THE HONG KONG POLYTECHNIC UNIVERSITY
INSTITUTE OF TEXTILES AND CLOTHING

DESIGN AND DEVELOPMENT OF ELECTRICALLY CONDUCTING TEXTILE SENSORS FOR SMART TEXTILES AND APPAREL

Joanna Hing Yee, TSANG

A thesis submitted in partial fulfillment of the
requirements for the Degree of Doctor of Philosophy

Aug 2006

CERTIFICATE OF ORIGINALITY

I hereby declare that this thesis is my own work and that, to the best of my knowledge and belief, it reproduces no material previously published or written, nor material that has been accepted for the award of any other degree or diploma, except where due acknowledgment has been made in the text.

TSANG, Hing Yee Joanna

To my husband Kwong,

for his encouragement and support.

To my mother Cecilia and father Piu,

sister Rosanna and brother Angus,

for their endless love, support and understanding.

ABSTRACT

The thesis presents a systematic study of sensing behaviour of the polypyrrole (PPy)-coated textile materials for large strain sensing purposes. This research is aimed at creating a conducting textile with superior sensing performance including low electrical resistance, high strain sensitivity and good environmental stability. It is also aimed to provide better understanding of the strain sensing mechanism and interaction between the PPy coating and textile substrate. The material system, fibre architecture and fabrication techniques have been investigated for producing flexible fabric strain sensors for particular applications. The study covers five related aspects, namely (1) fabrication techniques of the PPy-coated fabrics, (2) sensing performance of the PPy-coated fabrics with various stabilisation treatments, (3) characterisation of the PPy-coated fabrics fabricated under extremely low polymerisation temperature, (4) sensing mechanism of the PPy-coated fabrics and (5) product development using the newly developed flexible fabric strain sensors.

Fabrication techniques including (1) screen printing followed by chemical vapour deposition and (2) padding followed by chemical vapour deposition have been further developed in this project. The two fabrication processes and the conventional solution polymerisation technique are thoroughly described and compared. The chemical vapour deposition method can produce thinner, denser and uniformly distributed PPy coating layer on the textile substrate thereby enhancing the sensing performance.

Thermal annealing by vacuum drying and vacuum heat treatment plus large sized dopant application are the stabilisation treatments investigated for enhancing the environmental stability of the PPy-coated fabrics. Various characterisation techniques have been utilised to investigate the properties of PPy coating layer treated with different stabilisation methods. The study of the PPy-coated fabrics and pure PPy powders with different stabilisation treatments reveals that all the treatment methods can improve thermal stability, PPy chain ordering, surface smoothness and fabric hydrophobicity, resulting in enhancing the environmental stability as well as strain sensitivity. The most promising fabrication process with the above mentioned stabilisation treatments has been identified for producing high sensing capacity.

Electrically conductive fabrics prepared by the chemical vapour deposition process under extremely low polymerisation temperature (<-20°C) exhibit excellent strain sensitivity factor of over 400 at a strain of 50%. Particle size analyser, dynamic force mode and surface potential modes of scanning probe microscopy have been employed to characterise the properties of PPy coating on textile substrates. It is found that low temperature polymerisation produces smaller particle size of PPy with thinner, denser and smoother PPy coating on textile substrate which is beneficial to the sensing performance.

The present research discovers that the excellent strain sensing behaviour of the PPy-coated Tactel/Lycra knitted fabrics are mainly attributed to the high performance of the PPy-coated PU yarn as well as the excellent property of the knitted fabric structure. In-situ scanning electron microscopy observation demonstrates the crack-opening and crack-closing mechanism on the fibre surface. Electrical resistance of PPy-coated PU fibres with different pre-extension levels has been investigated in order to simulate the actual situation of PU fibres inside the knitted fabric substrate. The deformation mechanism of weft knitted fabric structure has also been studied.

The newly developed fabric strain sensors with excellent sensing performance are potentially applicable to many practical fields such as health and well being, wearable bio-medical monitoring, rehabilitation, toy and entertainment etc. This thesis demonstrates a prototype of instrumental dancing garment using the fabric sensor as a soft switch to control the instrumental music during dancing.

PUBLICATIONS

Refereed Journal Publications

1. **Tsang, H. Y. J.**, Leung, M. Y., Tao, X. M., Yuen, C. W. M., and Xue, P.
   "Effect of Fabrication Temperature on Strain Sensing Capacity of Polypyrrole-Coated Conductive Fabrics"
   Polymer International, accepted, August,2006.

2. **Tsang, H. Y. J.**, Leung, M. Y., Tao, X. M., Yuen, C. W. M., and Leung, C. W.
   "Development of Instrumental Dancing Garments with Fabric Strain Sensors"
   Journal of Industrial Textiles, submitted.

3. **Tsang, H. Y. J.**, Leung, M. Y., Tao, X. M., Yuen, C. W. M., Li, Y. and Cheng, X. Y.
   "Study of Polypyrrole Coated Stretchable Sensing Fabrics"
   Textile Research Journal, submitted.

4. Li, Y., Leung, M. Y., Tao, X. M., Cheng, X. Y., **Tsang, J.** and Yuen, C. W. M.
   "Polypyrrole-Coated Strain-Sensing Fabrics with High Sensitivity Prepared by Chemical Vapour Deposition"
   Journal of Material Science, submitted.

5. Li, Y., Cheng, X. Y., Leung, M. Y., **Tsang, J.**, Tao, X. M. and Yuen, C. W. M.
   "A Flexible Strain Sensor from Polypyrrole-Coated Fabrics"
   Synthetic Metals, 155 (1), 2005, p.89-94.

6. Li, Y., Leung, M. Y., Tao, X. M., Cheng, X. Y., **Tsang, J.** and Yuen, C. W. M.
   "Polypyrrole-Coated Conductive Fabrics as a Candidate for Strain Sensors"
   Journal of Material Science, 40(15), 2005, p.4093-4095.

Patent Application

Tao, X. M., Leung, M. Y., Yuen, C. W. M., Cheng, X. Y., **Tsang, H. Y. J.** and Li, Y.
"Methods for Coating Conducting Polymer"
US Patent, Application No. 11/222,179

Book Chapter

Leung, M. Y., **Tsang, H. Y. J.,** Tao, X. M. and Yuen, C. W. M.
"Stability Enhancement of Polypyrrole Coated Textiles"
Intelligent Textiles and Clothing, Editor: IN Mattila, H., Woodhead Publishing Ltd.

Conference Publications

1. **Tsang, H. Y. J**., Leung, M. Y., Tao, X. M. and Yuen, C. W. M.
   "Development of Textile E-sensor and Instrumented Dancing Garments"
   Ambience 05 Conference, Tampere, Finland, September 19-21, 2005, CD Rom

2. **Tsang, H. Y. J.**, Leung, M. Y., Tao, X. M., Yuen, C. W. M., Li, Y. and Cheng, X. Y.
   "Effect of Large Size Anion Dopant Application on Polypyrrole Coated Fabrics"
   Fiber Society Spring 2005 Conference, Technical Textiles from Fiber to Composites, St.Gallen, Switzerland, May 25-27, 2005, book of abstracts, p.92

3. Cheng, X. Y., **Tsang, H. Y. J.**, Li, Y., Leung, M. Y., Tao, X. M., Cheng, X. X., Xue, P. and Yuen, C. W. M.
   "Polypyrrole-Coated Large Deformation Strain Fabric Sensor and its Porperties Study"
   2006 Materials Research Society Spring Meeting, San Francisco, Ca., USA, April 17-21, 2006, MRS proceedings volume 920, Symposium S – Smart Nanotextiles, Editors: D. Diamond, X. Tao, G. Tröster, no. 0920-S05-08

4. Xue, P., Tao, X. M., **Tsang, H. Y. J.**
   "Investigation on PPy-coated XLA Fiber in Strain Sensing Application"
   International Fiber conference 2006, Seoul National University, Seoul, Korea, May 30- June 3, 2006

5. Xue, P., Tao, X. M., **Tsang, H. Y. J.** and Leung, M. Y.
   "PPy-Coated Electrically Conducting Fabrics with High Strain Sensitivity"
   2006 MRS Spring Meeting, San Francisco, Ca., USA, April 17-21, 2006

6. Cheng, X. Y., Kwok, W. Y., **Tsang, H. Y. J.**, Tao, X. M., Leung, M. Y., Yuen, C. W. and Xue, P.
   "Enhancement of the Environmental Stability of Polypyrrole-Coated Fabrics"
   Fiber Society 2004 Annual Meeting and Technical Conference, Cornell University, USA, October 11-13, 2004, book of abstract, p.82

ACKNOWLEDGEMENTS

First of all, I would like to express my deepest gratitude to my chief supervisor, Professor Xiao-ming Tao, Chair Professor of Textile Technology, Institute of Textiles and Clothing, who brought me to this interesting and promising research field. Her guidance and encouragement, drawn from her profound academic attainments and rich research experience, have been continuously enlightening my study at the Hong Kong Polytechnic University.

I would also like to express my special thanks to Dr. M. Y. Leung and Dr. C. W. M Yuen, my co-supervisors, for their valuable advice, support and patience throughout the whole research period.

Gratefully acknowledge to Dr. P. Xue, Dr. X. Y. Cheng and Dr. Y. Li, research fellows of the Nanotechnology Center of the Hong Kong Polytechnic University for their valuable advices and assistance in experimental design, sharing and discussion. Their expertise in mechanical engineering, electronic engineering and polymer science have provided me a lot of constructive suggestions during my study.

My thanks are also extended to the technical staffs in laboratories and workshops of the Institute of Textiles and Clothing, the Hong Kong Polytechnic University, for their assistance in experimental work. Sincere thanks to Mr. Yeung of Materials

Research Center of the Hong Kong Polytechnic University for his assistance in performing the experiments.

I wish to acknowledge the valuable assistance of my friend, Mr. C. W. Leung, who worked with me on the development of dancing garment. My thanks also give to Miss H. L. Lee, model of the dancing garment, for her patient and support during the development of prototype.

Finally, but not the least, my deepest gratitude goes to my husband, my parents and my sister and brother for their endless love, encouragement, and understanding during the past years. I dedicate this thesis to them.

This work has been financially support by the Innovation Technology Fund of The Hong Kong SAR Government is greatly appreciated [Project No. ITS/071/02]. I am especially acknowledge a postgraduate scholarship from the same source.

TABLE OF CONTENTS

LIST OF FIGURES

LIST OF TABLES

NOTATIONS

AQSA	Anthraquinone-2-sulfonic acid
CVD	Chemical Vapour Deposition
DBS	Sodium dodecylbenzenesulphonate
DFM	Dynamic Force Microscopy
DHBP	2,4-dihydroxybenzophenone
DS	Dodecylsulphate
e-textile	Electro-textile
IDG	Instrumental Dancing Garment
LT	Low Temperature
PA6	Polyamide, Nylon
Pad-CVD	Padding followed by Chemical Vapour Deposition
PET	Polyethylene terephthalate
PPy	Polypyrrole
Print-CVD	Screen Printing followed by Chemical Vapour Deposition
PU	Polyurethane, Lycra
RT	Room Temperature
SEM	Scanning Electron Microscopy
SP	Solution Polymerisation
SPM	Scanning Probe Microscopy
TGA	Thermogravimetry Analysis
VD	Vacuum Drying
VHT	Vacuum Heat Treatment
XPS	X-ray Photoelectron Spectroscopy
XRD	X-ray Diffraction

A_o	Area of the material
c	Course spacing
C_h	Crimps of the weave in the weft
C_v	Crimps of the weave in the warp
d	Distance between atomic layers in a crystal
D_a	Main diameter
E	Young's modulus
G	Shear modulus
G_c	Steady-state energy release rate
K	Gauge factor
L	Loop length
L_o	Length of the material
n	Order of diffraction
N	Number of grains
N_e	Number of ends per fabric width
N_p	Number of picks per fabric length
r	Yarn radius
R	Electrical resistance
R_a	Smoothness of the surface
RH	Relative humidity
R_h	Resistance of woven fabric measured in the weft direction
R_o	Initial electrical resistance
R_{shift}	Shift in the electrical resistance
R_v	Resistance of woven fabric measured in the warp direction
S_a	Mean grain size
S_o	Area of selected region
S_T	Total grain size
T	Temperature
t	Time
U	Total amount of strain energy
U_d	Strain energy density
V	Volume of the structure

V_{ac}	Oscillating voltage
VR	Variable resistor
V_{REF}	Voltage reference
w	Wale spacing
Z_o	Standard profile of a fibre surface
ε	Strain
$\acute{\varepsilon}$	Strain rate
η	Resistance of yarn per unit length of yarn
λ	Wavelength
v	Poisson's ratio
ρ_o	Resistivity of the material
σ	Stress
ω	Frequency

Subscripts

f	coating film
i	initial
max	maximum
min	minimum
r	relative
re	reference
s	substrate
re	reference

CHAPTER 1

INTRODUCTION

1.1 Background : Textile Sensors for Smart Textiles and Apparel

Smart textiles have attracted more and more attention in recent years. The research, development and application activities in smart textiles have grown tremendously over the past twenty years. Most smart fabrics are made by weaving metal wire into fabrics and incorporating small electronic components, sensors and circuitry into the structure of textile, thereby modifying the functionality of the apparel to produce smart metal-based wearable garments. The application of wearable electronics can be divided into five areas (Kim, Koncar, Devaux, Dufour and Viallier, 2004), namely (i) professionals (the need for “free hands function”), (ii) health care (monitoring, training result diagrams), (iii) everyday life (telephone, wellness), (iv) sports (training, performance measurement) and (v) leisure (aesthetic customisation network games). Typical examples of these types of smart textile products such as smart shirt, life shirt, wearable mother boards, cardiogram detection, smart bra, MP3 jacket, socks and gloves etc. (Meoli and May-Plumlee, 2002). However, many of the devices or systems available for wearable electronics rely upon electronic components attached to the textile materials, which may affect the comfortability of the wearer or alter the physical property of textile substrates.

Conducting polymer coated textile substrates have been found to have high potentials for the development of textile sensors, connectors and actuators. A more innovative and innocuous approach is to develop smart fabric sensors or wearable electronic devices by directly coating conducting polymers onto a textile substrate in order to eliminate the use of metal component within the fabrics. The major advantage of using conducting polymer coated fabrics as sensors is to retain the natural texture of the material so as to keep the comfortability and flexibility of the wearable electronics or electro-textiles. These materials normally work as strain or pressure gauge and find applications in wearable medical monitoring systems for clinical use (Brady, Diamond and Lau, 2005).

Despite the promising performance characteristics, the development of conducting textile structures is still at its earlier stage. The nano-structures of the conductive polymer film on the fibre surface play a vital role in determining the properties of the textile sensors. Hitherto, there are limited publications relating the electrical, mechanical and thermal properties of conducting textile structures to the morphology of the conductive coating on the fibre surface. In addition, very little publications concerning the effect of fibre architecture, deformation modes, moisture, acid and alkali perspirations, washing with reagents and fabrication processing conditions on the conductive textiles can be found. Hence, the present study is intended to investigate the relationships between the electrical conductivity, strain sensitivity and environmental stability of the textile sensors using various pretreatments, deposition and stabilisation treatments. These textile sensors with sensing techniques to detect the strain, humidity and temperature of flexible textile structures will be developed by applying the nano-structured conducting polymer coated on fabrics. In this study, high strain sensitivity and environmentally stable textile sensors will be designed and developed.

1.2 Objectives

The present study is aimed at developing various conducting fabric sensors with superior conductivity, strain sensitivity and environmental stability using different fabrication methods and preparation parameters. This thesis presents a systematic multi-scale study of the sensing behaviours of the polypyrrole (PPy)-coated textile fabrics with the following objectives:

1. To comparatively study various fabrication methods for developing the PPy-coated fabric sensors with superior strain sensing capacity and stability towards external environment.
2. To investigate the stabilisation treatments used for enhancing the environmental stability of the PPy-coated fabric sensors, and to study the resultant sensing consistency and strain sensitivity of the fabric sensors.
3. To explore the effect of fabrication methods with extremely low temperature polymerisation on the resultant sensing performance and environmental stability of the PPy-coated fabric strain sensors.
4. To characterise the developed conductive textile fabric sensors by studying their physical, mechanical, chemical and electrical properties using a series of analytical instruments.
5. To investigate the electro-mechanical behaviour of the PPy-coated fabrics and their strain sensing mechanism by studying the tensile property, surface morphology and coating thickness.

6. To develop a wearable sensing prototype by combining the newly developed textile sensors with various sensitivity levels.

1.3 Methodology

Figure 1.1 shows the framework of the study of the PPy-coated fabric strain sensors. It can be divided into two main parts, namely Literature Review and Proposed Schemes.

Problem Identification

High strain sensitivity and good environmental stability are the two critical requirements for the development of practical fabric strain sensors. However, very limited publications concerning both requirements simultaneously for developing PPy-coated fabric strain sensors.

Literature Review

A comprehensive literature review will be focused on the conductive polymer-coated textiles sensors based on various kinds of fabrication methods and materials. Literatures review will be conducted on (i) the recent developments of smart textiles and conductive polymer coated textile sensors, (ii) the electrical stability and degradation mechanisms of PPy films, (iii) the methods for enhancing the sensing performance of PPy-coated fabrics and finally (iv) the effect of fabric designs, fabrication methods, preparation conditions and surface treatments on the results of sensing performance. The review of sensing performance of the PPy-coated fabrics investigated by other researchers will also be carried out.

Figure 1.1 Framework of research methodology for PPy-coated fabric sensors

Proposed Schemes

As shown in Figure 1.1, there are several methodologies for studying the PPy-coated fabrics. It has been demonstrated that PPy-coated textiles developed by different fabrications would provide textile sensors with various sensitivity and conductivity that are suitable for different applications ranging from gas sensors, bio-sensors to strain sensors (Oh, Park and Kim, 2003; Tao, 2001; Zhang, Roy, Tessier and Dao, 2001). Since the strain sensitivity and stability of PPys properties are the most important factors governing the scope of its possible application for a strain sensor, thus the study will focus mainly on the investigation of the strain sensitivity and stability of textile sensors through various proposed methods. The newly developed methods are proposed to affect the structures, chemical properties, morphology and sensing performance of the PPy coating film on the textile substrates.

The research methodology with respect to the specific objectives of this study is summarised as follow:

Comparative study of various fabrication methods

Various fabrication methods will be comprehensively evaluated and compared with the sensing performance in order to produce different fabric sensors with a wide range of conductivity and strain sensitivity. Fabrication methods, namely screen printing followed by chemical vapour deposition and padding followed by chemical vapour deposition, are examined to enhance the sensing capacity of the PPy-coated fabrics. The effect of fabrication methods of the PPy-coated fabrics on the sensing performance including electrical conductivity, strain sensitivity and environmental stability will be systematically investigated.

The surface resistance of conductive materials will be measured by using the Keithley two-probe multi-meter. Tensile deformation will be carried out by means of the Instron 4466 model extensometer integrated with the computer data acquisition system. In addition, the extension device modified for on-line resistance recording during extension will be utilised in this study.

Investigation of the stabilisation treatments

Factors affecting the relative electrical resistance changes between the cyclic heating and cooling sensing curves of the flexible textile sensors with respect to the changes of environmental factors will be examined systematically. Various methods and theories employed for accelerating the ageing and enhancing the environmental stability of the conducting polymer will be investigated so as to optimise the performance of the flexible textile sensors and make it suitable for applying to wearable sensing products. Special techniques will be employed to stabilise the PPy-coated fabrics such as bulky anion dopant application and thermal annealing treatment.

Exploration of the new fabrication methods with extremely low temperature polymerisation

Extremely low temperature polymerisation will be investigated in order to synthesis a more thin, smooth, compact and dense PPy film for coating the textile substrates. A low temperature chamber of around -30°C will be utilised for fabricating PPy-coated fabrics. The sensing performance of various fabrication methods under low temperature polymerisation will be comparatively studied.

Characterisation of the developed conductive textile fabric sensors

In addition to the developed PPy-coated fabrics by different fabrication methods and conditions, pure PPy powders will also be produced for characterisation by a series of advanced instrumental techniques in order to provide deeper understanding of the behaviour of the PPy coating layer. The surface morphology will be characterised by scanning probe microscopy and scanning electron microscopy. The crystallinity, thermal property and particle size of PPy will be characterised by x-ray diffraction, thermogravimetric analysis and particle size analysis respectively.

Investigation of the electro-mechanical behaviour and strain mechanism of the PPy-coated fabrics

The electro-mechanical behaviour of PPy-coated polyamide and PPy-coated polyurethane fibres will be studied by using the Instron 4466 model extensometer integrated with the multi-meter and computer data acquisition system. In order to study the strain mechanism of PPy-coated fabric, firstly, the strain mechanism of PPy-coated fibres will be investigated by in-situ scanning electron microscope observation. Secondly, the electro-mechanical and morphological behaviours of PPy-coated polyurethane fibres with different pre-extension levels will also been studied in order to simulate the actuate state of polyurethane yarn inside the fabric substrate. The strain energy density of fibres with various levels of initial strain and elastic strain will be studied. Finally, the effect of the fabric knitted structure on the electro-mechanical behaviour will be evaluated and examined.

Development of wearable sensing product

A prototype of Instrumental Dancing Garment will be developed for demonstrating the application of PPy-coated fabric strain sensor into the conventional dancing garment. It will be developed to sense the body movements of dancer and transform the signals into specific musical instrumental sounds. The development of fabric sensor with optimum sensing capacity and environmental stability, design of connectors for signal transmission by using intrinsically conductive textile fibres, design of circuitry and computing program for signal transformation will be conducted.

1.4 Project Significance

Although there are numerous developments of textile electrical sensors by other researchers; little has been reported on the textile structure and interaction between conductive layer and substrates as well as the sensing performance of the sensors. The comprehensive investigation of the optimum fabrication parameters with respect to sensing performance and environmental stability will provide a new scientific understanding of the electro-mechanical behaviour and mechanism of the conducting textile strain sensors. It represents a great challenge and significant contribution to the advancement of fabrication knowledge and the development of various flexible conducting textile sensors. In addition, the successful design and development of various types of textile sensors for signal transmission are significantly valuable for smart products such as textile electronic products. These highly value-added products will bring great benefits not only to the textile and clothing industry, but also to chemistry, electronic, sports, multi-media and even rehabilitation fields.

1.5 Outline of the Thesis

The thesis comprises seven chapters which are summarised in the following.

Chapter 1 introduces the background information, objectives, research methodology and significance of the project.

Chapter 2 provides a comprehensive literature review for the recent development and potential application of conductive textiles sensors. Various fabrication processes of the PPy-coated textiles are compared in this chapter. The literature review also includes the explanation of the instability of PPy films and the proposed methods for its improvement.

Chapter 3 discusses the comparison of the PPy-coated fabrics prepared by various fabrication methods and treated with different stabilisation treatments. The comparison results are presented in terms of tensile behaviour and sensing performance which include electrical resistance, strain sensitivity, environmental stability towards temperature and relative humidity, and long term stability. This chapter also identifies the potential stabilisation treatment and fabrication procedures for producing the PPy-coated fabrics with superior sensing capacity and good stability.

Chapter 4 extends the study of the proposed polymerisation condition, i.e. the PPy-coated fabrics prepared at room temperature polymerisation and extremely low temperature polymerisation are compared and thoroughly investigated.

Determination of surface morphology and PPy coating thickness in micro-scale and nano-scale are presented.

Chapter 5 investigates the electro-mechanical behaviour of the PPy-coated fabrics and their strain sensing mechanism. The deformation mechanisms of various PPy-coated fibres are studied and observed by the in-situ scanning electron microscope. The study of the effect of pre-extension levels of the PPy-coated polyurethane fibres on the electrical and mechanical performance is carried out. The investigation of fibre materials, fabric structure and deformation mechanism of the weft-knitted Tactel/Lycra plain fabric with respected to the sensing capacity of the PPy-coated textiles is also conducted.

Chapter 6 illustrates the design and development of dancing garment prototype by using the newly developed fabric strain sensors. The design concept and design layout of Instrumental Dancing Garment development is demonstrated. The frameworks of prototype including the textile sensors, textile connectors, circuit design and computing programme design are thoroughly studied and discussed in this chapter. The potential application of the newly developed fabric strain sensors is also explored.

Chapter 7 summarises the major findings of the study and recommends the future work in the area of fabric sensors.

CHAPTER 2

LITERATURE REVIEW

2.1 Introduction

Nowadays customers demand interactivity, connectivity, mobility, ease of use, comfort and a “natural” interface for information processing. The enabling technologies of electronics, sensors, computing and communications are becoming pervasive. The integration of the enabling technologies into smart textiles and clothing is of critical need. Traditional textiles can be transformed into an interactive, intelligent infrastructure to facilitate pervasive information processing. Development of smart textile sensors will be the first step in the development.

2.1.1 Development and applications of conductive textiles

Conductive textile sensors have been studied for many years (Meoli and May-Plumlee, 2002). Recently, the art in integrating electronics with wearable systems or called smart textiles has garnered the attention for electronic, textile and clothing industries. Wearable electronics not only involve integrating electronic components on textiles but rather garments with embedded functionalities. These textile materials are able to transport and display data by using electrically conductive textile materials, such as flexible displays, sensors, embroidered switches etc. (Tao, 2001, 2005).

There are two common ways for developing conductive textiles. First, researchers developed highly conducting textile materials based on weaving or inserting fine intrinsically conductive wires such as copper and aluminium into a fabric. Second, conducting polymers coated textile substrates were found to have high potentials for the development of textile sensors, connectors and actuators.

Intrinsically conductive wires in fabrics

More than 20 years ago, conductive textiles were developed for electromagnetic interference shielding and antistatic applications (Cheng, Ramakrishna and Lee, 2000a; Cheng, Ramakrishna and Lee, 2000b; Cheng, Ueng and Dixon, 2001; Morgan, 2000). Start from 80s, techniques and applications for weaving, knitting or braiding metallised fabrics by using metal fibres or yarns such as copper, stainless steel, aluminium, nickel, even gold and silver had been reported (Smith, 1988). Furthermore, highly conductive fabric with soft handle, called silk organza, was reported by Post (1997). It contains two types of fibres, which were a plain silk yarn as the warp and a silk yarn wrapped with thin copper foil as the weft. The silk organza is shown in Figure 2.1.

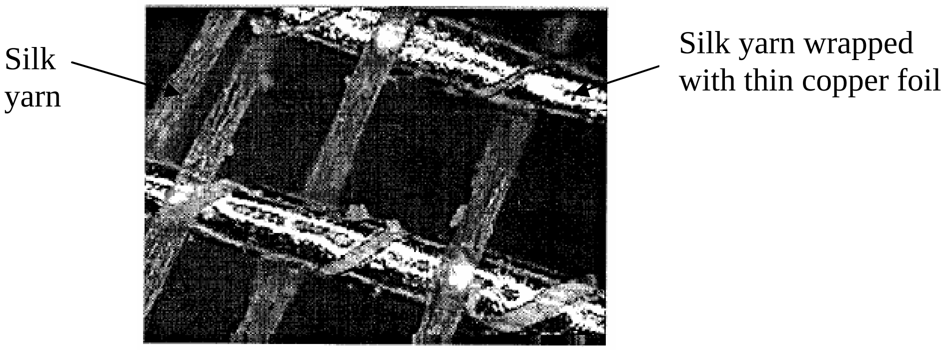

Figure 2.1 Micrograph of silk organza (Post, 1997)

Recently, there have been many innovating and advancing approaches toward integration of electronic components into textiles. Post (1997) built electronic circuits entirely out of textiles to distribute data and power, and perform touch sensing. He applied stainless steel fibres into textiles in order to connecting circuit boards for developing different types of textile electronics such as musical jacket, musical balls or electronic tablecloth. Figure 2.2 shows the prototype of musical jacket. Those circuits use conventional electronic components by sewing with conductive yarns, such as musical keyboards and graphic input surfaces.

Figure 2.2 Musical jacket (Post, Orth, Russo and Gershenfeld, 2000)

A research team developed transmission line using a woven fabric with conductive metal yarn in plain weave fabrics (Cottet, Grzyb, Kirstein and Troster, 2003; Marculescu, Marculescu, Zamora, Stanley-Marbell, Khosla, Park, Jayaraman, Jung, Lauterbach, Weber, Kirstein, Cottet, Grzyb, Troster, Jones, Martin and Nakad, 2003).

The idea for developing textile-based interconnect was for signal transmission. Insulated metal filaments twisted with polyester yarn woven in conventional plain weave structure have been chosen for development. This construction is the most elementary and simple textile structure. The selected material and weave provides a tight mesh of individually addressable wires that can be used as basic transmission lines, as well as whole circuits. However, the critical concern is the mechanical stability of the connection between the conductive fibres and electronic components. Figure 2.3 shows the woven fabric with insulated metal filaments.

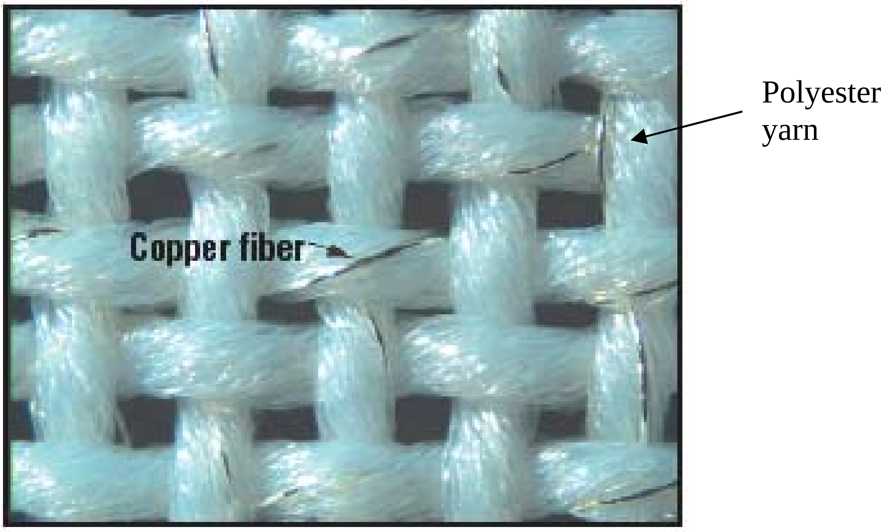

Figure 2.3 Woven fabric with metal fibres

(Cottet, Grzyb, Kirstein and Troster, 2003)

By the year of 1999, it was found that electro-textile (e-textile) using fibres and fabrics was not just to transmit signals but also to modulate signals, working as textile sensors. Philips Research Laboratories developed a wearable sensor jacket that uses advanced knitting techniques to form soft stretchable fabric sensors placed in the joint positions of jacket to measure upper limb and body movement (Farringdon, Moore, Tilbury, Church and Biemond, 1999). The structure of fabric sensor constructed by knitting elastic fibres with carbon fibres is shown in Figure 2.4. The resistance value could be changed when stretching the sensor. A tracking tape knitted with conductive fibre was developed for the purpose of transmitting an electrical signal and connected with sensors. The requirements of high conductivity and good stability are very useful for a tracking cables development, the knitted tracking was 10mm wide with only 3 ohms resistance over 100mm. When the sensor and tracking materials are relaxed, the sensors exhibit a resistance 25 times greater than that of the tracking. However, the ratio increases to 100 times during stretching. Therefore, the resistance of tracking will not affect the data obtained from the sensors as it possess much higher conductivity and stability to elongation. The sensor and tracking material is shown in Figure 2.5.

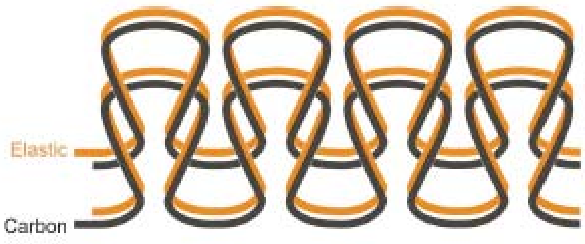

Figure 2.4 Knitted structure of fabric stretch sensor

(Farringdon, Moore, Tilbury, Church and Biemond, 1999)

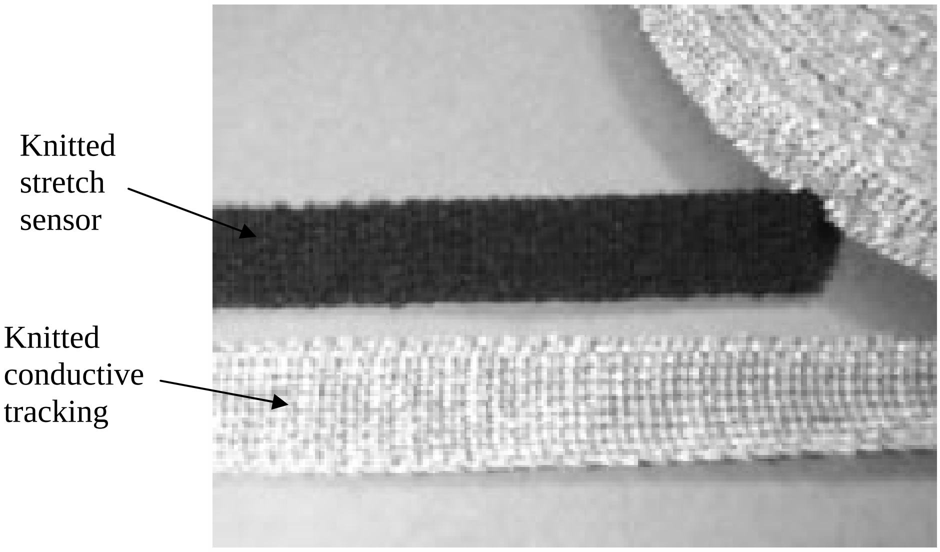

Figure 2.5 The black one is the stripe of stretch sensor knitwear and the white one is the knitted conductive tracking
(Farringdon, Moore, Tilbury, Church and Biemond, 1999).

Figure 2.6 The final sensor jackets. Sensors are shown in black, and are connected at each end by covered conductive tracking
(Farringdon, Moore, Tilbury, Church and Biemond, 1999).

The sensor jacket shown in Figure 2.6 includes knitted fabrics which have electrical properties suited for either sensing elongation or for use as non-sensing conductive tracking. A connection port on the jacket can be connected to other wearable devices for data collecting from the current limb movement and body position of the wearer.

In 2000, an detailed articles was published regarding the development of electronic embroidery which is the patterning of conductive textiles by numerically controlled sewing or weaving processes (Post, Orth, Russo and Gershenfeld, 2000). The aim of the research is to create computationally active textiles. Some unique applications, such as the construction of sensors, user interface elements in textiles and a complete process for creating flexible multilayer circuits on textile fabric substrates have been reported. Interactive electrical textiles embroidered with conductive threads has demonstrated their abilities to stitch multiple layers of fabric in one step and to precisely specify circuit layout with computer-aided design. Figure 2.7 shows one of the e-textile that developed by the authors.

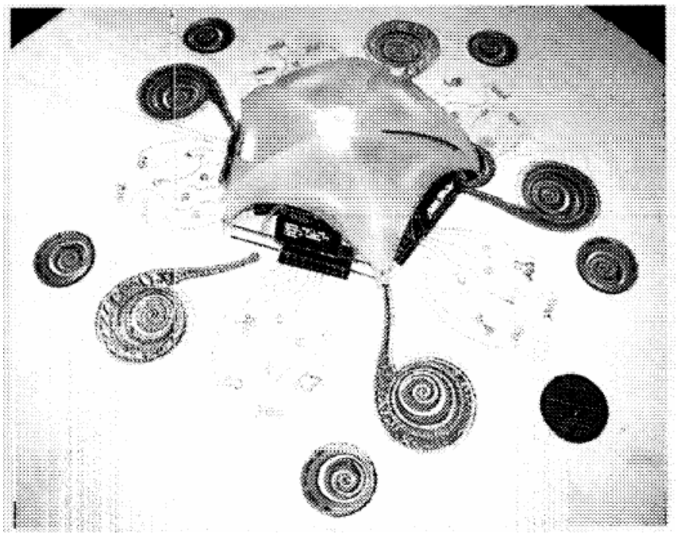

Figure 2.7 Electronic tablecloth

Other typical examples are textiles that react to deformation such as pressure sensors developed by Softswitch (Meoli and May-Plumlee, 2002; Rodie, 2004). SOFTswitch^{TM} technology turns fabrics into interactive electronic controllers, yet allows them to retain their textile aesthetics. The technology involves combining lightweight conductive textile materials with a quantum tunnelling composite that has pressure-sensitive switching properties. A switch incorporated into a sofa, chair, carpet or wall-covering allows the user to turn on and adjust a lighting or stereo system, or to control a climate or security system. Figure 2.8 shows the integrated textile keypad developed by Softswitch.

Figure 2.8 Integrated textile keypad (Meoli and May-Plumlee, 2002)

Recently, woven and knitted stainless steel fabrics were used as electrodes, as shown as ‘Textrodes’ in Figure 2.9, for the development of smart suit (Catrysse, Puers, Hertleer, Langenhove, Egmond and Matthys, 2004; Coosemans, Hermans and Puers, 2006; Hertleer, Grabowska, Langenhove, Catrysse, Hermans, Puers, Kalmar, Egmond and Matthys, 2004). The suit was intended for the monitoring of electrocardiogram and respiration rate of children in a hospital environment. The authors demonstrated the strong potential of using textile materials as sensor elements, antennae and interconnections in a wearable bio-instrumentation system. Figures 2.10 and 2.11 show the developed prototypes of respibelt for measuring respiration and baby suit for measuring heart rate and electrocardiogram respectively.

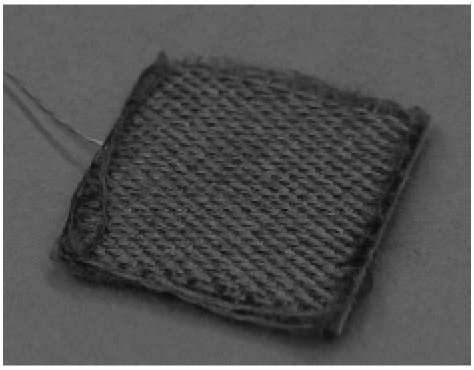

Figure 2.9 Photograph of a knitted 3 cm x 3 cm Textrode (Catrysse, Puers, Hertleer, Langenhove, Egmond and Matthys, 2004)

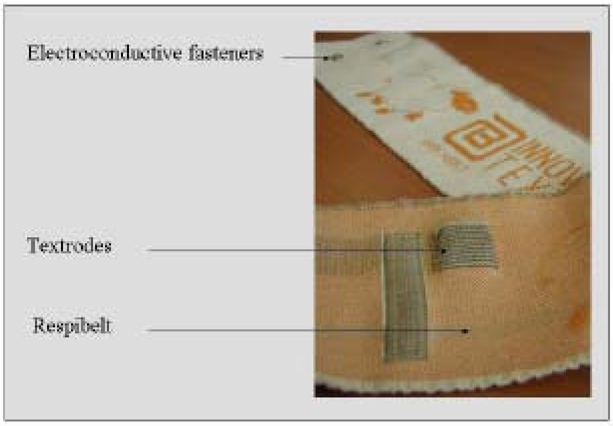

Figure 2.10 Prototype of Respibelt (Hertleer, Grabowska, Langenhove, Catrysse, Hermans, Puers, Kalmar, Egmond and Matthys, 2004)

(a) (b)

Figure 2.11 Body suit prototype, (a) inside showing the Textrodes and (b) backside (Coosemans, Hermans and Puers, 2006)

Figures 2.12 and 2.13 show the smart shirt and intelligent biomedical clothes developed by European funded projects: WEALTHY and MY HEART (Carpi and De Rossi, 2005; De Rossi, Loriga, Lorussi, Paradiso, Taccini, Tesconi and Tognetti, 2005; Pacelli, Loriga, Taccini and Paradiso, 2006). The fabric sensors implemented with the wearable systems can be used for medical monitoring of body parameters such as heart beat rate and breathing rate. The fabric sensors were made by commercial stainless steel threads twisted around a standard continuous viscose or cotton textile yarn. This system was designed for collecting risk factors to support citizens to fight against major cardio-vascular diseases and help avoid heart attack. Hence, it can provide the necessary motivation for the new life styles.

Figure 2.12 Wearable instrumented garment for monitoring vital signs (Smartex, http://www.smartex.it)

Figure 2.13 Intelligent biomedical cloth developed by MyHeart system (http://www.extra.research.philips.com/euprojects/myheart)

Although the above e-textiles, i.e. weaving thin wires of various metals have been developed with higher degrees of conductivity. The comfortability and strain sensitivity are still insufficient for strain sensors development.

Conducting polymers coated fabrics

Active research has been carried out to investigate the application of conducting polymers coated fabrics in corrosion protection, rechargeable batteries, electrochromic displays, conducting composite materials, biosensors, chemical gas sensors, actuators, electronics, electrochemical energy sources, artificial muscle devices, optical devices and smart fabrics (Brady, Lau, Megill, Wallace and Diamond, 2005; De Paoli, Panero, Passerini and Scrosati, 1990; Liu and Chung, 2003; Scrosati, 1993; Selampinar, Toppare, Akbulut, Yalcin and Suzer, 1995; Sree, Yamamoto, Deore, Shiigi and Nagaoka, 2002). These types of smart textiles can be produced by performing in-situ polymerisation of conducting polymers, such as polypyrrole (PPy) or polyaniline (PANI) in the presence of the textiles. The resulting smart fabrics are conductive while retaining the tactile properties of the original material. Because these smart materials do not compromise the tactile properties of uncoated material and provide excellent mechanical properties (Hu, Kaynak and Li, 2005), they have proven useful in the area of wearable sensing.

PPy based textiles and fibres were first developed by Milliken Research Corporation (Gregory, Kimbrell and Kuhn, 1989; Heisey, Wightman, Pittman and Kuhn, 1993). They have various levels of surface resistivity for different applications. They are produced by chemically polymerising pyrrole on the surfaces of fibres, yarns, and fabrics, encasing each individual fibre inside the textile assembly with a smooth, coherent coating of PPy.

For fabricating the conductive fibres and fabrics, in-situ chemical oxidative polymerisation using supercritical carbon dioxide aided process was explored (Harlin, Nousiainen, Puolakka, Pelto and Sarlin, 2005). PPy-coated polyamide fibres produced that can afford 10 times washing. The authors also reported that the PPy is mainly inside the fibre by using this fabrication method as supercritical carbon dioxide can swell the structure of the fibre and open the way for the monomer to penetrate into the polymer.

Previous studies by the team at The Hong Kong Polytechnic University have demonstrated that PPy-coated textile substrates possess strain, temperature and humidity sensing capacities. In addition, PPy-coated textile sensors have proved to be a flexible strain sensor that can respond to the repeated large strain deformation for up to 50% extension or more. Through a systematic study of various production methods for PPy-coated textiles, a new production method has been developed and a US patent has been registered (Tao, Leung, Yuen, Kwok and Ho, 2005).

PPy-coated textile can be developed as soft switches, strain sensors, pressure sensors, temperature sensors, gas sensor, and chemical sensors etc. It also can be used for communication, entertainment, healthcare, rehabilitation, sports trainings, safety, homeland security, computation, thermal uses, protective clothing, wearable electronics and fashions (De Rossi, Della Santa and Mazzoldi, 1999).

This kind of intelligent fabric also can act as sensor in the clothing which can adopt and respond to the wearers' needs and the environment. For example, it can be worn by senior citizens, the ill or high risk groups that will allow the constant medical monitoring of body parameters such as blood pressure, pulse, heart rate, body temperature, etc. Such smart shirt with sensors can bring the connectivity with the hospital so that medical aid can be reached in on time which promote "Personal Health Management" (Bhat, Seshadri, Nate and Gore, 2004). Users could take control of their own health status and adopt a permanent healthier lifestyle. This self-management of health would make people more independent, improve their quality of life and at the same time reduce health-care costs (Kirstein, 2004).

PPy-coated fabrics have been demonstrated to posses a sensing capacity of strain and temperature (De Rossi, Della Santa and Mazzoldi, 1997, 1999; De Rossi, Lorussi, Mazzoldi, Rocchia and Scilingo, 2001; Mazzoldi, De Rossi, Lorussi, Scilingo and Paradiso, 2002; Spinks, Wallace, Liu and Zhou, 2002). Wearable devices had been developed to read and record the posture and movements of a subject wearing the system. The sensory function was achieved by fabric strain sensors which were made with PPy-coated textiles. In the investigation, a sensing glove for recording the resistance changes caused by fabric strain due to finger flexion had been developed and a sensing sock for reading the resistance caused by fabric strain due to different compressive loads simulating foot-ground contact pressure was made. Figure 2.14 shows a smart sensing glove developed by De Rossi (De Rossi, Della Santa and Mazzoldi, 1999).

Figure 2.14 Smart sensing glove (De Rossi, Della Santa and Mazzoldi, 1999)

Figure 2.15 shows that the hardware sensors can be replaced by textile strain sensor for body kinematics, posture and gesture monitoring which is useful for rehabilitation or sports training purposes (De Rossi, Carpi, Lorussi, Mazzoldi, Scilingo and Tognetti, 2002).

(a) (b)

Figure 2.15 Body posture detection by (a) hardware sensors and (b) fabric sensor

Another group of researchers in Korea explored the polyethylene terephthalate (PET) fabric/PPy composite and Nylon 6/PPy composite fabrics for electromagnetic interference shielding (Kim, Kim, Byun, Jeong, Hong, Joo, Song, Kim, Lee and Lee, 2002; Kim, Jang, Byun, Lee, Joo, Jeong and Park, 2003), developed PPy-coated nylon woven fabric for heat generation fabric for medical uses (Lee, Park and Lim, 2003) and PPy-coated nylon/spandex stretchable conductive fabric for electrotherapy application (Kim, Oh and Bahk, 2004; Oh, Park and Kim, 2003). Recently, the concept of PPy-coated fabrics for development of a cooling fabric and heating fabric has been demonstrated (Hu, Kaynak and Li, 2005; Kaynak and Hakansson, 2005). But the cooling and heating effects have not been well achieved yet and optimisation of synthesis conditions is needed to further study.

In addition to the 2-dimensional fabric strain gauges, PPy-coated polyurethane foam sensor with 3-dimensional structure which sensitive to pressures exerted from all three dimensions was developed (Brady, Diamond and Lau, 2005; Brady, Lau, Megill, Wallace and Diamond, 2005). The authors used PPy coated polyurethane foam for developing a breathing monitor, whereby the foam sample was incorporated into a harness to wrap around the ribcage area. The movement of the ribcage during breathing exerts pressure on the conducting foam causing an increase in conductivity of the material.

2.1.2 Performance of PPy-coated fabric strain sensors

The application of PPy-coated textile sensors for wearable products or garments is still at a preliminary stage. Some problems, including the stability of the PPy-coated textile with respect to repeated cyclic temperature and humidity changes, have not been systematically studied and solved. The research about interactive effect of the parameters, strain, humidity and temperature during simultaneous measurement by the textile sensors has not yet been conducted. Table 2.1 summarised the fabrication methods and sensing performances of the PPy-coated textiles by other researchers. It shows the very limited publications concerning PPy-coated textiles as strain sensors. The best strain sensitivity of PPy-coated fabric possesses the factor of about 15 at 1.5% of fabric strain which was developed by De Rossi, Della Santa and Mazzoldi (1997).

Firstly, either chemical polymerisation or electro-chemical polymerisation could be used to form a layer of conducting PPy on the fabric substrates. Material selection and fabrication methods are critical issue for satisfying both adequate electrical and mechanical properties of the fabric strain sensors. Conductive sensors for wearable products need comfort, durability and stability in long term storage and daily usage. Therefore, different fabrication methods should be considered in order to provide optimum sensing capacities and good environmental stability that would not affect the excellent mechanical and physical properties of the textile substrates such as mechanical strength and flexibility.

Secondly, it is found that very limited publications concerning PPy-coated textiles as a strain sensor for large deformation. In general, circumference of body skin can be increased up to 20% with muscle contraction, the skin extension is up to 50% with bending at a joint in the longitudinal direction (Kim, Oh and Bahk, 2004). Therefore, using fabric strain sensor for wearable product, sensing capacity for large deformation up to 50% is needed to be considered. However, from the literature review, the strain sensitivity factor is only around 2.8 at 50% of fabric strain for the fabric sample prepared by chemical polymerisation (Kim, Kim, Chun, Park, Jeon, Lee, Hong, Joo and Kim, 2003).

Thirdly, the major requirement of a sensor is the reliability, which refers to an estimate for the ability of a system to function properly over time. Conductivity stability and reliability are closely related. Because fabric strain sensors will be exposed to use and care of the garments, time dependent effects will be more significant. Therefore for the reliability viewpoint, the environmental stability should be well considered while maintaining necessary mechanical properties of the PPy-coated fabric sensors. The literature review shows that the conductivity losses are quite serious after storage of the PPy-coated textile strain sensor. Eight folds of conductivity loss were found after 60 days storage (Scilingo, Lorussi, Mazzoldi and De Rossi, 2003). Child and Kuhn (1997) discovered that a doped PPy-coated polyester fabric can retained 93% of samples' initial conductivity after 1 year storage. The samples were doped with additive 2,4-dihydroxybenzophenone (DHBP) during chemical polymerisation. However, this kind of stable PPy-coated textile was not considered as a strain sensor.

Fourthly, it is known that the substrate material, fabrication process and conditions may alter the coating thickness and strain sensitivity of the PPy-coated conductive fabrics. However, the mechanism of strain sensing capacity of the PPy-coated fabrics has not been revealed until very recently. Recently, the electro-mechanical behaviour of the PPy-coated conductive composites and the sensing behaviour of PPy-coated polymer fibres was studied (Xue and Tao, 2004, 2005; Xue, Tao, Kwok and Leung, 2004). Their electro-mechanical behaviour under tensile load was experimentally studied. In addition, the morphology, conductivity, and mechanical properties of PPy-coated conductive fibres/yarn, and the mechanisms also investigated in multi-scales. The studies were concentrated on the PPy-coated fibres and yarns instead of fabrics.

A systematic study on electro-mechanical properties of knitted structure was reported (Zhang, Tao, Wang and Yu, 2005). The effective resistance of a knitted fabric has three components: (i) the resistance due to stretching the yarn in the V-segment of a knitted loop, (ii) the resistance due to yarn transfer from the horizontal part to the V-segment, and (iii) the resistance due to the yarn contact resistance. In the PPy-coated fabric, the first two components play a dominancy role.

Table 2.1 Summary of fabrication methods and sensing performance of PPy-coated textiles

Researchers	Materials and Fabrication Methods	Strain Sensitivity	Stability
(Child and Kuhn, 1997)	PPy-coated polyester fabric by chemical polymerisation		~33% conductivity loss after 120 days retained 93% of samples initial conductivity after 1 year storage if the sample with additive (DHBP)
(De Rossi, Della Santa and Mazzoldi, 1997, 1999)	PPy-coated Lycra fabric by chemical polymerisation	~15 at 1.5% fabric strain	--
(De Rossi, Carpi, Lorussi, Mazzoldi, Scilingo and Tognetti, 2002; Mazzoldi, De Rossi, Lorussi, Scilingo and Paradiso, 2002)	Fabrics coated with carbon loaded rubber by physical coating	2.5 at 1% fabric strain	--
(Kim, Byun, Jeong, Hong, Joo, Song, Park and Lee, 2002; Kim, Kim, Byun, Jeong, Hong, Joo, Song, Kim, Lee and Lee, 2002)	PPy-coated polyester fabric by chemical and electrochemical polymerisation in sequence		~60% and ~30% conductivity loss of the sample prepared by chemical polymerisation and electrochemical as well as chemical polymerisation after 80 day storage
(Scilingo, Lorussi, Mazzoldi and De Rossi, 2003)	PPy –coated Lycra/cotton fabric by chemical polymerisation	13 at 1.5% fabric strain	8 times conductivity loss after 60 days storage
(Oh, Park and Kim, 2003)	PPy-coated Nylon/spandex fabric by chemical polymerisation	Below 1 at 50% fabric strain	No change with 600 sec
(Kim, Kim, Chun, Park, Jeon, Lee, Hong, Joo and Kim, 2003)	PPy-coated PET/spandex fabrics by chemical or electrochemical polymerisations	~2.8 and ~1.6 at 50% fabric strain of the samples prepared by chemical and electrochemical polymerisation and chemical polymerisation only	--
(Spinks, Wallace, Liu and Zhou, 2003)	PPy-coated Nylon/polyurethane fabric by chemical polymerisation	~2 at 50% fabric strain	--
(Wallace, Spinks, Kane-Maguire and Teasdale, 2003)	PPy-coated Lycra fabric	4 at 5% fabric strain, 1.5 at fabric strain 5% to 60%	--

2.2 Fabrication of Electrically Conductive Textiles

2.2.1 Selection of conducting materials

Electrically conductive fibres can be intrinsically conductive or become conductive by integrating with electrically conductive materials. Carbon fibres represent a class of intrinsically conducting fibres and have been used to sense strain under tension and bending loading (Cho and Choi, 2000; Cho, Choi and Yoon, 2002; Wang and Chung, 1996). However, most carbon fibres are brittle in nature with low elongation, it possesses a modulus of about 200GPa or more, while most textile fibres have a modulus in the magnitude of several GPa. Introducing rigid carbon fibres into a textile structure may alter its strain and flexibility significantly. Besides, the measurement range of carbon-fibre-based sensors is limited to small strains, while fabric sensor is needed to operate at up to 50% of strain. Therefore, it is desirable to explore other kinds of electrically conductive textiles to serve in these applications.

Conjugated organic polymer systems are a field of increasing scientific and technical interest, offering a wide range of chemical, electrical, and magnetic properties. Because of their unusual electronic properties, electroactive conducting polymers, such as PANI, PPy and polythiophene (PTh) have found their way into many important technological applications. PPy was selected for this study because of its good electrical conductivity, good environmental stability in ambient conditions, chemical and thermal stability, inexpensive, ease of preparation and fewer toxicological problems when compared to the other conducting polymers. PPy is more suitable for applying to wearing products which may contact with human skin.

Polypyrroles (PPys) are formed by the oxidation of pyrrole or substituted pyrrole monomers. Figure 2.16 shows the chemical structure of pyrrole (C_4H_5N) and the structural formula of PPy. Electrical conductivity of PPy involves the movement of positively charged carriers or electrons along the polymer chains, i.e. hopping of these carriers between chains. The conjugated structure allows mobility of charge carriers along polymer chains via a rearrangement of double bonds (Kurosawa, 2004).

pyrrole

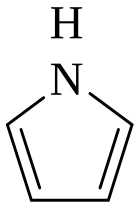

polypyrrole (α-α)

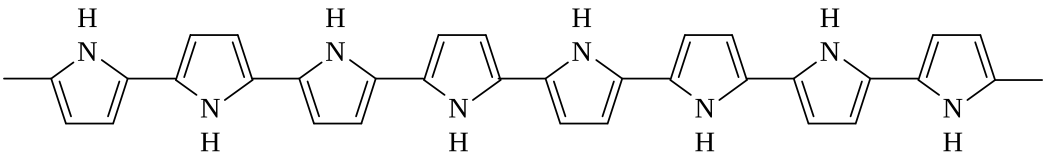

Figure 2.16 Chemical structures of pyrrole and polypyrrole

2.2.2 Fabrication methods of PPy

There are two main methods used to synthesise PPy, (i) electro-chemical polymerisation and (ii) chemical polymerisation. For the electro-chemical polymerisation, PPy can be formed by the oxidation of pyrrole at a suitable anode. Upon application of a positive potential, an insoluble conducting polymeric material is deposited at the anode. Figure 2.17 simply shows the polymerisation reaction (Wallace, Spinks, Kane-Maguire and Teasdale, 2003).

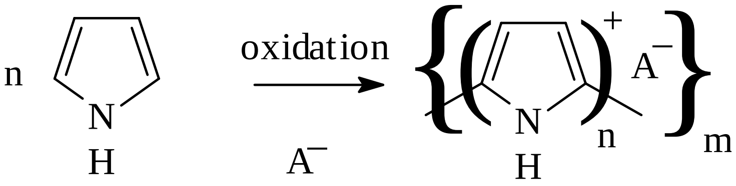

Where n=3-4, m relates to the polymer chain length

Figure 2.17 Electro-chemical polymerisation of PPy

PPy can also be formed by chemical polymerisation in solution by the use of a chemical oxidant (Wallace, Spinks, Kane-Maguire and Teasdale, 2003). According to the literature, transition metal ions are the most used oxidising agents for pyrrole polymerisation. Example of these metallic salts include $Fe_2(SO_4)_3$, $FeBr_3$, $CuCl_2$, $Fe(ClO_4)_3$, and $CuBr_2$. One of the most often used oxidising agents for pyrrole polymerisation are oxidative transition metal ions, i.e. ferric chloride ($FeCl_3$), and the polymerisation process can be simply shown in Figure 2.18 (Rodriguez, Grande and Otero, 1997).

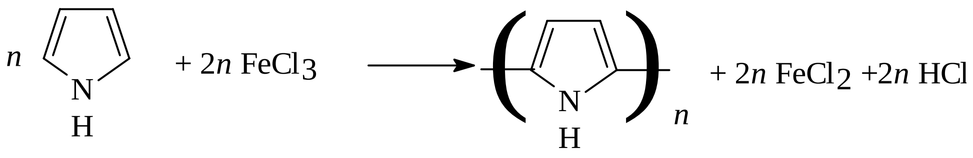

Figure 2.18 Chemical polymerisation process of pyrrole and $FeCl_3$
(Rodriguez, Grande and Otero, 1997)

The above two fabrication methods have also been used for producing PPy-coated fabrics as shown in Table 2.1. In addition, vapour phase in situ deposition has also been employed for fabricating PPy-coated yarn, for example, by passing pyrrole vapour over cotton yarn coated with the oxidant $FeCl_3$ (Tan and Ge, 1996).

2.2.3 Properties of PPy

As an intelligent material, conducting polymers must be capable of stimuli recognition, information processing and response actuation. As a result, they must possess appropriate chemical properties that can change in response to external stimuli, as well as appropriate electrical properties that allow information to be transported within the structure and switches to be actuated. The mechanical property is also necessary to be considered.

In order to optimise the performance of e-textile materials, the relationships between the structure and the properties must be clarified. The review of the electrical, chemical and mechanical properties of PPy structures is discussed below.

Electrical properties – Conductivity

The electrical properties of intelligent materials are important to transport information from one part of the structure to another, store information, trigger responses, convert and store energy. Electrical conductivity in PPy involves the movement of positively charged carriers or electrons along polymer chains and hopping of these carriers between chains (Wallace, Spinks, Kane-Maguire and Teasdale, 2003).

The experimental parameters used during synthesis have an essential effect on the polymer conductivity. In particular, the electrochemical conditions, solvent, counterion and monomers used during synthesis influence the electronic properties of the resulting polymer. By employing different metallic salts such as $FeCl_3$, $Fe(NO_3)_3$, $Fe(ClO_4)_3$, $Fe_2(SO_4)_3$ etc. for polymerising pyrrole, different conductivity values between 10^{-5} and 200 Scm^{-1} can be obtained (Rodriguez, Grande and Otero, 1997). In addition, it was also found that the quality of the films obtained deteriorated with the presence of nucleophiles during polymerisation. Water itself can act as a nucleophile, attacking the pyrrole ring to form carboxyl groups that break down the polymer chain, thereby causing a decrease in conductivity with adverse effect on mechanical properties (Wallace, Spinks, Kane-Maguire and Teasdale, 2003). It was shown that the presence of small amounts of water affected the rate of growth and polymer conductivity.

Mechanical properties

It is recognised by researchers that the mechanical properties of PPys vary widely from strong, tenacious materials to extremely brittle ones. As a consequence, it is necessary to understand how the mechanical properties are affected by the chemical structure, processing conditions and the conditions of use. It is apparent that the composition of polymer and the polymerisation conditions have significant effects on the polymer properties (Wallace, Spinks, Kane-Maguire and Teasdale, 2003).

Lower polymerisation temperature has been observed to have a significant improvement of the mechanical properties including tensile strength and elongation to break of PPy films (Wallace, Spinks, Kane-Maguire and Teasdale, 2003). There are many other factors that affect the mechanical properties apart from synthesis temperature, such as density, solvent used during polymerisation, types of counterion used, molecular weight of the PPy, crosslinking, degree of molecular order and environmental effects.

Chemical properties

The chemical properties of the resultant structure determine the sensing ability of the PPy-coated textiles to respond to stimuli appropriately. In addition, these properties determine how the conducting polymer interacts with other materials in the construction of intelligent textile composite.

PPys are inherently versatile molecular structures capable of undergoing many interactions such as PPy/Cl, PPy/dodecylsulphate (PPy/DS) and PPy/polyacrylic acid (Shirota, 1997). Most particularly, they are strong anion exchangers that are also capable of undergoing hydrophobic interactions. Other ion exchange groups such as carboxyl groups or self-doping sulphonate groups can be interacted with the monomer prior to polymerisation in order to modify the resultant properties. Hence, there are many parameters that may affect the chemical properties of PPy by incorporating a range of chemically functional counterions into PPys. The fact that pyrrole can be polymerised from aqueous solutions enables a wide range of counterions to be included in the structure.

All forms of PPy have low crystallinity (Nowak, 1995). Although polymerisation occurs at the α-carbons, Nuclear Magnetic Resonance technique indicate the involvement of β-carbons in the bonding which may denote the presence of branching. The most widely accepted spatial orientation of pyrrole moieties along the main chain of ideally α- α couple PPy is the one pyrrole units alternate in a planar arrangement. Thieblemont *et al.* pointed out that the desired polymerisation process was α-α coupling of oxidised pyrrole units to give an ideal polymer chain (Thieblemont, Gabelle and Planche, 1994; Thieblemont, Planche, Petrescu, Bouvier and Bidan, 1994). However, similar to other polymers, PPy contains abundant defects. Figure 2.19 shows the ideal PPy chain and the possible reaction ways for pyrrole-pyrrole linkages in PPy generation (Rodriguez, Grande and Otero, 1997). Diffraction patterns indicate poly (β, β'-dimethylpyrrole) packs with the chains oriented parallel to each other; whereas PPy chains are aligned at random (Street, 1986). The results proved the existence of various reaction ways for pyrrole-pyrrole linkages in PPy chain.

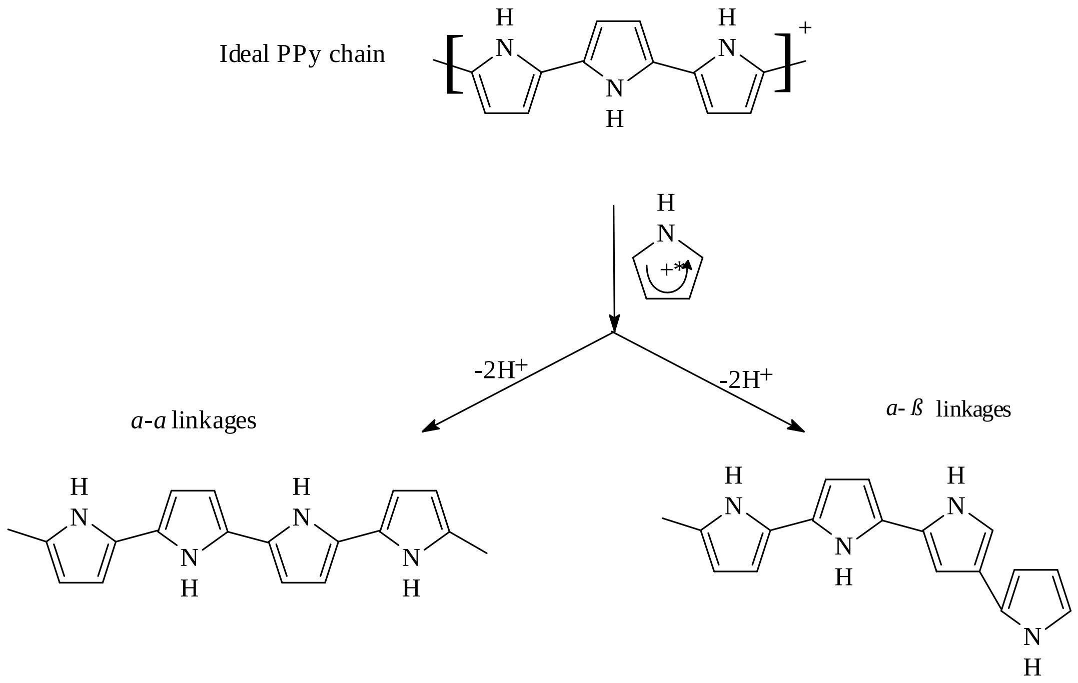

Figure 2.19 Possible reaction ways for pyrrole-pyrrole linkages in PPy generation (Rodriguez, Grande and Otero, 1997)

2.3 Instability of PPy Films

The electronic conductivity of PPy is ascribed to electrons hopping along and across polymer chains with conjugated double bonds (Liu and Hwang, 2001). As the mobility or number of the charges varies, the conductivity is changed. The theoretical mechanism of the mobility in PPys is still not fully understood, it was claimed that the factors affected the conductivity of PPys were the conjugation length of polymer chains and the distances between inter-chains (Gustafsson, Inganas, Nilsson and Liedberg, 1988). Wang and Rubner (1990) summarised two major factors that determined the length of polymer chain which thus affected the stability of conducting polymer. They were either intrinsic or extrinsic in nature. Intrinsic instability is mainly related to the conformation changes in the polymer backbone that are activated at the thermal annealing process.

External environment including water vapour and oxygen may also affect the conductivity stability which is called "Extrinsic instability" (Billingham, Calvert, Foot and Mohammad, 1987; Inganas and Salaneck, 1985; Samuelson and Druy, 1986). It is believed that the instability of PPy in ambient condition is due to the reaction of the polymer backbone with oxygen and/or water and/or damaging radiation leading to an irreversible loss of conjugation and conductivity (Cheah, Forsyth and Truong, 1998; Cheah, Forsyth, Truong and Olsson-Jacques, 1997; Chen, Devaux, Issi and Billaud, 1994; Child and Kuhn, 1997; Kuhn, Child and Kimbrell, 1995; Liu and Hwang, 2001; Thieblemont, Brun, Marty, Planche and Calo, 1995; Wang and Rubner, 1991). Literature also found that the reaction of PPy with water might affect the stability more seriously (Liu and Hwang, 2001; Thieblemont, Gabelle and Planche, 1994; Thieblemont, Planche, Petrescu, Bouvier and Bidan, 1994). Since the oxygen and hydrogen may react with the nitrogen and carbon in the PPy polymer chain, this may open the aromatic ring, shorten the PPy polymer chains and degrade conductivity consequently.

There are two major mechanisms postulated, i.e. the reactions of PPys with oxygen and/or water attacking at the α and β positions of pyrrole unit. Gustafsson *et al.* proposed that the hydroxide ion (OH^-) attack at the β-position on the pyrrole unit is one of the most important solution degradation reactions (Gustafsson, Lundstrom, Liedberg, Wu and Wennerstrom, 1989). The oxidised polymer chains may undergo nucleophilic attack by the oxygen nucleophilic species of the surrounding polymerisation media giving C-O bonds. Oxidation and phototropic processes may transform C-O bonds into C=O bonds. Figures 2.20 and 2.21 show the possible degradation mechanisms that explain the formation of a carboxyl group and as a result shortening the polymer chain (Chen, Devaux, Issi and Billaud, 1994). This chemical reaction between polymer chain and oxygen, water or damaging radiation causes the formation of carboxyl, ester or hydroxyl groups, thereby leading to the reduction of positive charge carriers on the polymer chain (Billingham, Calvert, Foot and Mohammad, 1987).

Another mechanism proposed that the hydroxide ion might attack the α-position of the pyrrole unit causing disrupt conjugation (Cheung and Stevens, 1988). This nucleophilic attack and pyrrole ring opening mechanism have been proposed by Otero, Tejada and Elola (1987) as an explanation for the degradation of PPy at the anodic potentials in aqueous solutions. The absorption of water molecules also occurs on the N^+ of the polymeric backbone via hydrogen bonds. Liu and Hwang (2001) observed that two kinds of adsorbed water, fixed and removable water, exist after the reaction between PPy and water as shown in Figure 2.22. The fixed water is bond to the N+ of PPy by hydrogen bonds, and is designated as chemisorbed water while the removable water is attached to the fixed or the removable water by hydrogen bonds, and is designated as physisorbed water.

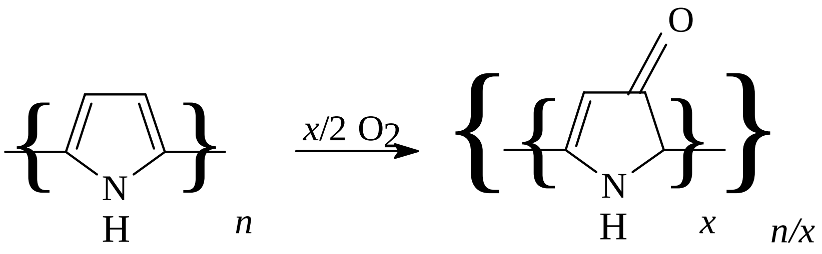

Figure 2.20 A possible degradation mechanism of PPy by oxygen attack (Chen, Devaux, Issi and Billaud, 1994)

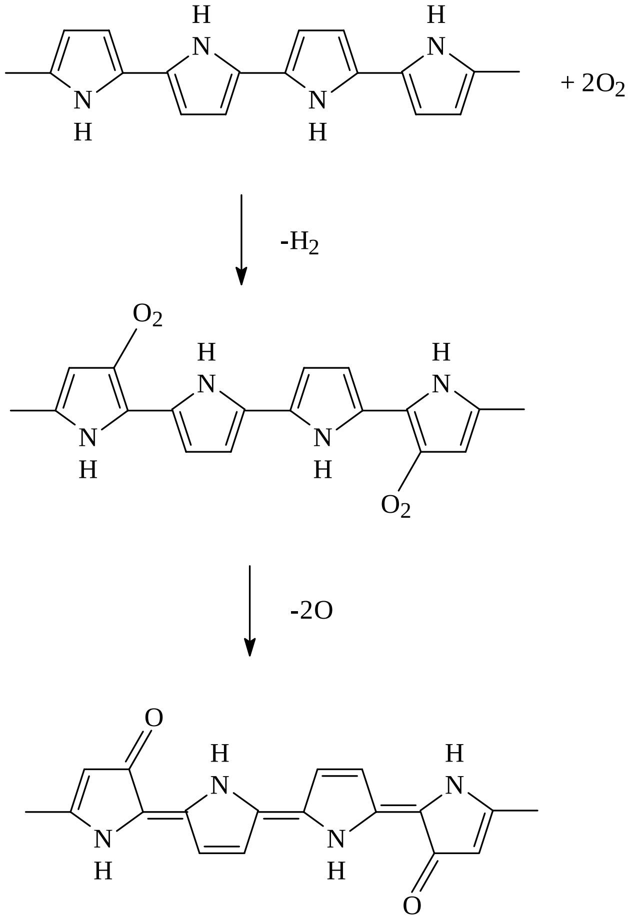

Figure 2.21 Chemical structure degradation of PPy in air (Chen, Devaux, Issi and Billaud, 1994)

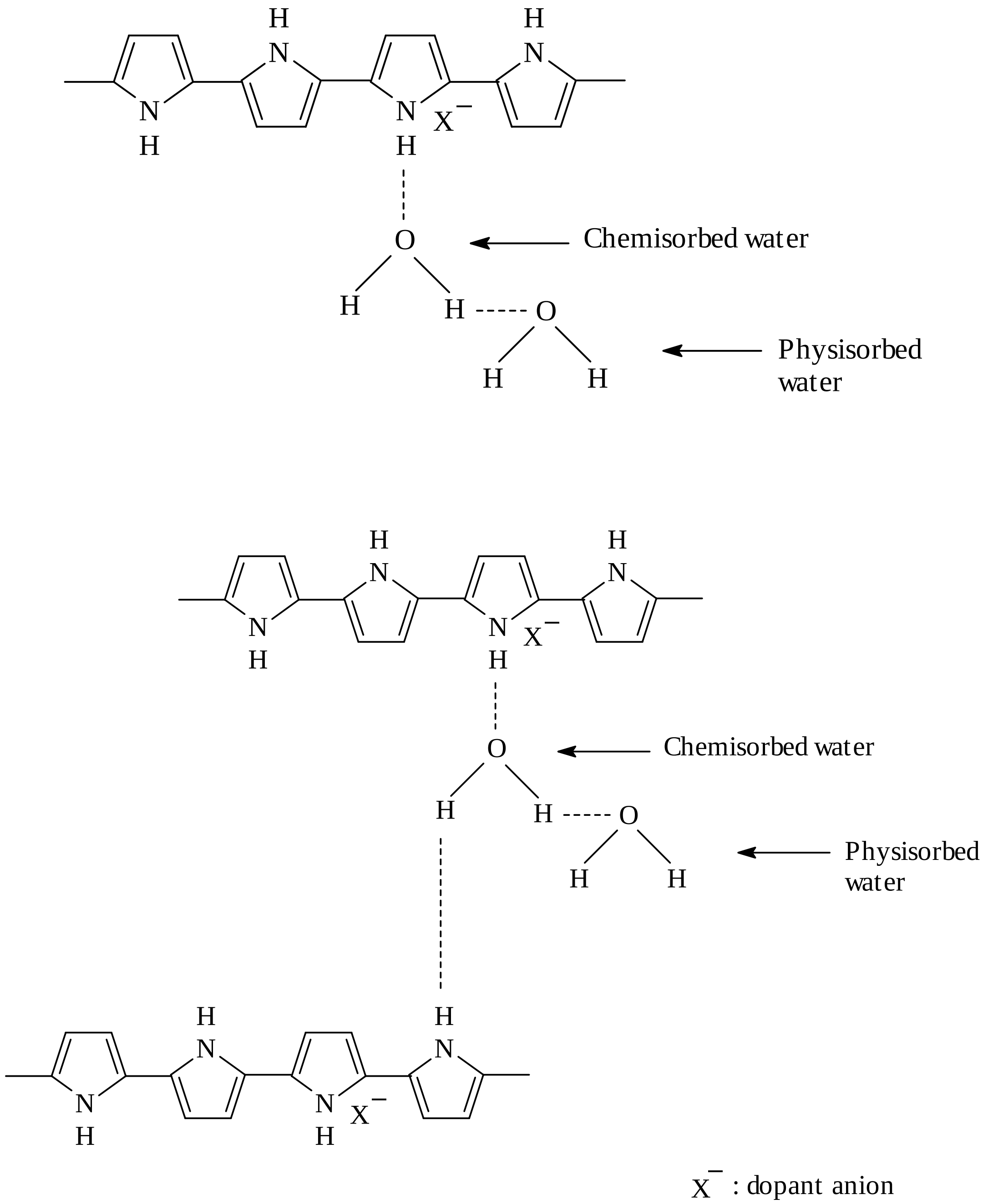

Figure 2.22 The interaction between PPy and fixed and removable water (Liu and Hwang, 2001)

Chen, Devaux, Issi and Billaud (1994) conducted a comparative study on the degradation of PPy and discovered that the conductivity of PPy decreased very fast when exposed to air, but was stable at 200°C under an argon atmosphere. It confirmed that oxygen caused extrinsic instability of PPy films. Liu and Hwang (2001) examined the amount of N^+/N ratio of aged samples and Kuhn, Child and Kimbrell (1995) studied the amount of carboxyl functionality after the ageing of PPy coated fabrics by X-ray photoelectron spectroscopy (XPS) analysis. They found that there was a large increase of oxygen content in the aged samples which supported the degradation mechanisms based on the atmospheric oxidation. This indicated that the rate of degradation would be related to the oxygen concentration within the PPy film. The authors also explained the conductivity loss through two subsequent steps, i.e. the diffusion of oxygen into the film, and the reaction of the oxygen with the PPy backbone.

Munstedt (1988) claimed that there was no chemical mean to obtain conducting polymers which were completely stable in air. The mechanism of diffusion of oxygen in air through the polymer was also reported (Chen, Devaux, Issi and Billaud, 1994; Ennis and Truong, 1993; Kuhn, Child and Kimbrell, 1995; Liu and Hwang, 2001), which stated that the diffusion coefficient increased with the relative humidity of the air. This mechanism is more active for chemically polymerised PPy owing to the larger surface area of the polymer particles (Chen, Devaux, Issi and Billaud, 1994). Besides the coefficient of air humidity, the amount of oxygen absorbed by the films and the time were proportional to the degradation of PPy films in terms of the reduced conductivity decay according to the findings of Ennis and Truong (1993).

The effect of alkali treatment on the stability of PPy film was studied (Cheah, Forsyth and Truong, 1998; Neoh, Young, Kang and Tan, 1997). It was observed that prolonged alkali treatment could lead to polymer ring oxidation and ion exchange between PPy and OH^- at the initial stage, giving rise to the formation of covalent bonds such as C-O and C=O. These covalent bonds may bind the hydroxyl ion to the pyrrole structure, and therefore shorten the conjugation length. The reactions causing conductivity instability are only in the initial stages because the PPy can be stablised after reaching the equilibrium.

Besides the intrinsic and extrinsic instability mechanisms, the thickness and surface morphology of the PPy films prepared will affect intrinsic or extrinsic instability. Wang and Rubner (1991) compared their results with Munstedt and found that the influence of film thickness on the stability was also significant. The thickness of their benzenesulphonate doped PPy film was one third of that of Munstedt with the same treatments. It revealed that thicker samples were 5 times more stable, i.e. without significant decrease in conductivity when stored in ambient conditions.

A study of PPy surface morphologies by Liu and Hwang (2001) revealed that a more porous morphology and larger specific surface facilitated the diffusion of attacking gas into the film. The surface morphology effects of PPy on poly(etheretherketone) (PEEK) and poly(methylmethacrylate) (PMMA) was investigated (Guernion, Ewen, Pihlainen, Ratcliffe and Teare, 2002). The authors found that smooth surface layer of PPy film on PEEK presented approximately three times more stable over time than the rougher surface of PPy coated on PMMA. The morphology of PPy may be affected by the dopant applied, solvent, and the condition of polymerisation such as applied voltage, concentration of chemicals, and reaction temperature.

2.4 Methods for Stabilising PPy Coating

Since late 80s, a considerable number of researches have studied the mechanism of the degradation of PPy as discussed in Section 2.3. A higher conjugation and doping level in the polymer backbone were the desirable characteristics of PPy film with a higher molar mass. The stability can be enhanced due to the decrease in the permeability of the PPy films to oxygen and water, and hence retarded oxidation. Long deposition time, lower applied potential, low reaction temperature, and higher concentrations of monomer and electrolyte are favourable for the conductivity and stability (Rodriguez, Grande and Otero, 1997). Furthermore, researchers also proposed that encapsulation could be used to enhance stability (Kuhn, Child and Kimbrell, 1995). When the extrinsic instability is dominant, it is possible to encapsulate the polymer with appropriate barrier materials (Samuelson and Druy, 1986), or prepare denser morphologies (Bloor, Hercliff, Galiotis and Young, 1985), both of which inhibit diffusion of chemical agents to the active sites within the polymer. In addition, enhanced stability could be achieved through treatment with simple acids and alkalis (Cheah, Forsyth, Truong and Olsson-Jacques, 1997) as well as with addition of dopants (Cassignol, Olivier and Ricard, 1998).

2.4.1 Dopants and small size anions

The applications of dopant on the morphology of PPy films had been discussed by Salmon, Diaz, Logan, Krounbi and Bargon (1982). More porous morphology films with smaller sized dopants were found to be responsible for the relative instability of the films. The Anthraquinone-2-sulfonic acid (AQSA) doped film was much more stable, due to the smoother and denser film formed, which thus inhibited oxygen penetration. AQSA doped PPy films exhibited superior conductivity and stability to others.

Munstedt (1988) studied the ageing of benzenesulfonate and perchlorate doped PPy and demonstrated that the dopants could improve the intrinsic stability of PPy films. Other researchers found that the PPy polymer doped with aromatic anions (p-toluene sulphonate and p-chlorobenzene sulphonate) exhibit better stability and higher electrical conductivity (Kim, Lee, Moon and Kim, 1995; Truong, Ennis, Turner and Jenden, 1992; Turcu, Neamtu and Brie, 1993). Furthermore, Kim, Lee, Moon and Kim (1995) explored that the polymer doped with 0.01M of hydroquinone in the system, the conjugation length was frozen even after 1200 redox cycles according to the results of UV-visible and Raman spectroscopy.

The application of dopants on the stabilisation of PPy films may be explained as follows. Firstly, the carbonium chains doped with counter-anions balance the charge on the PPy chains and thus reduce the opportunities for oxygen to attack C or N in the PPy chain. Secondly, dopants can affect the morphology of PPy films. It is believed that a denser and smoother surface morphology can inhibit the oxygen attack on the PPy chains.

2.4.2 Acid and alkali treatments

Cheak, Forsyth and Truong (1998) showed that the stability of PPy could be improved by acid and alkali treatments. The concentration of the solution, temperature and duration time are the parameters that affect the degree of stabilisation. Increasing the treatment temperature can accelerate the exchange of the counterion. PPy films treated at a high temperature decay more slowly and have higher residual conductivity (Truong, Ennis and Forsyth, 1995). In addition, it was found that the alkali treatment could provide the best stability because of the OH^- blocking the reactive sites for oxygen and water. However, the alkali treatment of the PPy films might result in the deprotonation of the pyrrole structure leading to the loss of conductivity (>40%) at the initial stage (Cheah, Forsyth, Truong and Olsson-Jacques, 1997). The authors also explained that higher stability could be achieved through longer treatment times but at the expense of conductivity. It was, however, important to note that the initial alkali treatment had already resulted in the significant loss of conductivity. Hence, the stability observed for the sample during thermal ageing could be the result of the PPy film reaching an equilibrium stable state with respect to the chemical (structural) changes which affected the conductivity in the degradation process. These results agreed with Munstedt's assumption that the improved stability was the result of the OH^- blocking the reactive sites for oxygen and water.

Apart from the alkali treatment, many investigations of PPy doped with various protonic acids were conducted (Oh, Park and Kim, 2004). It was found that both HCl and sulphonic acid were the best dopants in terms of conductivity and stability. This was due to the fact that the inter-chain interaction, protonation of the pyrrole structure (Cheah, Forsyth, Truong and Olsson-Jacques, 1997) and the conformation of conducting polymer were varied by the change of chemical structure and the charge transfer with dopants. These also affected the conductivity and the thermal stability of the PPy film.

Munstedt (1988) reported an increase in long term stability for PPy films treated with sulphuric acid (H_2SO_4) and sodium hydroxide (NaOH) at elevated temperatures (80°C and 140°C). The enhanced stability was attributed to the decrease in permeability of the PPy films to oxygen and water. He revealed the improved stability of the treated film which could retain up to 70% of its initial conductivity after 100 days at 140°C. Cheah, Forsyth, Truong and Olsson-Jacques (1997) conducted the XPS of PPy film. Their results indicated that both acid and alkali treatments resulted in the elimination of reactive sites for oxygen. An increase in the C-Ox species was observed in both acid and alkali treated samples, which could be the result of the elimination of reactive sites in the PPy structure.

2.4.3 Thermal annealing

Wang and Rubner (1991) heated the PPy samples at 120°C for 24 hours and then cooled to room temperature. It was found that the conductivity was increased after the heat treatment and the conductivity increment was due to annealing effects resulting in the improvement of the local ordering within the PPy films. The thermal annealing also induced a decrease of defect concentration, thereby increasing the conjugation length of the PPy films (Turcu, Neamtu and Brie, 1993). It was pointed out the initial stage of annealing could cause the restructuring of the PPy polymers (Singh, Narula, Tandon, Rao, Panwar, Mansingh and Chandra, 1996). This might be partly due to the evaporation of residual solvent. The solvent plays an important role in the specific salvation process which stabilises the π segments along the polymer chain, thereby reordering the polymer chain with annealing. Large numbers of voids and pores were observed in scanning electron microscopy micrographs with increasing annealing time which might hinder the path of conducting channels and thus decrease the conductivity. The cauliflower structure was totally disappeared after annealing the PPy films and poly(N-methylpyrrole-pyrrole) [P(NMPY-PY)] for 29 and 39 hours. No change in the conductivity was observed, indicating that a complete ordering of the polymeric chain occurred. It appeared that the ordering of the polymeric chain was a crucial factor in the determination of conductivity.

2.4.4 Addition of large size anion

PPy films doped with large organic anion dodecylbenzenesulphonate (DBS) were studied by Gao and Tian (1995). The results revealed that the stability of PPy film could be enhanced due to the remaining of DBS ions inside the PPy films instead of doping and undoping of small anion freely inside the PPy films during the redox process. Therefore, the negative charges inside the PPy films had to be compensated by the incorporation of cations such as Na^+ or H^+ from the DBS solution.

2.4.5 Application of E-field

It is believed that the structure of PPy film can be changed by applying a high voltage at polymerisation. Onyang and Li (1995) found that a 65% and 47% increase in conductivity of the film doped with TsO^- and NO_3^- respectively after applying a higher voltage to the film. The PPy(TsO^-) film remained stable but the PPy(NO_3^-) dropped back to its original value quickly after the treatments. The results indicated that the counter-anions played an important role in the increase of conductivity by applying higher voltage. As proposed by the authors, the doped counter-anions are used for balancing the charges on the chains inside the PPy films. When a voltage is applied to the films, the electric field is set up between the two electrodes on which the voltage is applied. The counter-anions doped in the film will tend to move under the electric field. When the applied voltage is high enough, the counter-anions move to a quasi-stable, higher-energy position. At this time, the chain structure of the film changes and its conductivity increases. After removing the voltage, the quasi-stable structure may relax. Due to its larger size, the relaxation of the TsO^- counter-anion is more difficult when compared with NO_3^- and BF_4^-. Hence, the higher conductivity state after the voltage treatment remains for a longer period for the $PPy(TsO^-)$ film.

Apart from the single way of voltage applied, cyclic redox reaction of PPy between potentials of -0.9V and +0.3V was reported by Kim, Lee, Moon and Kim (1995). The conjugation length was shortened just in one cycle of redox reaction. The shortening of conjugation length in one redox cycle might be caused by the conformational changes from trans to gauche in structure. No shift was found of the conductivity after 1200 cycles of the redox reaction.

2.4.6 Others

The PPy film thickness and layer structure might attribute to the stability of conductivity (Munstedt, 1988). Rupprecht (1999) found that the thicker the PPy film (100 microns from 4 & 35 microns) the more stable the conductivity on the thermal treatment at 200°C. Truong, Ennis and Forsyth (1995) claimed that thicker films showed better stabilisation as the rate of decay was slower and the loss of conductivity was smaller. They stated that the layered structure might be useful in understanding the stabilisation. It was suggested that as the outer layers are oxidised, the average conductivity of the affected region will be decreased. A barrier to oxygen diffusion at the outer boundaries is formed and at the same time the oxygen permeability of the material is decreased and the rate of conductivity decay is reduced. Ultimately, the stage is reached where the oxidised outer skin protects the pristine core from further oxidation. They called “self-stabilisation” of thick PPy/ p-toluene sulphonate films.

Apart from addition of organic dopants, Liu and Hwang (2001) investigated the modification of by metal iron. Cu(I) was used to enhance the conductivity and stability of PPy. The reason arises from the deposition of Cu(I) onto PPy, mainly on the N^+. Consequently, the original N^+ is stabilised in the Cu-PPy complex. Cu-PPy composite can also exhibits a less porous structure morphology films. Since a more porous morphology and larger specific surface facilitate the attacking gas diffusing into the films, Cu-modified PPy may contribute the relative stability from the view point of the decrease in permeability of the PPy film to water.

Moss (1992) explored different kinds of stabiliser coating on the pores of the polymers and thus protecting the surface against oxidative attack. It revealed that the Irganox 1010TM (primary stabiliser) and Irgafos 168TM (secondary stabiliser) combination would inhibit the degradation of PPy to the highest extent incorporating both high temperature processing stability and long term low temperature stability.

2.5 Textile Fabrics with PPy Coating

Textiles have been claimed as an ideal substrate for conducting polymer because of their high surface area, wide range of mechanical properties, high flexibility, and large-scale availability (Kuhn and Child, 1998). The Milliken Research Corporation is the front-runner investigating the application of PPys coated textile materials. Various fabrication methods including electro-chemical polymerisation, situ polymerisation and chemical deposition of PPy on various types of yarn and fabric structures have been studied (Gregory, Kimbrell and Kuhn, 1989, 1991; Kuhn, 1993; Kuhn, 1997; Kuhn and Child, 1998; Kuhn, Child and Kimbrell, 1995; Rodriguez, Grande and Otero, 1997). PPy-coated substrates can produce conductive materials with different levels of surface resistance and suitability for different applications.

One of the most important considerations for using the PPy-coated materials is the environmental instability of the polymer. As discussed in Section 2.4, considerable efforts have been made to stabilise the conductivity of the PPy-films over the past few decades. These approaches can be considered for PPy-coated fabrics.

Child A. D. of Milliken Research Corporation investigated the stabilisation method for PPy-coated textile in the late 90s (Child, 1998, 1998b). Addition of DHBP was introduced for stability enhancement. This additive did not serve as dopant, but was used in conjunction with aryl sulphonate dopants. The sample containing DHBP displayed an initial increase in conductivity, and then a slower decrease when compared with the control sample without the dopant. The control lost nearly 50% of its initial conductivity, whereas the sample of the invention of dopant applied lost only 11% of its initial conductivity after 60 hours. Child stated that the addition of the specific dopant might cause (i) variation in the morphology of the conducting polymer film and (ii) the increased order of the polymer by the additive during thermal ageing.

An encapsulating barrier coating, such as polyvinylidene chloride and AQSA, specifically for oxygen was recommended for improving the stability of the PPy coated fabrics (Child and Kuhn, 1997; Kuhn, Child and Kimbrell, 1995). The most stable fabric that Child and Kuhn (1994) encapsulated had a room temperature half-life of approximately five years.

A number of researchers other than Milliken Research Corporation had investigated the stabilisation of PPy-coated textiles. Thieblemont, Planche, Petrescu and Bouvier (1993) found that PPy doped with 2-naphthalenesulfonate was more stable than those doped with the usual p-toluene sulphonate . Kim *et al.* revealed that PET fabric/PPy composites prepared by only chemical polymerisation had more serious conductivity decay than the composites prepared by electro-chemical polymerisation (Kim, Kim, Byun, Jeong, Hong, Joo, Song, Kim, Lee and Lee, 2002). It was claimed that dense structure of PPy coating formed by electro-chemical polymerisation are more defensive to attack by oxygen, resulting in much better environmental stability. Furthermore, they also found that PPy-Nylon 6 composite fabrics prepared by electro-chemical polymerisation on chemical polymerisation possessed a higher stability in their conductivity when compared with those prepared by chemical polymerisation only. The conductivity of electro-chemical polymerisation on the chemical polymerisation composite had an almost constant value at 180°C for 600 mins (Kim, Jang, Byun, Lee, Joo, Jeong and Park, 2003).

Crowley & Cassidy (2003) reported that smoother morphology could be produced by doping with larger anionic species such as PPy/DS and PPy/DBS when compared with the cauliflower-like appearance of PPy/Cl^{-} or PPy/ClO_4^{-} films.

For fabricating the conductive fibres and fabrics, Harlin, Nousiainen, Puolakka, Pelto and Sarlin (2005) explored a new method of in-situ chemical polymerisation using supercritical carbon dioxide aided process. PPy-Polyamide (PA6) fabrics produced can afford 10 times of washing. It was also reported that PPy was mainly inside the fibre as the supercritical carbon dioxide could swell the structure of the fibre and open the way for the monomer to penetrate into the polymer.

2.6 Study of Electro-mechanical Properties of Conductive Fabrics

Electro-mechanical properties, crucial for the sensor development, have been extensively investigated by the research team of The Hong Kong Polytechnic University, including PPy-coated fibres, PPy-coated woven fabric and intrinsically conductive knitted textiles. The theoretical studies on mechanisms are reviewed as follows.

2.6.1 PPy-coated fibres

Electro-mechanical and morphological studies on PPy-coated PA6 and polyurethane (PU) fibres have been reported (Xue, Tao, Kwok and Leung, 2004). It has been found that the electro-mechanical behaviour of the conductive fabrics depends strongly on the microstructure of the coating layer, the material of the substrate, as well as textile structures. On PA6 fibres, PPy forms a continuous layer with finer, denser, and more uniform grains than those on the PU fibres. A smooth and uniform coating and matched mechanical properties will lead to a satisfied performance of conductive fibre sensors.

The R/R_o calculated from the change in the dimension of the sample by using the following equation:

$$R = \rho \frac{L_o}{A_o} \frac{(1+\varepsilon)}{(1-\nu\varepsilon)^2} \tag{2.1}$$

or

$$\frac{R}{R_o} = \frac{(1+\varepsilon)}{(1-\nu\varepsilon)^2} \tag{2.2}$$

where R is the electrical resistance of PPy-coated fibres when elongated. R_o is the initial electrical resistance equal to $\rho_o \frac{L_o}{A_o}$. ρ_o, L_o and A_o is the resistivity, length and area of the material. ν is the Poisson's ratio of PPy-coated fibres when elongated along their longitudinal direction. ε is the strain applied along the longitudinal direction of the fibre.

Figure 2.23 compared the predictions from Equation 2.2 and measured values of R/R_o versus strain of PPy-coated PA6 and PPy-coated PU fibres respectively. For the PPy-coated PA6 fibres, the dimensional change due to tension is the main cause of the resistance variation, especially when the applied strain is not large as shown in Figure 2.23 (a). In contrast, the resistance variation with applied strain for PPy-coated PU fibres is mainly attributed to damage to the coating layer as shown in Figures 2.23 (b) and 2.24.

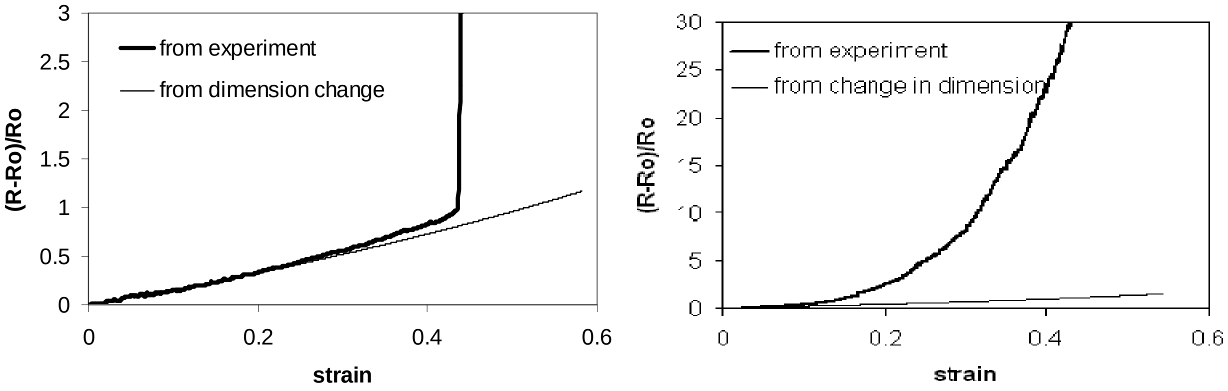

(a) (b)

Figure 2.23 Comparison of the calculated (Equation 2.2) and measured values of R/R_o for (a) PPy-coated PA6 fibres and (b) PPy-coated PU fibres

The Young's modulus of the PA6 fibre is much larger than PU fibre. In fact, under the same level of the applied stress, the PPy-coated PU fibre will experience much larger deformation than the PPy –coated PA6 fibre. A larger strain must result in higher strain energy. It is the surface cracks that release the large strain energy stored in the PPy-coated PU fibre. The steady-state energy release rate, G_c, is given as (Beuth, 1992; Chen, Cotterell and Wang, 2002):

$$G_c = \frac{1}{2}\bar{E}_f \varepsilon^2 \pi h_f g(\alpha,\beta) \qquad (2.3)$$

The factor $g(\alpha,\beta)$ is a function of the Dundurs parameters, α and β, which for plane strain condition are give by:

$$\alpha = \frac{\bar{E}_f - \bar{E}_s}{\bar{E}_f + \bar{E}_s} \quad , \qquad \beta = \frac{G_f(1-2\upsilon_s) - G_s(1-2\upsilon_f)}{2G_f(1-\upsilon_s) + 2G_s(1+\upsilon_f)'} \tag{2.4}$$

Where E is the plane strain tensile modulus and G is the shear modulus. The subscripts, f and s, stand for the coating film and substrate, respectively. Of these two parameters, α is much more important. Restricting β to the practical limits of β=0 or β= α /4, the function, g, will increase with parameter α. Therefore, the larger difference between Young’s moduli of the coating film and the substrate will lead to easy cracking.

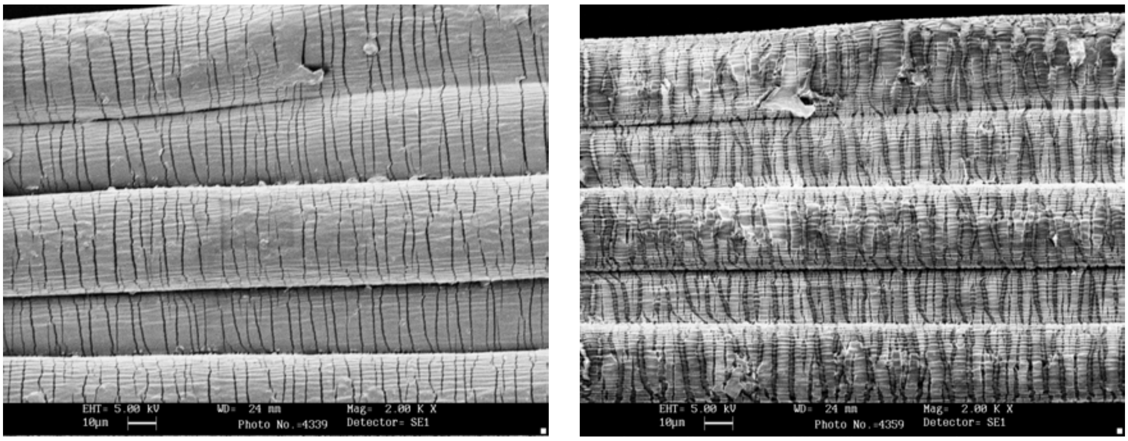

(a) ε=3.8%　　　　(b) ε=30%

Figure 2.24 SEM microphotographs of PPy-coated PU yarn at different strain level

The phenomenological electro-mechanical model has been developed that correlates the resistance change to applied strain, the damage level of the fibres, and the temperature and relative humidity, which provides a theoretical basis for the analysis and design of electrically conductive fabrics. Based on the experimental results and

Ohm’s law, the electro-mechanical model of the PPy-coated PA6 fibres can be expressed by:

$$\frac{R}{R_o} = \frac{\rho}{\rho_o}(1+\varepsilon)(1+2\nu\varepsilon+3\nu^2\varepsilon^2)\left(\frac{1.82}{1+e^{0.077\dot{\varepsilon}/\dot{\varepsilon}_{re}}}\right)\cdot \left[0.06\left(\frac{T}{T_{re}}\right)^2 - 0.31\left(\frac{T}{T_{re}}\right)+1.34\right]\cdot\left[0.616\left(\frac{RH}{RH_{re}}\right)+0.416\right] \quad (2.5)$$

where ε is the strain applied along the longitudinal direction of the fibre, $\acute{\varepsilon}$ is the strain rate, *T* is the temperature, and *RH* is the relative humidity, ρ is the resistivity of the material and υ is the Poisson’s ratio. $\acute{\varepsilon}_{re}$, T_{re} *and* RH_{re} are the reference strain rate, the reference temperature, and the reference relative humidity, respectively.

2.6.2 Conductive woven fabrics

The electro-mechanical properties of a conductive fabric not only depend on the materials used, but on the structure of the fabric. A model was proposed for PPy-coated plain weave fabric under unidirectional tension (Xue, Tao, Leung and Zhang, 2005). The authors represented a plain weave fabric coated with conducting polymer by an electrical network as illustrated in Figure 2.25. If the variations of yarn and structural evenness are ignored, the resultant total resistance of a plain weave fabric can be simply expressed as:

Warp direction: $R_v = \dfrac{\eta(1+C_v)(N_p-1)}{N_e}$ (2.6)

Weft direction: $R_h = \dfrac{\eta(1+C_h)(N_e-1)}{N_p}$ (2.7) where R_v, R_h are the equivalent resultant resistance of the fabric measured in the warp and weft directions, respectively; N_p is the number of picks per fabric length and N_e is the number of ends per width; η is the resistance of yarn per unit length of yarn; C_v and C_h are the crimps of the weave in the warp and weft directions, respectively.

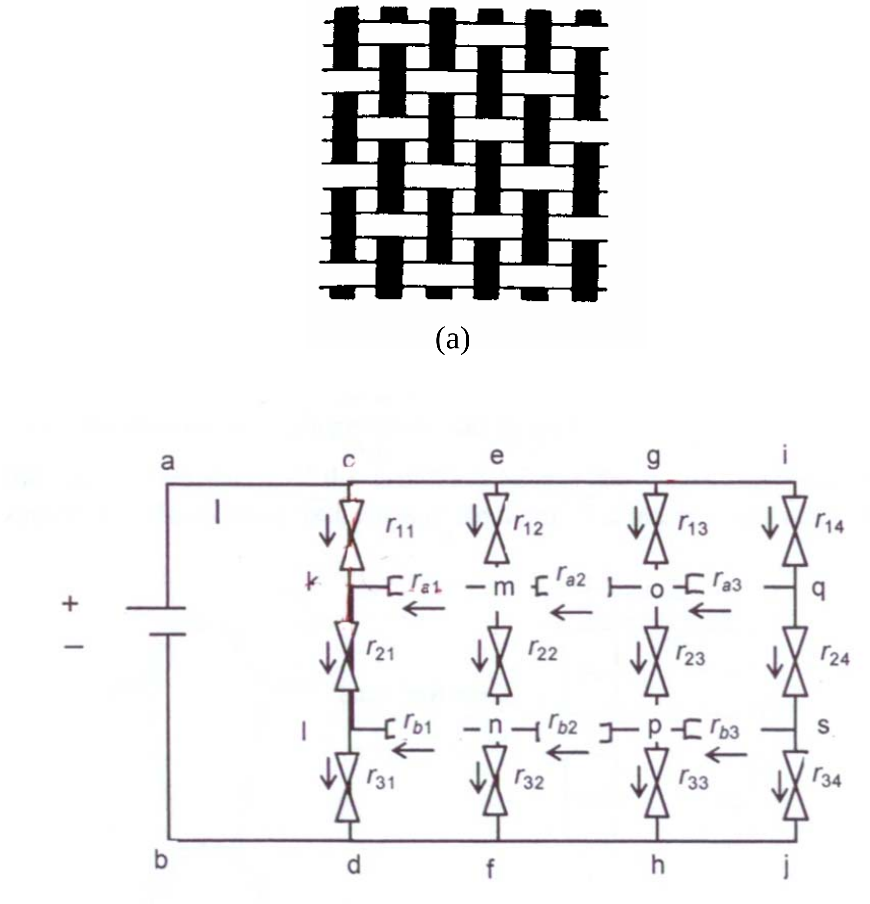

(a)

(b)

Figure 2.25 (a) Plain weave fabric structure and (b) electrical network representing a segment of the conductive woven fabric (Xue, Tao, Leung and Zhang, 2005)

During the unidirectional tensile deformation (for example in the warp direction), the change in the resistance of the fabric can be expressed as:

$$dR_v = \frac{(N_p - 1)(1 + C_v)}{N_e} d\eta + \frac{(N_p - 1)\eta}{N_e} dC_v + \frac{\eta(1 + C_v)}{N_e} dN_p - \frac{\eta(N_p - 1)(1 + C_v)}{N_e^2} dN_e \tag{2.8}$$

It can be seen that the change in resistance under large deformation comes from contributions of the yarn and from the geometrical change in the structure of the fabric during tensile deformation, such as change in the crimp of the weave and changes in the densities of the pick and end.

2.6.3 Conductive knitted fabrics

An electrically conductive knitted fabric can be depicted as a circuit network, as shown in Figure 2.26 (Zhang, Tao, Wang and Yu, 2005). The authors proposed a two-dimensional hexagon model was used to represent the loop configurations. The intrinsic resistance of the yarn and the contact resistance both contribute to the electrical properties of the fabric. The resistance of the intrinsically conducting yarn was calculated by Ohm's law and the contact resistance was determined experimentally. The experimental setup for measuring the contact resistance and contact force is shown in Figure 2.27. The equivalent resistance of the fabric was then obtained based on the circuit network.

It was found that the contacting resistance at the overlapped points in the knitted fabric governed the change in resistance of stainless steel fabrics. The contacting resistance plays a very important role in the sensitivity of the intrinsically conductive knitted fabric sensor. The resistance of the fabric decreases as the fabric is stretched in either wale or course directions.

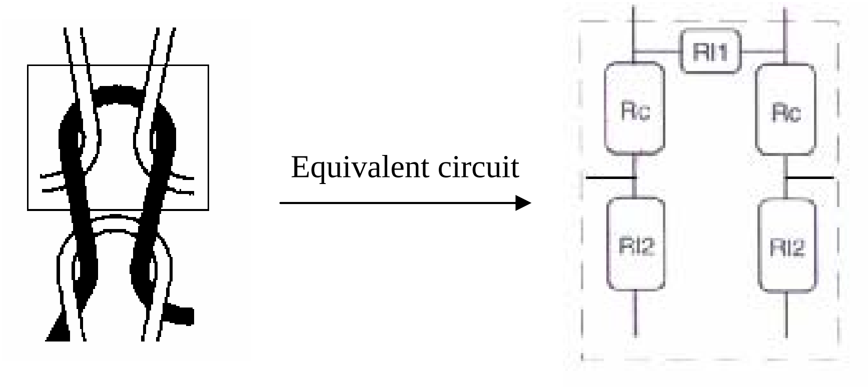

Figure 2.26 Circuit representing a unit loop of the conductive knitted fabric (Zhang, Tao, Wang and Yu, 2005)

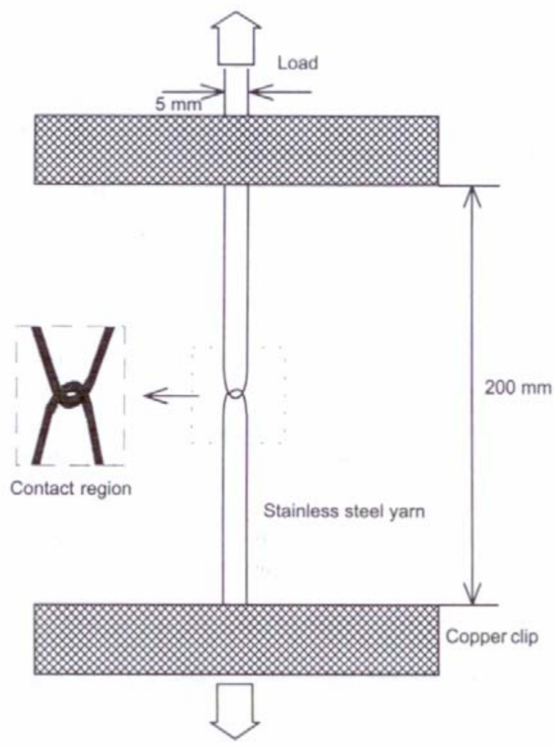

Figure 2.27 Experimental setup to measure the contact resistance and contact force at the overlapped point (Zhang, Tao, Wang and Yu, 2005)

2.7 Summary

Smart or intelligent textiles and apparel are the trend in recent years. Textile-oriented sensors have recently become the subject of great interest and significantly important to the market. Although there are numerous investigations of textile electrical sensors by other researchers, it is still lack of understanding of textile structure and interaction between conductive layer and substrates as well as the environmental stability of the sensors. It is evident that there is a need for comprehensive study of the fabrication parameters towards superior sensing performances and environmental stability, and the study of the interaction between the conducting polymer layer and various types of textile substrates of electrical textile sensors.

Different methods for stabilising the PPy films have been reviewed and discussed in this chapter. There are pros and cons of each method. Among all the stabilisation methods, some of them may not be applicable to textiles sensors. For examples, acid and alkali treatments may cause damages on the textile substrates and also lower the electrical conductivity dramatically that may not be suitable for sensor development. High voltage application during synthesis of PPy film may not be also applicable to conductive textile strain sensor development. It is because very thick layer of PPy film may be produced on the textile substrate which may not be beneficial for strain sensitivity. Therefore, large size anion application, thermal annealing, encapsulating barrier coating application and low temperature polymerisation are being planned to use for stabilising the PPy-coated fabrics in this research project.

Previous studies on mechanisms of the strain sensitivity of PPy-coated fibres, PPy-coated woven fabric and stainless steel conductive knitted fabric, have been reviewed. In this study, the mechanisms of strain sensitivity of PPy-coated knitted fabrics fabricated under low temperature polymerisation will be further investigated.

CHAPTER 3

STABILISATION OF POLYPYRROLE-COATED FABRIC STRAIN SENSORS

3.1 Introduction

Review of literatures in Chapter 2 indicates that there are still many unsolved problems concerning the PPy-coated fibres and fabrics as strain sensors. The most important considerations for using the PPy-coated fabric as a strain sensor are their conductivity, strain sensitivity and environmental stability. Over the past few decades, considerable efforts have been made to stabilise conductivity of PPy films (Billingham, Calvert, Foot and Mohammad, 1987; Cheah, Forsyth and Truong, 1998; Cheah, Forsyth, Truong and Olsson-Jacques, 1997; Chen, Zhang, Wang and Shi, 2003; Chen, Devaux, Issi and Billaud, 1994; Munstedt, 1986, 1988; Neoh, Young, Kang and Tan, 1997; Omastova, Kosina, Pionteck, Janke and Pavlinec, 1996; Thieblemont, Planche, Petrescu and Bouvier, 1993; Truong, Ennis, Turner and Jenden, 1992) or PPy-coated materials (Child, 1998a, 1998b; Child and Kuhn, 1994, 1997; Kim, Lee, Moon and Kim, 1995; Kim, Kim, Byun, Jeong, Hong, Joo, Song, Kim, Lee and Lee, 2002; Omastova, Pavlinec, Pionteck and Simon, 1997). Hitherto, the effects of PPy degradation on the strain sensitivity of PPy-coated fabric sensor have not been studied in detail. On the other hand, the highest strain sensitivity achieved was 15 at 1.5% of fabric strain (De Rossi, Della Santa and Mazzoldi, 1997).

Very few publications have been found concerning the long-term environmental stability and the strain sensitivity of the PPy-coated fabrics.

In this chapter, three fabrication methods will be first examined, that is the conventional method called solution polymerisation (SP), screen printing followed by chemical vapour phase deposition (Print-CVD) and padding followed by CVD (Pad-CVD). Two stabilisation techniques are then employed, namely doping and thermal annealing. The study is aimed at enhancing the sensitivity and environmental stability of the PPy-coated fabric sensors.

3.2 Experimental

3.2.1 Materials and reagents

The material used was a plain knitted fabric of 83% polyamide (Tactel) and 17% spandex (Lycra) with the weight of 195gm/m^2, which was supplied by Sunikorn Knitters Limited (HK). The fabric density was 43 courses/cm and 22 wales/cm, and the linear density of the Tactel yarn was 702 denier/68 filaments and the Lycra yarn was 40 denier/5 filaments.

Pyrrole (99%) and ferric chloride hexahydrate ($FeCl_3 \cdot 6H_2O$) obtained from Sigma-Aldrich Chemical Company were used as the monomer and the oxidising agent respectively without further purification. Sodium dodecylbenzenesulphonate (DBS) (approximate 80%) obtained from the same company was used as a doping agent.

The untreated textiles were first washed with 1g/l non-ionic detergent solution (Lentol B) at 60°C for 30 minutes and then rinsed thoroughly. The samples were left to dry in a standard conditioning room at 21°C and 65% relative humidity for 24 hours before fabrication.

3.2.2 Sample fabrication

3.2.2.1 PPy-coated fabrics

1. Solution Polymerisation (SP)

Four pieces of Tactel/Lycra fabrics with the size of 100mm x 100mm were firstly immersed into the beaker containing 0.1 mol/l of $FeCl_3 \cdot 6H_2O$ solution. The beaker was kept shaking for 30 minutes followed by the addition of 0.05 mol/l of pyrrole for another 30 minutes of shaking. After the chemical polymerisation, the PPy-coated fabrics with black colour developed were then washed thoroughly with de-ionised water followed by rinsing with ethanol and drying at either 21˚C or in a vacuum oven set at -760mmHg and 40˚C for 16 hours.

2. Padding followed by Chemical Vapour Phase Polymerisation (Pad-CVD)

The PPy-coated fabrics were prepared by combining padding with CVD. Four pieces of Tactel/Lycra fabrics of 178mm x 127mm were immersed into the ethanol solution containing 0.1 mol/l of $FeCl_3 \cdot 6H_2O$ for 15 minutes and kept stirring. The wet uptake was controlled to be around 80% by using a padding machine (model PA-0). The padded fabrics were then transferred to a desiccator containing 10ml of pyrrole for CVD. Vapour phase polymerisation was carried out under vacuum set at -760mmHg and 21˚C for 24 hours. 10 minutes was required to achieve the set value. After the CVD process, a layer of PPy-coating was formed on the fabric surface. The coated fabrics were then washed thoroughly with de-ionised water followed by rinsing with ethanol and drying at either 21˚C or in a vacuum oven set at -760mmHg and 40˚C for 16 hours.

3. *Screen Printing followed by Chemical Vapour Phase Polymerisation (Print-CVD)*

Screen printing followed by chemical vapour phase polymerisation was used to fabricate the PPy-coated fabrics (Tao, Leung, Yuen, Kwok and Ho, 2005). The emulsion was firstly prepared by using 1900ml of white spirit, 400ml of water and 50g of emulsifier with well mixing and stirring. The print paste was then prepared by mixing 200g of the emulsion with 30g of $FeCl_3 \cdot 6H_2O$. Four pieces of Tactel/Lycra fabrics with a size of 178mm x 127mm were firstly printed by flat screen with the print paste and then transferred to a desiccator containing 10ml of pyrrole for CVD. Vapour phase polymerisation was carried out under vacuum set at -760mmHg and 21˚C for 24 hours. 10 minutes was required to achieve the set value. After the CVD process, a layer of PPy-coating was formed on the fabric surface. The coated fabric was then washed thoroughly with de-ionised water followed by rinsing with ethanol and drying at either 21˚C or in a vacuum oven set at -760mmHg and 40˚C for 16 hours.

3.2.2.2 Pure PPy powders

The production of pure PPy powders was similar to the fabrication method of Print-CVD, but the print paste was applied onto a glass plate instead of fabric. The emulsion was firstly prepared by using 1900ml of white spirit, 400ml of water and 50g of emulsifier with well mixing and stirring. A layer of print paste containing 200g of emulsion and 30g of $FeCl_3 \cdot 6H_2O$ was applied onto a glass plate and then transferred to a desiccator containing 10ml of pyrrole for CVD. Vapour phase polymerisation was carried out under vacuum set at -760mmHg and 21˚C for 24 hours. 10 minutes was required to achieve the set value. After the CVD process, pure PPy powder was formed on the surface of glass plate. The powder was then washed thoroughly with de-ionised water followed by rinsing with ethanol and drying at either 21˚C or in a vacuum oven set at -760mmHg and 40˚C for 16 hours.

3.2.3 Stabilisation treatments

Stabilisation treatments required for the PPy-coated textiles must be carefully selected in order not to damage the physical and mechanical properties of textile substrates, such as the stretch and recovery property which are very important for the development of a stretchable sensing sensor. Among all the stabilisation treatments discussed in the Literature Review, some of them may not be applicable to the stretchable textiles sensors. For example, acid and base treatments may cause damage to the textile substrates and reduce the electrical conductivity dramatically. High voltage application during the synthesis of PPy film cannot be used for the development of conductive textile strain sensor due to the formation of random and thick layer of PPy film. The thick layer coating will significantly reduce the strain sensitivity of the textile sensor. Low temperature thermal annealing and addition of large size anion were selected for stabilising PPy-coated fabrics that are described in the following.

3.2.3.1 Thermal annealing

In general, polymeric textile materials cannot withstand too high temperature. Hence, lower temperature annealing was carried out by means of vacuum drying

(VD) at 40˚C for 16 hours and vacuum heat treatment (VHT) at 60˚C for 40 hours under the vacuum atmosphere set at -760mmHg.

3.2.3.2 Addition of dopants

In this study, DBS ($C_{18}H_{29}NaO_3S$) was selected as the doping agent used for the fabrication of the PPy-coated fabric sensors. The procedure of dopant addition for different fabrication methods are reported in the following.

1. Solution Polymerisation (SP)

Four pieces of Tactel/Lycra fabrics with the size of 100mm x 100mm were immersed into the beaker containing 0.1 mol/l of $FeCl_3{\cdot}6H_2O$ solution. The beaker was kept shaking for 30 minutes followed by the addition of 0.017 mol/l of DBS and 0.05 mol/l of pyrrole with another 30 minutes of shaking. The samples were then washed and dried as stated previously.

2. Padding followed by Chemical Vapour Phase Polymerisation (Pad-CVD)

Fabrics samples were immersed into the aqueous solution containing 0.011 mol/l of DBS for 15 minutes with constant stirring, and the wet uptake was controlled to be around 80%. The padded fabrics were then immersed in ethanol solution with 0.1 mol/l of $FeCl_3{\cdot}6H_2O$ for another 15 minutes and with constant stirring, and the fabrics were padded again with around 80% wet uptake. The padded fabrics were subsequently transferred to a desiccator containing 10ml of pyrrole for CVD. The samples were then washed and dried as stated previously.

3. *Screen Printing followed by Chemical Vapour Phase Polymerisation (Print-CVD)*

The solution of 6.54g of DBS in 30ml of deionised water was added into the print paste containing 200g of the emulsion and 30g of $FeCl_3 \cdot 6H_2O$. Fabrics were firstly printed by flat screen and subsequently transferred to a desiccator containing 10ml of pyrrole for CVD. The samples were then washed and dried as stated previously.

4. *Pure PPy Powders*

The solution of 6.54g of DBS in 30ml of deionised water was added into the print paste containing 200g of the emulsion and 30g of $FeCl_3 \cdot 6H_2O$. A layer of print paste was applied onto a glass plate and then transferred to a desiccator containing 10ml of pyrrole for CVD. The samples were then washed and dried as stated previously.

3.2.4 Characterisation of PPy-coated fabrics

Electrical Resistance and Strain Sensitivity Measurements

The PPy-coated fabric specimen with a size of 25.4mm x 76.2mm in wale direction was attached vertically by two pairs of copper plates with a gauge length of 25.4mm. A DC electrical current was supplied and the electrical resistance was measured. Measurement of the electrical resistance of conductive textile sensor under large strain deformation was carried out using a two-probe multi-meter Keithley Model 2010. Simultaneously, ten consecutive cycles of unidirectional extension up to 50% were carried out by Instron tensile tester (Model 4466). The crosshead speed of the tensile extension was set at 1mm/sec and the gauge length was 25.4mm. Ten specimens of each fabrication methods were tested. One typical specimen from each fabrication method was selected for representing the figure of strain versus relative electrical resistance change. The strain sensitivity of a fabric sensor is represented by the gauge factor defined as the fraction of the increment in its electrical resistance, $\Delta R/R_o$, per unit strain, that is:

$$K(gaugefactor) = \frac{R - R_o}{\varepsilon_{\max} R_o} \tag{3.1}$$

Where R is the resistance of fabrics under maximum strain, R_o is the initial resistance at the relaxed state, ε is the unidirectional tensile strain of fabrics, and $\varepsilon_{\max}$ is referred to 50%.

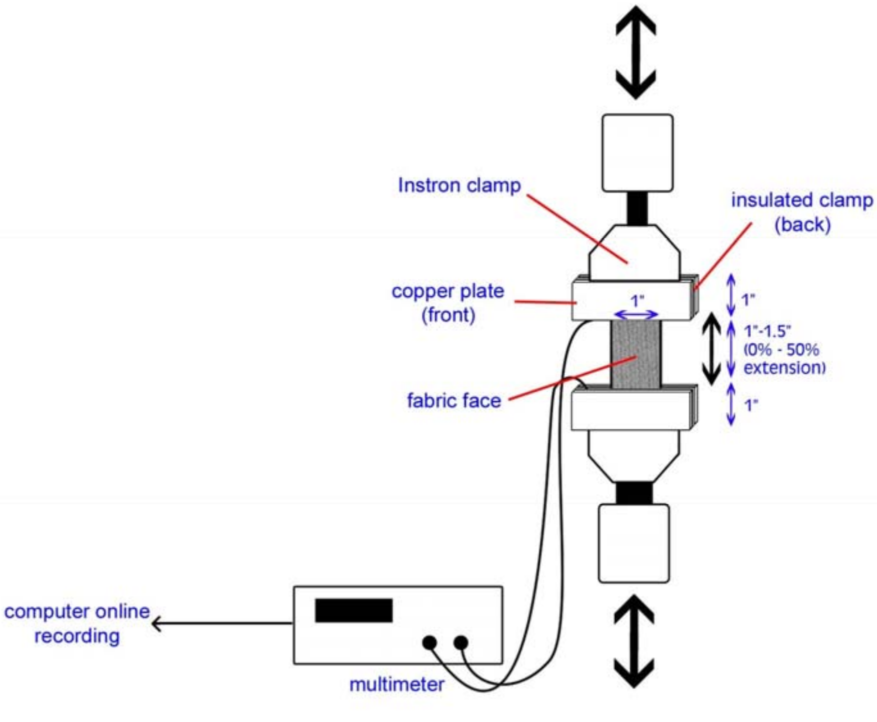

Figure 3.1 Schematic diagram of instrumental set up for testing electrical resistance and strain sensitivity of PPy-coated fabrics

Temperature and Humidity Control

HOTPACK environmental chamber was used to condition the PPy-coated fabrics at different temperature and relative humidity. Fabric specimen was placed in the dynamic temperature and humidity chamber with (i) temperature being adjusted to 20˚C, 35˚C, 50˚C and 60˚C respectively at 65% relative humidity, and (ii) humidity being adjusted to 40%, 55%, 70% and 90% respectively at 20˚C. The electrical resistance was measured in every 2 hours after the adjustment of temperature and humidity.

Morphology

Scanning electron microscope (SEM Model Lecia Cambridge stereoscan 440) was used to study the morphology of the PPy-coated fabric surfaces. The microphotographs were obtained at an accelerating voltage of 20 kV and at 5 k magnification.

Degree of Crystallinity

The degree of crystallinity of the fabrics was measured by the X-ray Diffractometer (Bruker D8 Advance XRD System) equipped with a solid-state of germanium crystal detector. A Cu K_α X-ray source was running at 40 kV and 40 mA. The scanning range was set from 2° to 60° with the scan speed of 1 sec/0.03° increment. Three specimens from each sample were tested and the average value was taken.

Thermal Analysis

Thermogravimetric Analysis (TGA) is a technique used for rapidly evaluating the percentage of volatiles as well as the onset of thermal decomposition temperature of conducting polymer. In this study, the thermal study of the PPy-coated fabrics and pure PPy powders was conducted using a Netzch STA449C TGA/DSC analyser. 5-6mg of sample was placed in the sample holder with a rise of temperature from 30°C to 700°C at a rate of 10°C/min. The sample was heated in the nitrogen gas at a flow rate of 20 ml/min in order to eliminate possible chemical reactions of polymer backbone with oxygen. Three specimens from each sample were tested and the average value was taken.

Contact Angle Measurement

The measurement of hydrophobicity of the fabrics was carried out by means of a contact angle meter, Tantec, CAM-micro. The contact angle was measured directly from the image at 3 sec after the distilled water droplet was placed on the fabric surface. The droplet size was 1 μl and the distance between the syringe and sample was 5 mm. Five specimens from each sample were tested and the average value was taken.

3.3 Effect of Fabrication Methods on Sensing Performance

The experimental results of electrical resistance and gauge factor of the PPy-coated fabrics prepared by different fabrication methods at room temperature (21°C) are shown in Table 3.1. When compared, the lowest electrical resistance of conductive fabric with 14kΩ/in^2 can be obtained by SP. However, the gauge factor is only 6 at a strain of 50% which is crucial to the development of flexible fabric strain sensor. Under 10 cyclic tensions, the resistance variation results of the PPy-coated fabrics prepared by different fabrication methods are shown in Figures 3.2 to 3.4.

Table 3.1 Initial resistance and gauge factor of the PPy-coated samples subjected to different fabrication methods

Sample No.	Fabrication Method	Initial Resistance (R_o) ($k\Omega/in^2$) [s.d.]	Gauge Factor[a] ($\frac{\Delta R}{\varepsilon_{\max} R_o}$) [s.d.]
S1a	Solution Polymerisation	14 [1.97]	6 [0.72]
S1b	Padding followed by CVD	98 [9.47]	9 [1.70]
S1c	Printing followed by CVD	100 [2.33]	20 [1.33]

[a] strain = 50%

It is obvious that the PPy-coated fabric prepared by the Print-CVD method exhibits the highest gauge factor up to 20 at 50% of fabric strain. On the other hand, the Pad-CVD and SP can only produce conductive fabrics with lower gauge factors of about 9 and 6 respectively. The samples prepared by the Print-CVD or Pad-CVD fabrication methods show repeatable sensing curves during the cyclic strain tests. The sample made by the Print-CVD method demonstrates excellent linearity and small hysteresis of the sensing curves among ten cycles. The difference in the strain sensitivity between three fabrication methods is believed to be partially due to the thickness and morphology of conductive film formed on the textile substrates. In general, a low sensitivity is associated with a thick coating composed of multi-layers of PPy deposited on the surface of the fabrics during the SP (Li, Cheng, Leung, Tsang, Tao and Yuen, 2005). The multi-layers of PPy may not change in the same way when the fabrics are elongated. Therefore, a more smooth, dense and thin layer of PPy-coating is beneficial to the strain sensitivity of the sensors.

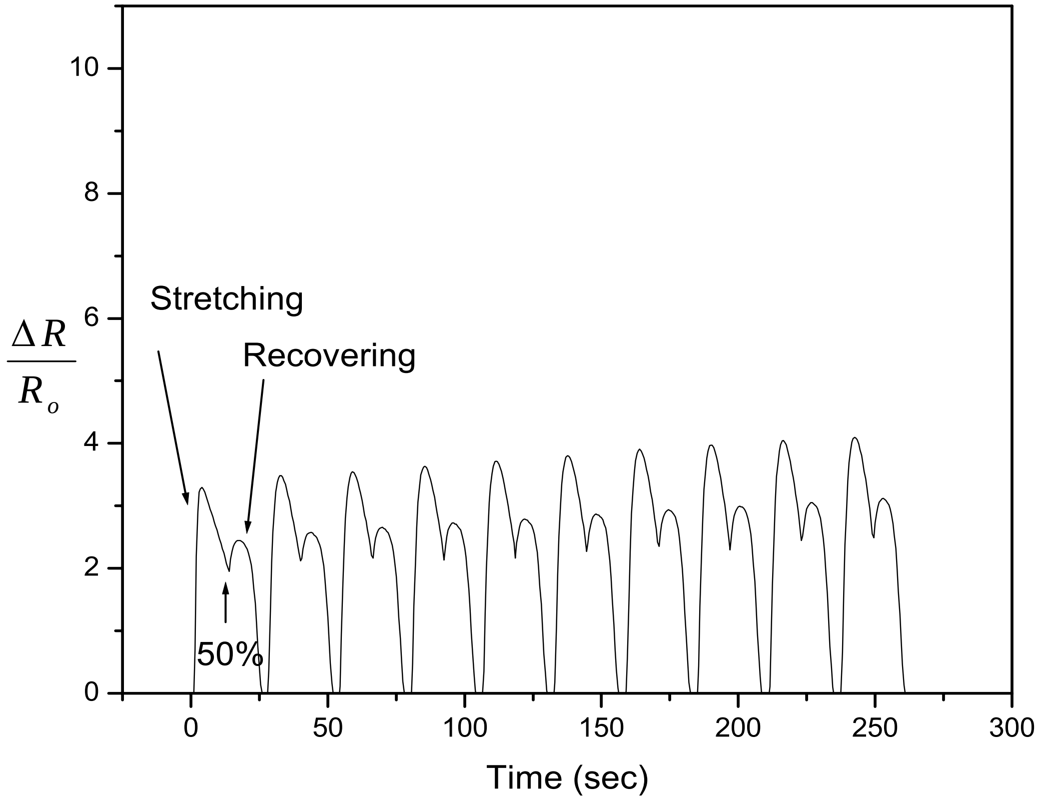

Figure 3.2 Relative resistance change as a function of time in a cyclic tensile test of the PPy-coated fabrics fabricated by solution polymerisation (S1a)

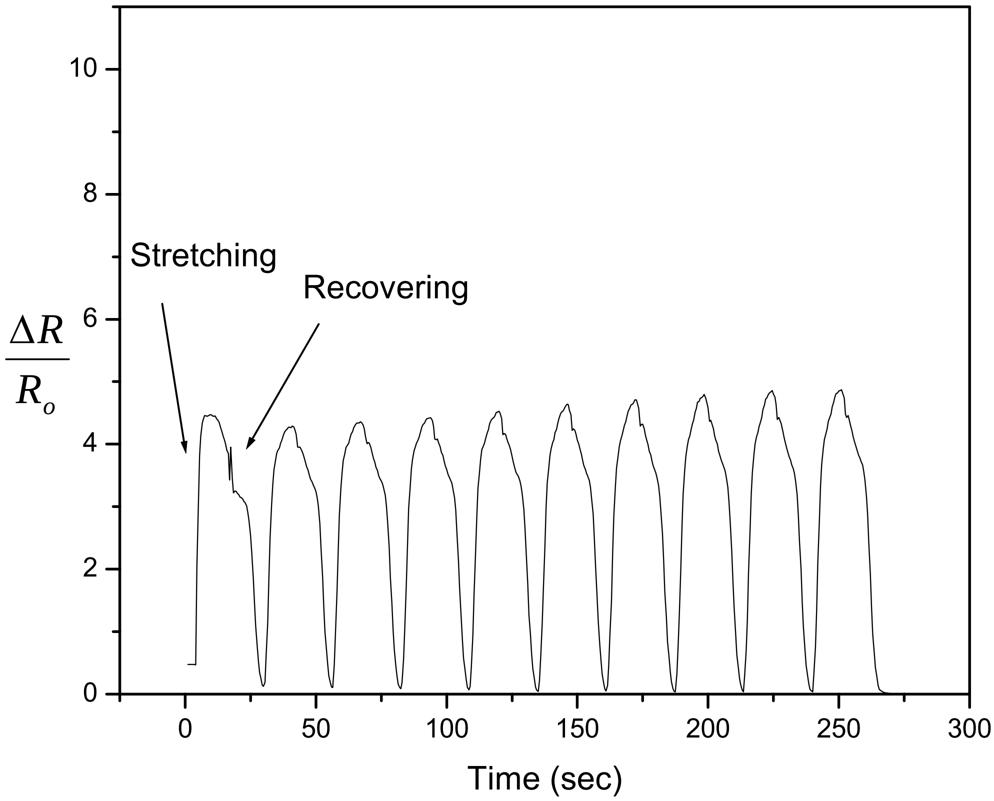

Figure 3.3 Relative resistance change as a function of time in a cyclic tensile test of the PPy-coated fabrics fabricated by Pad-CVD (S1b)

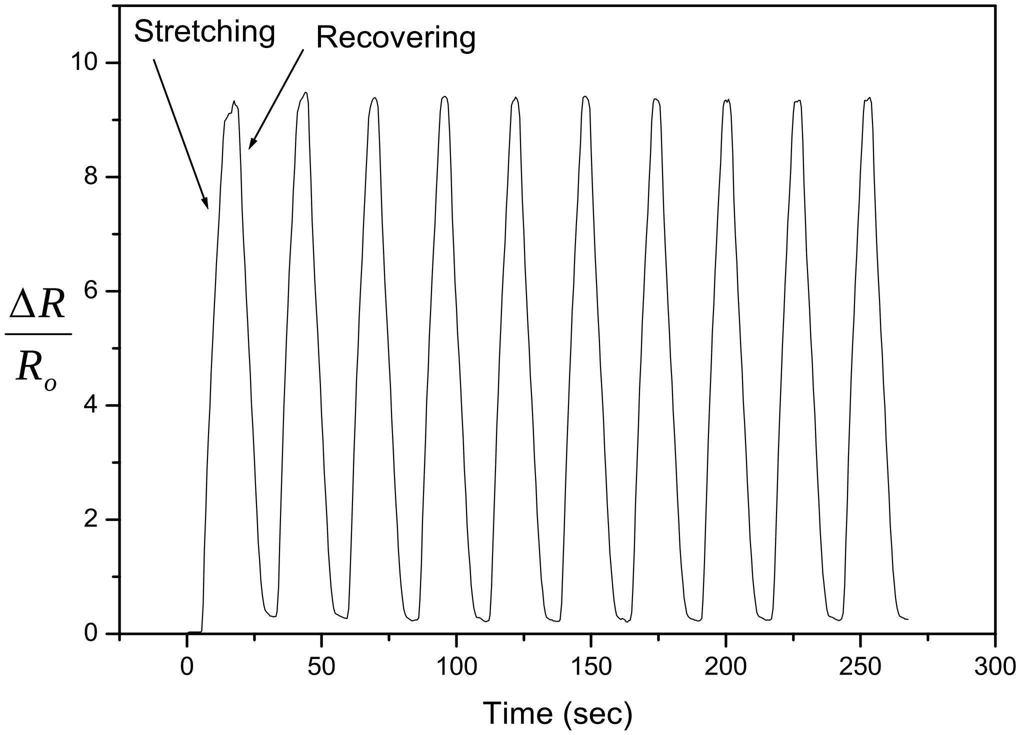

Figure 3.4 Relative resistance change as a function of time in a cyclic tensile test of the PPy-coated fabrics fabricated by Print-CVD (S1c)

The preliminary results indicate that the fabric sensor produced by SP exhibits poor sensing behaviour as non-linearity will occur during stretching and recovery. Double peaks are exhibited at every tensile cyclic of stretching and recovering. For the stretching curve of every cycle, the resistance change could be divided into two phases. In the initial phase, the resistance increased gradually up to 22% of fabric strain, followed by a second phase in which the resistance decrease gradually to 50% of fabric strain. In the initial phase, the yarn transfer from the horizontal part to the V-segment of the knitted loops and the damage of PPy film on the Lycra yarn due to yarn stretching is the dominant factor contributes to the increasing of resistance of the knitted fabric. In the second phase, the yarn contacting resistance is the dominant factor contributes to the decreasing of resistance of the fabric. Hence, the

SP fabrication method is not considered for the development of fabric strain sensor in this study.

The chemical vapour polymerisation method demonstrates better strain sensing capacity either by the Pad-CVD and Print-CVD. There are no obvious double peaks exhibit in Figures 3.3 and 3.4, single phase of resistance change is illustrated up to 50% of fabric strain for the samples prepared by Pad-CVD and Print-CVD methods. It is because better quality of PPy coating with thinner and more uniform characteristics are produced on the textile fabrics which can postpone the commencement of PPy film damage at longer strain. Therefore, the resistance due to stretching the yarn in the V-segment of a knitted loop and yarn transfer from the horizontal part to the V-segment are the key factors governing the strain sensitivity of those samples. The mechanism of the strain sensing behaviour of PPy-coated fabrics will be discussed in Chapter 5.

Among the three fabrication methods, the Print-CVD method is worthwhile to be further studied and evaluated, particularly the stabilisation treatments of the PPy-coated fabrics as discussed in the following sections.

Vapour deposition has been utilised for producing PPy film (Dillingham, Cornelison and Bullock, 1994; Gaynor and Desu, 1994; Gaynor, Senkevich and Desu, 1996; Lee, 2001; Plank, Dinardo and Vohs, 1997; Porter, Caple and Caple, 1994; You, Yang, Lang, Moore, Wu, Mcdonald and Lu, 1993). The CVD process of PPy-coated fabric can eliminate solvent effects, which allows for better control of film uniformity and thickness. The result was supported by Lee (2001) found that the vapour-deposited

PPy thin film was highly ordered that the oligomer chains were directed almost parallel to the Cu(110) surface plane. Therefore, the PPy-coated fabrics prepared by the CVD methods have improved sensing performance, partially because of more ordered and dense PPy chains deposited on the textile substrate.

Figures 3.5 to 3.8 show SEM micrographs of uncoated Tactel/Lycra fabric (control) and PPy-coated fabrics prepared by the SP, Pad-CVD and Print-CVD. The fabrics coated with PPy formed by CVD exhibit very smooth surfaces covered with very thin continuous layer of PPy coating, while the fabrics prepared by the SP demonstrates a very rough and thick surface. There is no obvious difference in fibre diameters between the Pad-CVD samples, Print-CVD samples and uncoated control samples as shown in Figures 3.5, 3.7 and 3.8 with the fibre diameter of around 13µm. However, it can be seen in Figure 3.6 that fibre diameters of the sample fabricated by SP are in the range of 15µm to 20µm. SP produces thicker PPy coating layers on the fabric substrate. As a result, the samples prepared by the CVD can exhibit better sensing performance while the SP shows relatively low strain sensitivity.

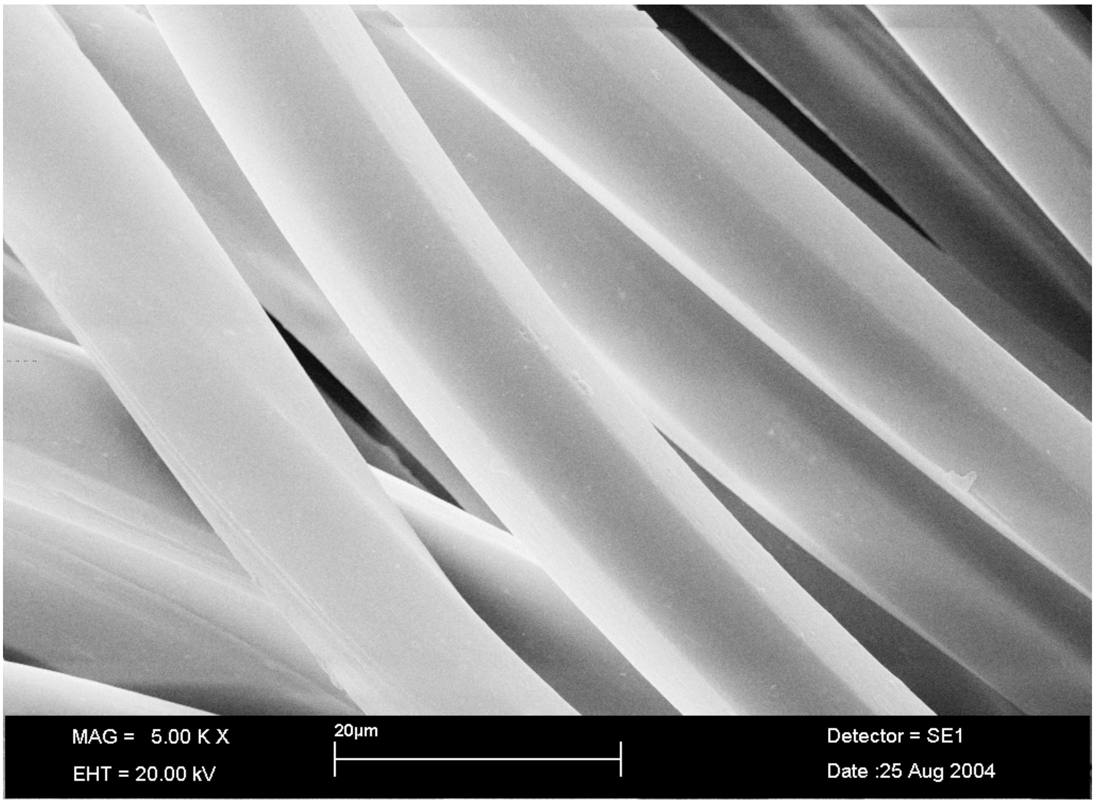

Figure 3.5 SEM photograph of uncoated control Tactel/Lycra fabric

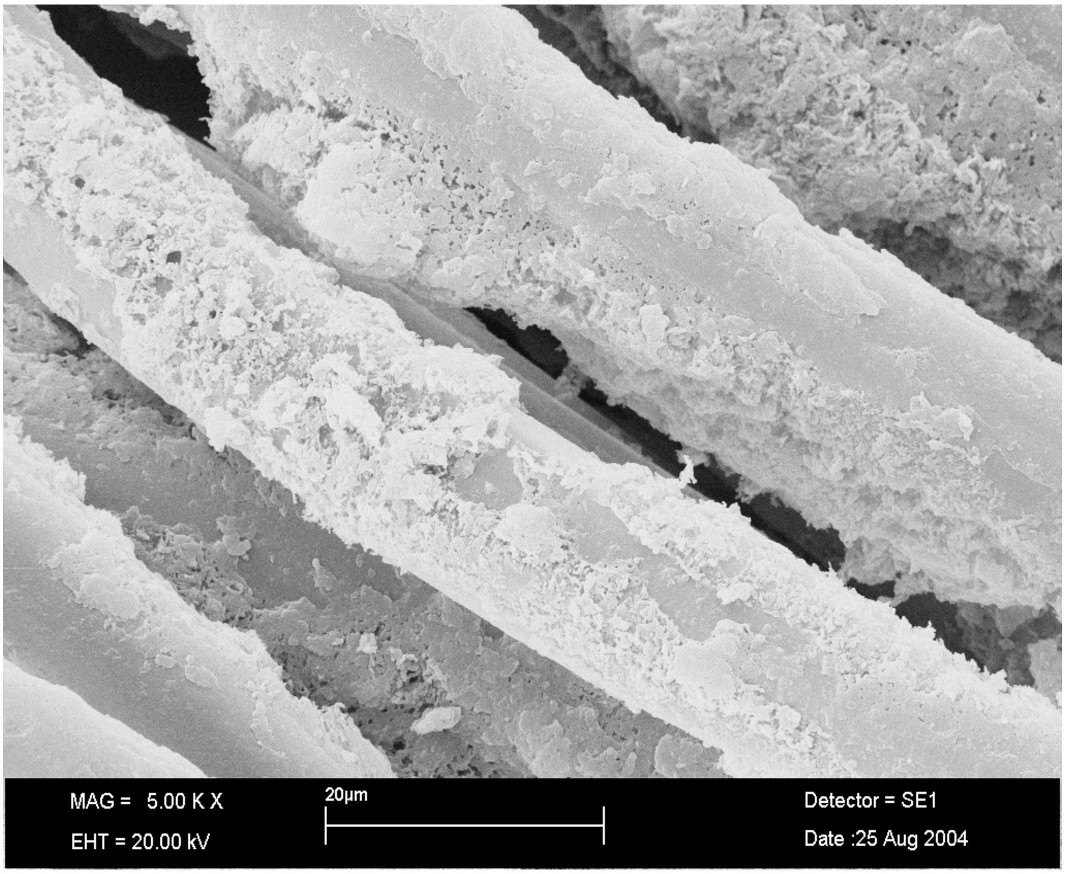

Figure 3.6 SEM photograph of PPy-coated fabric prepared by solution polymerisation (S1a)

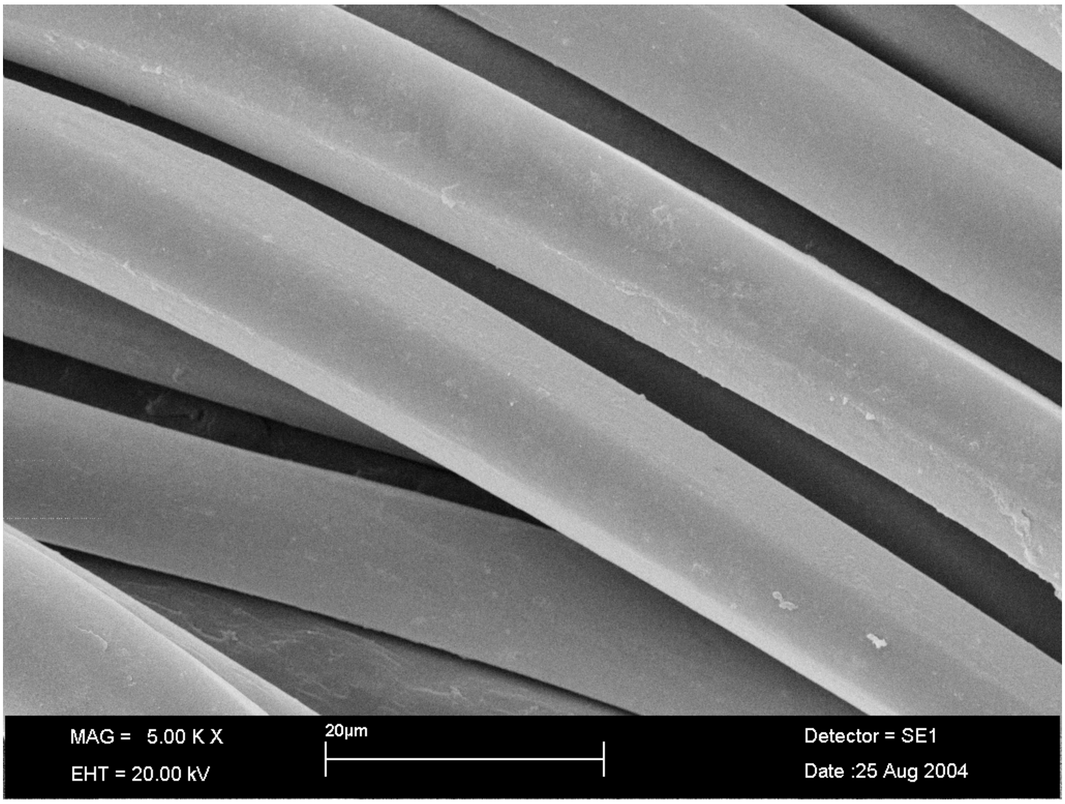

Figure 3.7 SEM photograph of PPy-coated fabric prepared by Pad-CVD (S1b)

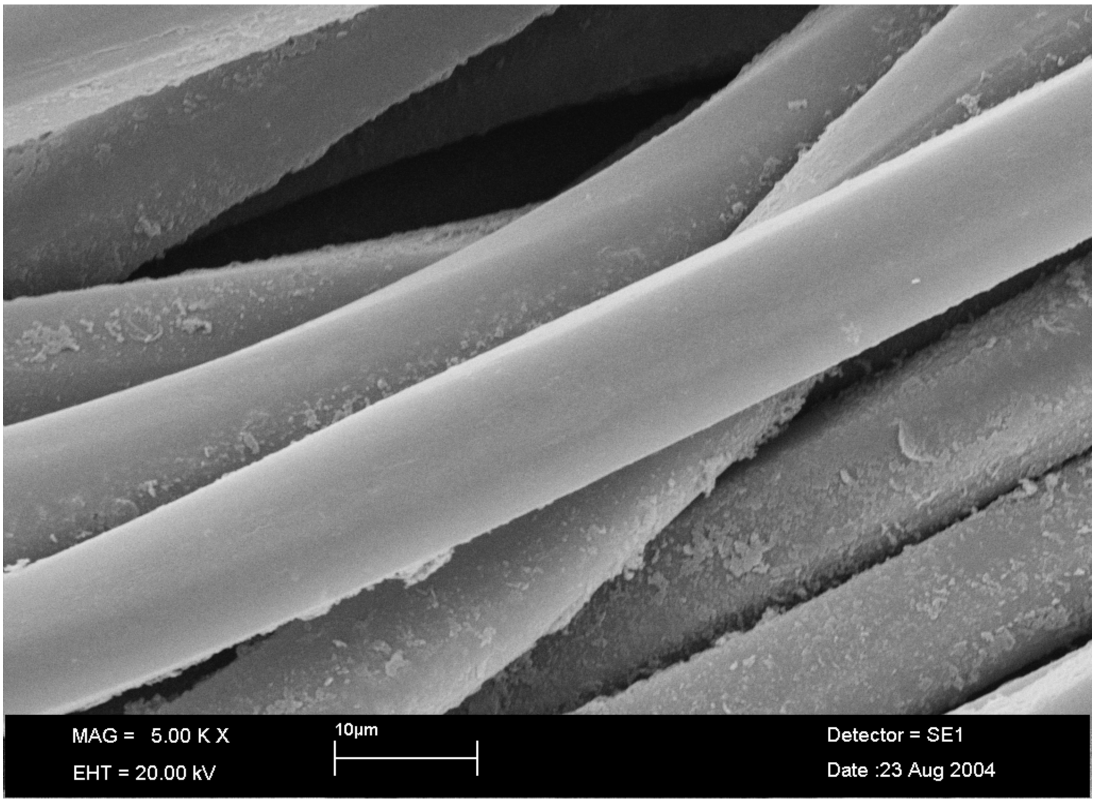

Figure 3.8 SEM photograph of PPy-coated fabric prepared by Print-CVD (S1c)

3.4 Stabilisation of the PPy-Coated Fabrics

The PPy-coated fabrics samples prepared by the Print-CVD method were selected for investigating stabilisation treatments. The procedures of applying stabilisation treatments to the fabrication process are illustrated in Figure 3.9. Four types of PPy-coated fabric samples with different stabilisation treatments were produced, namely, (i) untreated samples, (ii) VD samples, (iii) VD + VHT samples and (iv) VD + VHT + DBS samples.

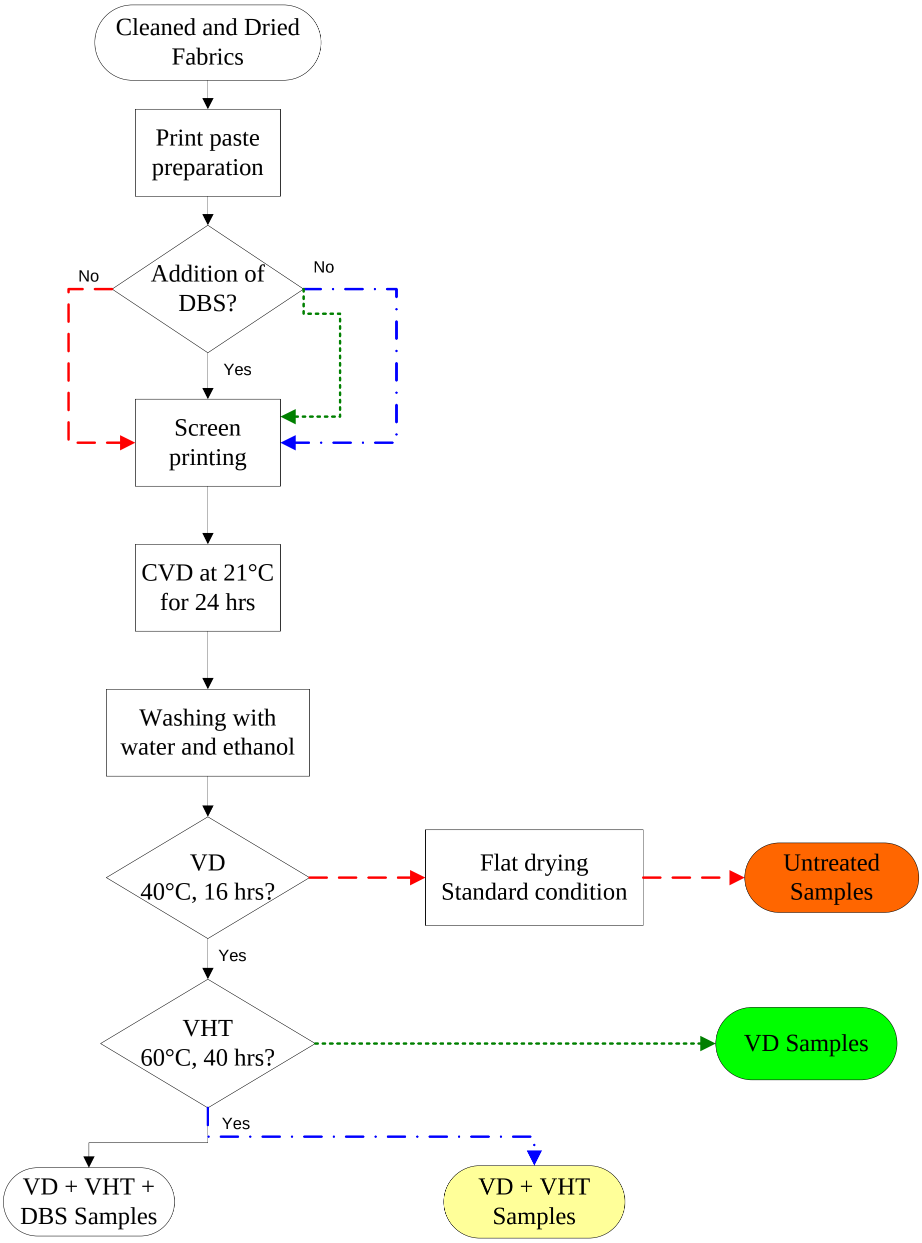

Figure 3.9 Fabrication procedures of PPy-coated fabrics with various stabilisation treatments

As the thermal annealing effect can improve the local ordering within the PPy coating, VD and VHT were used to stabilise the PPy-coated samples. The restructuring of the PPy polymers induced by thermal annealing may be due to the evaporation of residual solvents (Singh, Narula, Tandon, Rao, Panwar, Mansingh and Chandra, 1996; Turcu, Neamtu and Brie, 1993). Furthermore, thermal annealing can induce the reordering of PPy which is beneficial to the electrical conductivity of the PPy film, for instance an increase in the conductivity of PPy film was found after thermal annealing at 120°C for 24 hours (Wang and Rubner, 1991). Owing to the fact that PPy is coated on Tactel/lycra textile substrate, thus the temperature of heat treatment cannot be too high as the lycra fibres will melt within the range of 230°C to 290°C, and also sticking may occur at approximately 150°C (Cook, 1984). It has been reported that heat treatment at 190°C or higher will make the PPy-coated fabric non-conductive (Omastova, Kosina, Pionteck, Janke and Pavlinec, 1996; Omastova, Pavlinec, Pionteck and Simon, 1997). This may be probably due to the serious oxidation degradation of the PPy-coated fabric which occurs at the high temperature. Hence, heat treatment under vacuum is selected for this investigation so as to lower the temperature required for the thermal annealing process.

Conventionally, the small-sized counterion Cl^- within the PPy films is used for the electrical neutralisation and can easily be removed at higher temperatures. When the small inorganic anions Cl^- are used as dopant and counterion, they may have the interaction with water molecules. As a result, they will either move freely inside the PPy film or leave the PPy film completely resulting in poor stability of conductivity. The electrical neutralisation may be achieved by other ions (OH^- obtained from the hydrolysis of water, or CO_3^{2-} from the dissolved CO_2, etc.), and the conductivity will be altered. Since the absorbed water molecules may form a thin layer on the surface at high humidity, thus they can easily enter the PPy film and attack the pyrrole ring to decrease the conductivity.

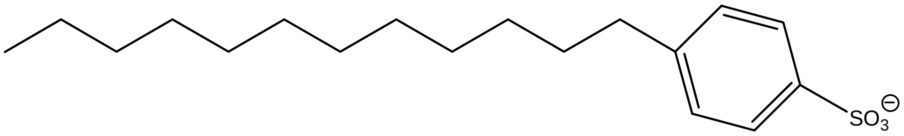

Figure 3.10 Structure of DBS

Addition of the DBS anions can enhance the thermal stability due to their large molecular size. The structure of DBS is shown in Figure 3.10. It is believed that DBS anions will be closely attached to the PPy coating and built inside the PPy film (Gao and Tian, 1995). These large sized DBS anions are trapped in the polymer during polymerisation and cannot freely move in or out of the film because of the steric hindrance effect (Pei and Qian, 1991). DBS was selected for the investigation. The effect of stabilisation treatments on the electromechanical behaviour and surface morphology are discussed in the following section.

3.4.1 Tensile behaviour of PPy-coated fabrics with stabilisation treatments

The tensile behaviour of the uncoated control Tactel/Lycra plain knitted fabric, PPy-coated fabric without treatment, and PPy-coated fabrics with different stabilisation treatments is depicted in Figures 3.11 to 3.13. Figure 3.11 demonstrates the tensile property in terms of stress versus strain curve with 50% extension and recovery of the uncoated control Tactel/Lycra knitted fabric. Figure 3.12 compares the tensile properties of the uncoated control and PPy-coated Tactle/Lyrca knitted fabrics. Figure 3.13 shows the effects of the coating layer with different stabilisation treatments on the tensile properties of the PPy-coated fabrics. It can be seen from Figure 3.11 that the uncoated control fabric exhibits a non-linear tensile behaviour. It was selected for the development of conductive fabric strain sensor because this stretchable textile material had a low elastic modulus and small hysteresis. As shown in Figure 3.12, there is no obvious change in the tensile property of the fabric after being coated with PPy. This is due to the fact that the PPy coating film is so thin that it does not affect tensile property of the textile fabric. It only changes the electrical properties of the fabric.

Figure 3.13 shows the comparison of tensile behaviour between the three different stabilisation treatments. This is no significant change in the tensile property of all the samples with different stabilisation treatments. It is concluded that all the stabilisation treatments do not affect the tensile property of the fabrics. Hence, all the coated conductive fabrics retain excellent elasticity and recovery properties.

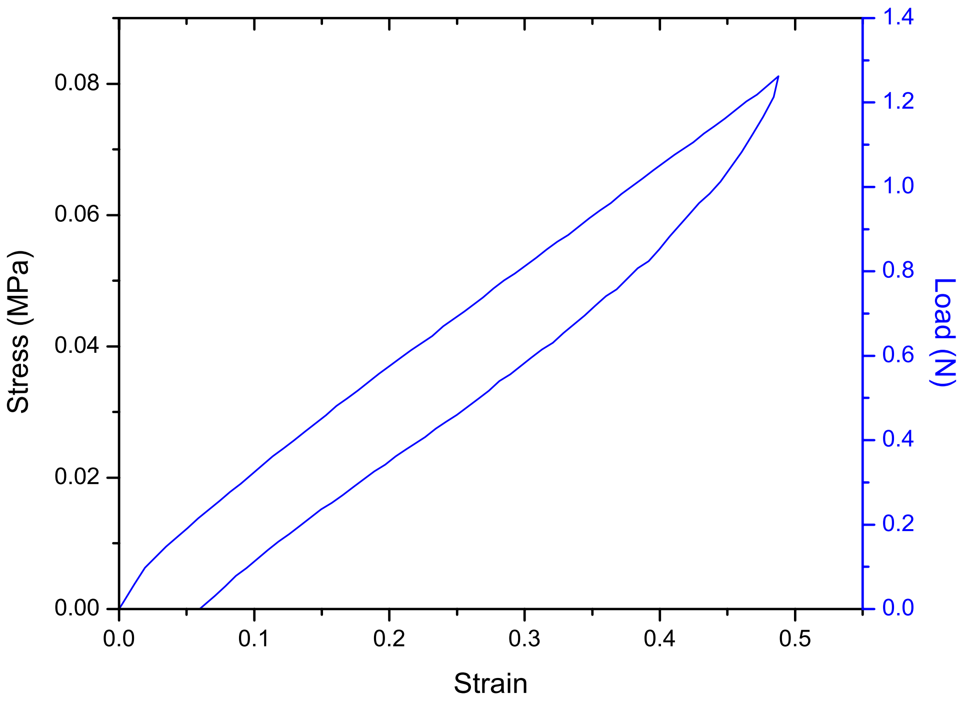

Figure 3.11 Stress versus strain curve of the uncoated control Tactel/Lycra fabric in the wale direction

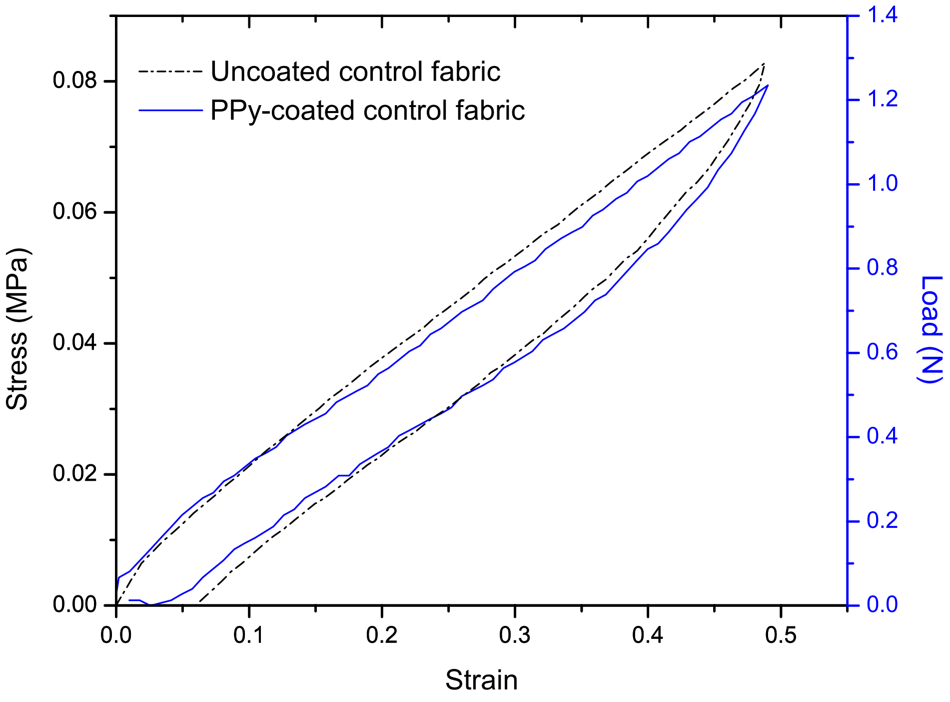

Figure 3.12 Stress versus strain curves of the uncoated control and PPy-coated fabrics in the wale direction

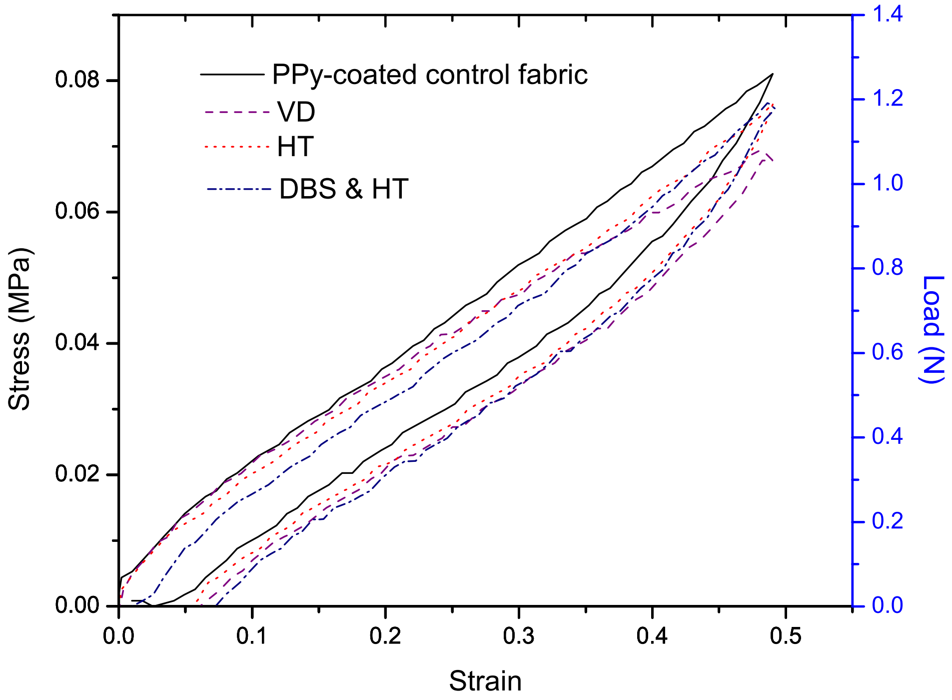

Figure 3.13 Stress versus strain curves of the PPy-coated fabric with different stabilisation treatments in the wale direction

3.4.2 Sensing performance of the PPy-coated fabrics

Electrical resistance and strain sensitivity

The experimental results of the PPy-coated fabrics with different stabilisation treatments are summarised in Table 3.2. Each stabilisation treatment can improve the conductivity of the PPy-coated fabrics to same extent. When compared, the initial resistance of the treated and untreated samples dropped from 40% to 80% with respect to different stabilisation treatments.

Table 3.2 Initial resistance and gauge factor of the PPy-coated samples subjected to different stabilisation treatments

Sample No.	Treatment Methods	Initial Resistance (R_o) (kΩ/in^2) [s.d.]	Gauge Factor[a] ($\frac{\Delta R}{\varepsilon_{\max} R_o}$) [s.d.]
S1c	No Treatment	100 [2.33]	20 [1.33]
S2a	VD	20 [3.57]	60 [8.04]
S2b	VD + VHT	20 [3.26]	110 [11.10]
S2c	VD + VHT + DBS	60 [6.44]	184 [11.49]

[a] strain = 50%

Furthermore, the VD treatment at 40°C shows a significant increase in the strain sensitivity of the PPy-coated fabrics under large cyclic tension. The values of gauge factor for samples with or without VD are approximately 60 and 20 respectively at 50% of fabric strain, implying that VD can tremendously improve the gauge factor of sample when compared with the untreated samples. In addition, the employment of VD and VHT at 60°C for 40 hours can further enhance the gauge factor of the sample to 110.

Figures 3.14 to 3.17 indicates that the strain sensitivity and repeatability of the sensing performance of the PPy-coated fabrics with different stabilisation treatments, namely (i) without any treatment (Figure 3.14), (ii) with VD (Figure 3.15), (iii) with VD + VHT (Figure 3.16), and (iv) with VD + VHT + DBS (Figure 3.17). Using the same dimension scale, it is very obvious that the addition of VD and VHT can significantly improve the strain sensitivity of the PPy-coated fabric. In both cases, the sensing curves have an excellent repeatability.

As shown in Table 3.2 and Figure 3.17, the addition of dopant DBS lead to a significant improvement of the strain sensitivity. Textile sensor fabricated with VD + VHT + DBS can achieve a very high gauge factor of about 184 at 50% of strain. In addition, the sensing curves show a very good linearity and repeatability.

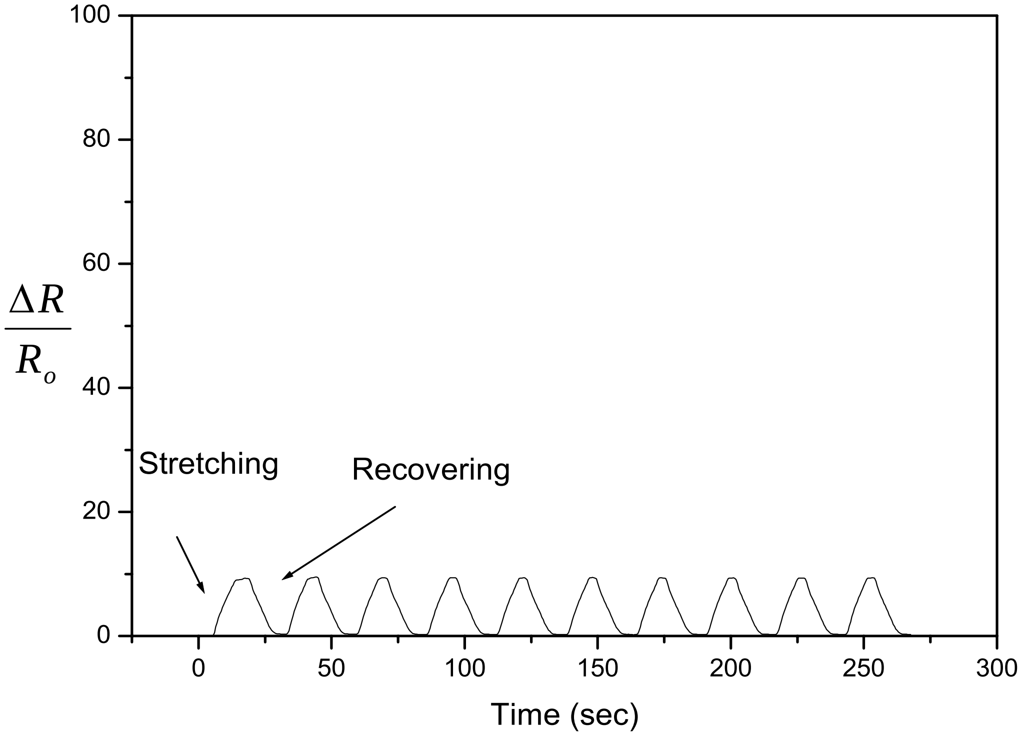

Figure 3.14 Relative resistance change as a function of time in a cyclic tensile test of the untreated PPy-coated fabrics (S1c)

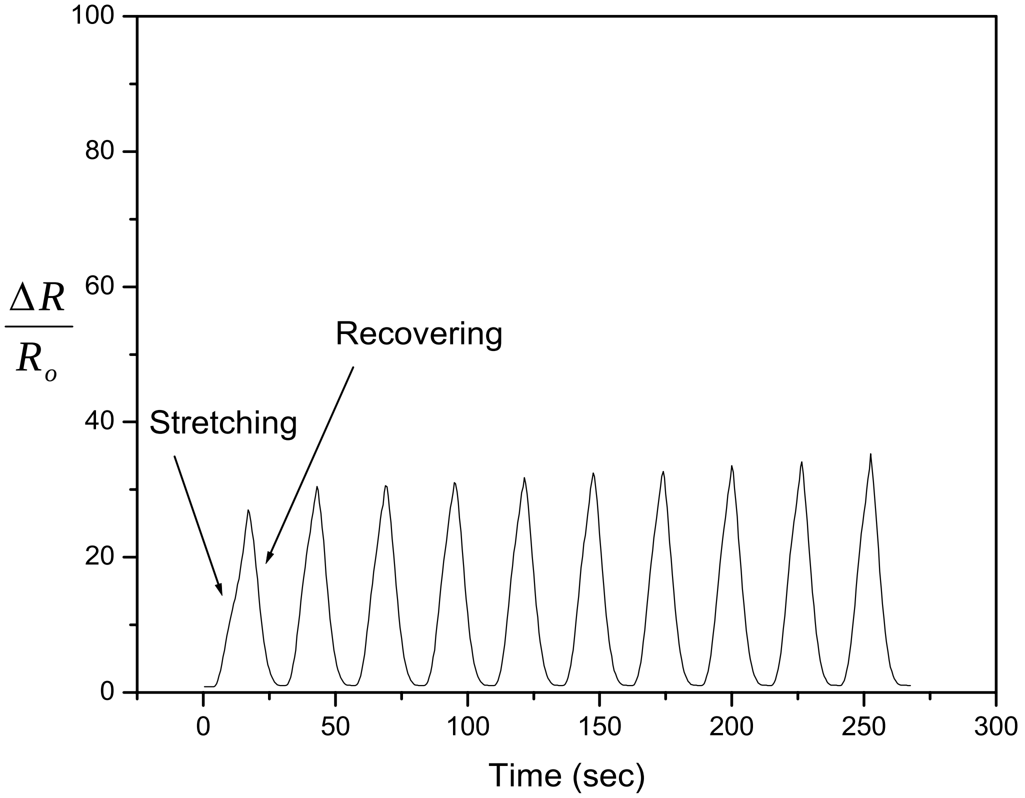

Figure 3.15 Relative resistance change as a function of time in a cyclic tensile test of the PPy-coated fabrics with VD treatment (S2a)

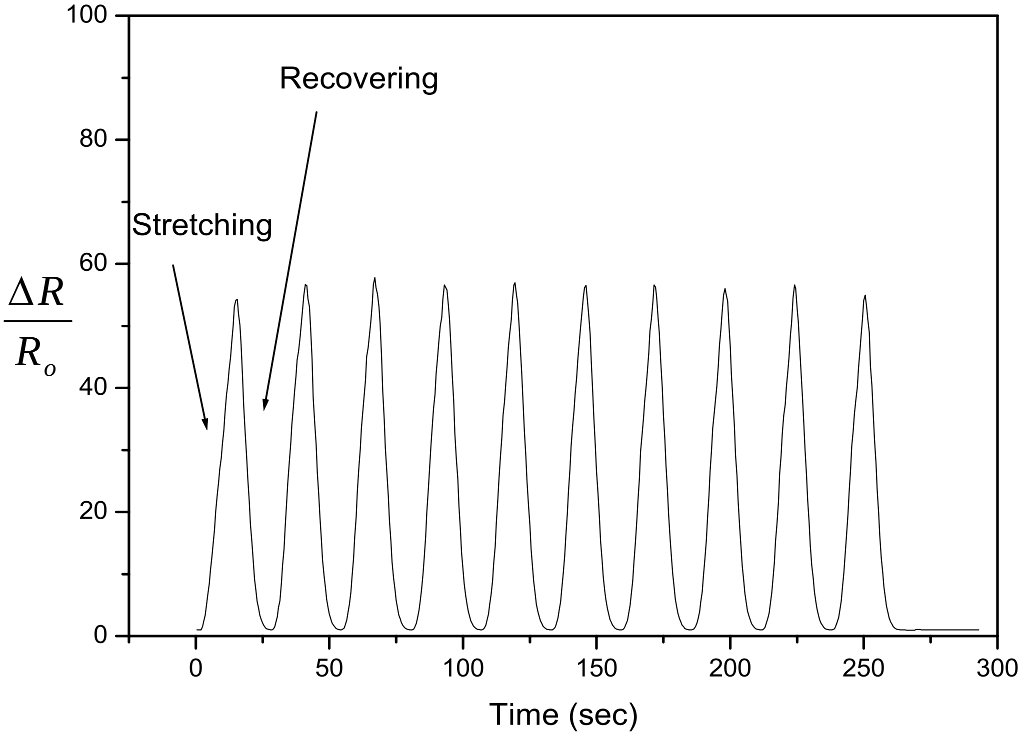

Figure 3.16 Relative resistance change as a function of time in a cyclic tensile test of the PPy-coated fabrics with VD + VHT (S2b)

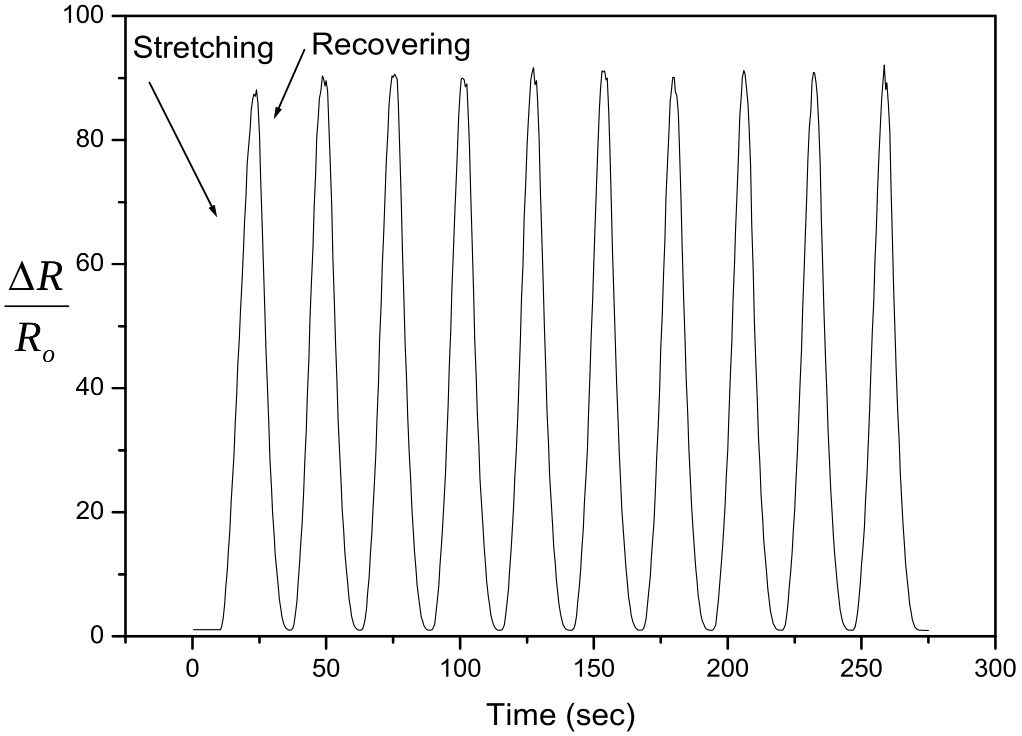

Figure 3.17 Relative resistance change as a function of time in a cyclic tensile test of the PPy-coated fabrics with VD + VHT + DBS treatment (S2c)

Effect of temperature and relative humidity on the stability of PPy-coated fabrics

For fabric strain sensors, the resistance change versus temperature and RH under normal environmental conditions should be minimised so that more environmentally stable PPy-coated fabrics can be produced with lower thermal and RH sensitivities. The thermal behaviour of samples with (i) no stabilisation treatment, (ii) VD + VHT, (iii) VD + VHT + DBS treatment are shown in Figure 3.18 to 3.20. It can be seen that the relative resistance is increasing during the temperature cycles. On the contrary, the samples with VD + VHT or VD + VHT + DBS treatments can significantly reduce the relative resistance change versus cyclic temperature change. The hysteresis between heating and cooling curves can also be reduced by the stabilisation treatments.

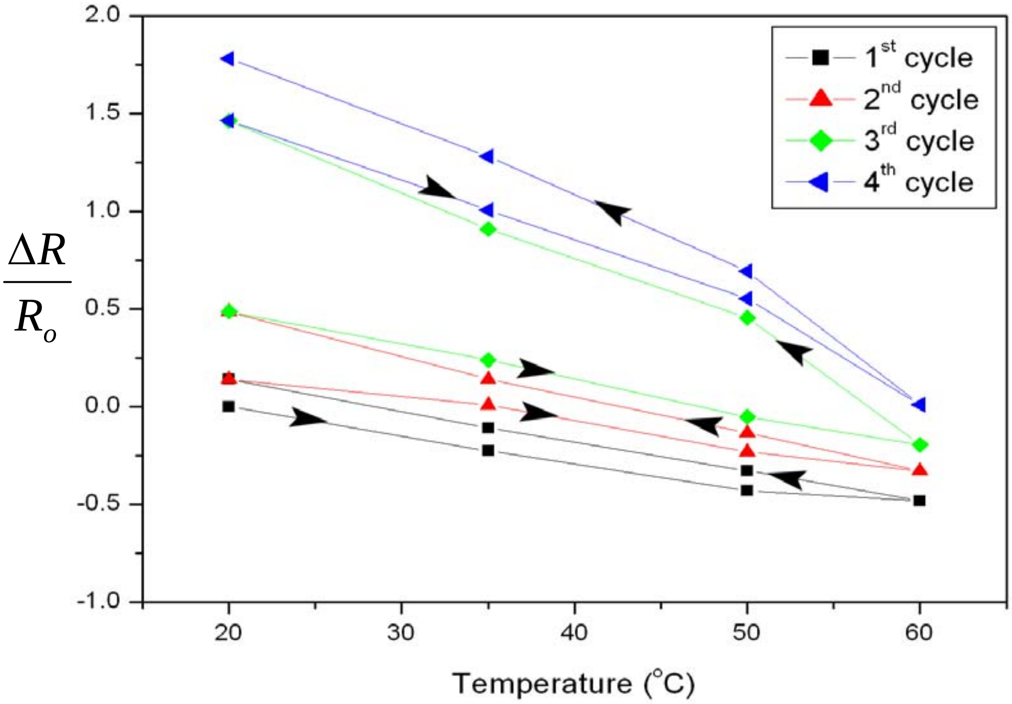

Figure 3.18 Cyclic temperature sensitivities of the untreated PPy-coated fabric (S1c)

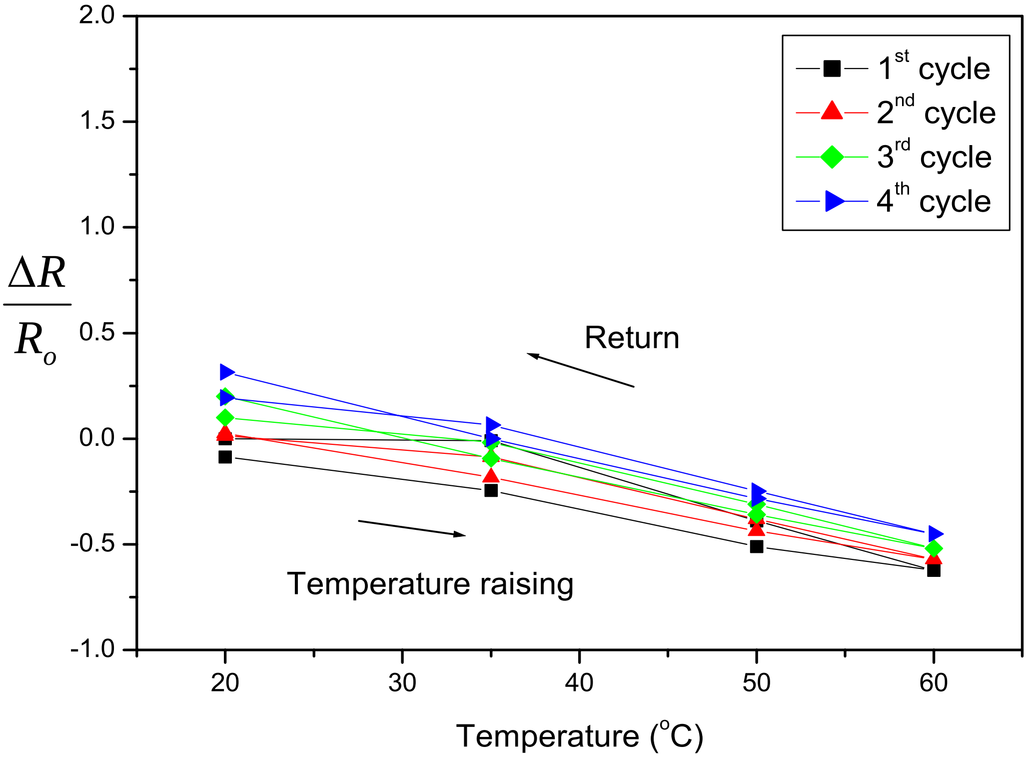

Figure 3.19 Cyclic temperature sensitivities of the PPy-coated fabric with VD + VHT (S2b)

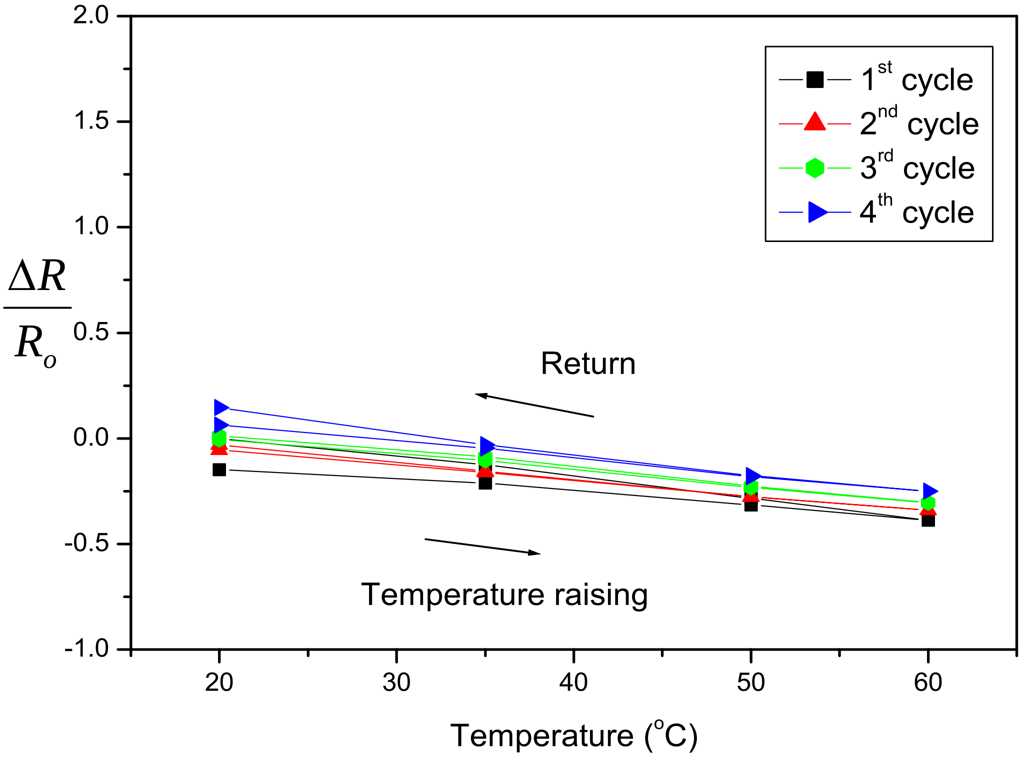

Figure 3.20 Cyclic temperature sensitivities of the PPy-coated fabric with VD + VHT + DBS treatment (S2c)

Figure 3.21 shows that the relative electrical resistance of the untreated PPy-coated sample varies tremendously after 2 cycles of humidity ageing. The sample is very unstable in an environment with humidity fluctuations. Similar to the change of temperature, the sample with VD + VHT significantly improves the stability of e-textile sensors with respect to humidity change, as shown in Figures 3.22. The application of VD + VHT + DBS can further improve the stability of humidity with very slight changes in the relative resistance towards humidity change as shown in Figure 3.23. The VD + VHT + DBS treated sample almost has no change in electrical resistance when the humidity varies from 40% to 90%. The hysteresis is very small. Therefore, it is obvious that both VHT and DBS application can significantly enhance the stability of humidity sensing performance of the textile sensors by reducing the relative resistance change from cyclic RH change.

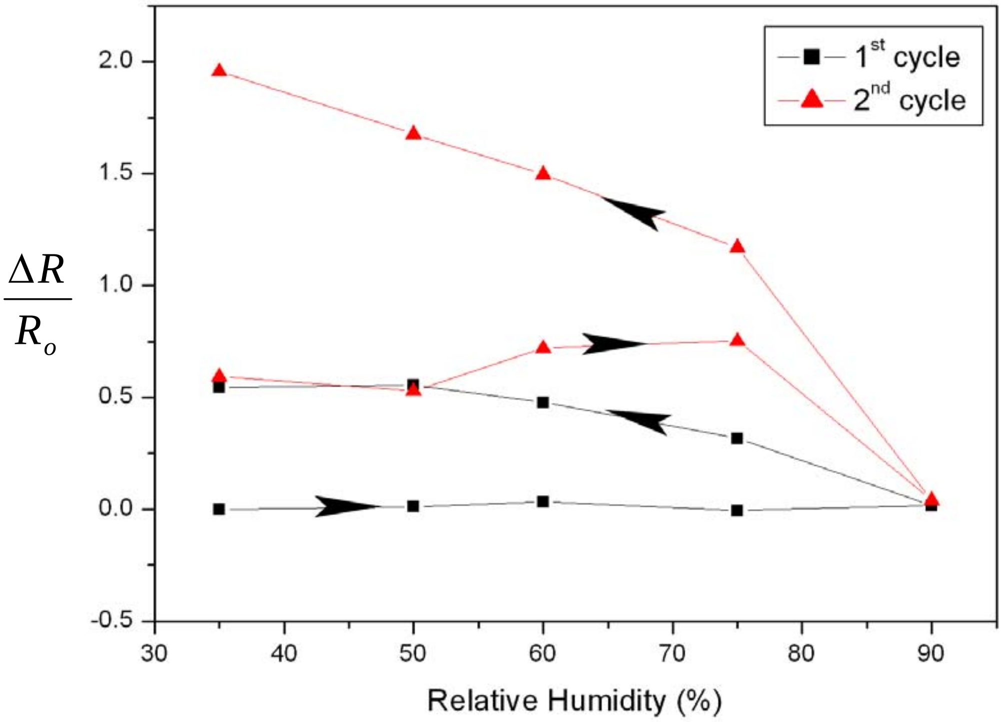

Figure 3.21 Cyclic humidity sensitivities of the untreated PPy-coated fabric (S1a)

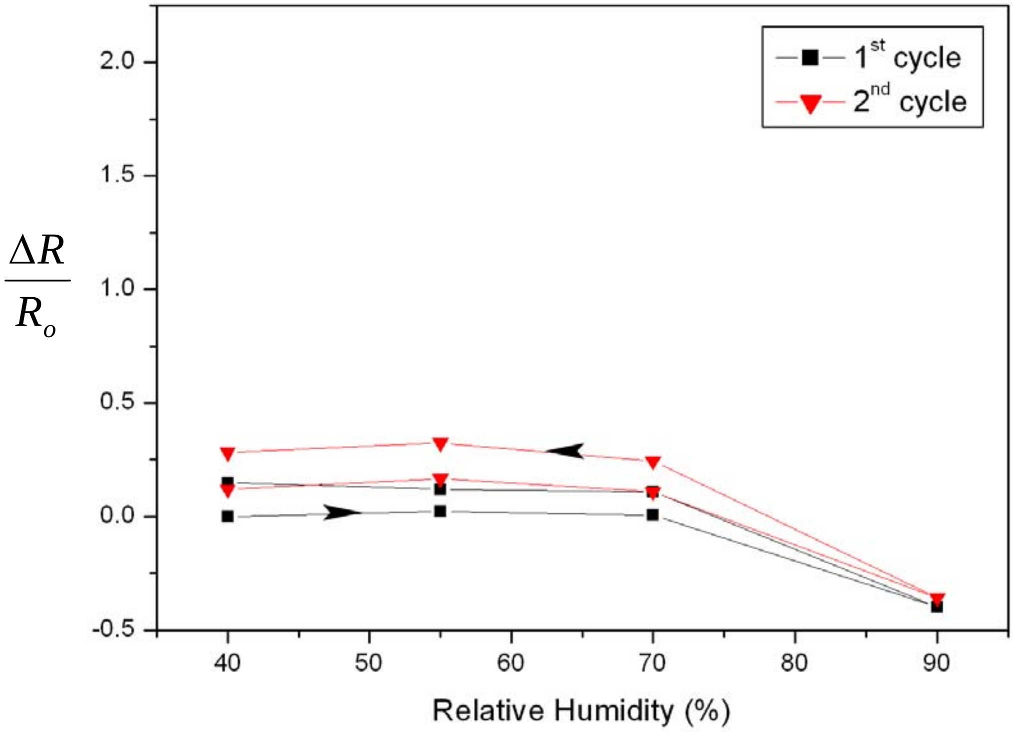

Figure 3.22 Cyclic humidity sensitivities of the PPy-coated fabric with VD + VHT (S2b)

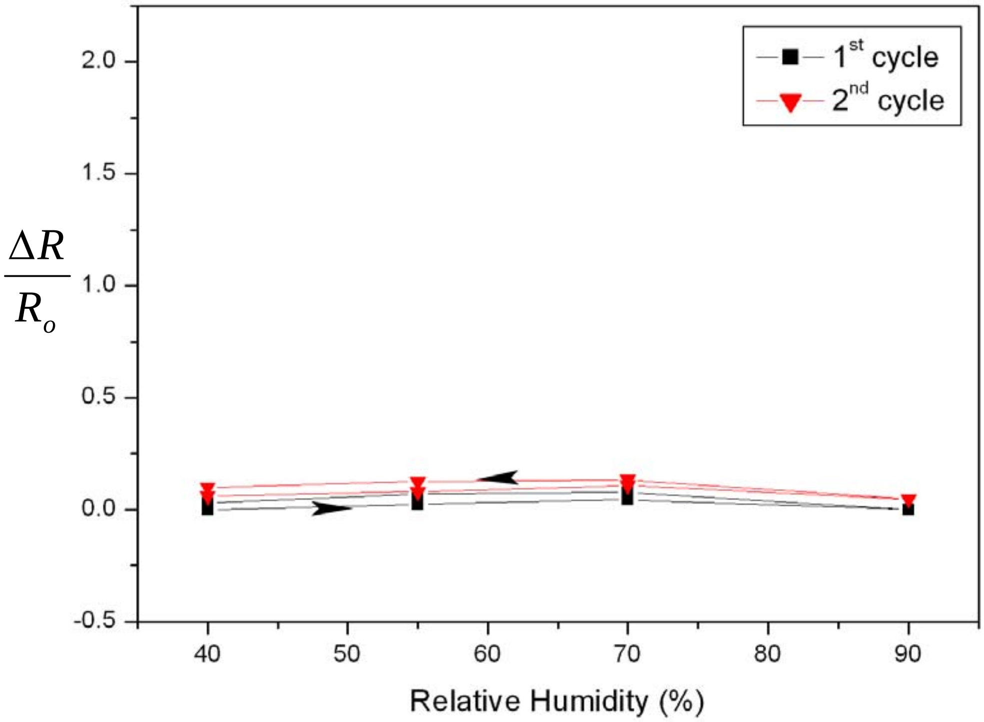

Figure 3.23 Cyclic humidity sensitivities of the PPy-coated fabric with VD + VHT + DBS treatment (S2c)

Long-Term Environmental Stability

Another direct indication of the stability is the variation of the conductivity and gauge factor of the sensor after a prolonged storage. Table 3.3 summarises the changes of electrical resistance and gauge factor of the PPy-coated fabrics with different proposed stabilisation treatments after storing the samples for 1 year. Figures 3.24 to 3.26 compare the relative resistance change of the PPy-coated fabrics with different stabilisation treatments under cyclic tension after storing for 1 year.

As for the sample that has no stabilisation treatment, the electrical resistance of the sensor increases more than 20000% compared to the initial resistance after storing for 1 year as shown in Table 3.3. As a result, its sensing curve of resistance change versus strain cannot be plotted due to very high initial resistance value before extension. All the three proposed stabilisation treatments can successfully reduce the resistance increment. However, the gauge factor values of the VD and VD + VHT treated samples are reduced to 50% and 30% respectively after storing for 1 year. As shown in Figures 3.24 and 3.25, some small peaks can be found on the sensing curves of the VD and VD + VHT treated samples after storage. It may be due to the decay of the PPy film coatings caused by the presence of air and water over a long period of time. When compared, the most stable sample is the VD + VHT + DBS treated PPy-coated fabric which can retain almost the same gauge factor of about 180. However, the resistance of the sample is increased approximately to 450%, i.e. from 60kΩ to 278.5kΩ after storing for 1 year. Figure 3.26 demonstrates the resistance change versus cyclic strain which shows that there is no significant change in the linearity and repeatability of the strain sensing curves except the first cycle.

Table 3.3 Resistance and gauge factor of the PPy-coated samples subjected to different stabilisation treatments

		Resistance		Gauge Factor[a]	
Sample No.	Treatment Methods	(R_o) (kΩ/in^2) [s.d.]	(R_{1yr}) (kΩ/in^2) [s.d.]	($\frac{\Delta R}{\varepsilon_{\max} R_o}$) [s.d.]	($\frac{\Delta R}{\varepsilon_{\max} R_{1yr}}$) [s.d.]
S1c	No Treatment	100 [2.33]	20308 [3732]	20 [1.33]	Overflow (over 120MΩ)
S2a	VD	20 [3.57]	3900 [153.6]	60 [8.04]	32 [5.34]
S2b	VD + VHT	20 [3.26]	218 [9.00]	110 [11.10]	80 [10.65]
S2c	VD + VHT + DBS	60 [6.44]	278.5 [8.45]	184 [11.49]	180 [9.80]

[a] strain = 50%

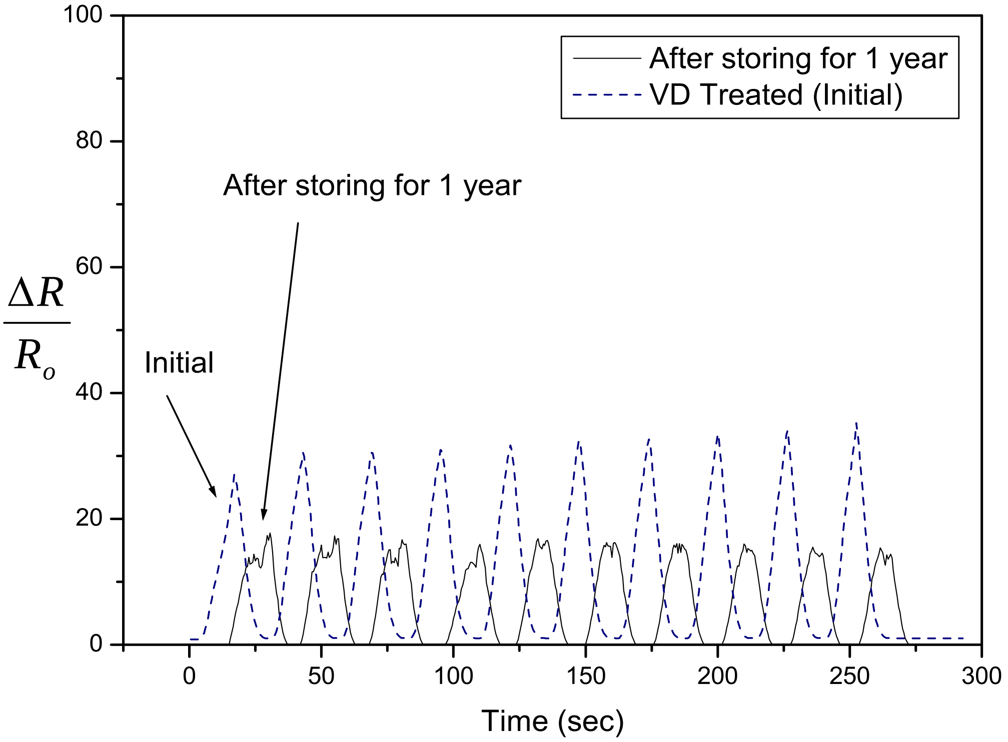

Figure 3.24 Relative resistance change as a function of time in a cyclic tensile test of the VD treated PPy-coated fabric before and after storage (S2a)

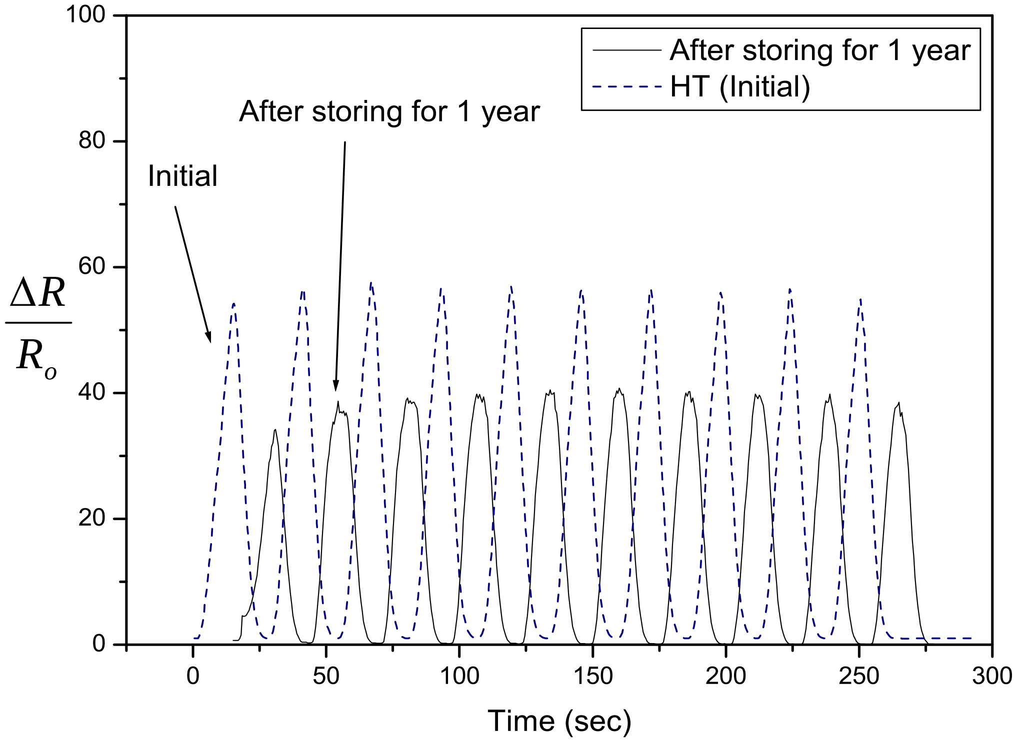

Figure 3.25 Relative resistance change as a function of time in a cyclic tensile test of the VD + VHT treated PPy-coated fabric before and after storage (S2b)

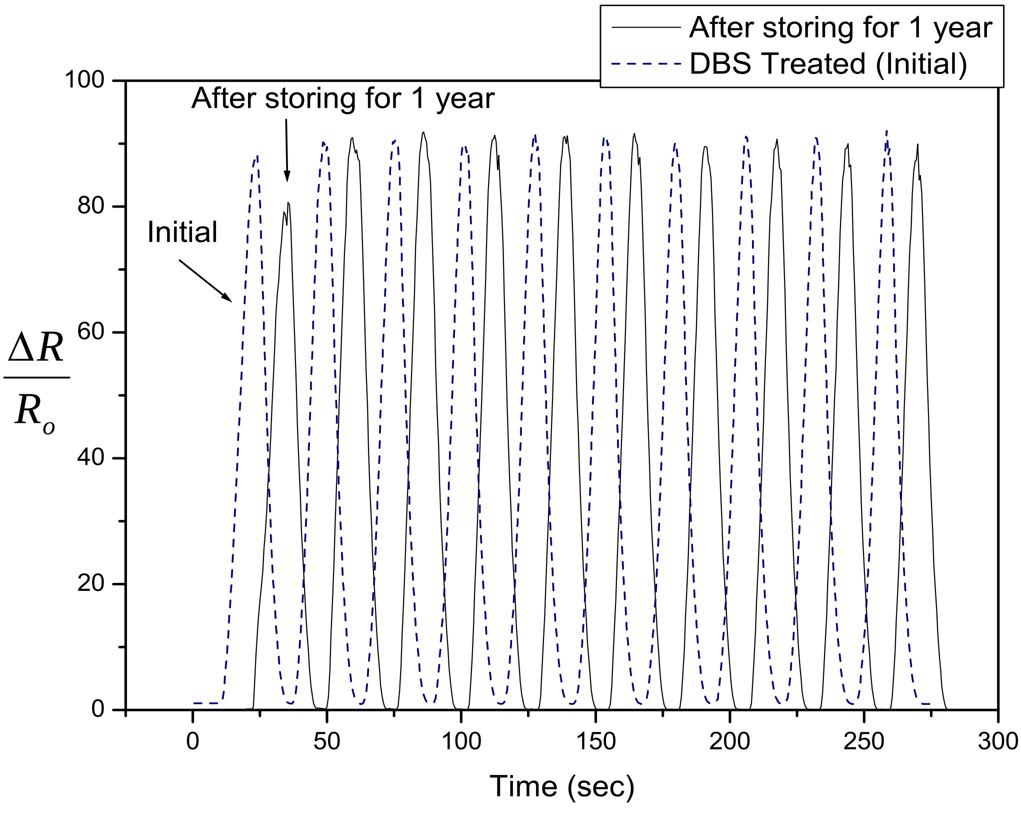

Figure 3.26 Relative resistance change as a function of time in a cyclic tensile test of the VD + VHT + DBS treated PPy-coated fabric before and after storage (S2c)

The results of the electrical conductivity, strain sensitivity, thermal and RH stability and long-term environmental stability show that the VD, VHT processes as well as the addition of DBS can improve the sensing performance of the fabric sensor. This is due to the fact that both stabilisation methods can change the characteristics of the PPy film structure and surface morphology owing to the thermal annealing effect induced by the VD and VHT, and large sized molecules trapped into the PPy film. The property of film structure and surface morphology are further investigated in the following sections.

3.4.3 Surface morphological study of PPy-coated fabrics

The surface morphology of PPy-coated fabric with different stabilisation treatments is depicted in Figures 3.27 to 3.29. According to the SEM photographs shown in Figures 3.28 and 3.29, the PPy-coated fabric samples with the VHT and DBS treatments exhibit compact and smooth surface morphology when compared with the untreated sample or only with VD treatment. These results agree with the findings obtained by Omastova, Pavlinec, Pionteck and Simon (1997) who found that the PPy films doped with DBS have a much smoother morphology than the cauliflower-like appearance of the PPy/Cl films.

It is found that the smoother and denser surface morphology of large anionic molecule DBS doped PPy coating can inhibit the penetration of oxygen resulting in greater environmental stability of the PPy film. The results of SEM examination further confirm the stability enhancement induced by the DBS application. These results fully agree with the findings obtained by Liu and Hwang (2001) which revealed that a more porous morphology and larger specific surface could facilitate the attacking gas diffusing into the film.

On the other hand, there is no significant change in the fibre diameters between the uncoated control sample, PPy-coated control sample and the PPy-coated samples with different stabilisation treatments as compared with the SEM photograph shown in Figure 3.5. The overall results illustrate that the stabilisation treatments greatly affect the surface morphology of the PPy coating but only have minor effect on the coating thickness deposited on textile substrates.

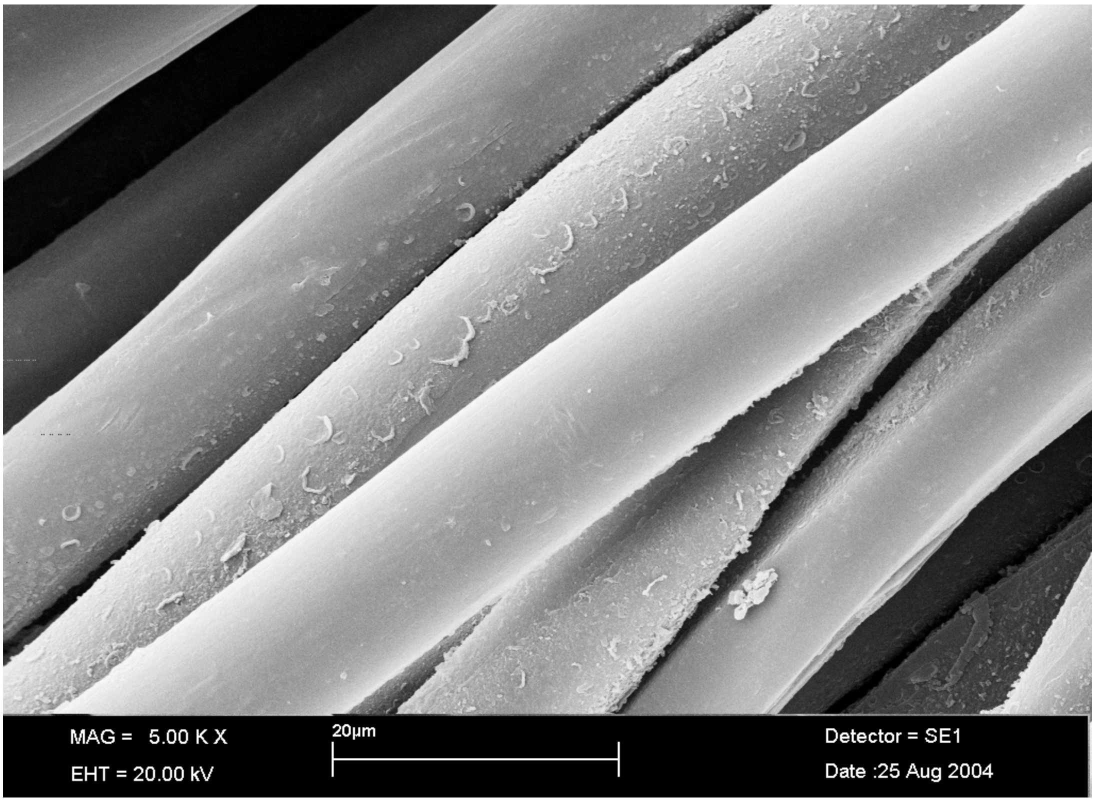

Figure 3.27 SEM photograph of the VD treated PPy-coated fabric (S2a)

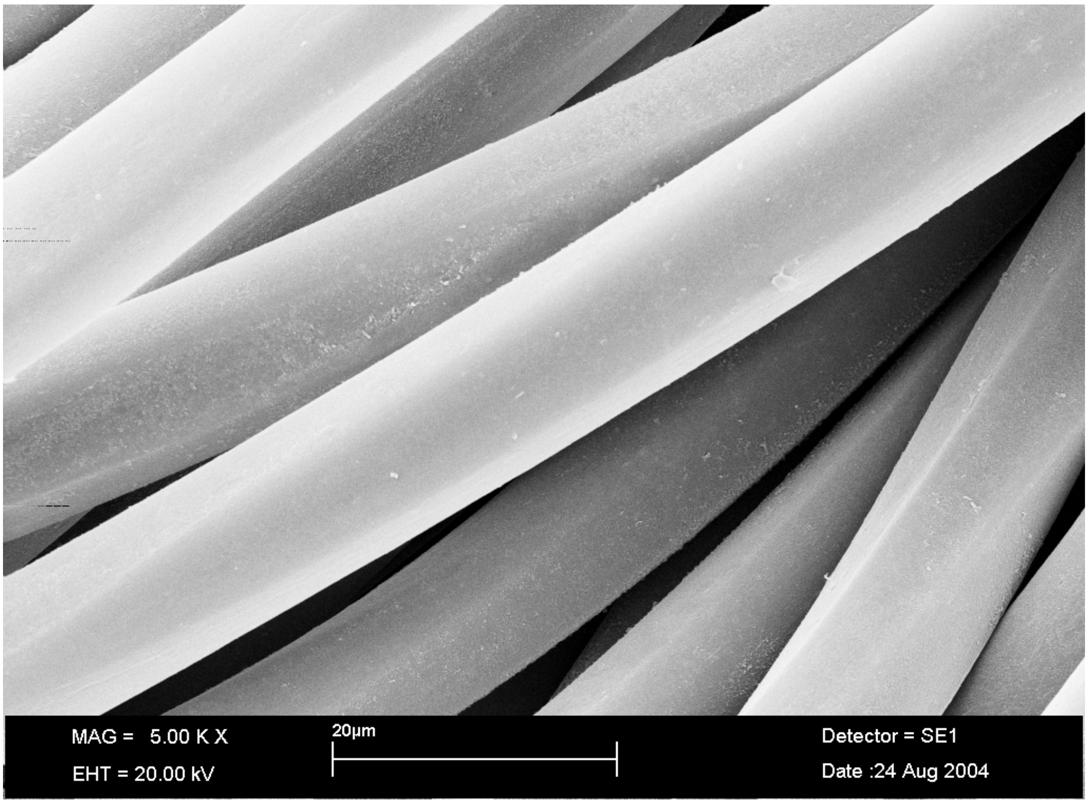

Figure 3.28 SEM photograph of the VD + VHT treated PPy-coated fabric (S2b)

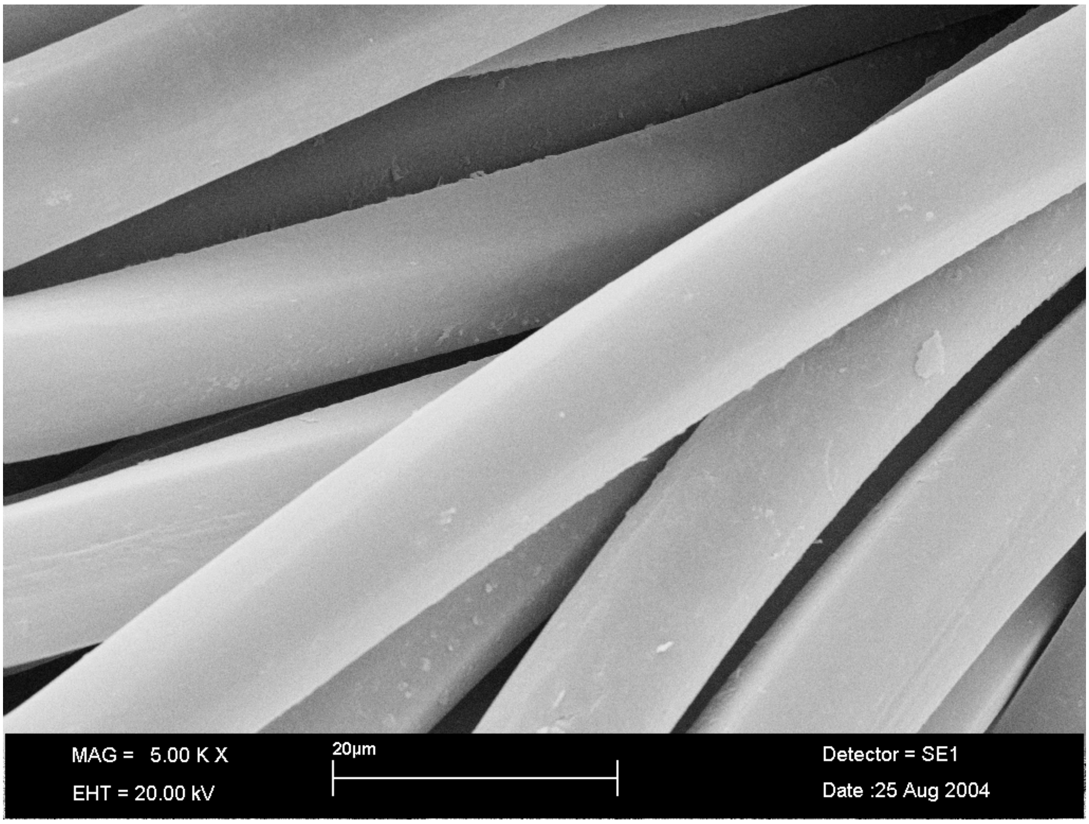

Figure 3.29 SEM photograph of the VD + VHT + DBS treated PPy-coated fabric (S2c)

3.4.4 Contact angle measurement

Review of literatures indicated that the instability of PPy coating in ambient conditions was mainly due to the reaction of the polymer backbone with either oxygen, water and/or harmful radiation. This led to an irreversible loss of the conjugation bonding resulting in reduced conductivity (Liu and Hwang, 2001; Thieblemont, Planche, Petrescu, Bouvier and Bidan, 1994). In order to verify this hypothesis, the property of fabric surface hydrophobicity was carried out by measuring the contact angle of water droplets on the fabric surfaces. It is anticipated that a more hydrophobic surface can obstruct water attack and thus improve the environmental stability.

Table 3.4 shows the contact angle of water droplet on the uncoated control fabric, the PPy-coated untreated fabric and the PPy-coated fabric with stabilisation treatments. The contact angle is 108° for the uncoated control Tactel/Lycra knitted fabric. As for the contact angles of the treated samples, the result indicates that the addition of PPy coating can slightly affect the surface tension of the fabric when compared with the droplet angle of uncoated control fabric, i.e. 110° and 108° respectively. Moreover, there is an increase in the contact angle of the fabrics from 110° to 112° and 114° when the PPy-coated fabric treated with VD, VD + VHT and VD + VHT + DBS application respectively. The results indicate that more hydrophobic surfaces of the PPy-coated conductive fabrics can be created using both the VHT and DBS stabilisation treatments. The hydrophobic surface is probably attributed to the higher density and orientation of the PPy coating. In order to verify the results, more advanced chemical analyses of the PPy-coating were conducted as shown in the following sections.

Table 3.4 Contact angle of water droplet on the PPy-coated fabrics

Sample No.	Treatment Methods	Contact Angle [s.d.]
Control	No PPy Coating	108° [1.41]
S1c	No Treatment	110° [2.12]
S2a	VD	110° [1.41]
S2b	VD + VHT	112° [0.00]
S2c	VD + VHT + DBS	114° [0.00]

3.4.5 X-ray Diffraction (XRD) Analysis

The comparison results of the wide angle XRD analysis of the uncoated control fabric and PPy-coated fabrics are presented in Figure 3.30 with the main peaks appearing at 2θ of 32.6°, 38.9°, 42.6° and 51° respectively. The X-ray diffraction of the Tactel/Lycra crystal shifts very little after the deposition of the PPy coating, indicating that the PPy coating is thin and the PPy so formed is mainly amorphous. The diffraction spectra obtained from the PPy pure powders with different treatments are shown in Figure 3.31. The results demonstrate that the majority of PPy powders are essentially amorphous, and also show the presence of a broad high-angle asymmetric scattering peak stretching from 2θ of 14.5° to 30°. The high-angle peak appearing at 2θ of 26.5° and the *d* spacing can be calculated through the Bragg's Law as following:

$$n\lambda = 2d\sin(\theta) \tag{3.2}$$

where *n* is the order of diffraction, λ is the wavelength of the incident X-ray beam (1.5418 Å) and *d* is the distance between atomic layers in a crystal.

Therefore, the *d* spacing of the high-angle peak appearing at 2θ of 26.5° is 0.34nm. The appearance of this peak is believed to be due to the location of the PPy chains close to the interplanar Van der Waals distance for aromatic groups (Cheah, Forsyth and Truong, 1998), which is corresponding to the interplanar spacing of the pyrrole chains. This diffraction peak observed in the PPy powder with VD + VHT + DBS application is sharper than that of the powder without treatment. The sharpest diffraction peaks obtained for the VD and VD + VHT powders indicating more ordered pyrrole chain structures can be obtained after the VD and VHT treatments.

The overall XRD results indicate that higher ordered orientation of PPy can be produced by the VD, VHT and DBS treatments. They can provide the fabric sensor with higher conductivity and better environmental stability. This is reflected by the electrical resistance of the PPy-coated fabric as shown in Tables 3.2 and 3.4. The VD + VHT + DBS treated sample demonstrates lower resistance, 60 kΩ, when compared with the untreated sample, 100 kΩ, respectively. However, the VD and VD + VHT treated samples exhibit the lowest electrical resistance of 20 kΩ.

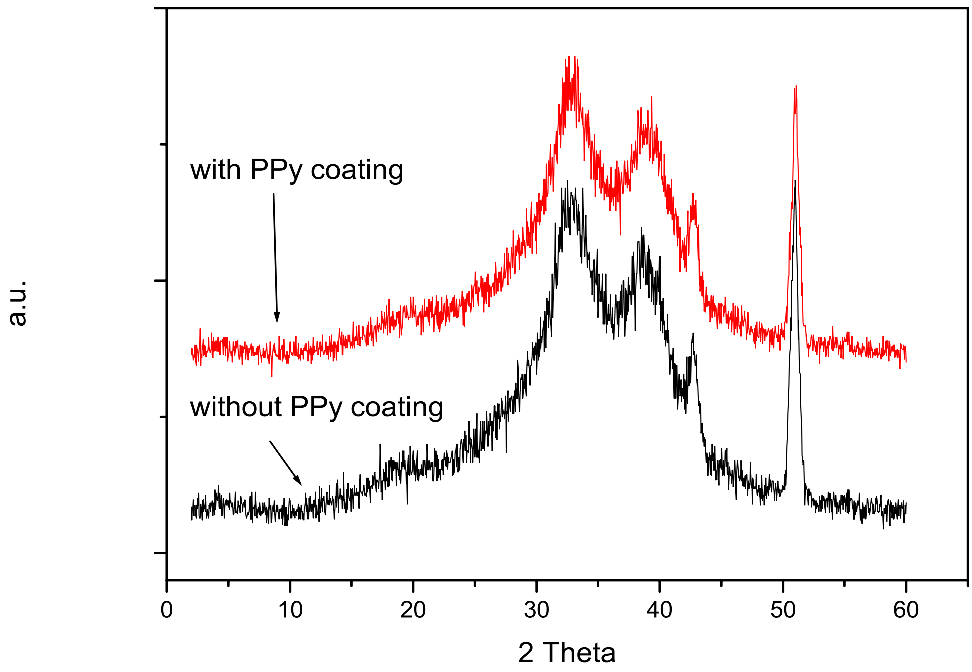

Figure 3.30 XRD patterns of uncoated control and PPy-coated fabric

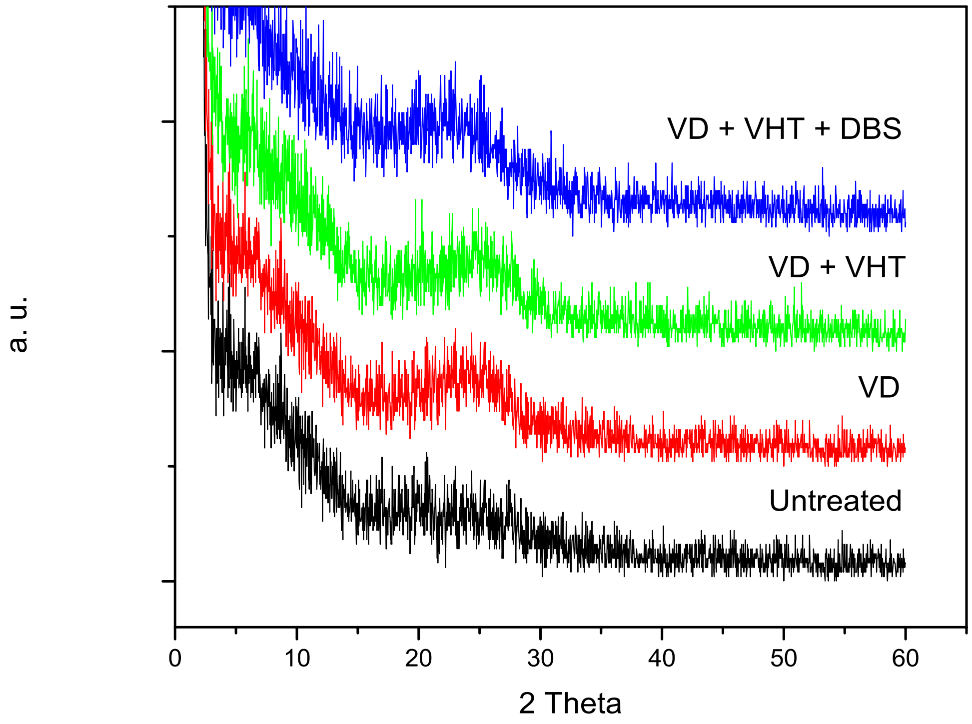

Figure 3.31 XRD patterns of PPy powders prepared with different stabilisation treatments

3.4.6 Thermal Analysis

TGA is useful to characterise the PPy-coated fabrics and pure PPy powders. It is a key indication of the thermal stability of the e-textile sensors. This technique is used to investigate the thermal behaviour of the PPy coating layers with different stabilisation treatments. The results of TGA are summarised in Table 3.5 and Figures 3.32 and 3.33.

Table 3.5 TGA data of the PPy powders prepared with different stabilisation treatments

Sample No.	Treatment Methods	1st Onset Temp (°C)	2nd Onset Temp (°C)	5% Weight Loss (°C)	Weight Loss at 100°C (%)
S3a	No Treatment	78.6	188.6	29.9	14.56
S3b	VD	72.3	211.8	48.5	7.35
S3c	VD + VHT	92.3	212.6	91.4	5.37
S3d	VD + VHT + DBS	86.1	221.7	166.2	3.8

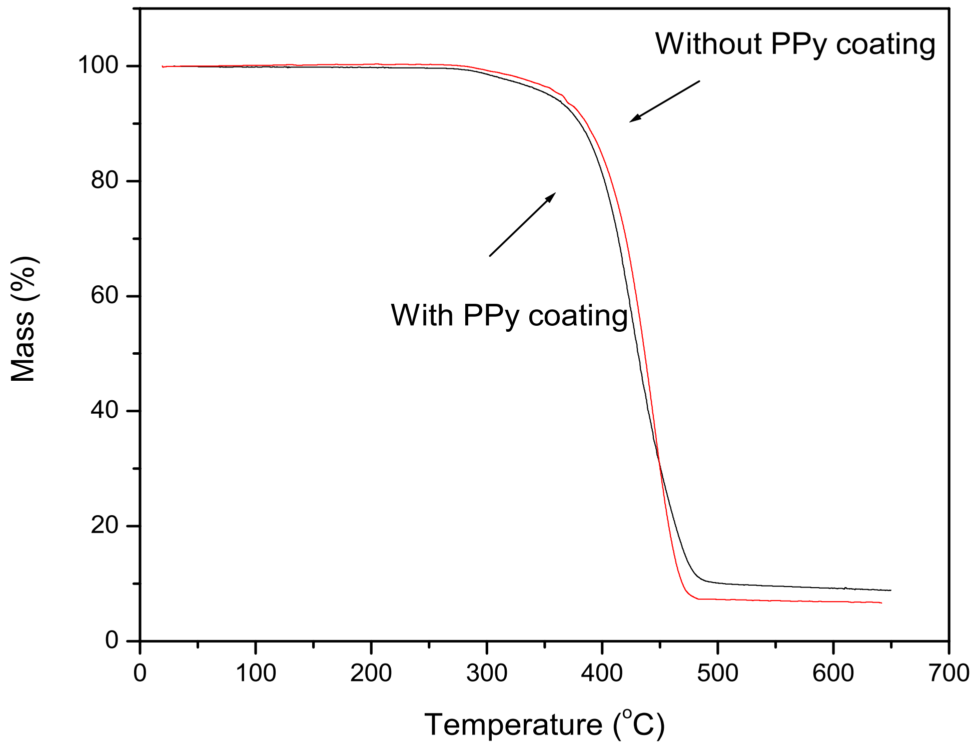

Figure 3.32 TG curves at 10°C min^{-1} in dry nitrogen of uncoated control and PPy-coated fabrics

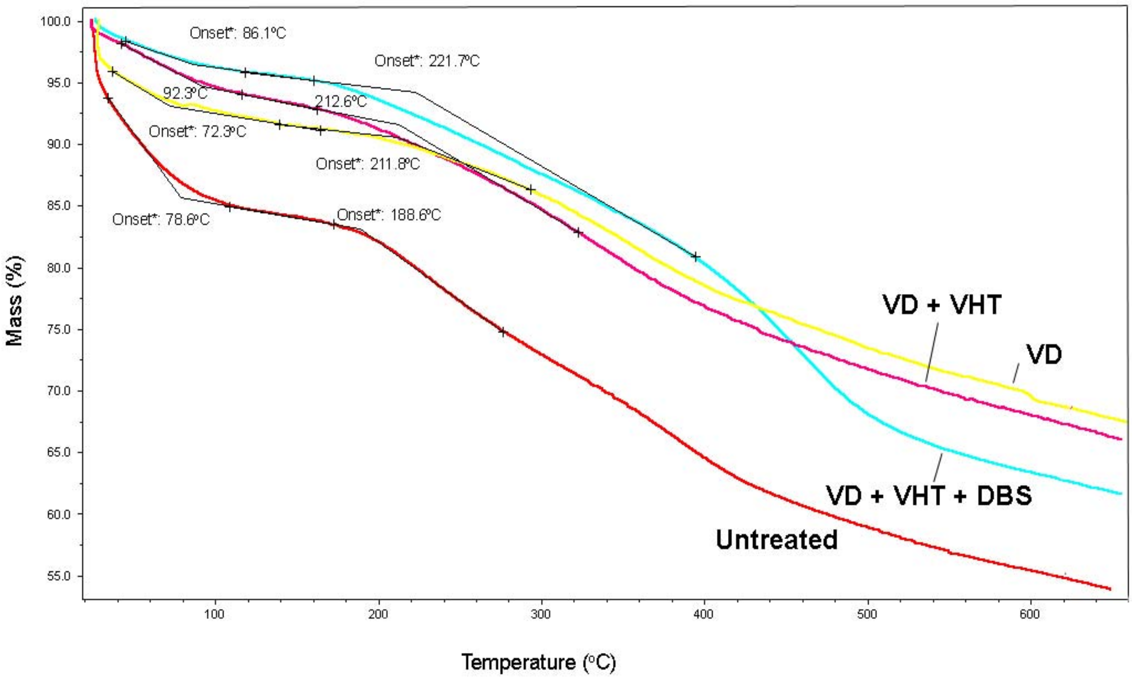

Figure 3.33 Comparison of TG curves at 10°C min^{-1} in dry nitrogen of PPy powders with different stabilisation treatments

Figure 3.32 exhibits TG curves of the uncoated control and PPy-coated untreated fabrics. The thermal stability of the fabrics changes very little after the deposition of the PPy coatings by the Print-CVD fabrication, which is probably due to very small content of PPy present on the conductive fabrics. In order to study the actual thermal behaviour of the PPy coatings treated with various stabilisation treatments, the TGA is conducted on the PPy powders as shown in Figure 3.33. The curves of mass loss versus temperature show two significant mass losses. The first that occurs at low temperature between 30°C and 100°C can be ascribed to the evaporation of water and residual washing solvents, i.e. ethanol, which has lower boiling point. This is in good accordance with the results reported by Cassignol *et al.* and Kang *et al.* (Cassignol, Olivier and Ricard, 1998; Kang, Neoh and Ong, 1991). It is noticed that the weight loss of the VD, VHT and DBS treated samples within the temperature range of 30°C to 100°C are lesser than the untreated sample. The weight loss of the untreated sample, the VD, VD + VHT and VD + VHT + DBS treated samples is 14.56%, 7.35%, 5.37% and 3.8% respectively. This may be due to the more hydrophobic nature of the treated samples. The results obtained from the thermal analysis are relevant to the results of contact angle measurement of the PPy-coated fabrics with different stabilisation treatments.

The second major mass loss observed at around 200°C of all curves is due to the decomposition of the polymer structures. It is found that the stabilisation treatments of the VD and VD + VHT as well as the VD + VHT + DBS treatment can improve the thermal stability of the PPy coating as reflected by the polymer degradation temperatures of 211.8°C, 212.6°C and 221.7°C respectively when compared to the untreated PPy powder which shows the degradation temperature of 188.6°C. It is concluded that doping with aromatic surfactants can further enhance the thermal stability of the PPy coating. This is probably due to the higher thermal stability of aromatic surfactants employed as dopant during the synthesis of the PPy powders.

The temperature that causes the weight loss of 5% increases dramatically from 30°C to 48.5°C, 91.4°C and 166.2°C for the untreated PPy powder, VD, VD + VHT and VD + VHT + DBS treated respectively. The untreated sample that undergoes the higher mass loss is suspected to have a greater affinity for water than the treated samples. This is also supported by the results of contact angle measurement of the PPy-coated fabrics, which show that the treated samples have greater fabric hydrophobic surface. As a result, it is evident that all the stabilisation treatments can improve the thermal stability of the PPy coated fabrics.

It can be concluded that the DBS application can significantly enhance the thermal stability of the PPy-coated fabrics. The results agree with the finding of Khalkhali and Keivani (2005). They had studied the thermal stability of the PPy films prepared with different dopants during synthesis, such as PPy/BS benzene sulphonate, PPy/PTS toluene sulphonate, PPy/DNS 1,5-naphthalenedisulphonate, PPy/DS sodium dodecyl sulphate and PPy/DBS. Of all the organic dopants being studied, they found that the benzene based dopants producing more thermally stable polypyrrole films with superior conductivity and mechanical properties as well.

3.5 Implementation of the Most Promising Stabilisation Treatment to the Other Fabrication Methods

From the above results of three stabilisation treatments, it is discovered that the combination of all 3 stabilisation treatments will give the most promising result of sensing performance as well as environmental stability. The procedure of stabilisation treatment is firstly (i) addition of DBS dopant during fabrication, (ii) then VD the PPy-coated fabric and finally (iii) VHT conducted for stabilising PPy-coated fabric. In order to verify this stabilisation treatment is applicable to the other fabrication methods as well, the study of the sensing performance and long term stability of PPy-coated fabrics fabricated by SP and Pad-CVD with the most promising stabilisation treatment has been conducted and summarised as follows.

The experimental results of PPy-coated fabrics prepared by SP and Pad-CVD with the most promising stabilisation treatment are summarised in Table 3.6. It shows that the conductivity can be improved with the stabilisation treatment on the PPy-coated fabrics prepared by CVD method. Furthermore, it is obvious that the stabilisation treatment can also improve the strain sensitivity for both fabrication methods. It demonstrates that the samples prepared by CVD methods with stabilisation treatment performed better environmental stability as the strain sensitivity can almost maintained as original, the strain sensitivity only loss 10% for the samples prepared by Pad-CVD, however, 26% strain sensitivity loss for the SP samples after 1 year storage.

Table 3.6 Initial resistance and gauge factor of PPy-coated samples subjected to different fabrication methods with DBS + VD + VHT

		Resistance			Gauge Factor[a]		
Sample No.	Fabrication Method	Untreated	DBS + VD + VHT		Untreated	DBS + VD + VHT	
		(R_o) (kΩ/in^2) [s.d.]	(R_o) (kΩ/in^2) [s.d.]	(R_{1yr}) (kΩ/in^2) [s.d.]	$(\frac{\Delta R}{\varepsilon_{\max} R_o})$ [s.d.]	$(\frac{\Delta R}{\varepsilon_{\max} R_o})$ [s.d.]	$(\frac{\Delta R}{\varepsilon_{\max} R_{1yr}})$ [s.d.]
S4a	SP	14	19.2	93	6	17	12.5
		[1.97]	[2.94]	[14.72]	[0.72]	[1.10]	[2.47]
S4b	Pad-CVD	98	87	526	9	56	50
		[9.47]	[11.65]	[81.97]	[1.70]	[5.72]	[8.82]

[a] strain = 50%

The relative resistance change versus strain of the PPy-coated fabrics prepared by SP and Pad-CVD with stabilisation treatment is shown in Figures 3.34 and 3.35. By comparing the strain sensitivity of samples under cyclic large strain, the stabilisation treatment still can possess good linearity and repeatability of the sensing curves. Furthermore, it exhibits minor changes of the sensing curves of samples after 1 year of storage. It is concluded that the most promising stabilisation treatment can be implemented to different fabrication methods for producing the PPy-coated fabrics. The stabilisation treatment can enhance the sensing performance and environmental stability of the PPy-coated fabrics.

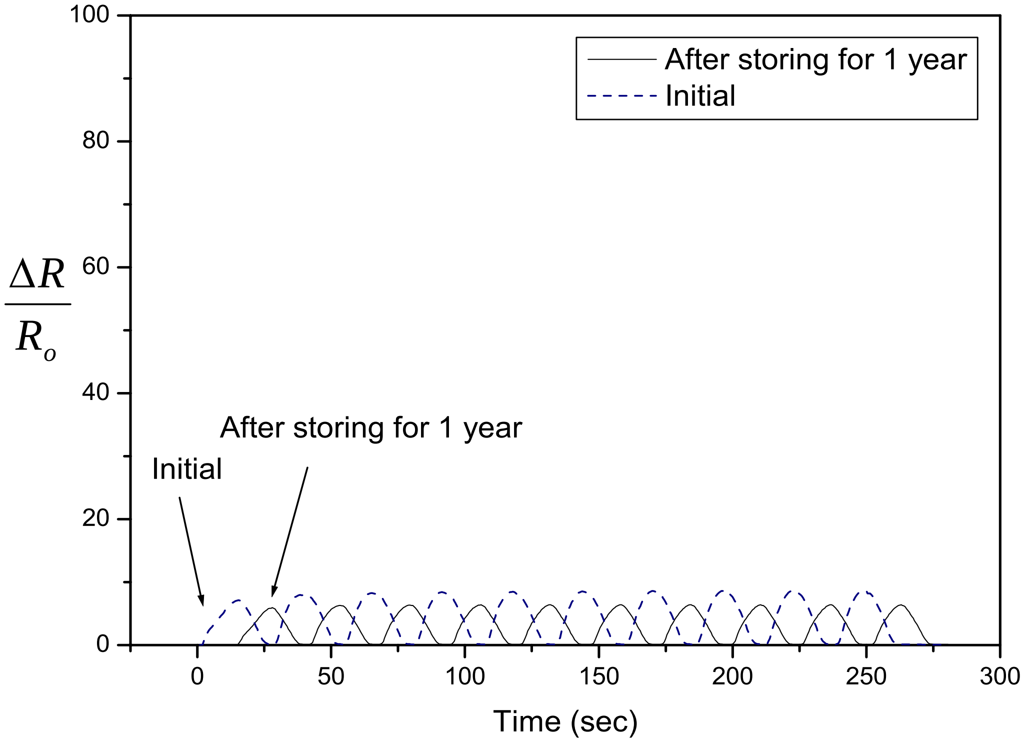

Figure 3.34 Relative resistance change as a function of time in a cyclic tensile test of the stabilisation treated PPy-coated fabric before and after storage that fabricated by SP (S4a)

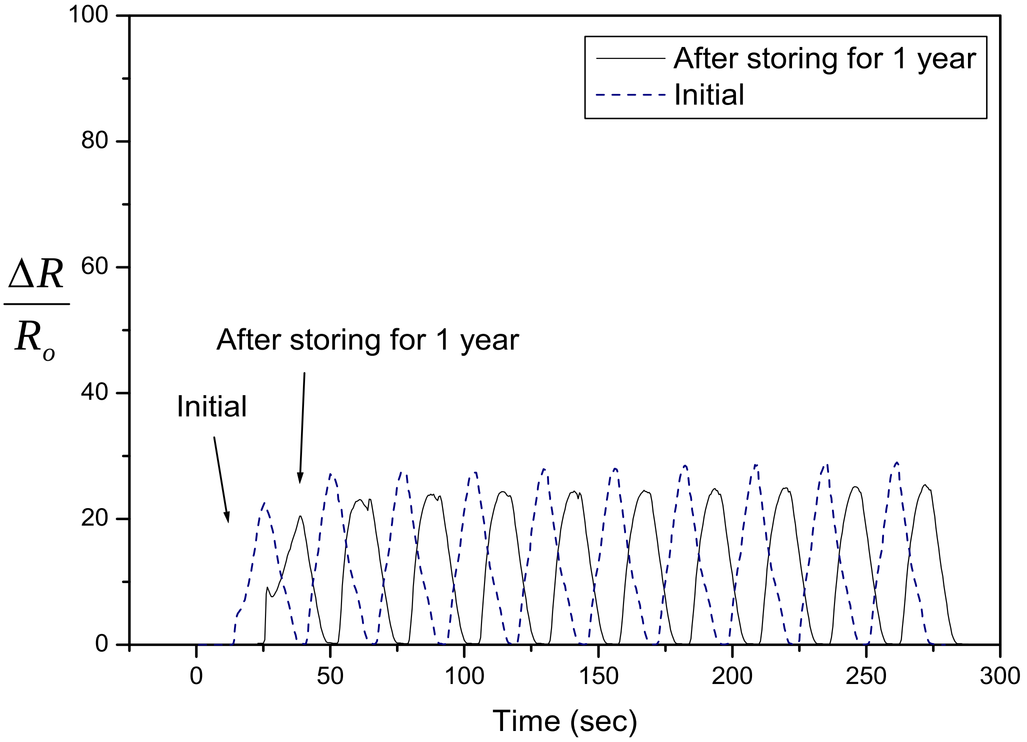

Figure 3.35 Relative resistance change as a function of time in a cyclic tensile test of the stabilisation treated PPy-coated fabric before and after storage that fabricated by Pad-CVD (S4b)

3.6 Concluding Remarks

The sensing performance, including electrical resistance, strain sensitivity and environmental stability of PPy-coated fabrics with different treatments such as the VD and VHT as well as DBS dopant application, has been studied. The experimental results reveal that the proposed VHT method can significantly enhance the gauge factor without affecting the initial resistance and the repeatability of the sensing function. Furthermore, the samples fabricated with DBS and subjected to vacuum heat treatment can also significantly improve the environmental stability of electrical conductivity. The proposed stabilisation treatments are very suitable for the PPy-coated stretchable sensors containing spandex or elastane materials.

After investigating the three proposed stabilisation treatments, it is discovered that the combination of all 3 stabilisation treatments will give the most promising result of sensing performance as well as environmental stability. The procedure of stabilisation treatment is firstly (i) addition of DBS dopant during fabrication, (ii) then VD the PPy-coated fabric and finally (iii) VHT conducted for stabilising PPy-coated fabric. It is found that very thin, smooth and continuous PPy coating layer can be formed on the fibre surface by means of the developed CVD fabrication process. The PPy-coated fabrics produced by the CVD methods possess very good strain sensitivity and environmental stability when compared with conventional SP fabrication method.

CHAPTER 4

EFFECT OF FABRICATING TEMPERATURE ON SENSING PERFORMANCE

4.1 Introduction

Various fabrication and stabilisation methods have been discussed in Chapter 3. In this chapter, the effect of fabrication temperature on the sensing capacity of polypyrrole (PPy)-coated conductive fabrics is further studied. It is believed that polymerisation temperature can affect the interface, structure and morphology of PPy films coated on textile fabrics and their sensing performance. Recently, there have been some reports concerning the low temperature (LT) polymerisation of PPy synthesis. The effect of synthesis parameters on the particle size and conductivity of the resulting PPy-silica colloidal nano-composites had systemically studied (Lascelles, Mccarthy, Butterworth and Armes, 1998). It was found that polymerisation at 0°C led to nano-composites with the highest conductivities and smaller particle diameters. The lowest temperature polymerisation of PPy reported by Yoon *et al.* showed that higher conductivity of pure PPy film was produced by electrochemical polymerisation at -40°C (Yoon, Sung, Kim, Barsoukov, Kim and Lee, 1999).

For the development of PPy-coated fabrics, Kaynak and Beltran (2003) also proposed that the LT polymerisation of pyrrole conducted at 5°C on the surface of poly(ethylene terephthalate) (PET) fabrics could help to obtain thinner coatings resulting in more adherent film and more ordered structure of PPy with higher conductivity. LT polymerisation of conducting polymer by vapour deposition concerned about the development of conducting polymers for biomedical applications was reported (Jiang, Tessier, Dao and Zhang, 2002). The authors introduced a 3-steps method combining gas phase phosphonylation with vapour deposition for PPy polymerisation at 4°C.

In the literature, the aim of adopting LT for the synthesis of PPy films or PPy-coated fabrics is mainly for enhancing the stability of conductivity. There is no report discussing the effect of LT polymerisation on the strain sensing capacity and long term environmental stability of the PPy-coated fabrics which are critical for the development of e-textile strain sensor. Comparative studies of the effect of polymerisation temperature on the coating interface, structures and morphology of the PPy-coated fabrics as well as the strain sensing properties are discussed in this chapter.

4.2 Experimental

4.2.1 Materials and sample fabrication

4.2.1.1 PPy-coated fabrics

The materials and fabrication methods used for producing room temperature (RT) PPy-coated fabrics are the same as those stated in Chapter 3. For the samples prepared by LT, the chemical vapour deposition (CVD) was conducted under vacuum set at -760mmHg and -25°C for 72 hours. 10 minutes was required to achieve the set value. All the samples are treated with the stabilisation treatments including sodium dodecylbenzenesulphonate (DBS) application and vacuum drying (VD) at 40°C in a vacuum oven set at -760mmHg for 16 hours. The annealing process was also carried out by heating the dried fabrics at 60°C for 40 hours in a vacuum oven set at -760mmHg.

4.2.1.2 PPy-coated fibres

The materials used were polyamide (PA6) multi-filaments with triangular profile in 78 denier/51F and polyurethane (PU, Lycra) in 140 denier/12F, which were supplied by Dupont. Figures 4.1 (a & b) show SEM photographs of the cross sectional features of PA6 and PU fibres. The fabrication of PPy-coated fibres is similar to the fabrication method of Pad-CVD. The major difference between them is using filter paper instead of padding to remove the excessive solution on the fibres after immersed into the aqueous and ethanol solutions. The fabrication procedures are stated in the following.

Individual yarns were mounted on a sample holder in relaxed state as shown in Figure 4.2. Four sample holders with yarns were firstly immersed into an aqueous solution containing DBS (0.011 mol/L) for 15 minutes and then an ethanol solution of ferric chloride hexahydrate ($FeCl_3{\cdot}6H_2O$) (0.1 mol/L) for another 15 minutes. They were then transferred to a desiccator containing 10ml of pyrrole for CVD. Vapour phase polymerisation was carried out under vacuum set at -760mmHg and -25˚C (LT) for 72 hours or at room temperature 21˚C (RT) for 24 hours. 10 minutes was required to achieve the set value. After the CVD process, a layer of PPy-coating was formed on the fibre surface. The coated yarns were then washed thoroughly and vacuum dried at 40˚C for 16 hours in a vacuum oven set at -760mmHg. The annealing process was then carried out by heating the dried yarns at 60˚C for 40 hours in a vacuum oven set at -760mmHg.

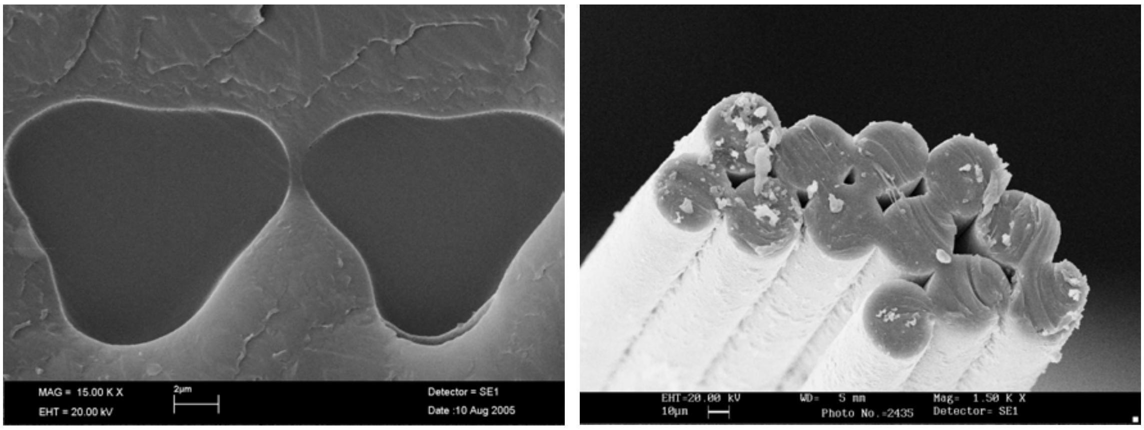

(a) (b)

Figure 4.1 SEM photographs of the cross section of (a) PA6 fibres and (b) PU fibres

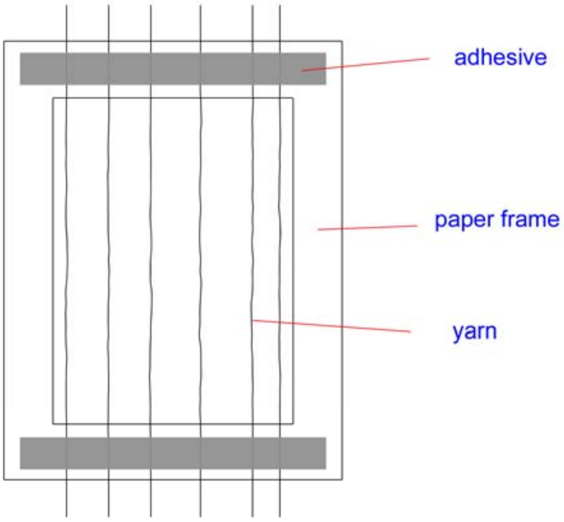

Figure 4.2 Schematic drawing of a yarn sample to be fabricated

4.2.1.3 Pure PPy powders

The emulsion was firstly prepared by using 1900ml of white spirit, 400ml of water and 50g of emulsifier with well mixing and stirring. A layer of print paste containing 200g of emulsion, 30g of $FeCl_3{\cdot}6H_2O$ and solution of 6.54g of DBS in 30ml of deionised water was applied onto a glass plate and then transferred to a desiccator containing 10ml of pyrrole for CVD. Vapour phase polymerisation was carried out under vacuum set at -760mmHg and 21˚C for 24 hours or -25˚C for 72 hours. 10 minutes was required to achieve the set value. After the CVD process, pure PPy powder was formed on the surface of glass plate. The powder was then washed thoroughly with de-ionised water followed by rinsing with ethanol and VD at -760mmHg and 40˚C for 16 hours in a vacuum oven. Vacuum heat treatment (VHT) was also carried out by heating the dried powders at 60˚C for 40 hours in vacuum oven set at -760mmHg.

4.2.2 Characterisation of the PPy-coated fibres and fabrics

The characterisation methods and procedures of the PPy-coated fabrics and pure PPy powders have been reported in Chapter 3. Other characterisation methods of the PPy-coated yarns and PPy powders are summarised in the following.

Electro-mechanical tensile test of the PPy-coated yarns

The electrical resistance of the PPy-coated yarns was measured by the two-probe method with a Keithley 2010 multi-meter while they were extended. The load and deformation were obtained and recorded by an Instron mechanical testing system (Model 4466). A single yarn was attached vertically to a piece of paper of 100mm apart with a rectangular hole cut in the centre as shown in Figure 4.3. The single yarn was clipped vertically by two pairs of copper plates with a gauge length of 25.4mm as shown in Figure 4.4. Prior to the application of a vertical tensile load, the paper was cut horizontally along the dashed line as shown in Figure 4.3. The crosshead speed was 2mm/min. At least three specimens from each sample were tested and the average value was taken. Moreover, cyclic test with five consecutive cycles of unidirectional extension up to 50% was also carried out by the same setup of tensile test but with the crosshead speed of 5mm/min. All electro-mechanical tests were carried out at 21˚C and 65% RH. The strain sensitivity of a yarn sensor as represented by the gauge factor in Equation 3.1 is also calculated.

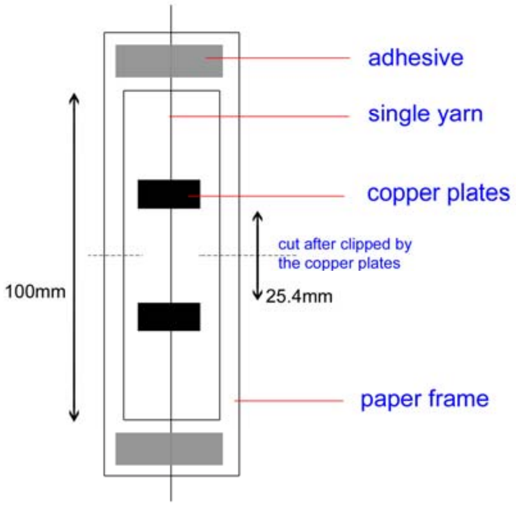

Figure 4.3 Schematic diagram of a yarn sample mounted in a frame

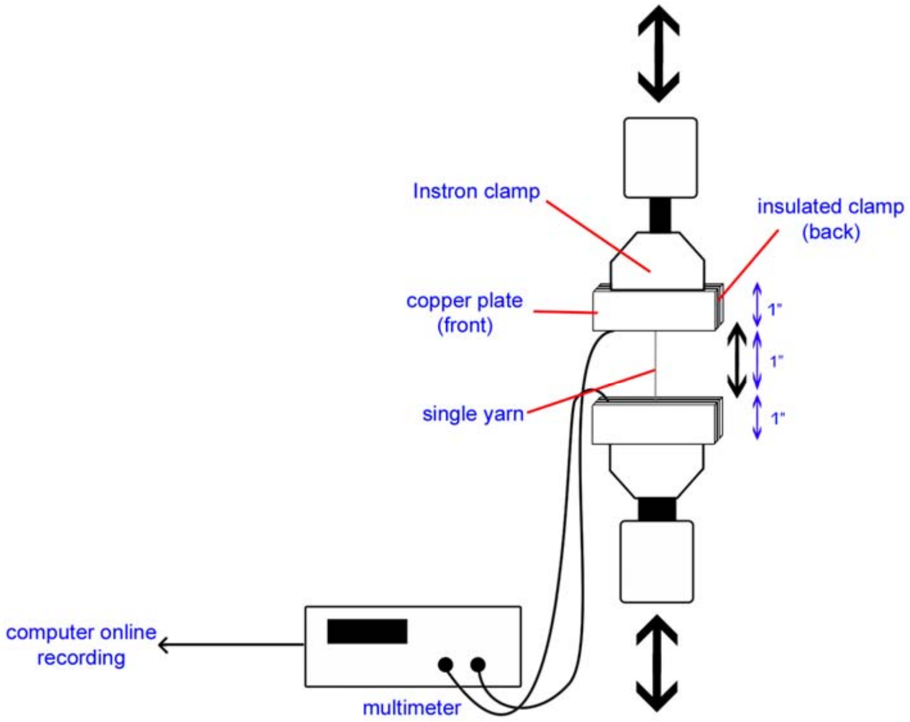

Figure 4.4 Schematic diagram of instrument setup for electrical resistance and strain sensitivity testing of the PPy-coated yarns

Fibres Morphology Study

The measurement with Dynamic force microscope (DFM) mode was carried out by using a scanning probe microscope system (SPM Model Seiko SPI4000 series) under ambient conditions. Standard silicon nitride tip was used. Topographical and phase images with the scanned area of 2µm x 2µm and 1µm x 1µm of the PPy coating on the PA6 and PU fibres were obtained. In addition, analysis of the grain size and surface smoothness of the PPy-coated PU fibres with the scan area of 1µm x 1µm were also conducted by SPM.

Coating Thickness Study

The PPy-coated PA6 fibres were embedded into a mold with resin, and then cut by ultra-microtome to form thin and smooth slices. The slices were scanned by SPM and the cross-sectional images of fibres were reported. Surface potential detection of the standard Tapping Mode measurement was carried out by a SPM system (Digital Instruments NanoScope IV) under ambient conditions. Standard silicon nitride tip was used. Surface topographical and surface potential images with the scanned area of 37µm x 37µm and 10µm x 10µm respectively of the PPy coated PA6 fibres were obtained.

Particle Size Analysis

Particle size analyser (Beckman Coulter LS13320 series) with Universal Liquid Module and Polarised Intensity Differential Scattering (PIDS) system was utilised for measuring the particle size of PPy pure powders. The range of particle size being detected was 40nm to 200 µm and the sample scanning was repeated with 4 times.

4.3 Effect of Polymerisation Temperature on the Sensing Performance of the PPy-Coated Fabric Sensors

Three aspects of fabric sensor, namely electrical conductivity, strain sensitivity and environmental stability, are involved in the study. The comparison between the PPy-coated fabrics prepared at RT and LT is conducted.

4.3.1 Electrical resistance and strain sensitivity

The experimental results of the PPy-coated fabrics fabricated by different polymerisation temperatures and various fabrication methods namely solution polymerisation (SP), screen printing followed by CVD (Print-CVD) and padding followed by CVD (Pad-CVD) are shown in Table 4.1. It is obvious that the PPy-coated fabrics prepared by the polymerisation at LT exhibit lower initial resistance (R_o) and higher strain sensitivity when compared with the fabric sensors produced at RT. The lowest electrical resistance, i.e. 8.76k kΩ/in^2, and the highest gauge factor, i.e. 450, obtained by the LT Pad-CVD respectively, the results are 10 times and 8 times better than those of the RT Pad-CVD.

Table 4.1 Changes in resistance and gauge factor of the PPy-coated fabrics subjected to different polymerisation temperatures

Sample No.	Treatment Methods	Resistance (R_o) (kΩ/in^2)		Gauge Factor[a] $(\frac{\Delta R}{\varepsilon_{\max} R_o})$	
		RT [s.d.]	LT [s.d.]	RT [s.d.]	LT [s.d.]
S4a & S5a	SP	19.2 [2.94]	16 [1.06]	17 [1.10]	20 [4.47]
S4b & S5b	Pad-CVD	87 [11.65]	8.76 [0.66]	56 [5.72]	450 [47.5]
S2c & S5c	Print-CVD	60 [6.44]	11.5 [3.35]	184 [11.49]	230 [32.6]

[a] strain = 50%

The results shown in Table 4.1 are in good accordance with other investigations concerning the effect of polymerisation temperature on the electrical conductivity of PPy films. Rodriguez, Grande and Otero (1997) found that the electro-polymerisation temperature had a substantial influence on the kinetics of polymerisation as well as on the conductivity, redox properties and mechanical characteristics of the film. According to the study of Lee (2001), the PPy films prepared in propylene carbonate solution at -20°C were much more conductive, i.e. 300S cm^{-1}, than those prepared at 20°C, i.e. 97 S cm^{-1}. Spectral analysis of the material prepared at the lower temperatures shows a more regular structure. At higher temperatures, the side-reactions such as solvent discharge and nucleophilic attacks on polymeric radicals cause the formation of more structural defects, resulting in lower conductive films.

By comparing the strain sensitivity of samples under cyclic large deformation as shown in Figures 4.5 to 4.7, the fabrication methods of LT CVD, including LT-Print-CVD and LT-Pad-CVD, demonstrate significant increase in the strain sensitivity of the PPy-coated fabric when compared to the LT SP. Very high strain sensitivity factors, i.e. about 230 and 450 at 50% strain, are achieved. Under 10 consecutive extension-recovery cycles, the sensing curves of those samples prepared by LT indicate very good linearity and repeatability. The strain sensitivities of the PPy-coated fabrics fabricated by the LT CVD methods are tremendously higher than those obtained by other researchers as reviewed in Table 2.1 of Chapter 2.

CVD fabrication method is better than solution polymerisation at both RT and LT because CVD can produce PPy coating layer in more thinner and orderly oriented distribution on the textile substrate which is beneficial to higher strain sensitivity and stability. The sensing performance of the PPy-coated fabric is highly dependent on the polymerisation temperature.

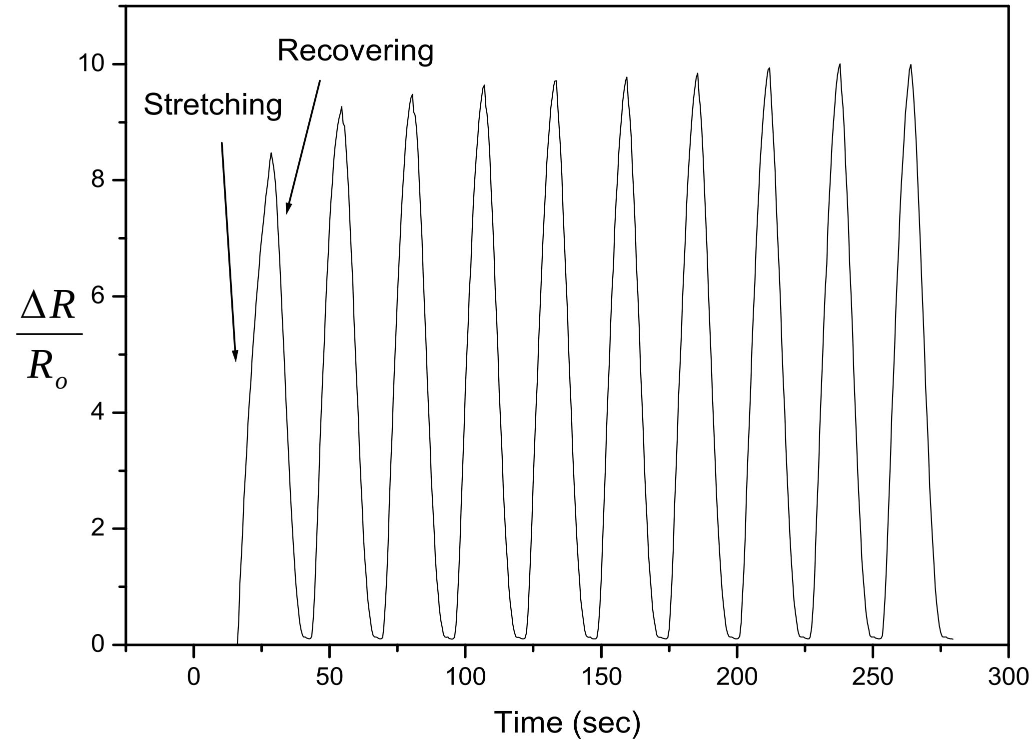

Figure 4.5 Relative resistance change as a function of time in a cyclic tensile test of the PPy-coated fabrics fabricated by LT-SP (S5a)

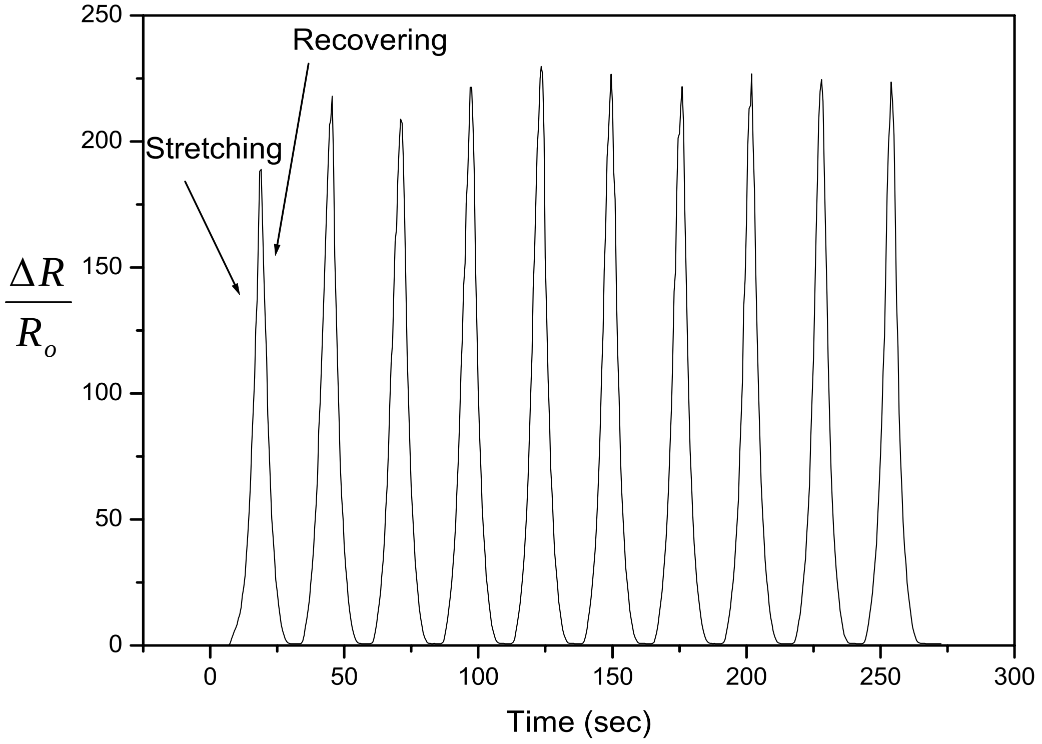

Figure 4.6 Relative resistance change as a function of time in a cyclic tensile test of the PPy-coated fabrics fabricated by LT-Pad-CVD (S5b)

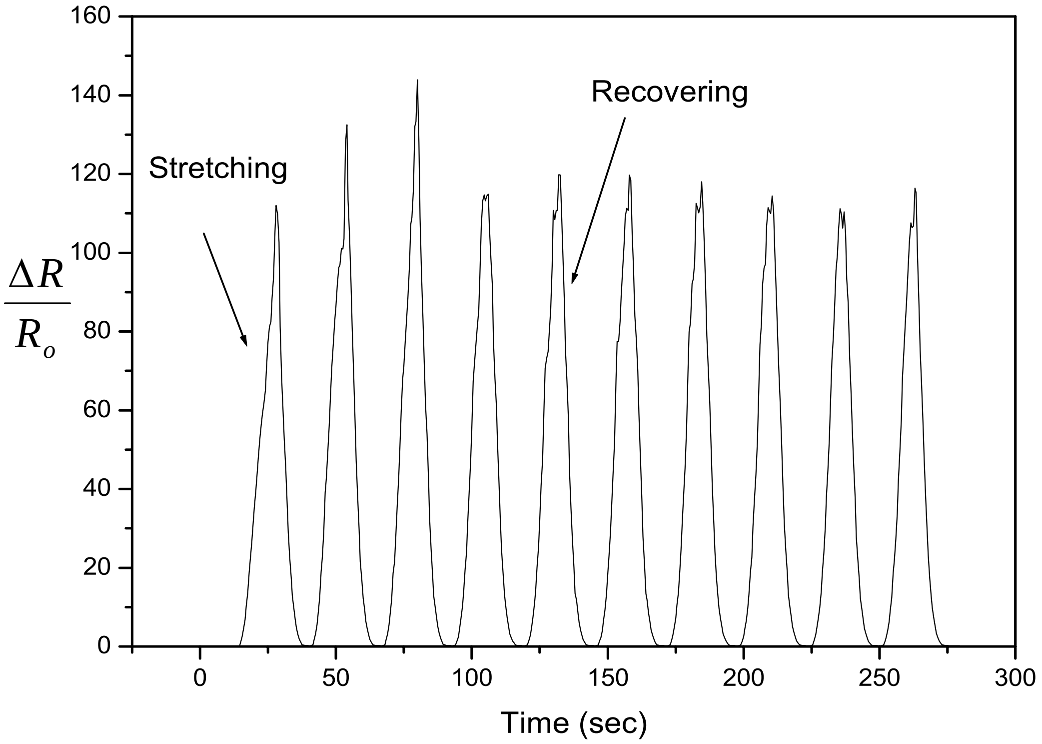

Figure 4.7 Relative resistance change as a function of time in a cyclic tensile test of the PPy-coated fabrics fabricated by LT-Print-CVD (S5c)

4.3.2 Environmental stability

Stability is essential to the textile strain sensors. A direct indication of the stability is the extent of variation of the conductivity of sensor after a prolonged storage. The electrical resistances and gauge factor changes after storing for one year is shown in Table 4.2. It is found that the change in electrical resistance of the sensor prepared at RT varies is around 450% after storing for one year. However, the sensor prepared by LT polymerisation dramatically reduces the change in electrical resistance after one year when compared with the fabric sensor prepared by RT polymerisation. The LT-Pad-CVD samples varied from 8.76 kΩ to 9.25 kΩ which is about 5.6% change in electrical resistance after storing for one year.

Figures 4.8 to 4.10 demonstrate that the strain sensitivities of the PPy-coated fabric sensors prepared by LT-Print-CVD and LT-Pad-CVD are maintained after the storage. The strain sensitivities drop less than 10% after storing for one year. The linearity and repeatability also change very little after the long-term storage.

Table 4.2 Changes in resistance and gauge factor of the PPy-coated samples subjected to different polymerisation temperatures

Sample No.	Treatment Methods	Resistance		Gauge Factor[a]	
		(R_o) (kΩ/in^2) [s.d.]	(R_{1yr}) (kΩ/in^2) [s.d.]	($\frac{\Delta R}{\varepsilon_{\max} R_o}$) [s.d.]	($\frac{\Delta R}{\varepsilon_{\max} R_{1yr}}$) [s.d.]
S5a	LT-SP	16 [1.06]	73 [17.00]	20 [4.47]	15.3 [2.07]
S5b	LT-Pad-CVD	8.76 [0.66]	9.25 [1.05]	450 [47.5]	413 [21.18]
S5c	LT-Print-CVD	11.5 [3.35]	43 [7.56]	230 [32.6]	218 [29.20]

[a] strain = 50%

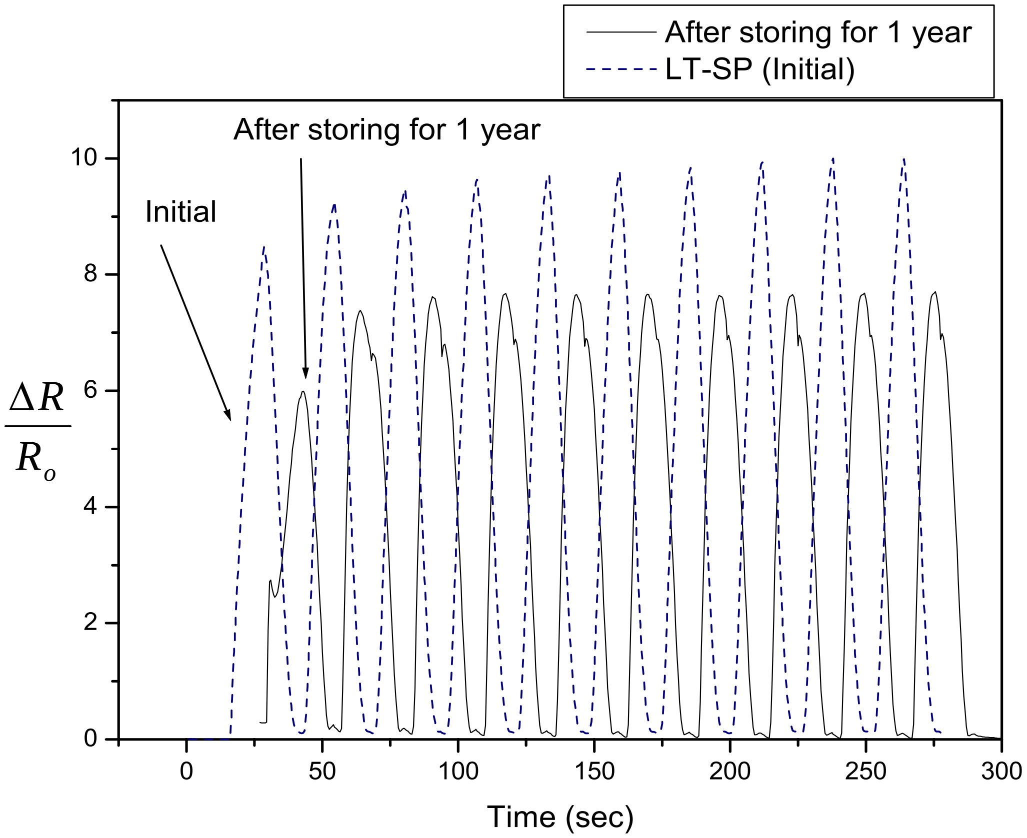

Figure 4.8 Relative resistance change as a function of time in a cyclic tensile test of the PPy-coated fabrics fabricated by LT SP before and after storage (S5a)

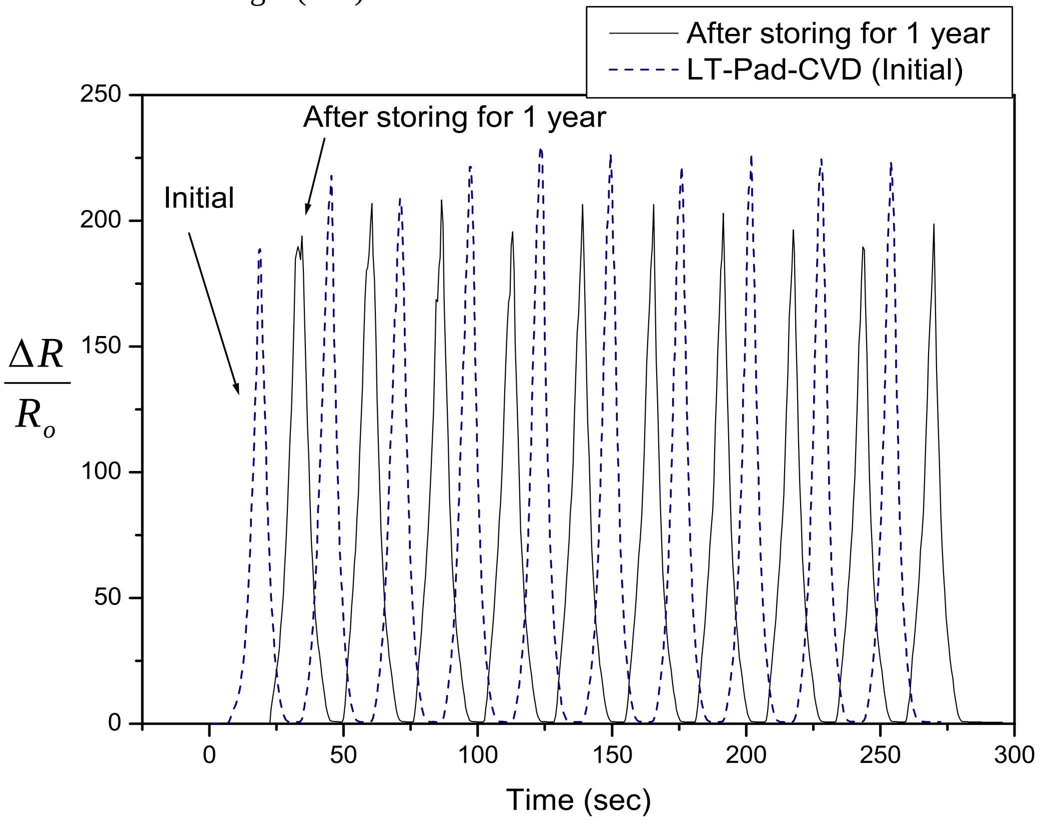

Figure 4.9 Relative resistance change as a function of time in a cyclic tensile test of the PPy-coated fabrics fabricated by LT Pad-CVD before and after storage (S5b)

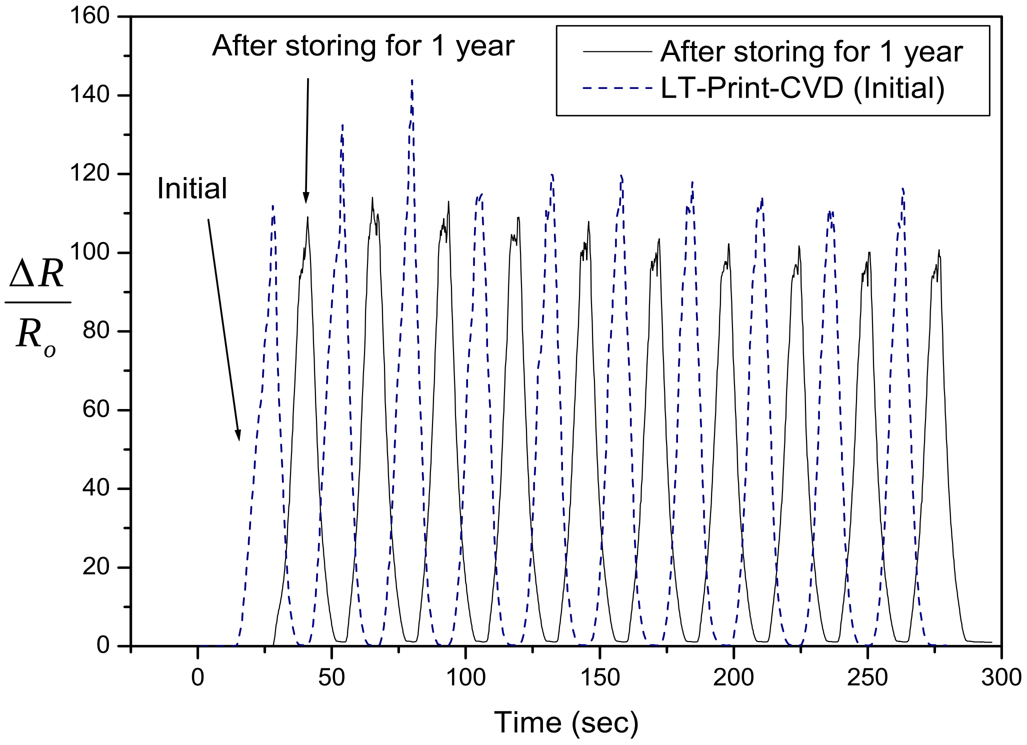

Figure 4.10 Relative resistance change as a function of time in a cyclic tensile test of the PPy-coated fabrics fabricated by LT Print-CVD before and after storage (S5c)

4.4 Tensile Behaviour of the PPy-coated Fabrics with Different Fabrication Temperatures

Figure 4.11 depicts the tensile behaviour of the PPy-coated fabrics prepared by different fabrication methods at LT, namely LT-SP, LT-Pad-CVD and LT-Print-CVD, with stabilisation treatment.

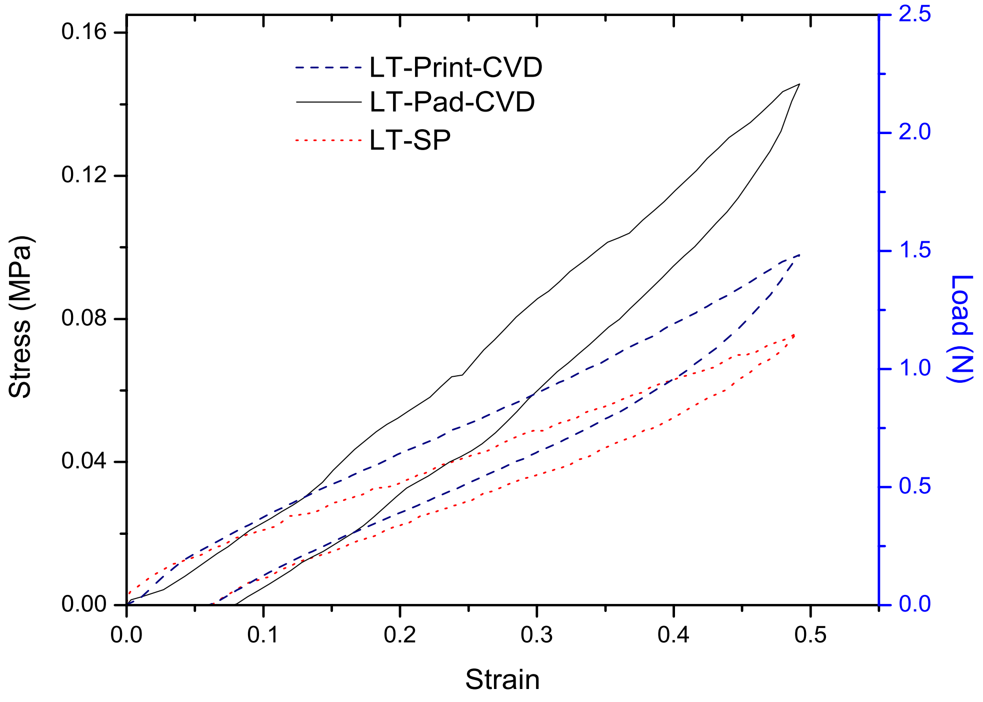

Figure 4.11 Tensile behaviour of the PPy-coated fabrics prepared by different LT fabrication methods in the wale direction

According to the results stated in Chapter 3, there is no change in the tensile properties of different PPy-coated fabrics prepared by different RT fabrication methods. However, Figure 4.11 shows that there is a significant difference in the tensile property of the PPy-coated fabric prepared by LT-Pad-CVD when compared with that of the PPy-coated fabrics prepared by LT-SP and LT-Print-CVD. The PPy-coating made by LT-Pad-CVD can stiffen the textile fabric with the stress rising up to 0.15 MPa and 0.075 MPa at 0.5 strain for the LT-Pad-CVD and RT-Pad-CVD respectively. Various performance of tensile loading reflects the difference in the interfacial structure as well as the interaction of the coating layer and the substrate fabric (Xue, Tao, Kwok and Leung, 2004). Therefore, the LT-Pad-CVD fabrication method can make more compact, dense and stronger PPy coating layer on the textile substrate, leading to stronger interface for the PPy/Tactel/Lycra system. It is also explained extremely high strain sensitivity resulted from the PPy-coated fabric prepared by the LT-Pad-CVD.

4.5 Electrical and Mechanical Properties of the PPy-Coated Yarns with Different Polymerisation Temperatures

The tensile properties of the PPy-coated PA6 and PU fibres had been studied (Xue, Tao, Kwok and Leung, 2004). It is shown that the electro-mechanical behaviour of the conductive composites depends strongly on the micro-structure of the coating layer and the material of the substrate. In the present study, the tensile and electro-mechanical behaviour of the PPy-coated PA6 and PU yarns prepared at different polymerisation temperatures are compared.

Prior to tensile testing, the electrical resistance had been measured. It is noticed that with the same sample preparation conditions at RT, the PPy-coated PA6 yarns possess higher conductivity when compared with the PPy-coated PU yarns. The initial resistance of the PPy-coated PU yarns is almost 50 times higher than that of the PPy-coated PA6 yarns, i.e. 35000kΩ/inch and 680kΩ/inch respectively. However, fabrication conducted at low polymerisation temperature can lower down the electrical resistance of both the PPy-coated PA6 and PU yarns with their initial resistances being 151kΩ/inch and 260kΩ/inch respectively. The conductivity of PA6 yarn is higher than the PU yarns irrespective of the samples of whether are prepared at RT or LT. This is due to higher quality of PPy coatings being formed on the PA6 fibres as the morphology of the PPy coating film is highly dependent on the substrate. Xue and Tao (2005) found that the interaction between PA6 fibre and PPy was stronger than that between PU fibre and PPy because the morphology of both systems was different resulting in various electrical conductivity. It is found that PPy coating film formed on the PA6 fibre is composed of well-connected PPy granules, covering up the whole fibre surface with finer, denser and more uniform grains than those of PPy on the PU fibre. These morphological differences can explain why the electrical conductivities of PA6 fibres are higher than Lycra fibres when the samples are prepared at either RT or LT.

Figures 4.12 and 4.13 show the relative resistance change versus strain curve of PPy-coated PA6 and PU yarns prepared at different polymerisation temperatures. For the PPy-coated PA6 yarns shown in Figure 4.12, the electrical resistance increases with the increased strain, and the relationship between $(R-R_o)/R_o$ and strain is almost linear under tensile loading until fracture. There is no significant difference in the electro-mechanical behaviour between the PPy-coated PA6 yarns prepared at RT and LT. Lam found that the loop shape was changed by the fibre rotation and sliding during large deformation of textile fabric composite. When the strain of fabric composite was increased to 30%, the fibre would be elongated to the maximum order of 1 to 1.8% (Lam, 2004). Therefore, the resistance change versus yarn strain before 20% needs to be considered. It is also found that the sample prepared by the LT CVD exhibits slightly higher yarn strain sensitivity than the sample prepared by the RT CVD.

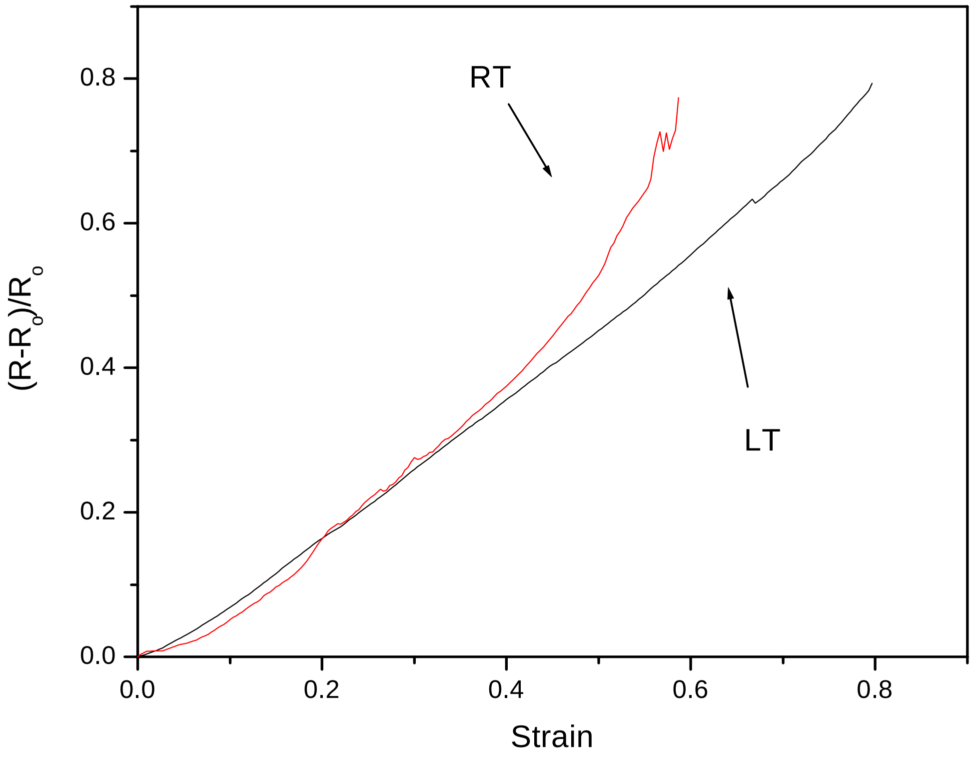

Figure 4.12 Relative resistance change versus strain curves of PPy-coated PA6 yarns prepared by RT CVD and LT CVD

In Figure 4.13, the electro-mechanical behaviour of the PPy-coated PU yarn prepared by the LT CVD is significantly different from that of the sample prepared by the RT CVD. There is a rapid change in electrical resistance for the RT sample with small strain, and the electrical resistance becomes overflow with less than 20% yarn strain. This may be due to too high initial resistance value in the relaxed state of yarn. On the contrary, the resistance change can be divided into two phases for the sample prepared by the LT CVD. In the initial phase, the resistance increases gradually followed by the second phase in which the resistance increases non-linearly and rapidly. Xue and Tao (2005) suggested that for the PPy-coated PU fibres, the variation of resistance with applied strain is mainly attributed to the damage of the coating layer. Hence, the significant difference between the RT CVD and LT CVD prepared PPy-coated PU yarn may be mainly due to the quality of the coating layers formed on the fibre substrates. The performance of coating layer developed by different temperatures will be characterised and discussed in the next section of this Chapter.

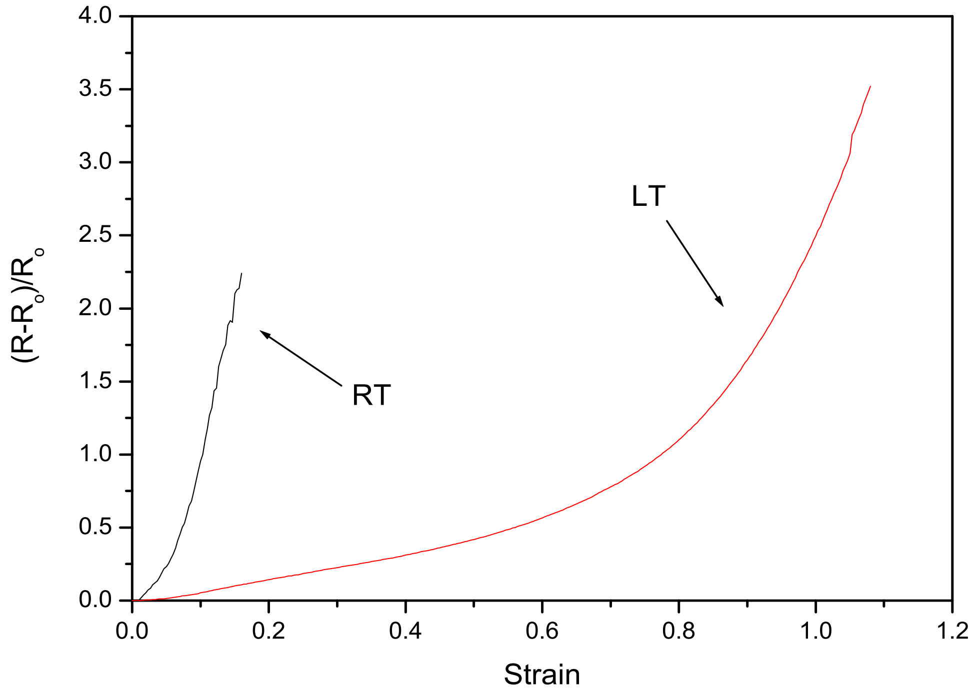

Figure 4.13 Relative resistance change versus strain curves of PPy-coated PU yarns prepared by the RT CVD and LT CVD

Figures 4.14 and 4.15 depict the comparison of stress versus strain curves of the PPy-coated PA6 and PU yarns fabricated at different polymerisation temperature. Figure 4.14 demonstrates that the LT CVD makes the PPy coating slightly stiffer than the RT CVD. As a result, more denser and compact layer of PPy coating may be formed by the LT CVD. This hypothesis will be discussed in the next section of this Chapter. Figure 4.15 exhibits almost no difference in the tensile behaviour of PPy-coated PU yarns fabricated by the RT CVD and LT CVD.

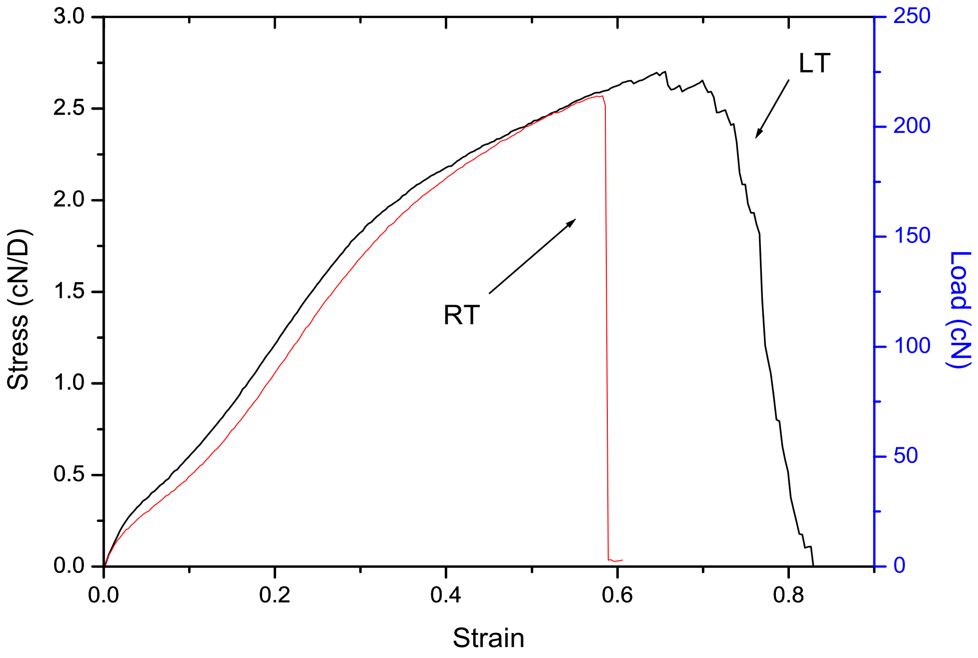

Figure 4.14 Stress versus strain curves of PPy-coated PA6 yarns prepared by the RT CVD and LT CVD

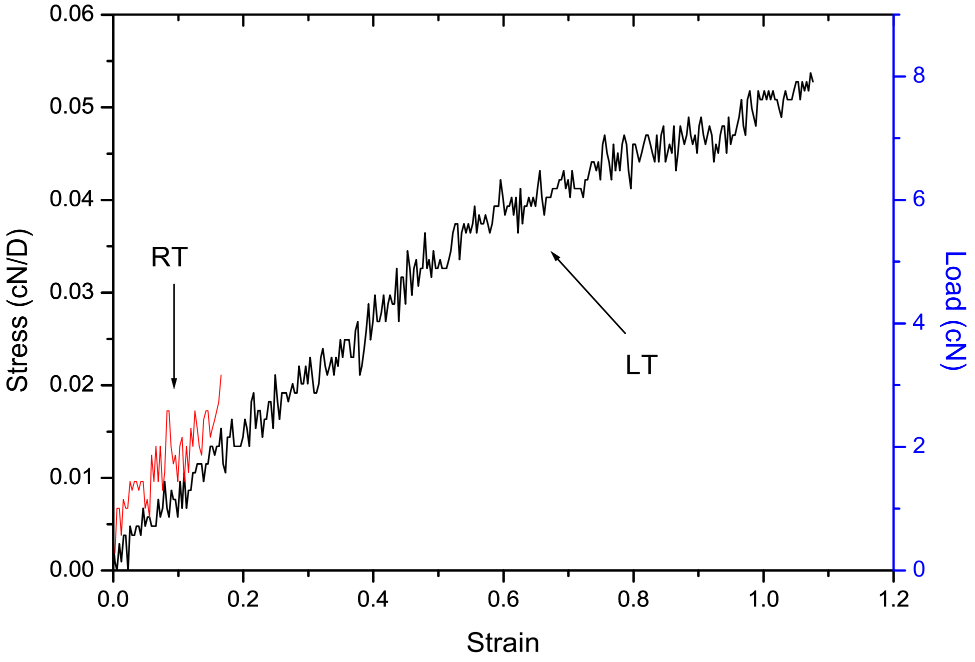

(b)

Figure 4.15 Stress versus strain curves of PPy-coated PU yarns prepared by the RT CVD and LT CVD

4.6 Characterisation of the PPy-Coated Fabrics and PPy Powders

Similar to Section 3.4 of Chapter 3, various characterisations of the PPy-coated fabrics, PPy-coated fibres and pure PPy powders were conducted in order to explore deeper understanding of the PPy coating film prepared at different polymerisation temperatures.

<u>Contact Angle Measurement</u>

It is anticipated that a more hydrophobic surface can obstruct water attack resulting in improving the environmental stability. Table 4.3 shows that the fabric sensor prepared by LT polymerisation can improve the hydrophobic property of the fabric for all fabrication methods. The contact angle can be increased up to 130° for the sample prepared by the LT-Pad-CVD. The formation of more hydrophobic surface is probably attributed to the higher density and orientation of the PPy coating. Therefore, it has only 5% change in electrical resistance after storing for one year, which is very outstanding for long term environmental stability.

Table 4.3 Contact angle of water droplet on the PPy-coated fabrics

Sample No.	Fabrication Method	Contact Angle	
		RT [s.d.]	LT [s.d.]
S4a & S5a	SP	110° [0.00]	125° [2.24]
S4b & S5b	Pad-CVD	117° [1.73]	130° [1.41]
S2c & S5c	Print-CVD	114° [0.00]	124° [0.00]

X-ray Diffraction (XRD) Analysis

The diffraction spectra obtained from the PPy pure powders produced by the RT CVD and LT CVD are shown in Figure 4.16. The results demonstrate that the majority of PPy powders are essentially amorphous, and also show the presence of a broad high-angle asymmetric scattering peak stretching from 2θ of 14.5° to 30°. The diffraction peak at 2θ of 26.5°, giving *d* spacing of 0.34 nm observes in the PPy powder prepared by LT CVD is much sharper than that of the RT CVD, indicating a more ordered pyrrole chain structure obtained (Cheah, Forsyth and Truong, 1998). The overall XRD results indicate that higher ordered orientation of PPy can be produced by the LT CVD for it can provide the fabric sensor with higher conductivity and better environmental stability. This is reflected by the electrical resistance of the PPy-coated fabric which is reduced by almost 10 times. There is only about 5% change in electrical resistance after storing for one year if the fabric sensors are produced by LT CVD method.

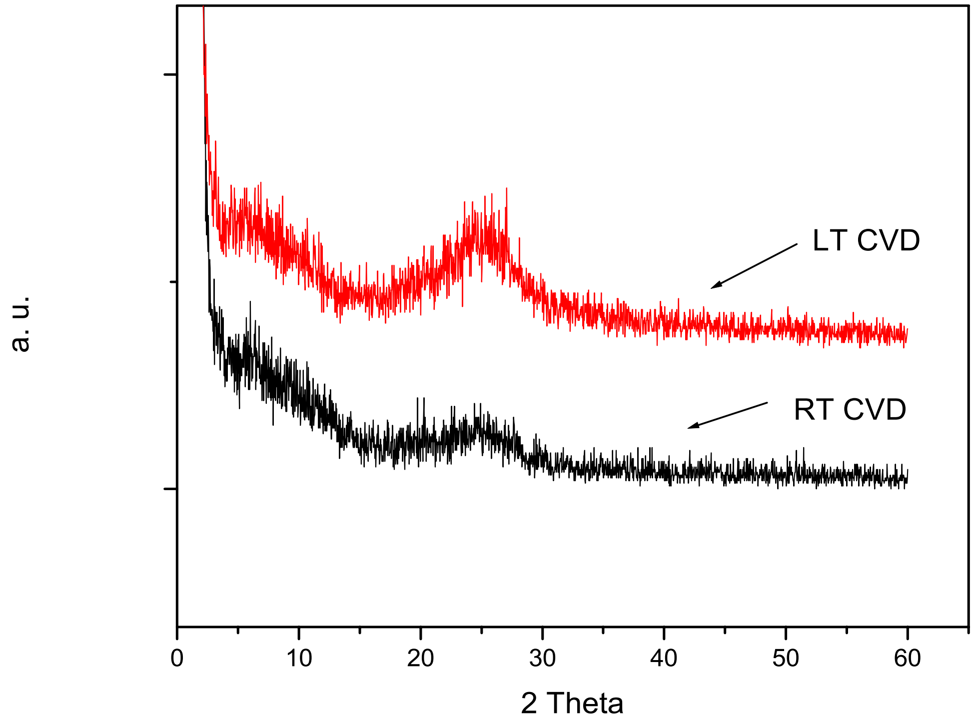

Figure 4.16 XRD patterns of PPy powders prepared by RT CVD and LT CVD

Thermal Analysis

The results of TG analysis are shown in Table 4.4, Figures 4.17 and 4.18. The thermal stability of the fabrics changes very little after the deposition of the PPy coatings by either the RT CVD or LT CVD, which is probably due to very small content of PPy present in the conductive fabrics. In order to study the actual thermal property of PPy coatings fabricated by the RT CVD and LT CVD, the TG analysis was conducted on the PPy powders as shown in Figure 4.18. For the first mass loss ascribed to the evaporation of water and residual washing solvents, it is noticed that the weight loss of the LT samples within the temperature range of 30°C to 100°C is 0.7% which is lesser than the RT sample. The RT CVD samples undergoing higher mass loss is suspected to have a greater affinity for water than those of the LT CVD. The first onset temperature is also higher for the LT sample, which is 101.5°C as compared to 86.1°C for the LT and RT sample respectively. This may be due to more hydrophobic nature of the LT samples. This result is relevant to those of the contact angle measurement of the PPy-coated fabrics at different polymerisation temperatures in which the LT CVD shows greater fabric hydrophobic surface. As a result, it is evident that the LT CVD can improve the thermal stability of the PPy-coated fabrics.

Figure 4.18 also shows that the LT CVD can improve the thermal stability of PPy coating as reflected by the polymer degradation temperatures of 245.5°C when compared with that of the RT CVD which shows the degradation temperature of 221.7°C. Furthermore, the temperatures that cause the weight loss of 5% are at 166.2°C and 183.3°C for the RT CVD and LT CVD respectively.

Table 4.4 TGA data of PPy powders prepared at different polymerisation temperatures

Sample No.	Fabrication Temperature	1st Onset Temp (°C)	2nd Onset Temp (°C)	5% Weight Loss (°C)	Weight Loss at 100°C (%)
S3d	RT	86.1	221.7	166.2	3.8
S6a	LT	101.5	245.5	183.3	3.1

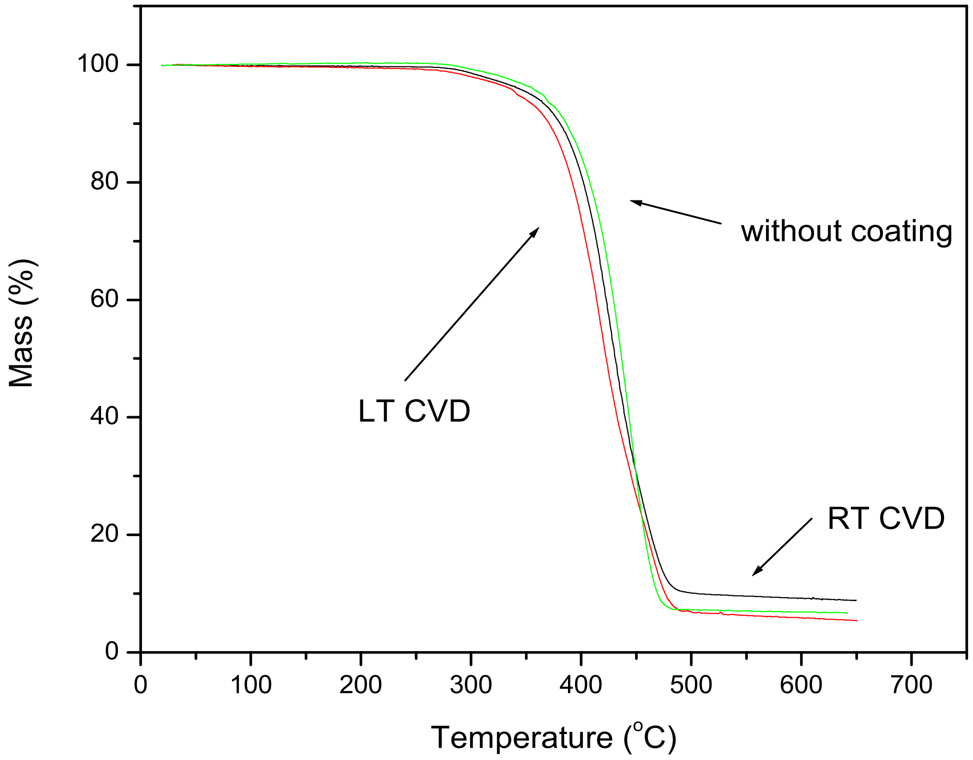

Figure 4.17 Comparison of TG curves at 10°C min^{-1} in dry nitrogen of PPy-coated fabrics fabricated by the RT CVD and LT CVD

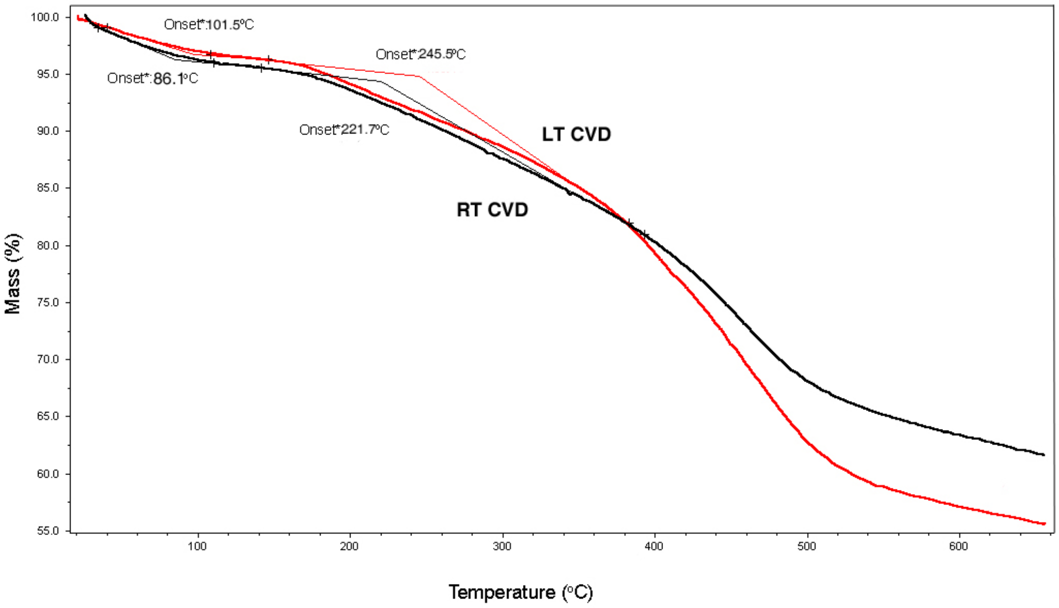

Figure 4.18 Comparison of TG curves at 10°C min^{-1} in dry nitrogen of PPy powders produced by the RT CVD and LT CVD

Particle Size Analysis

The particle size distribution of the PPy powders produced by the RT CVD and LT CVD has also been studied. The dramatic effect of a lower polymerisation temperature is illustrated in Figure 4.19. A relatively broad particle size distribution is obtained using the RT CVD with an average particle diameter of 360nm. However, a much narrower particle size distribution with a significantly reduced average particle diameter of 100nm is achieved by using the LT CVD. The particle size distribution of PPy powder may directly affect the coating thickness of textile fabrics, resulting in a thinner layer of PPy coating formed by the LT CVD on the textile fabrics which can be beneficial to higher strain sensitivity capacity. In addition, finer particle size can improve the arrangement or ordering of the PPy chain layer on the textile substrate leading to the formation of more compact and dense PPy coating layer. More uniform particle size may produce more evenly distributed layers and smoother morphology coating on the textile substrate. As a result, better environmental stability can be obtained.

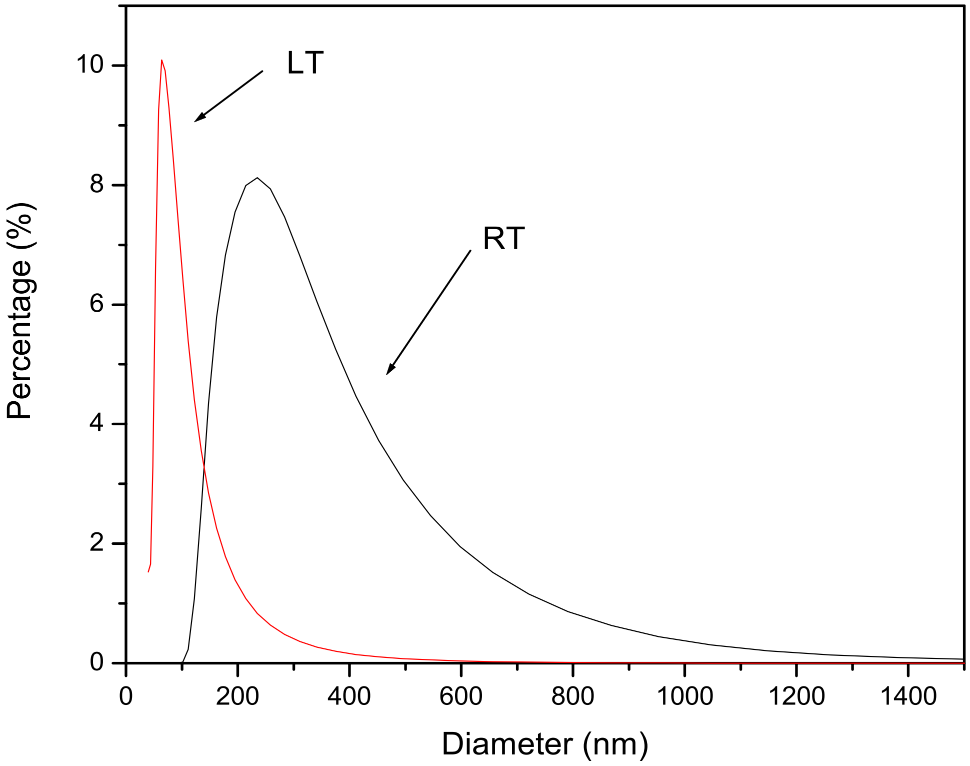

Figure 4.19 Comparison of particle size distribution of PPy powders prepared by RT CVD and LT CVD

The overall characterisation results can confirm the sensing capacities, good conductivity as well as good environmental stability of the fabric sensor produced by the LT CVD method.

4.7 Coatings Morphological Study by SEM and SPM

Xue and Tao (2005) compared the morphology and growth mode of the PPy film layer prepared by the RT CVD on the surface of the PA6 and PU fibres using SPM. It was found that a smooth and uniform coating could lead to a satisfactory performance of conductive fibre sensors. In the present study, comparison of the morphological study of PPy coating on the PA6 and PU fibres prepared at different polymerisation temperatures was investigated.

The SEM photographs shown in Figures 4.20 to 4.23 indicate the surface morphology of the PPy-coated PA6 fibres and PPy-coated PU fibres fabricated by the RT and LT CVD respectively. The SEM images demonstrate that the PPy coatings are smoother, more uniform and compact on the PA6 fibres than the PU fibres irrespective of whether the samples are prepared at RT or LT. The findings are similar to Xue's previous investigation on RT fabrication (Xue and Tao, 2005). When compared, PPy forms a continuous layer of finer, denser, and more uniform grains on PA6 substrate than those on the PU substrate. This is due to the strong interaction occurring between the substrate and PPy, resulting in fast nucleation rate and relatively small distance between nuclei. The nuclei grow quickly in the lateral directions and spread throughout the surface of the fibres. The initially connected layer comes from the multiple nucleation sites with either isotropic or anisotropic growth rates on the substrate. On the contrary, the interaction between the PU fibre and PPy is relatively weak; therefore, the nucleation rate is slow and the nuclei will grow both laterally and vertically in the form of islands.

By comparing the PPy-coated fibres fabricated by the RT and LT, it is obvious that either PA6 or PU fibres prepared by the LT CVD as shown in Figures 4.21 and 4.23 have a more compact and smooth surface morphology than that prepared by the RT CVD as shown in Figures 4.20 and 4.22.

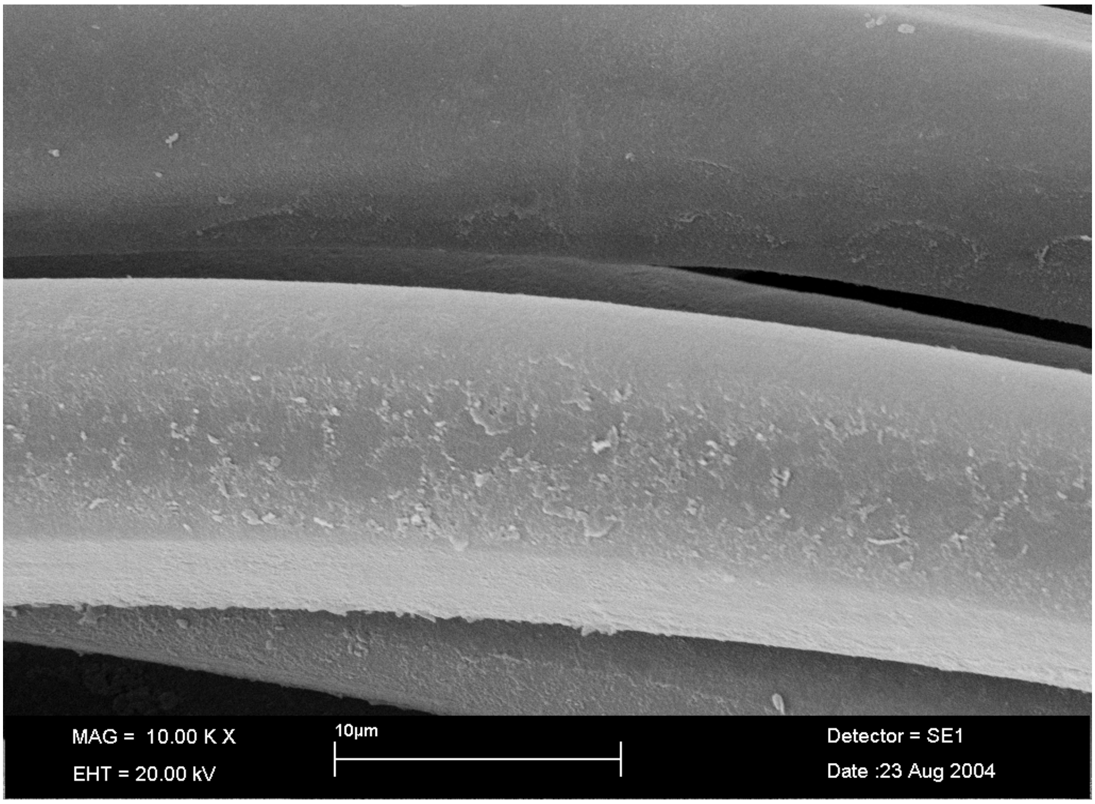

Figure 4.20 SEM photographs of the PPy-coated PA6 fibres prepared by room temperature (21°C) CVD

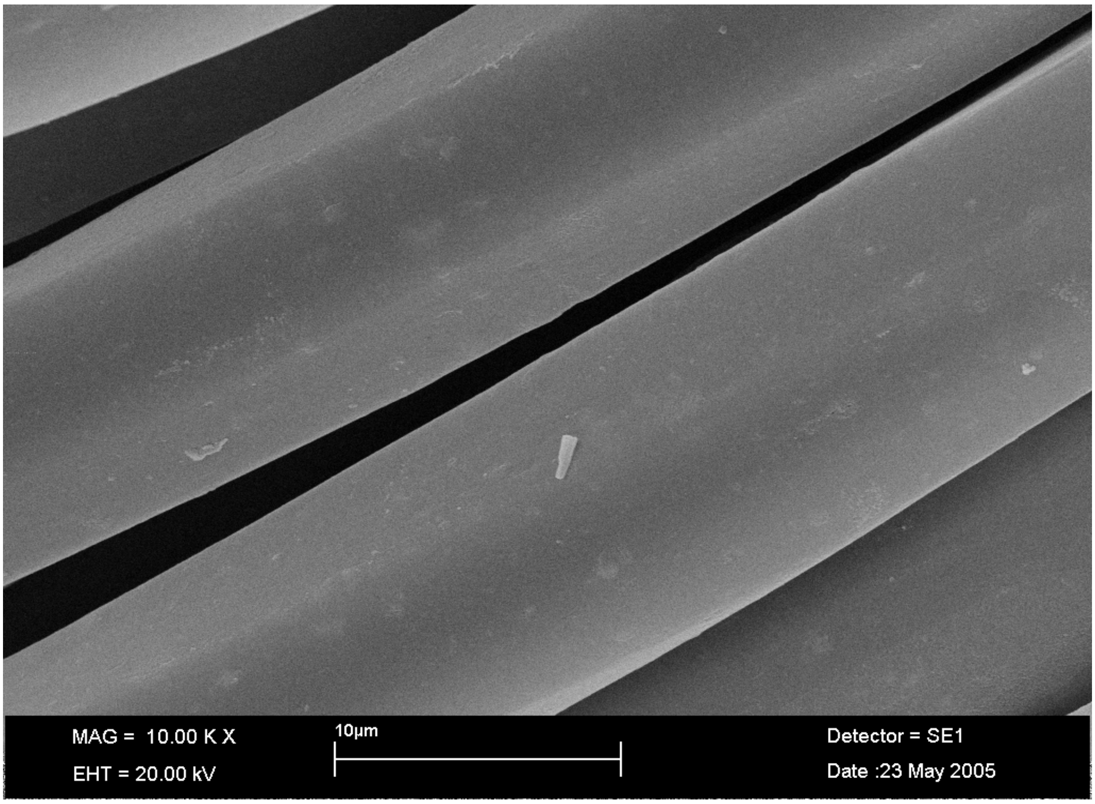

Figure 4.21 SEM photographs of the PPy-coated PA6 fibres prepared by low temperature (-25°C) CVD

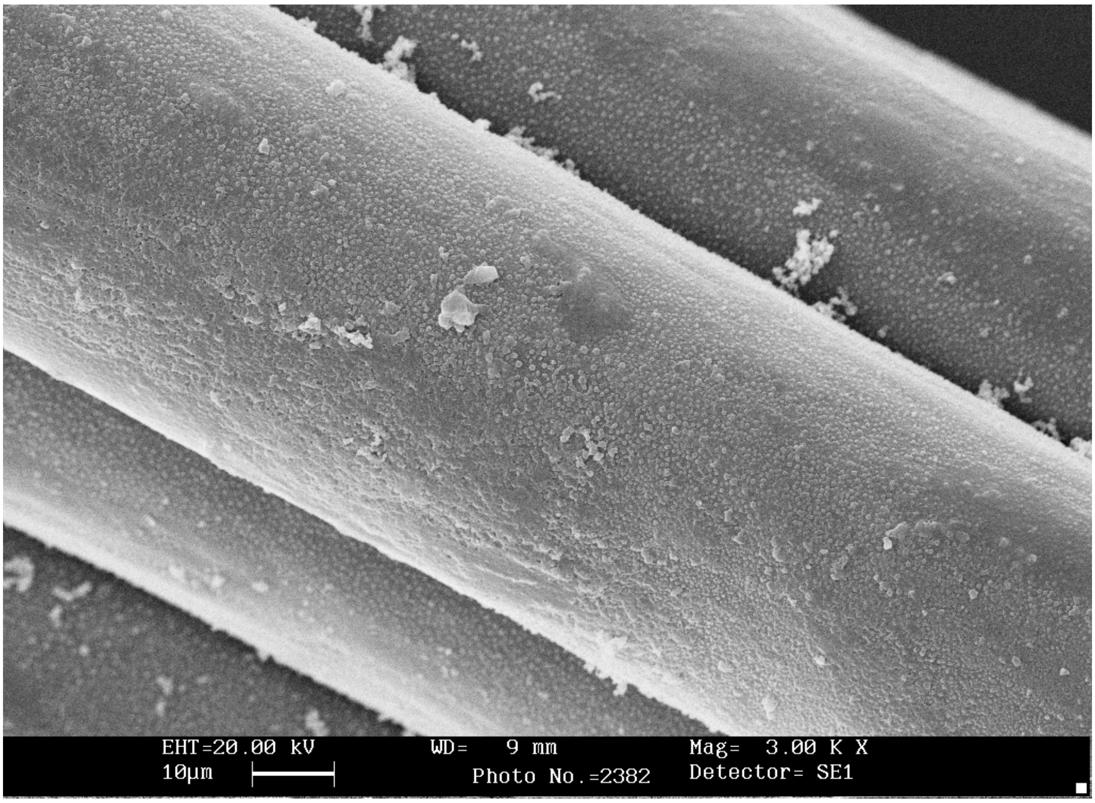

Figure 4.22 SEM photographs of the PPy-coated PU fibres prepared by room temperature (21°C) CVD

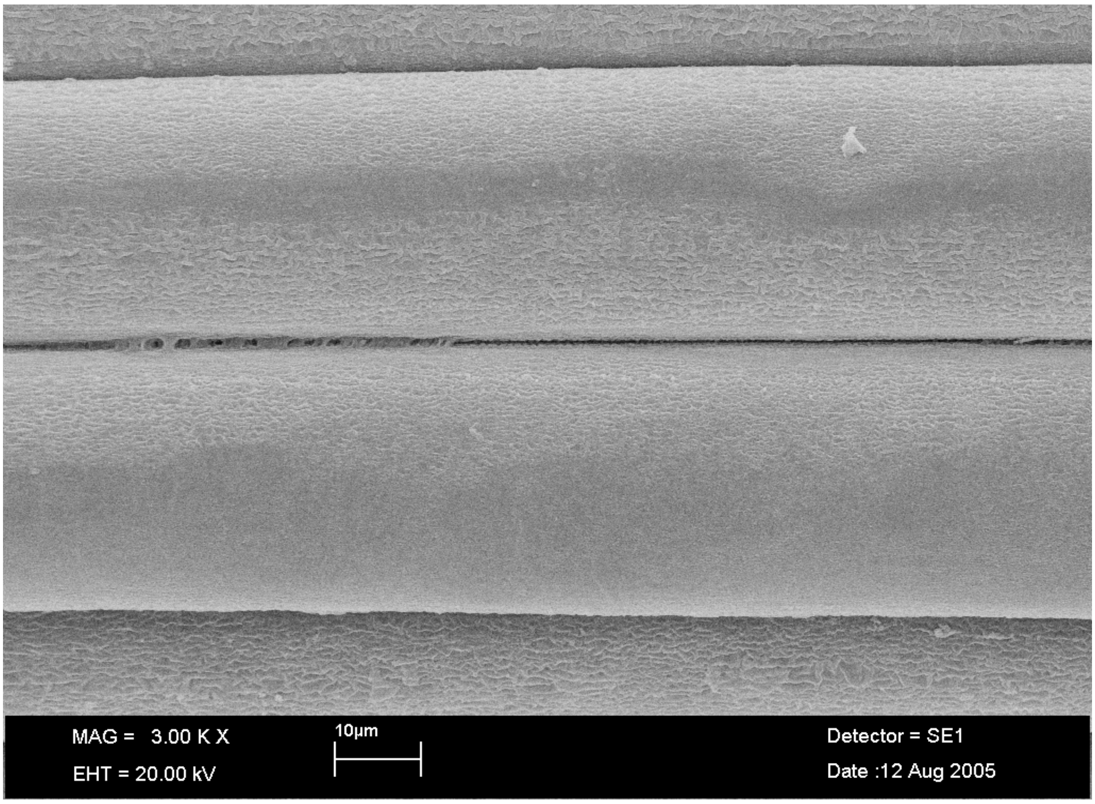

Figure 4.23 SEM photographs of the PPy-coated PU fibres prepared by low temperature (-25°C) CVD

SPM is used to provide more detailed topography information about the structures of the PPy layer coated on the PU fibres in micro and nano scales. SPM relies on a very sharp probe positioned within a few nanometers above the surface of sample. When the probe scanning relative to the sample, any change in the height of the surface causes the detected probe signal to change. A three dimensional map of surface height is carried out with a probe scanning over the surface while monitoring some interaction between the probe and the surface. Probe signals that have been used to sense surfaces include electron tunnelling current (STM), interatomic forces (AFM), magnetic force (MFM), electrostatic force (EFM) and thermal coupling (SThM), etc. In the past five years, Atomic Force Microscopy (AFM) has proven especially useful for the study of PPy morphology (Suarez and Compton, 1999). Silk, Hong, Tamm and Compton (1998a, 1998b) have examined the influence of the dopant on the roughness characteristics of PPy films.

Dynamic force microscope (DFM) mode is used for studying PPy-coated PU fibres and the working principle of DFM is shown in Figure 4.24. DFM is a tapping mode imaging which can eliminates frictional forces by intermittently contacting the surface and oscillating with sufficient amplitude to prevent the tip from being trapped by adhesive meniscus forces from the contaminant layer. For the circular type and soft sample like PU fibres, DFM is helpful to avoid tip slippage on the sample surface. It produces two types of information: (i) topography and (ii) phase. As the cantilever intermittent scans over a sample, it bends and the position of the laser beam on the detector shifts. The local height of the sample is measured by recording the vertical motion of the tip. Then, a three dimension topographical map of the surface is constructed by plotting the local sample height versus horizontal probe tip. The phase image in this DFM mode is created by detecting the phase shift. The weak interactions during intermittent scanning can significantly change the amplitude of tip oscillations and lead to a phase shift. Different structure of materials causing different values of phase shifts. Smaller phase shift can be detected for harder materials. Therefore, the phase image is very useful to show the sample with different materials.

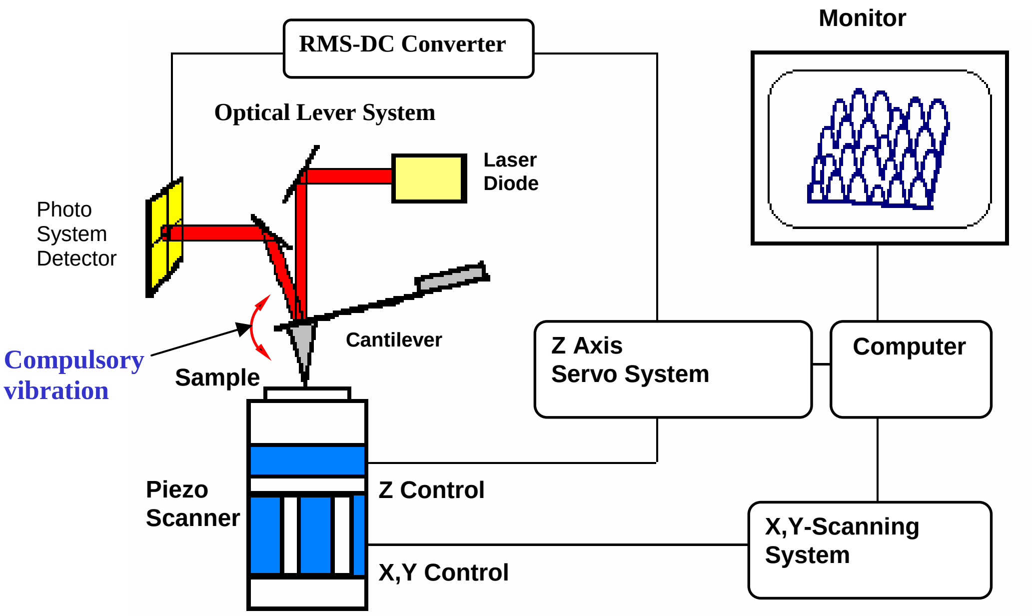

Figure 4.24 Principle of DFM mode (Seiko-Spi4000-Series, 2002)

Figures 4.25 to 4.28 exhibit the topographical and phase images of the PPy-coated PU fibres characterised by SPM. The results show that the PPy coating film fabricated by the LT CVD is composed of well-connected PPy granules, covering up the whole fibre surface with finer, denser, more uniform grains and evenly distributed layers than those of PPy coating fabricated by the RT CVD. On the contrary, the gap between the granules can be easily identified from the phase image of the RT CVD. Since lower polymerisation temperature can slow down the PPy polymerisation rate, thus the PPy particles can be densely arranged in order to form the continuous coating layers.

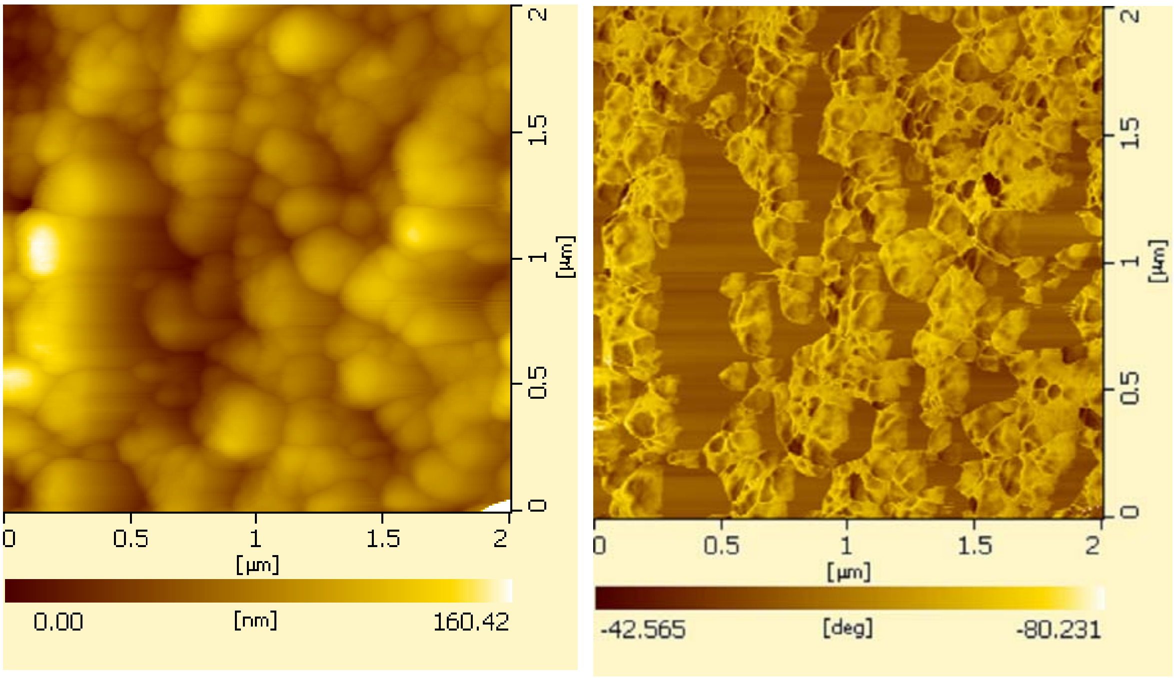

(a) (b)

Figure 4.25 Morphology of the PPy-coated PU fibre prepared by the room temperature (21°C) CVD with (a) topographical image and (b) phase image in 2μm x 2μm

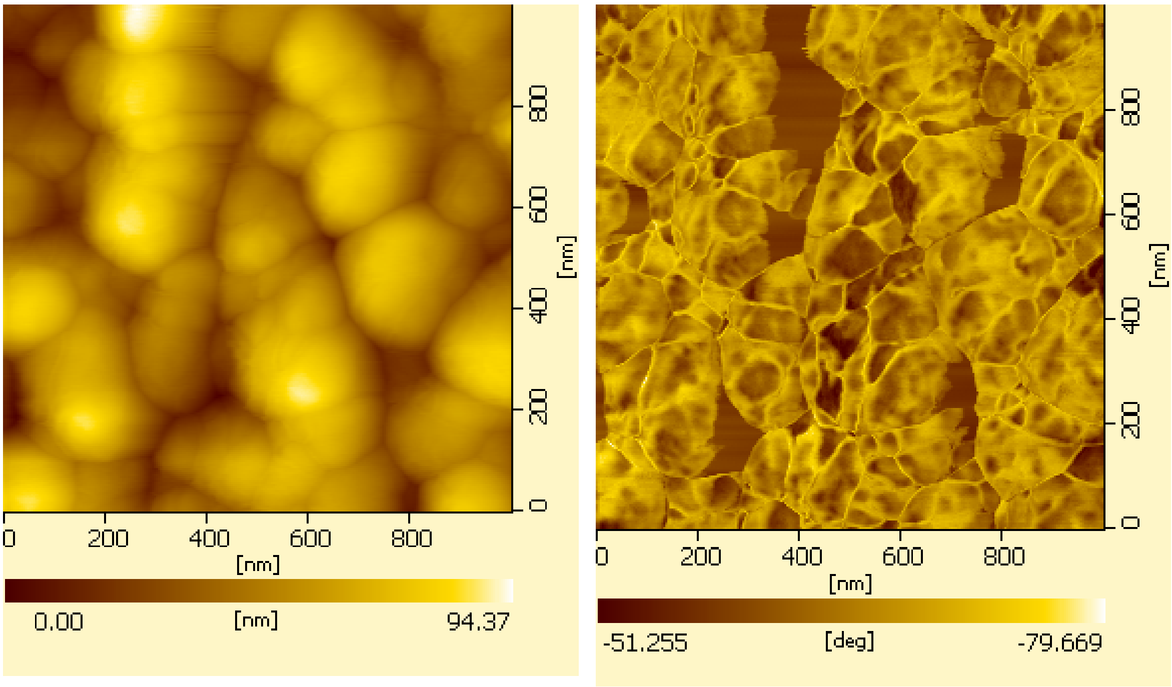

(a) (b)

Figure 4.26 Morphology of the PPy-coated PU fibre prepared by the room temperature (21°C) CVD with (a) topographical image and (b) phase image in 1µm x 1µm

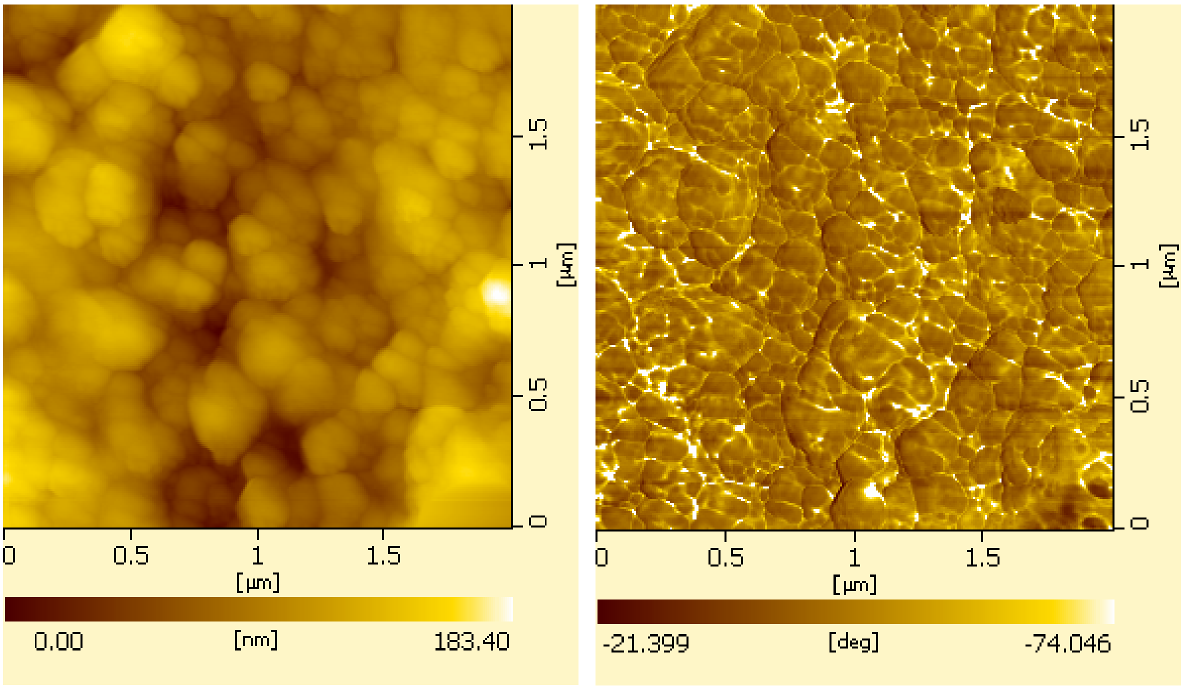

(a) (b)

Figure 4.27 Morphology of the PPy-coated PU fibre prepared by the low temperature (-25°C) CVD with (a) topographical image and (b) phase image in 2µm x 2µm

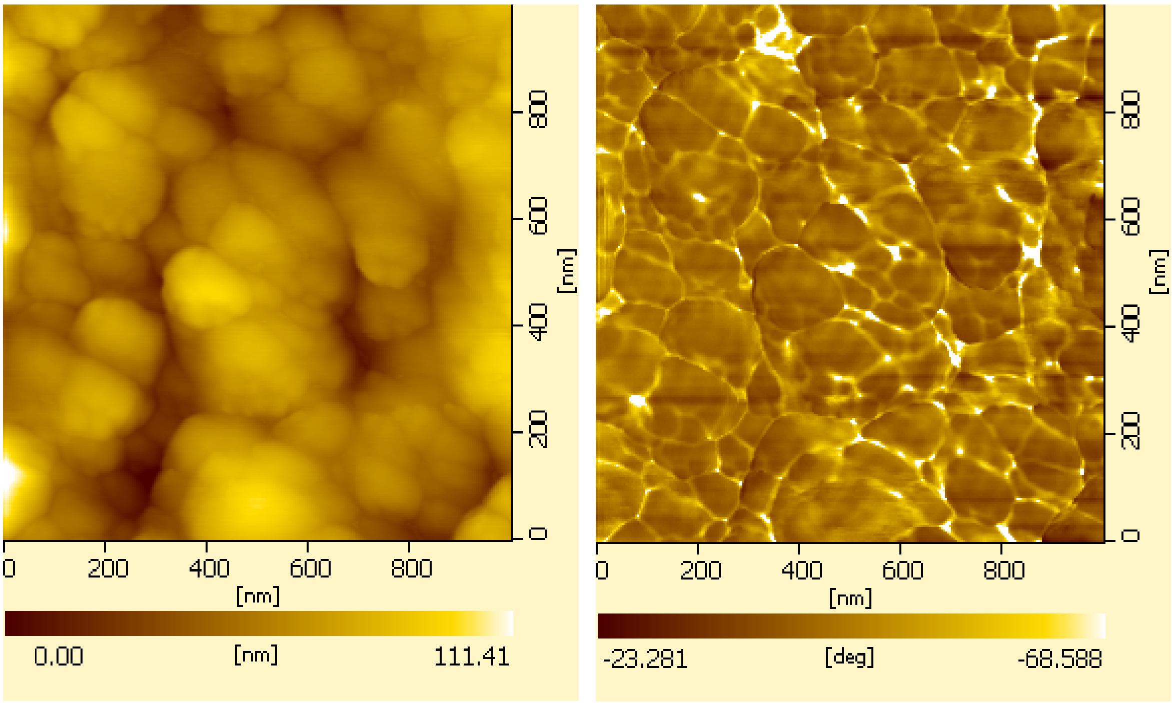

(a) (b)

Figure 4.28 Morphology of the PPy-coated PU fibre prepared by the low temperature (-25°C) CVD with (a) topographical image and (b) phase image in 1μm x 1μm

Grain size analysis and Surface smoothness analysis provide additional information beyond the standard morphology measurements. The grain size, diameter, distribution and average surface smoothness are involved in the study of the morphology of PPy coating layer on textile substrate. For each image, the morphological features at the surface are quantified by three parameters, i.e. the mean grain size, mean diameter and aveage surface smoothness, calculated for the whole area that analysed by SPM.

Firstly, a standard profile Z_0 is defined by:

$$Z_0 = \frac{1}{S_0}\int_{Y_b}^{Y_T}\int_{X_L}^{X_R} F(X,Y)dxdy \tag{4.1}$$

S_0 is the area of the selected region, Y_T, Y_b, X_R and X_L are the defined scan area, $F(X,Y)$ is the roughness curve relative to the centre plane.

The mean grain size (S_a) is a measure of the heterogeneity of the topography:

$$S_a = \frac{S_T}{N} \tag{4.2}$$

S_T is the total grain size and N is the number of grains.

When assuming the grain is circular, the mean diameter (D_a) is:

$$D_a = 2\sqrt{\frac{S_a}{\pi}} \tag{4.3}$$

Finally, the relative mean smoothness of the surface, R_a, is defined by:

$$R_a = \frac{1}{S_0}\int_{Yb}^{Y_T}\int_{X_L}^{X_R} \left|F(X,Y) - Z_0\right| dxdy \tag{4.4}$$

The comparison of grain size, diameter and surface smoothness between the PPy-coated PU fibres prepared by the RT CVD and LT CVD is summarised in Table 4.5.

Table 4.5 Comparison of average surface smoothness of the PPy-coated PU fibres subjected to different polymerisation temperatures

	RT	**LT**
Mean size (S_a)	4.16 x 10^4 nm^2	1.66 x 10^4 nm^2
Mean diameter (D_a)	2.3 x 10^2 nm	1.46 x 10^2 nm
Grain area	5.42 x 10^5 nm2	4.49 x 10^5 nm^2
Max. difference of height	94 nm	125 nm
Average surface smoothness (R_a)	15 nm	14.1 nm

With regard to the grain size analysis, the images and profiles of particle size distribution of the PPy-coated PU fibres produced by the RT CVD and LT CVD are shown in Figures 4.29 and 4.30 respectively. It can be seen that the maximum difference of grain height is not obvious between the PPy-coated PU fibres prepared by the RT CVD and LT CVD, i.e. 94nm and 125nm respectively. However, the size distribution is narrower for the sample prepared at LT, and so more smooth and uniform coating layer can be formed.

Furthermore, it is obvious that the mean grain size and diameter are larger for the sample prepared by the RT CVD. These results are in accordance with the particle size analysis of pure PPy powders as discussed previously in Section 4.6.

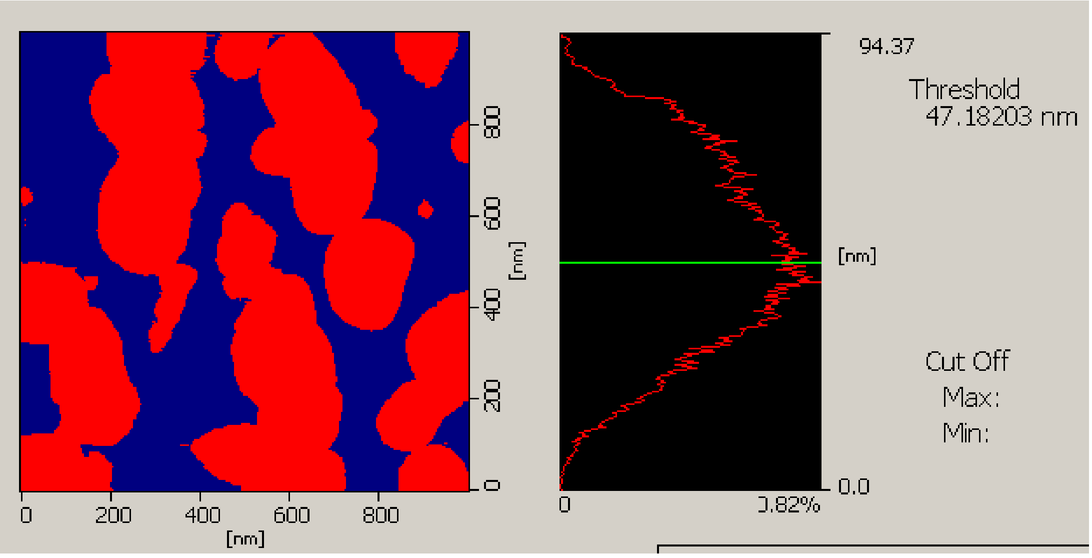

Figure 4.29 Profile of particle size distribution of the PPy-coated PU fibre prepared at room temperature (21°C)

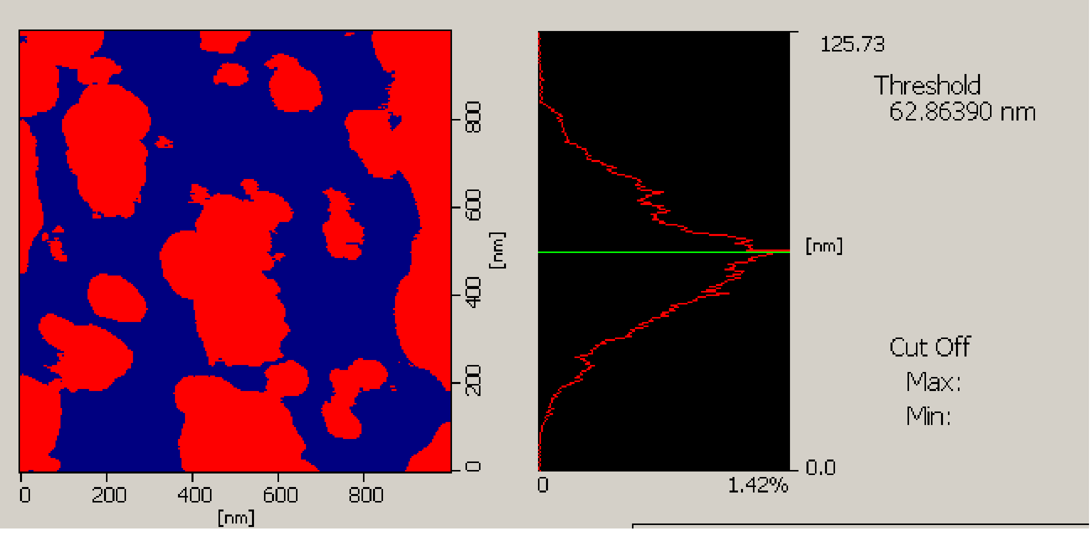

Figure 4.30 Profile of particle size distribution of the PPy-coated PU fibre prepared at low temperature (-25°C)

The data given from the surface smoothness analysis of the RT and LT samples are not significantly different, i.e. 15nm for RT PPy-coated PU fibres and 14.1nm for LT PPy-coated PU fibres. However, Figures 4.31 and 4.32 show that the depth features of surface smoothness of the PPy-coated PU fibres fabricated at RT and LT respectively exhibit larger particle size and height differences than those of the sample prepared at RT as shown in Figure 4.31. Furthermore, the surface roughness of LT sample shown in Figure 4.32 seems to be not so obvious when compared with the sample prepared at RT.

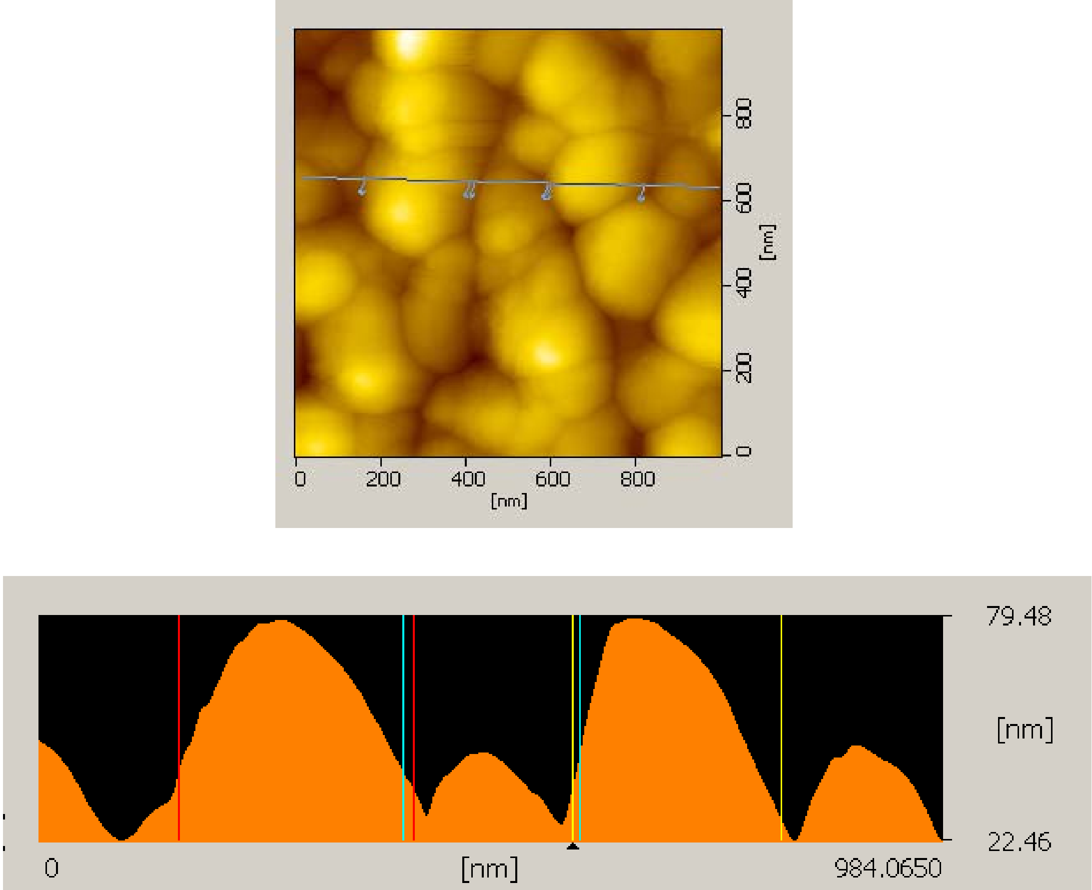

Figure 4.31 Depth features of surface smoothness of the PPy-coated PU fibre prepared at room temperature (21°C)

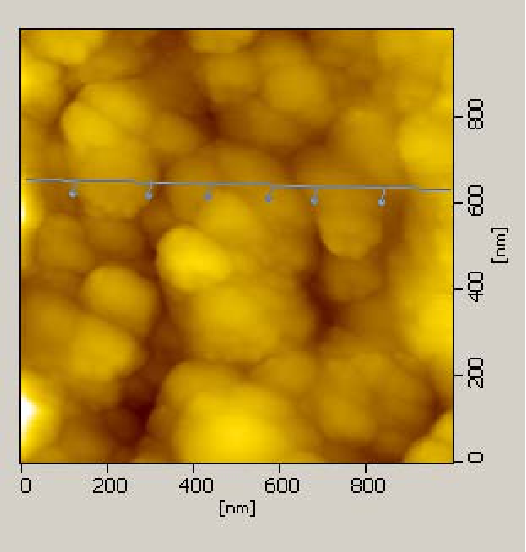

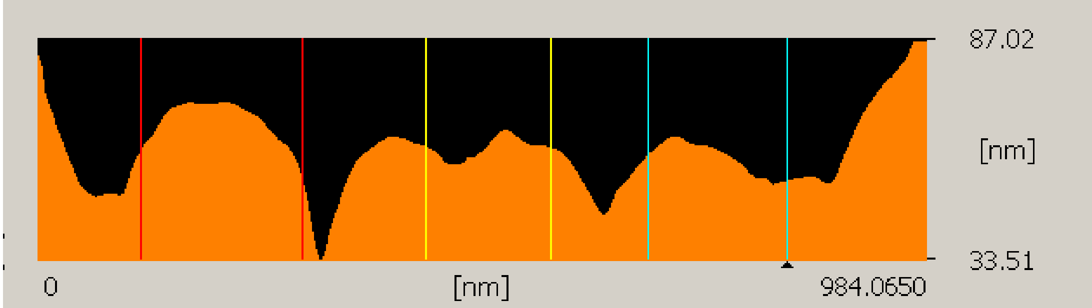

Figure 4.32 Depth features of surface smoothness of the PPy-coated PU fibre prepared at low temperature (-25°C)

Based on the SPM study, it is confirmed that denser and smoother surface morphology can be produced by the LT CVD fabrication method. The SPM results are similar to the findings obtained by Yoon et al. (Yoon, Sung, Kim, Barsoukov, Kim and Lee, 1999) who reported that the film densities of PPy were highly dependent on the preparation conditions.

It is believed that a smoother and denser surface morphology can inhibit the penetration of oxygen resulting in greater environmental stability of the PPy film. The results of SEM and SPM examination further explain the enhancement of stability induced by the LT CVD fabrication method. These results agree well with the findings obtained by Liu and Hwang who revealed that a more porous morphology and larger specific surface could facilitate the attacking gas diffusing into the film (Liu and Hwang, 2001).

4.8 Study of the PPy Coating Thickness by SPM

It is assumed that thinner coating layer is beneficial to the strain sensitivity of the PPy-coated fabric strain sensor. Investigation on the coating thickness is very essential to prove the above hypothesis.

Surface potential detection is a two-pass procedure where the surface topography is obtained by the standard Tapping Mode on the first pass while the surface potential is measured on the second pass as shown in Figure 4.33.

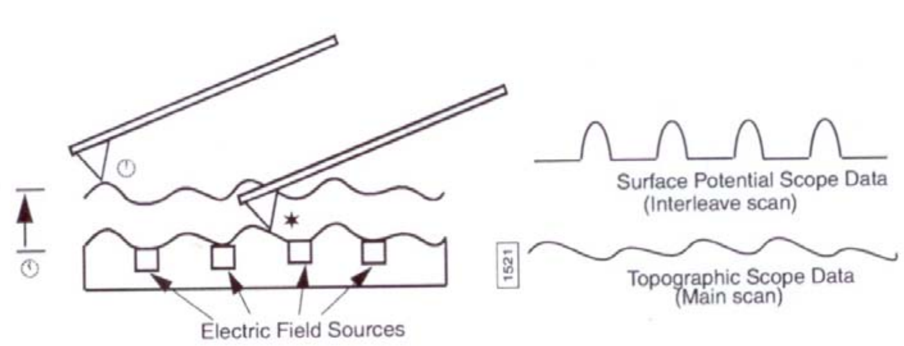

Figure 4.33 Lift Mode principle used in surface potential detection (Digital Instruments Inc., 1997)

For the first pass in Tapping Mode, the cantilever is mechanically vibrated near its resonant frequency by a small piezoelectric element in which a topography images obtained are shown in Figures 4.34 (a) and 4.36 (a). The substrate fibres are shown in the darker regions while the polymers used to embed the samples are in the lighter regions. These images show that the cross-sectional geometry of the PA6 fibre is triangular profile with the height of about 13µm. However, the electrically conductive layer existed between the two materials is not clearly shown in the topography images.

For the second pass, the tapping drive piezo is turned off and an oscillating voltage, $V_{AC} \sin\omega t$, is applied directly to the probe tip. If there is a difference in DC voltage between the tip and sample, there will be an oscillating electric force on the cantilever at the frequency, ω. This causes the cantilever to vibrate so that an amplitude can be detected. Consequently, the surface potential images are obtained as shown in Figures 4.34 (b), 4.35, 4.36 (b) and 4.37.

In this way, the coating thickness of the PPy layer on the PA6 fibres can be obtained with the brightest colour in the surface potential images. This is due to the fact that the PPy coating layer is electrically conductive, thereby causing DC voltage difference between the tip and conductive PPy coating. Figures 4.35 and 4.37 show the potential images of the cross section of the PPy-coated PA6 prepared at RT and LT respectively with the scan size of 10µm x 10µm. These figures clearly demonstrate that the PPy coating thickness of LT is thinner than the sample prepared at RT. The coating thickness is approximately 350nm for the sample prepared at RT and 200nm for the sample prepared at LT. The LT CVD can produce thinner PPy coating on textile substrate because finer particle size can be produced at LT. In addition, LT can slow down the polymerisation rate of PPy, forming more ordered and well arranged PPy layer on the surface; and resulting in producing thinner and more uniform coating layer.

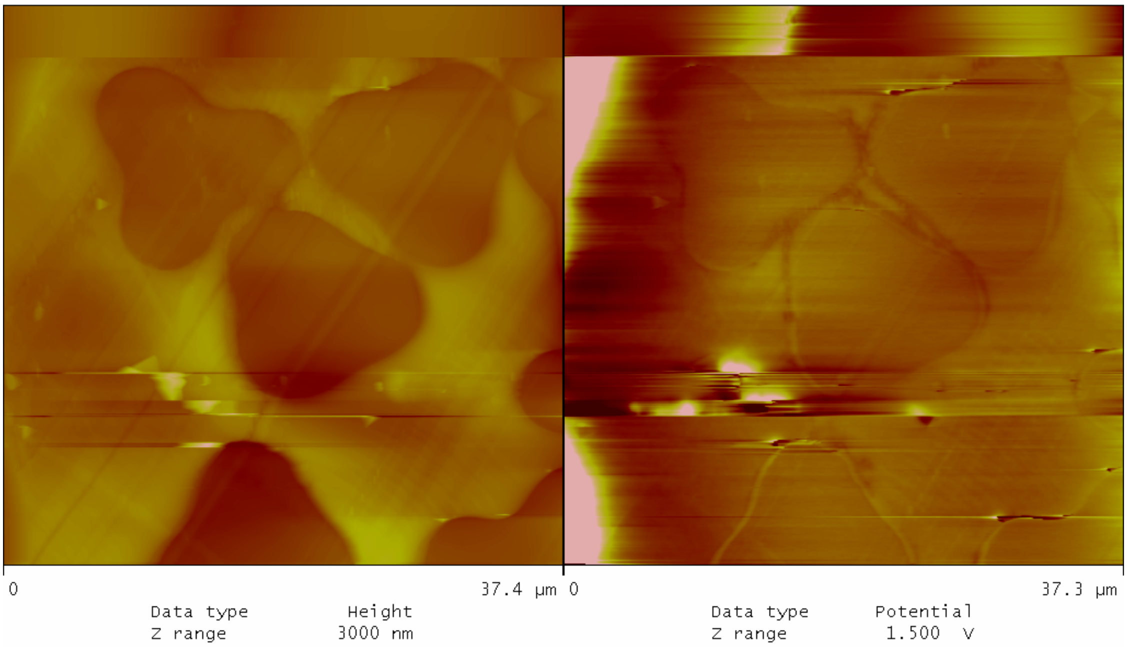

(a) (b)

Figure 4.34 PPy-coating thickness analysis of the PPy-coated PA6 fibre prepared at room temperature (21°C) (a) topographical image and (b) surface potential image in 37µm x 37µm

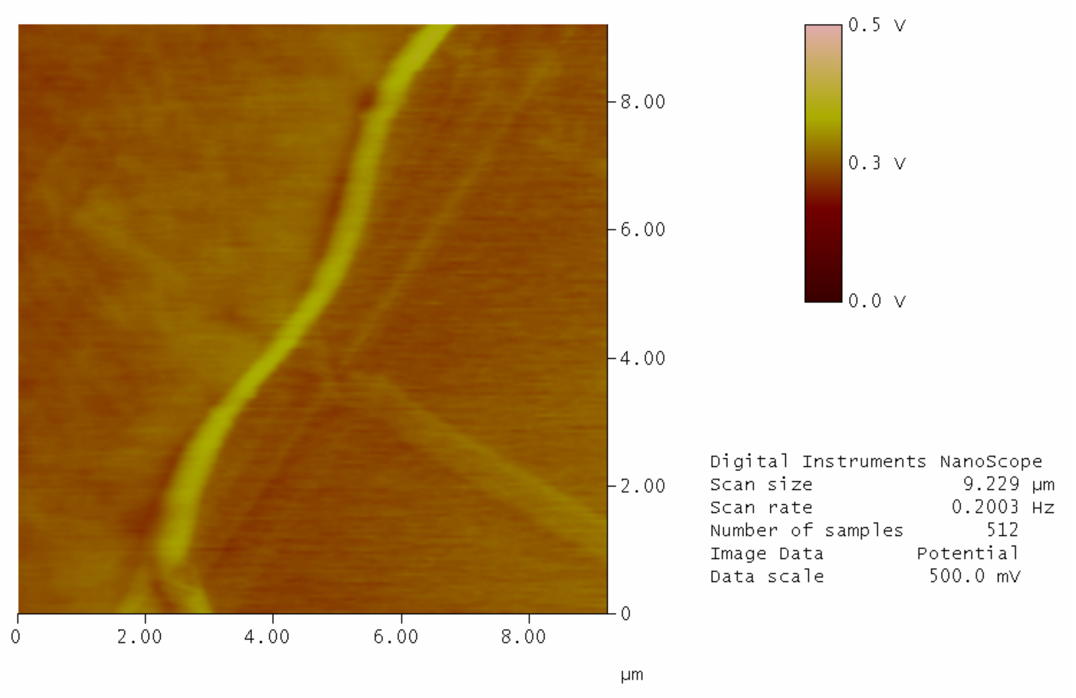

Figure 4.35 Surface potential image of the PPy-coated PA6 fibre prepared at room temperature (21°C) in 10µm x 10µm

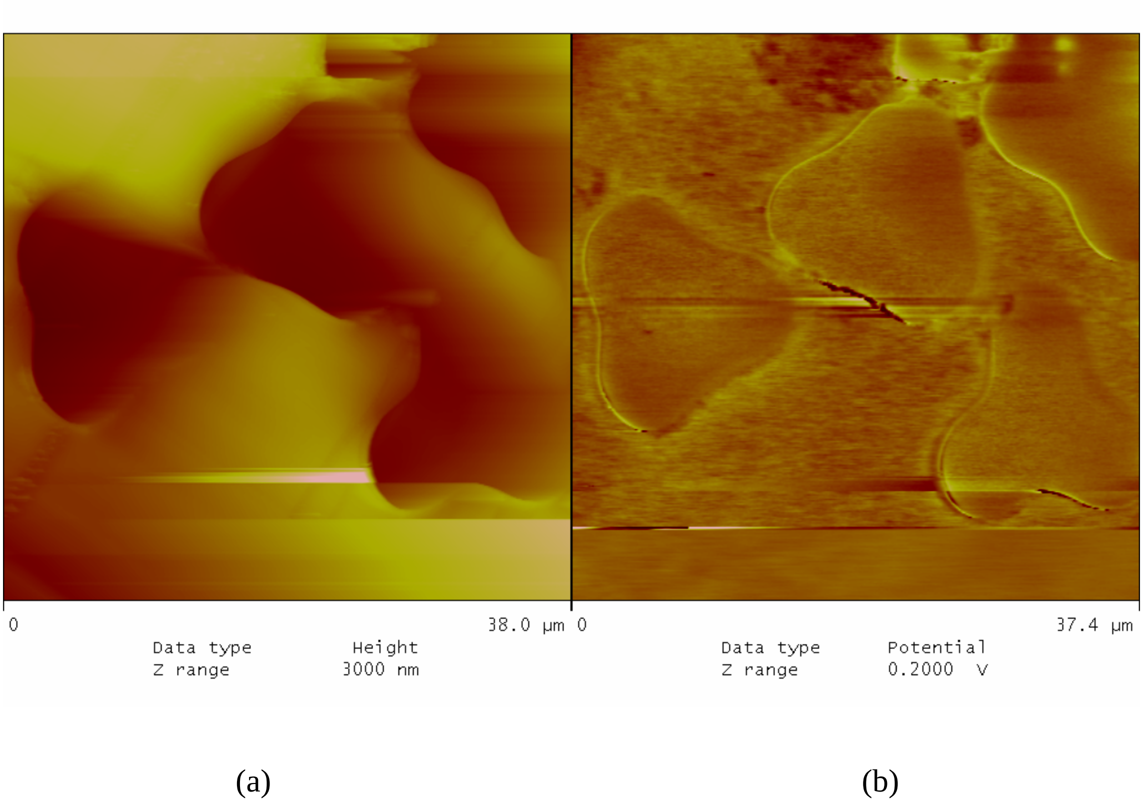

(a) (b)

Figure 4.36 PPy-coating thickness analysis of the PPy-coated PA6 fibre prepared at low temperature (-25°C) (a) topographical image and (b) surface potential image in 37µm x 37µm

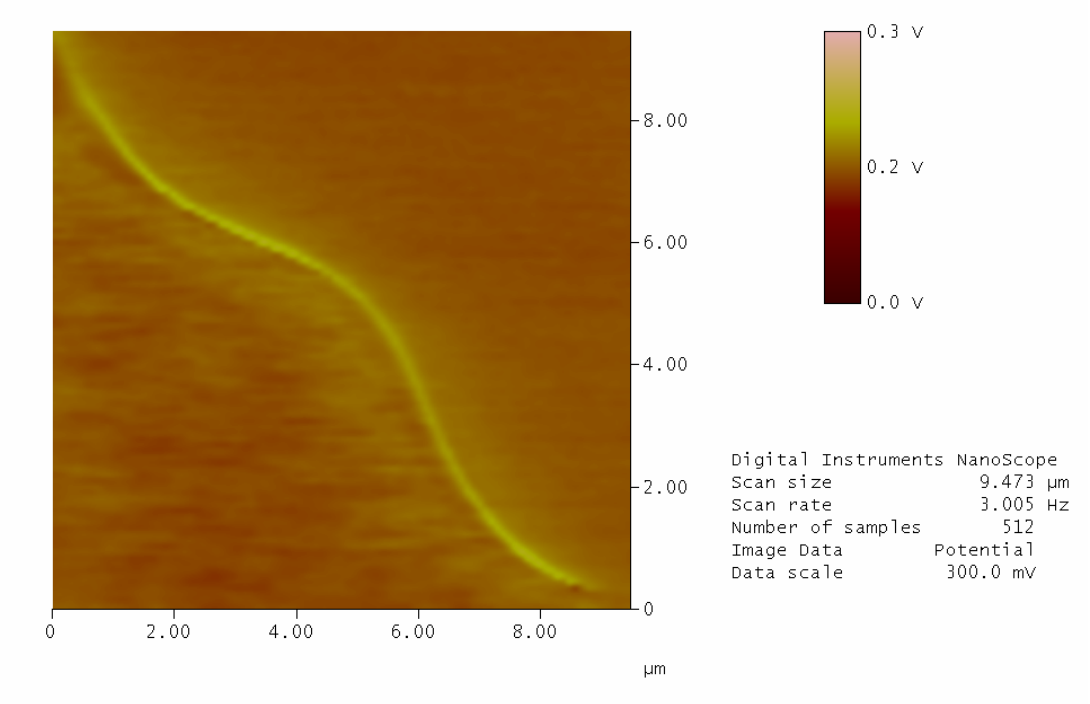

Figure 4.37 Surface potential image of the PPy-coated PA6 fibre prepared at low temperature (-25°C) in 10µm x 10µm

4.9 Concluding Remarks

A comparison study of polymerisation temperatures used for fabricating the PPy-coated fabric sensor was carried out. It referred to Chapter 3, it is confirmed that a smooth and dense layer of PPy film can increase its resistance to the attack of oxygen and water molecules, thereby enhancing its stability. It is evidenced that the lower fabrication temperature can help build up a thinner layer of coatings, resulting in more ordered structure of PPy with better sensing capacity.

Electrically conductive fabrics prepared by the CVD process at LT exhibit much higher strain sensitivity of over 400 at the strain of 50% with very large workable range of more than 50%. Furthermore, the LT CVD can produce the fabric sensor with higher electrical conductivity as well as better environmental stability. It is found that the particle size of PPy coating formed by the LT CVD is much smaller than the RT CVD. This produces a more oriented and structured film on the fabrics. The results of different characterisation methods, including thermal analysis, XRD polymer crystallinity analysis, surface morphology analysis by SEM and SPM etc., confirm that the LT CVD can deposit a thinner, smoother, more uniform and ordered structure of PPy film on the fabric surface, which is beneficial to the sensing performance and environmental stability.

CHAPTER 5

MECHANISM OF THE STRAIN SENSING BEHAVIOUR OF THE POLYPYRROLE-COATED FABRIC

5.1 Introduction

Fabric structure, fibre material, interfacial interaction between the polypyrrole (PPy) and the fabric, the structure and morphology of PPy coating layer are the crucial parameters that affect the sensing performance of the PPy-coated fabric sensor. The fabric used in this study is composed of polyamide (PA6) and Lycra (PU) fibres. It is essential to investigate the electro-mechanical behaviour of the PPy-coated PA6 and PPy-coated PU fibres that may be closely related to the sensing performance of the PPy-coated Tactel/Lycra knitted fabric.

The earlier investigations (Xue and Tao, 2004, 2005; Xue, Tao, Kwok and Leung, 2004) showed that the electro-mechanical behaviour of the conductive fibres depended strongly on the micro-structure of the coating layer and the fibres. The variation in the resistance of the PPy-coated PA6 fibres is mainly due to the change in the dimension of the fibres. In contrast, the variation in resistance with the applied strain for PPy-coated PU fibres is mainly attributed to the damage of the coating layer. Hitherto, very limited publications concerning the mechanism of the strain sensing behaviour of the PPy-coated knitted fabrics have been found. The strain sensing mechanism under unidirectional tension of the PPy-coated plain weave fabric was analysed by an electrical network (Xue, Tao, Leung and Zhang, 2005). A model based on a circuit network and two dimensional hexagon loop configuration was proposed for studying the electro-mechanical properties of stainless steel knitted fabric made from multi-filament yarn (Zhang, Tao, Wang and Yu, 2005). It was found that the key factor which governed the sensitivity of the stainless steel fabric sensor was the relationship between yarn contacting resistance and load. As a result, the fabric structure is crucial for fabric sensor development.

Chapter 4 shows that the strain sensitivity of the PPy-coated fabric prepared by padding followed by chemical vapour deposition (Pad-CVD) at low temperature (LT) reaches a very high strain sensitivity factor of 450 at a strain of 50%. It has been found that the surface morphology, coating thickness and structure of the PPy film affect the strain sensing behaviour of the PPy-coated fabrics. In order to understand the high strain sensitivity of the newly developed conductive fabric, the electro-mechanical properties of the PPy-coated PA6 yarn and PPy-coated PU yarn are tested. In addition, the observation of the morphological change during the fibre elongation is also conducted using simple tension instrument integrated with in-situ scanning electron microscopy (SEM). In this chapter, the main investigations are focused on (i) the LT fabrication of the PPy-coated fibres, (ii) the pre-extension level of PU fibres and (iii) the structure of knitted fabric in order to identify the deformation mechanisms of the PPy-coated fabrics.

5.2 Experimental

5.2.1 Materials and sample fabrication

The fabrication procedures of PPy-coated fabric and yarns under LT are the same as those stated in Section 4.2.1. The materials used for the mechanism study include PPy-coated fabric, PPy-coated PA6 yarn and PPy-coated PU yarn.

5.2.2 In-situ SEM observation set-up

SEM, Model Lecia Cambridge Stereoscan 440, integrating a tensile tester was employed to investigate the mechanism that governs the electro-mechanical behaviour of the PPy-coated fibres. This system enables the simultaneous observation of the morphological change of the PPy-coated fibres in micro-scale during tensile deformation. A single yarn was attached to a sample holder with a gauge length of 5mm, and was then elongated at a constant loading speed of 5μm/sec. The microphotographs were obtained at an accelerating voltage of 20 kV with different strain level. The tensile loading was extended to around 150% of fibre strain followed by an unloading procedure until the specimen returned to its original length.

5.3 Structure of Fabric Substrate

The fabric was a plain knitted fabric of 83% polyamide (Tactel) and 17% spandex (Lycra). It was knitted by plating technique, i.e. the simultaneous formation of one loop from two yarns as shown in Figure 5.1. The appearance of the knitted fabric after plating exhibits that one yarn (Tactel) will lie on the face of the fabric while the other yarn (Lycra) will lie on the back of the fabric as shown in Figure 5.2. The average loop length of PA6 yarn and Lycra yarn is 2.18mm/loop and 1.5mm/loop respectively. Lycra yarns are pre-extended by at least 45% in the fabric relax state. Figure 5.3 shows the Lycra loops with a smaller size.

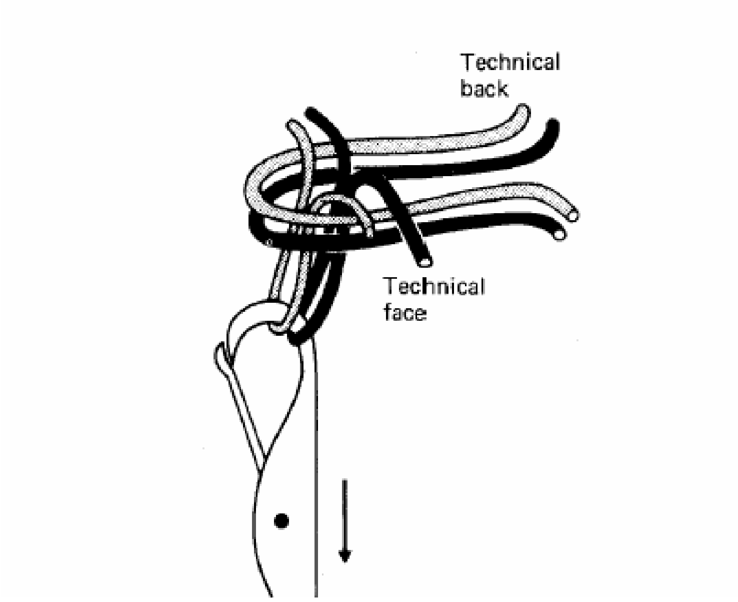

Figure 5.1 Plating relationship of two yarns

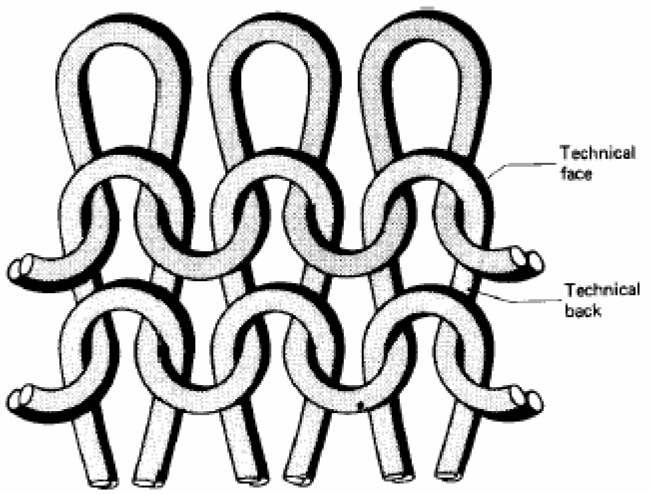

Figure 5.2 Schematic diagram of weft knitted fabric after plating

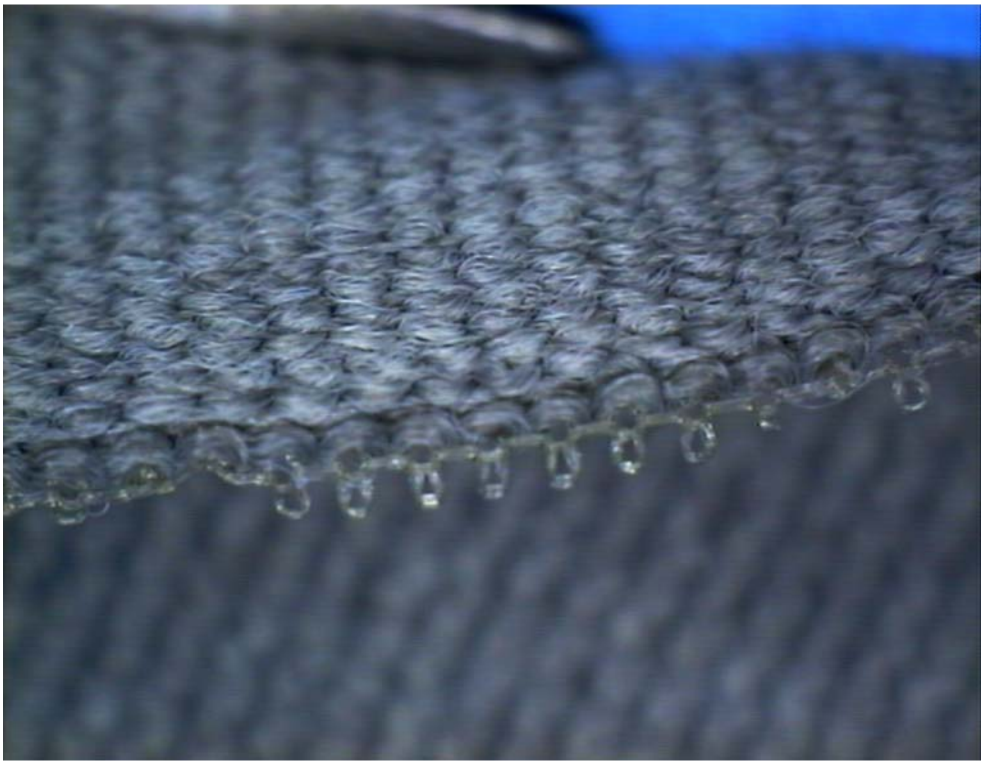

Figure 5.3 Lycra loops inside the PPy-coated fabric.

5.4 Electro-mechanical Behaviour of the PPy-Coated Fibres

5.4.1 Effect of substrate fibres

The resistance variation versus strain is shown in Figure 5.4. It can be seen that the two kinds of conductive yarns give the same order of resistance variation at the strain up to 60%. Beyond the strain of 60%, the electrically conductive PA6 fibres fracture gradually while the conductive PU yarn continues its deformation with more rapid variation in electrical resistance. The PU yarn experiences a much higher strain level than that of the PA6 yarn. Therefore, one of the key contributions to the high strain sensitivity of the developed conductive fabric under large deformation comes from the performance of the PPy-coated PU yarn.

Figures 5.5 and 5.6 show the tensile behaviour of conductive PA6 and PU yarns respectively. It is known that the PU yarn has much larger ultimate strain when compared with PA6 yarn. The former is over 550% while the latter is only about 60%. The PA6 yarn starts to break at around 60% strain. The Young's moduli of the PA6 and PU yarns are 6.67 and 0.06 cN/D, respectively. Hence, Lycra fibre is much softer and easy to deform than PA6 fibre.

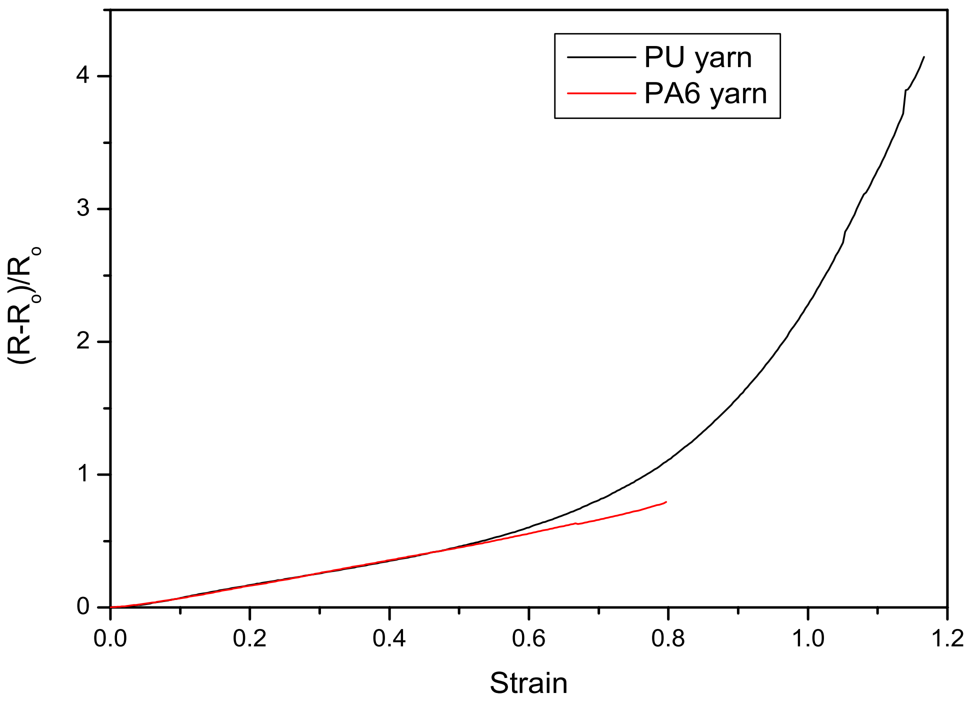

Figure 5.4 Resistance variation of the PPy-coated PA6 yarn and PU yarn prepared at low temperature

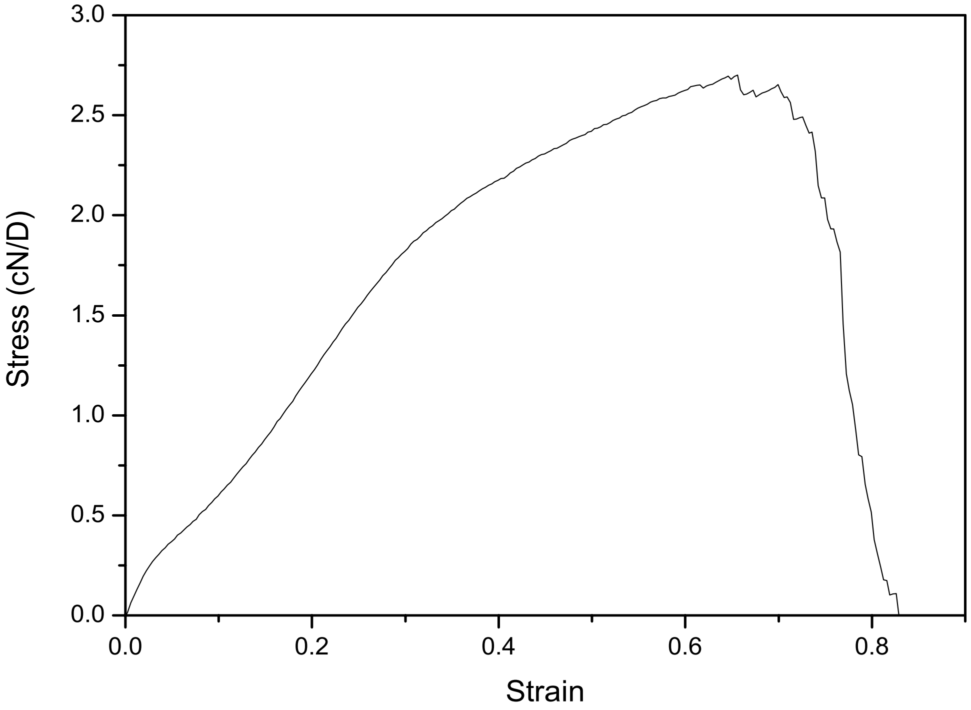

Figure 5.5 Stress versus strain curves of the PPy-coated PA6 yarn

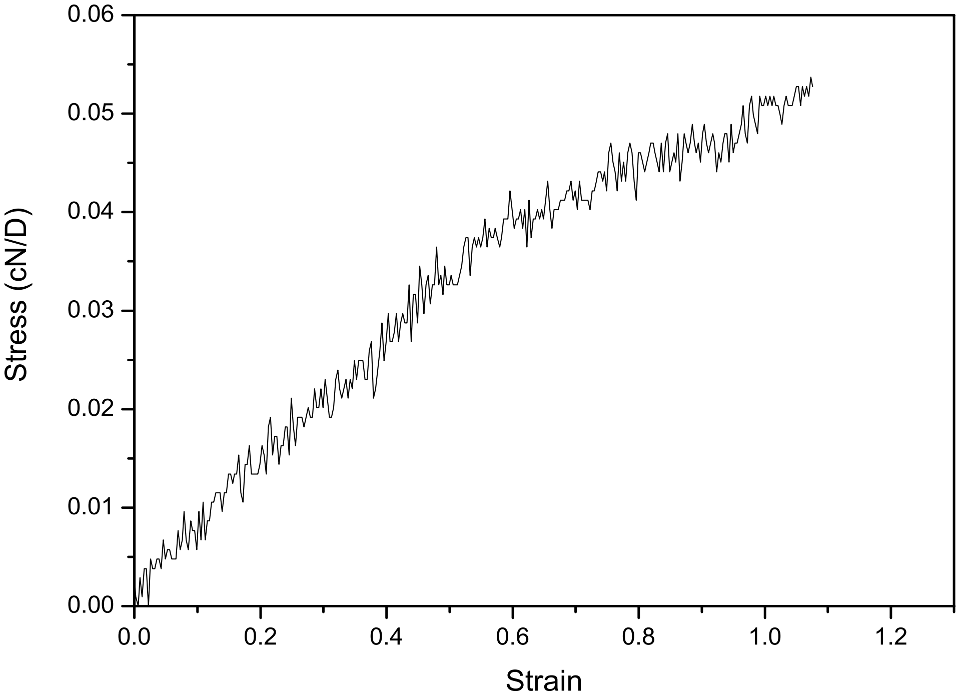

Figure 5.6 Stress versus strain curves of the PPy-coated PU yarn

SEM microphotographs of the two kinds of fibres at different strain levels are shown in Figures 5.7 to 5.9 with the magnification of 3000x and 1000x, respectively. The mechanisms governing the behaviour of these two kinds of conductive fibres are different from each other. After polymerisation of pyrrole, the PPy encases each single fibre of the yarn with a smooth, coherent layer of polymer. However, on the surface of PU fibres, very little micro-striations are found along the circumferential direction even before the specimen is extended ($\varepsilon = 0$). When compared with PPy which has a modulus of GPa, PU has a modulus of MPa (Xue and Tao, 2005), implying that the hard coating on the soft and extensible fibre is very easily damaged. As a result, even a slight extension during specimen preparation may cause these micro-defects on the surface.

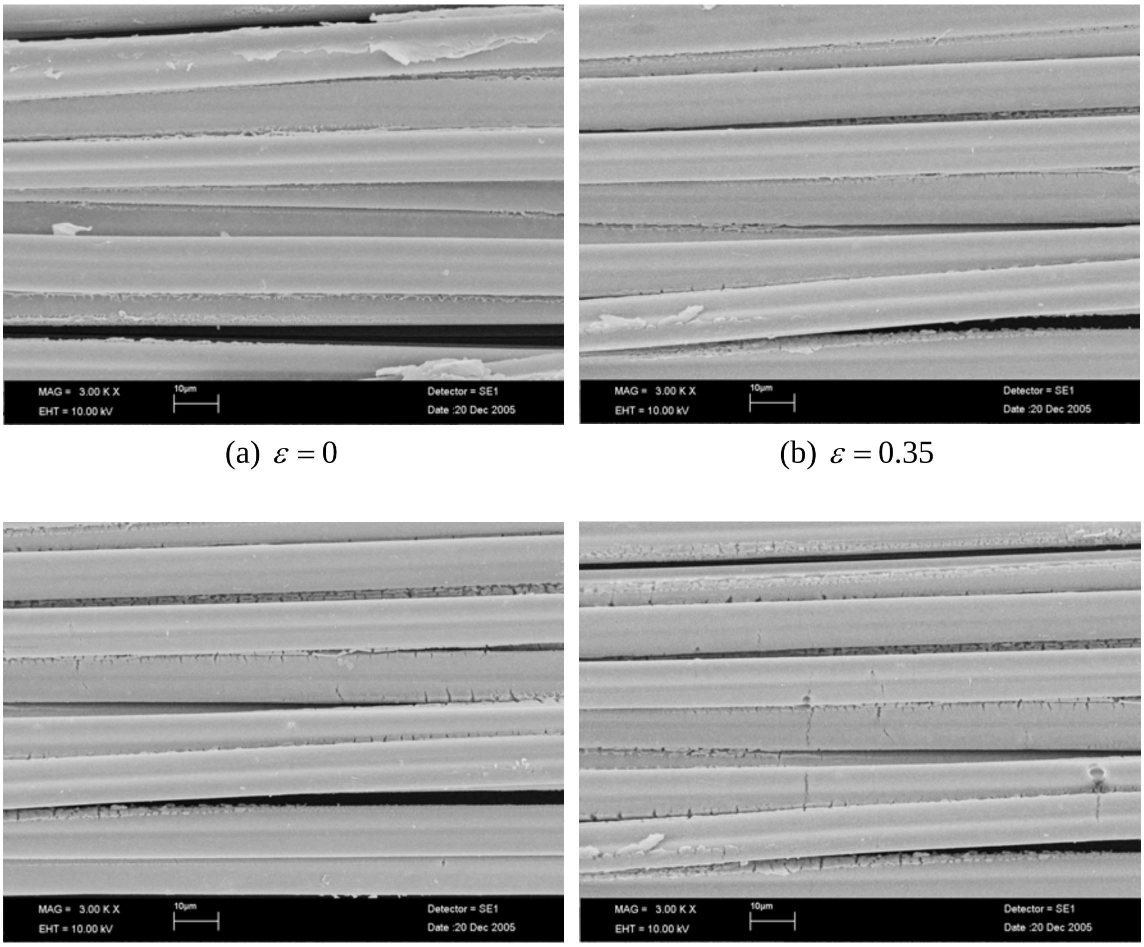

(a) $\varepsilon = 0$ (b) $\varepsilon = 0.35$

(c) $\varepsilon = 0.58$ (d) $\varepsilon = 0.66$

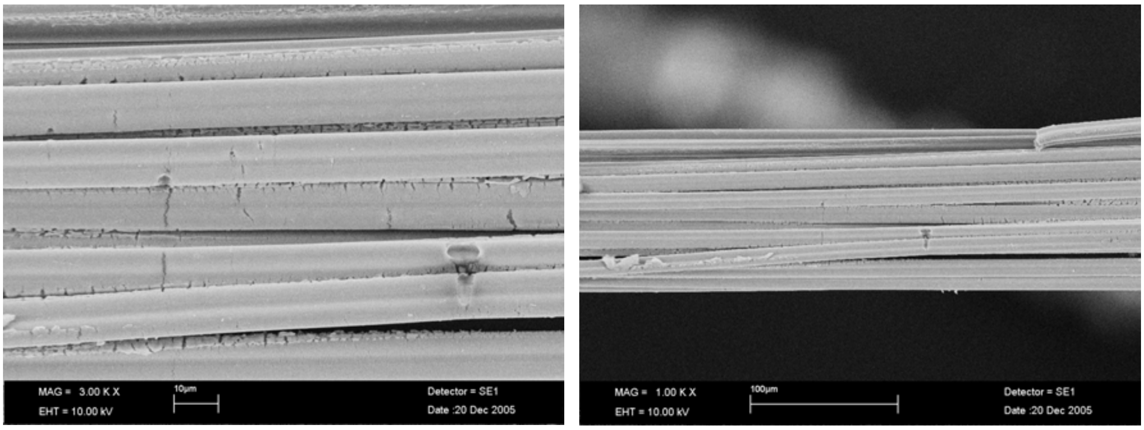

(e) $\varepsilon = 0.70$ (f) $\varepsilon = 0.75$

Figure 5.7 SEM microphotographs of the PPy-coated PA6 yarn at different strain levels

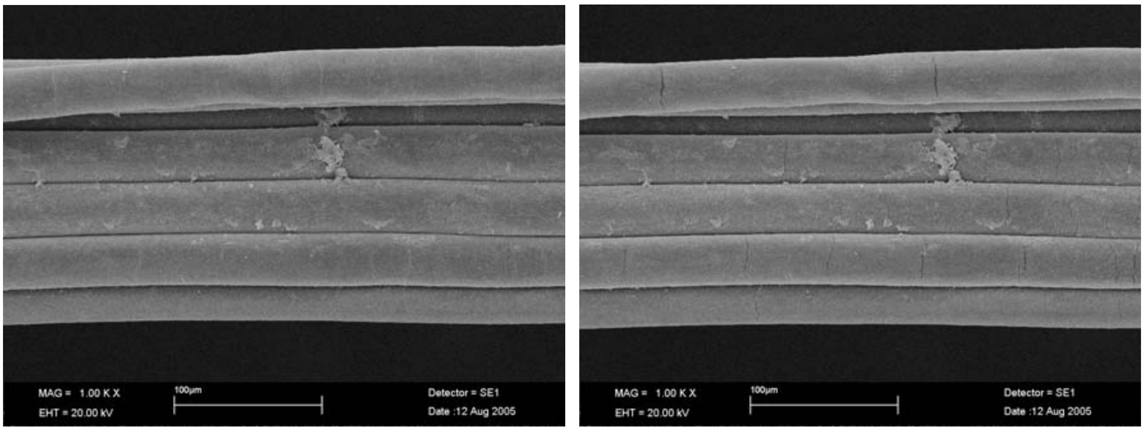

(a) $\varepsilon = 0$ (b) $\varepsilon = 0.10$

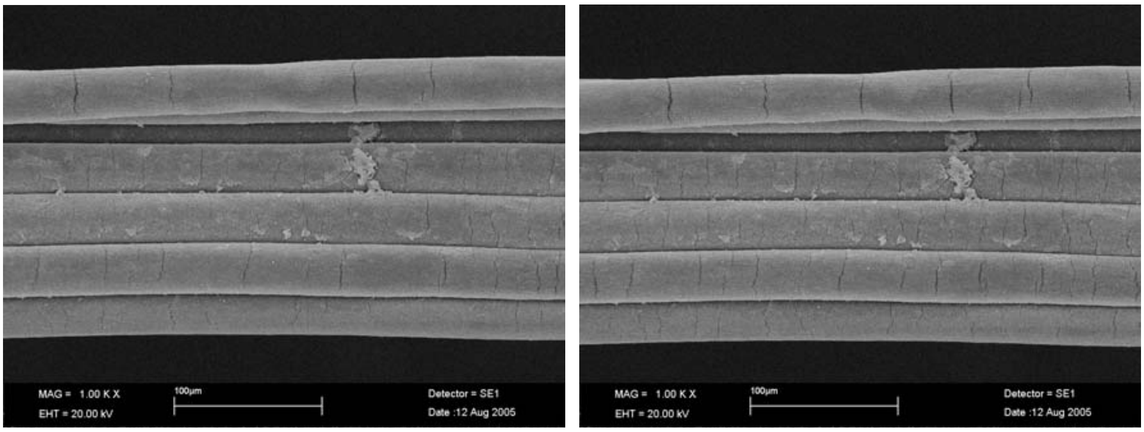

(c) $\varepsilon = 0.14$ (d) $\varepsilon = 0.18$

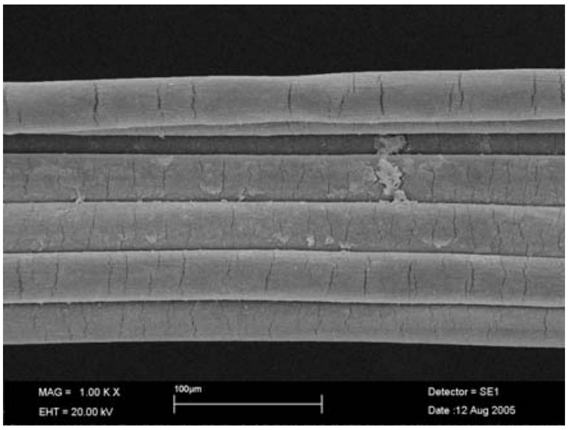

(e) $\varepsilon = 0.22$

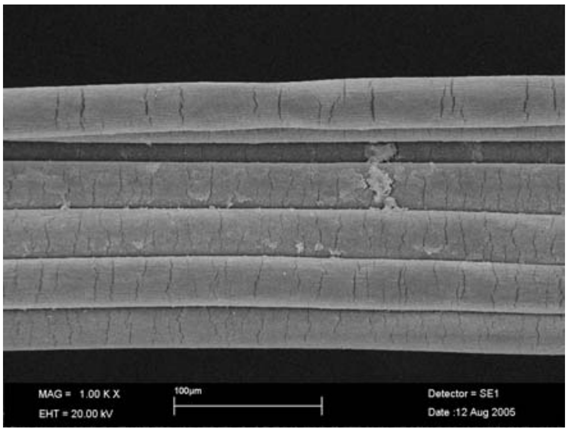

(f) $\varepsilon = 0.26$

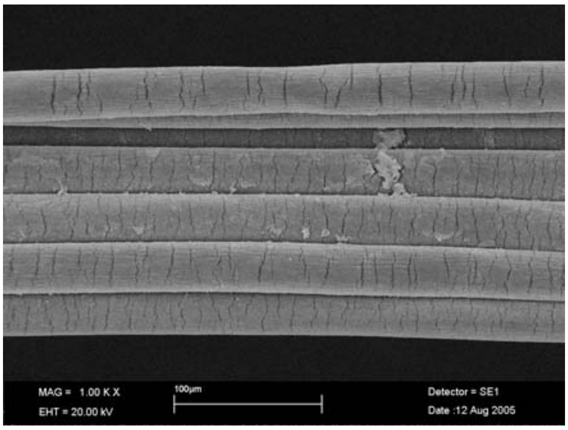

(g) $\varepsilon = 0.45$

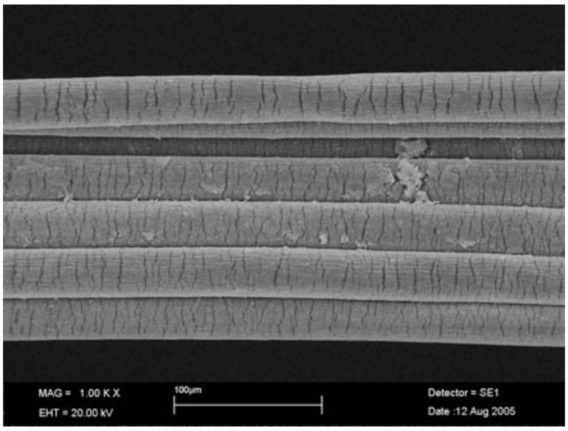

(h) $\varepsilon = 0.62$

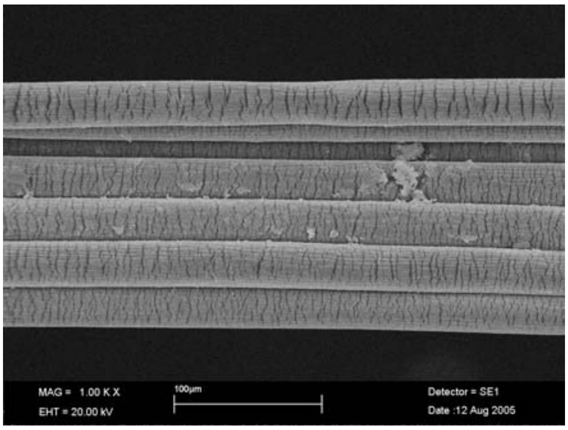

(i) $\varepsilon = 0.84$

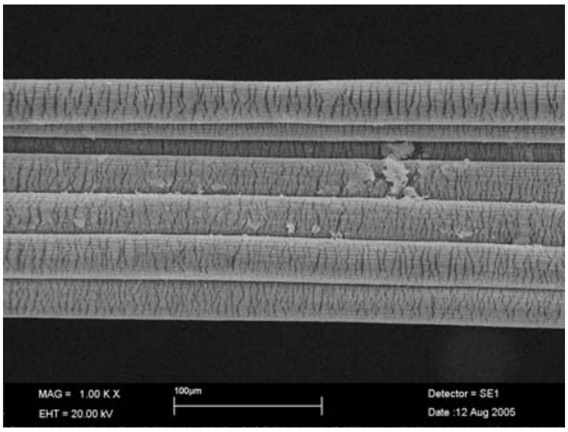

(j) $\varepsilon = 1.20$

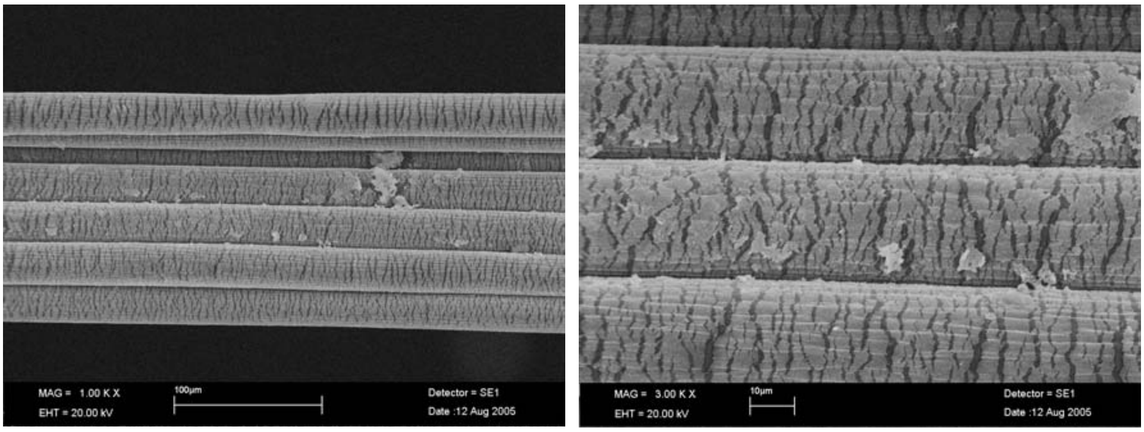

(k) $\varepsilon = 1.40$ (l) $\varepsilon = 1.40$

Figure 5.8 SEM microphotographs of the PPy-coated PU yarn at different strain levels during stretching

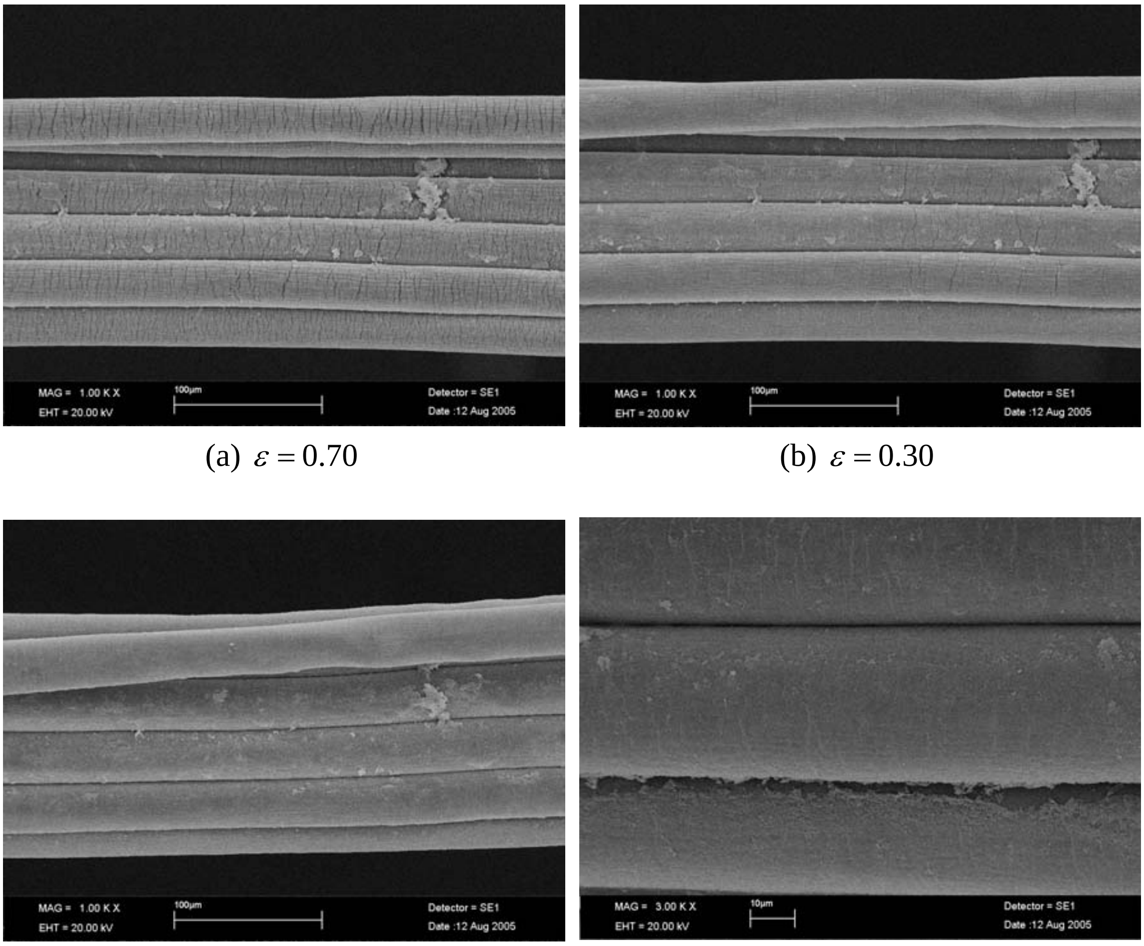

(a) $\varepsilon = 0.70$ (b) $\varepsilon = 0.30$

(c) $\varepsilon = 0$ (d) $\varepsilon = 0$

Figure 5.9 SEM microphotographs of the PPy-coated PU yarn at different strain level during unloading

From the in-situ SEM observations, it is obvious that the coating layer of the PA6 fibres can remain complete without any apparent damage until the longitudinal strain reaches about 58%. Once the damage occurs to the surface of the fibre, it fractures abruptly at about 70% strain as shown in Figure 5.7 (e and f). The resistance variation is mainly due to the change in dimension of the fibres. This phenomenon is similar to that of the PPy-coated PA6 fibres prepared at room temperature (RT) as reported in previous study (Xue, Tao, Kwok and Leung, 2004). This also explains that there is no significant differences between the electro-mechanical behaviour of the PPy-coated PA6 yarn prepared at RT and LT as discussed in Section 4.5.

In contrast, some obvious transverse micro-cracks are found on the coating layer of the PPy-coated PU fibres at an axial strain of 10%. As the tensile test is progressed, the early transverse cracks will propagate through the entire width of the fibre. In addition, more cracks are formed progressively along the fibre axis at the same time. The spacing between two adjacent cracks is getting smaller while the length of the cracks is getting longer. Below the axial strain of up to 120%, a conducting PPy network forming the current conducting paths still exists so that the PPy-coated PU fibres still possess the current-carrying capacity. The resistance variation of the applied strain is mainly attributed to these micro-cracks appearing on the coating layer. With the accumulation of damage, the continuous current conductive paths become longer and thinner, and the electrical resistance increases rapidly until the accumulated damage of the coating layer reaches a level sufficient to block the electrical conductivity of the PPy-coated fibres.

Under cyclic tension as shown in Figures 5.9 and 5.10, the micro-cracks are closing gradually when unloading the tension. All the cracks are closed when the strain is returned to 0%. In the repeated tension, the transverse cracks will re-open and then re-closed during loading and unloading respectively, resulting in the cyclic variation of electrical resistance. As a result, the electrical resistance of the PPy-coated PU yarn will increase, followed by a decrease in the cyclic tensile test as shown in Figure 5.10, which can be interpreted as the opening and closing of the transverse cracks. It can be seen that a shift in the electrical resistance (R_{shift}) may be produced when unloading to original. At the end of the first cycle, the electrical resistance connot return to its initial value, $R_{o.}$ This shift in resistance is probably attributed to the residual plastic deformation.

The different behaviour of these two kinds of conductive fibres can be further explained by the difference in mechanical properties as shown in Figure 5.6. The Young’s modulus of the PA6 yarn is much larger than the PU yarn, i.e. the former is about 110 times of the latter. In fact, under the same level of the applied stress, the PPy-coated PU yarn will experience much larger deformation than the PPy –coated PA6 yarn. Since a larger strain will result in higher strain energy, thus, the surface cracks may form easily due to the release of large strain energy stored in the PPy-coated PU yarn.

The phenomenon of crack-opening and crack-closing mechanism of the PPy-coated PU yarn is similar to the findings of the previous study obtained by Xue and Tao (2005). In this study, the PPy-coated PU yarn produced by the extremely low temperature polymerisation has been compared with the samples prepared by the room temperature polymerisation. It is found that the crack-opening of the LT PPy-coated PU yarn commences at a higher strain, i.e. 10% of strain for LT shown in Figure 5.8 (b) and 3.8% of strain for RT shown in Figure 2.19 (a). In order to obtain the same appearance of crack level of the RT sample at the strain of 3.8%, the LT sample needs to be extended to more than 50% of strain. This phenomenon can help to explain the electro-mechanical behaviour of the PPy-coated PU yarn as discussed in Section 4.5. The electrical resistance of RT sample becomes overflow when less than 20% of strain. On the contrary, the resistance change of the sample prepared by LT increases gradually with the strain up to 110%. The significant difference between the RT and LT CVD prepared the PPy-coated PU fibres may be probably due to the quality of the coating layers formed on the fibre substrates. The comparison of the PPy-coating layer at RT and LT has been presented in Chapter 4. It is found that the coating film prepared by the LT exhibits denser, smoother, thinner and uniformly distributed layer on the fibre surface. Owing to this high performance of the coating layer formed, the cracks will form at a higher strain and so a higher strain sensitivity is achieved finally.

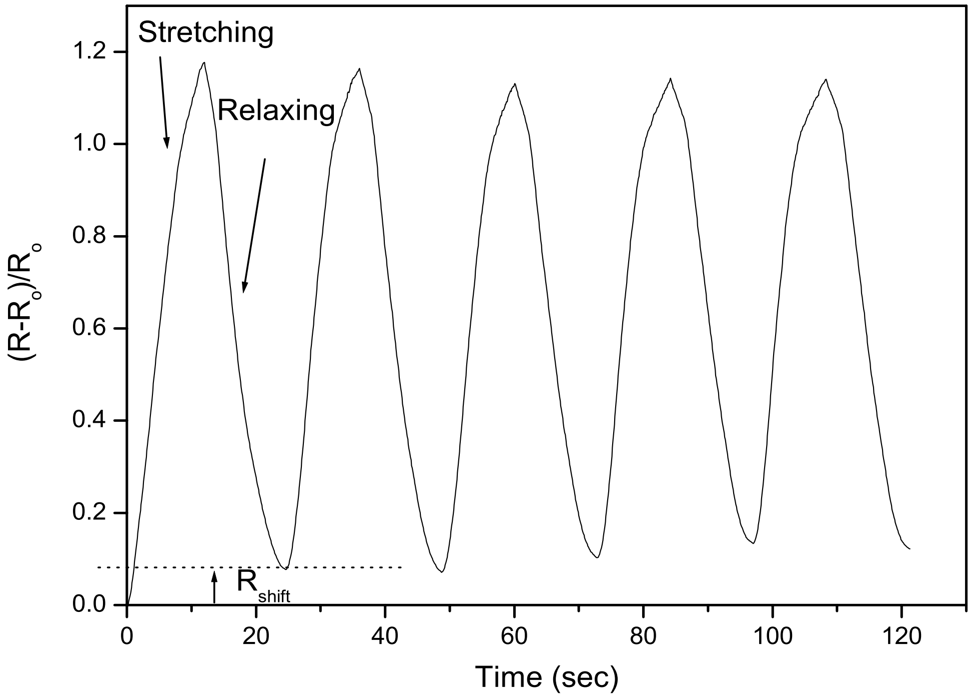

Figure 5.10 Relative resistance change as a function of time in a cyclic tensile test of the PPy-coated PU yarn

5.4.2 Effect of pre-extension level

The PU yarns were pre-extended at different levels, i.e. no pre-extension, 20%, 40% and 60% pre-extension, and coated with PPy in order to simulate the actual state of PU yarns inside a fabric. The experimental procedures involved the pre-stretch of the PU yarns with determined pre-extension levels and mounting on a frame. The PPy coating was formed on the PU yarns by means of LT CVD. The pre-extended PPy-coated PU yarn were then clamped on the Instron tensile tester and further extended for electro-mechanical tests.

The resistance variation versus strain of the PU yarns with different pre-extension levels is shown in Figure 5.11. It can be seen that beyond the strain of 50%, the electrically conductive PU yarn with 60% pre-extension continues its deformation with more rapid variation in electrical resistance as compared to the yarn with 0% pre-extension prior to the PPy coating. The electro-mechanical behaviour of the PU yarns with 20% and 40% pre-extension shows very slight difference in the variation of electrical resistance. It should be noted that for all the knitted fabric used in this research project, the PU yarns were set by the amount of at least 45% pre-extension. The relative electrical resistance changes of PU yarn with 40% and 60% pre-extension can reach up to 80 and 100 respectively at 250% of strain. Therefore, another key reason for the high strain sensitivity of the developed conductive fabric under large deformation is due to the unique performance of the PPy-coated PU yarn with specific pre-extension levels.

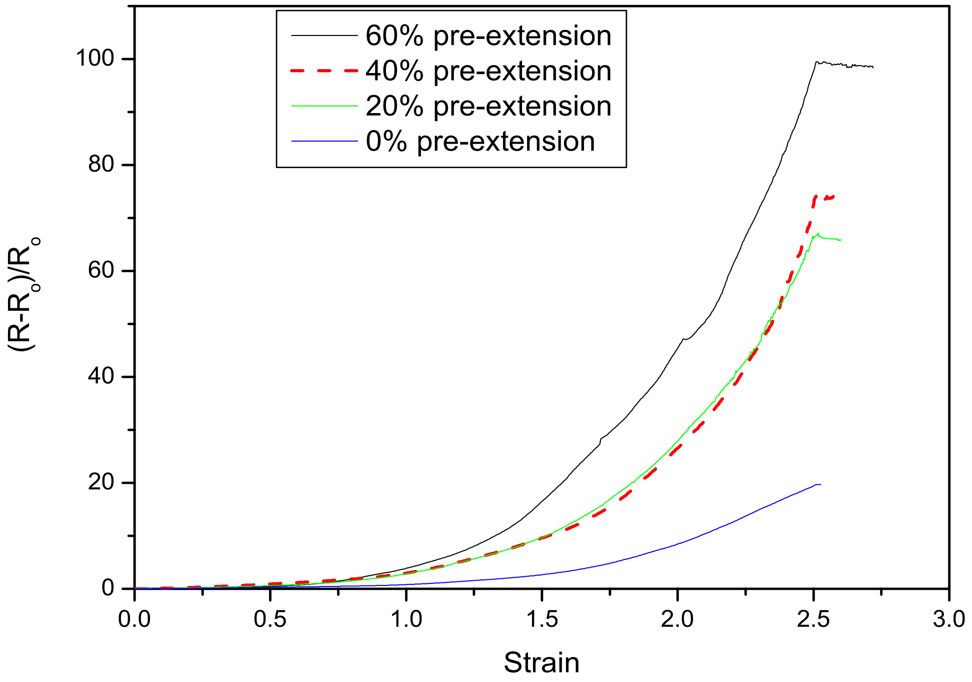

Figure 5.11 Resistance variation of the PPy-coated PU yarn with different pre-extension levels

The SEM microphotographs of the PPy-coated PU yarn with different pre-extension levels at large deformation are shown in Figures 5.12 (a-d). These figures show the morphology of the PPy-coated PU yarn with the pre-extension of 0%, 20%, 40% and 60% respectively at 50% of strain level. The PU yarns were coated with PPy under the pre-determined extension levels, and then further extended for the in-situ SEM observation. Hence, the actual strain of the PU yarns is different from that of the PPy coating. The ultimate strain of the PU yarns shown in Figure 5.12 (a –d) are 50%, 80%, 110% and 140%, respectively. It can be seen that the cracks are wider, longer, deeper and more acute with higher pre-extension of the PPy-coated PU yarn. As for the yarn without pre-extension, the micro-cracks are observed on the surface of coating film. However, the distance between cracks along the circumferential direction is shorter, and the amount of cracks is lesser than other samples with higher pre-extension level. The conducting PPy network still exists and possesses the current-carrying capacity.

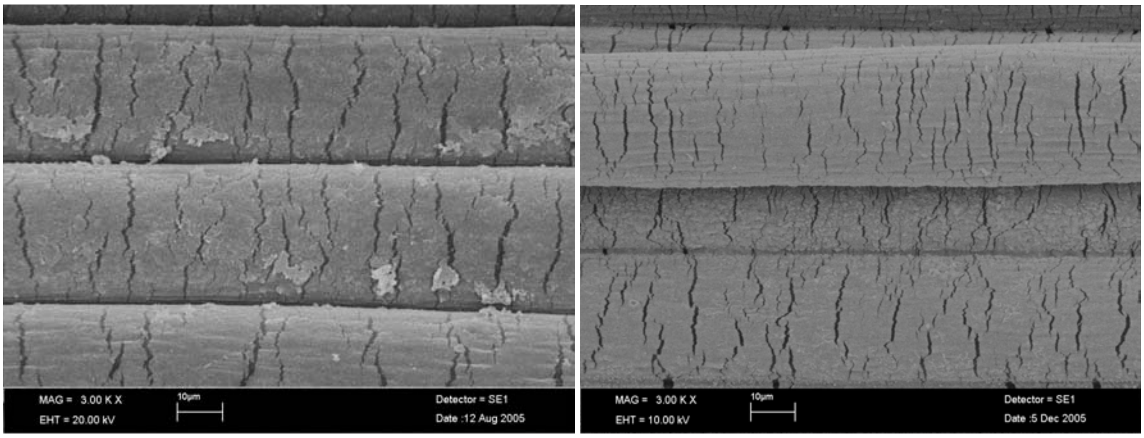

(a) $\varepsilon = 0.50$, 0% pre-extension (b) $\varepsilon = 0.50$, 20% pre-extension

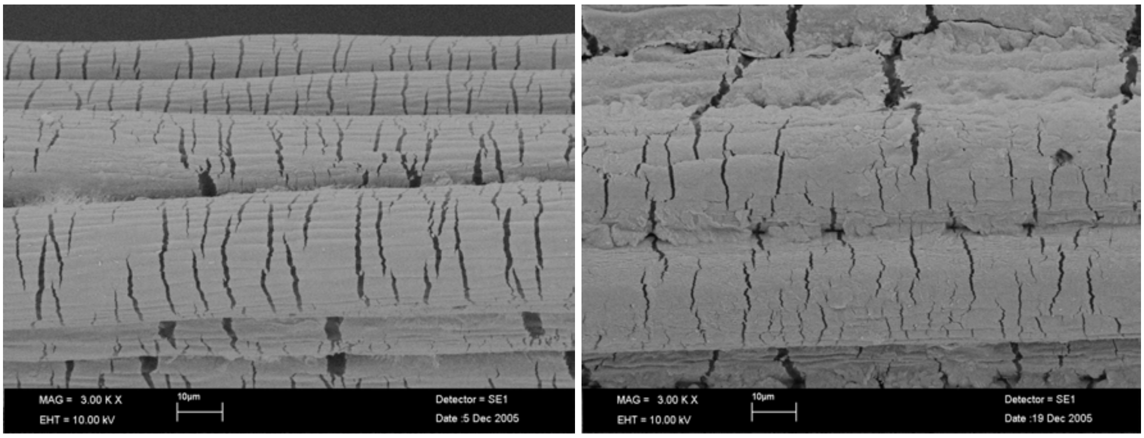

(c) $\varepsilon = 0.50$, 40% pre-extension (d) $\varepsilon = 0.50$, 60% pre-extension

Figure 5.12 SEM microphotographs of the PPy-coated PU yarn with different pre-extension at certain strain level

On the other hand, for the yarn with 60% pre-extension level, more obvious and deeper cracks are observed when compared with the other samples having the same elastic strain at 50%. The damage of the coating layer is much more serious than the other samples as reflected by the termination of some areas of the PPy network due to the blocking and cutting of the paths by the thick and deep cracks. As a result, the electrical resistance increases rapidly after 50% of strain. This can explain the higher strain sensitivity of the PPy-coated PU yarn with larger pre-extension level as shown in Figure 5.11.

As a matter of fact, higher pre-extension level will result in higher strain energy. It is the surface cracks that release the large strain energy stored in the PPy-coated PU yarn (Beuth, 1992; Chen, Cotterell and Wang, 2002; Xue, Tao, Kwok and Leung, 2004). The relationship between the strain energy and pre-extension level is illustrated in the following (Patnaik and Hopkins, 2003).

The product of stress and strain represents the strain energy density (U_d). The total amount of strain energy (U) stored in the structure is obtained by integrating the density function over the volume as:

$$U = \int_v U_d dv \tag{5.1}$$

where U is the total amount of strain energy stored in the volume V of the structure. The strain energy density U_d, or strain energy per unit volume, is defined as:

$$U_d = \int_\varepsilon \sigma d\varepsilon \tag{5.2}$$

where σ and ε are the uniaxial stress and strain, respectively. According to the experimental data shown in Figure 5.13, the relationship of stress and strain of PU yarn is bi-linear, and expressed by the following equations:

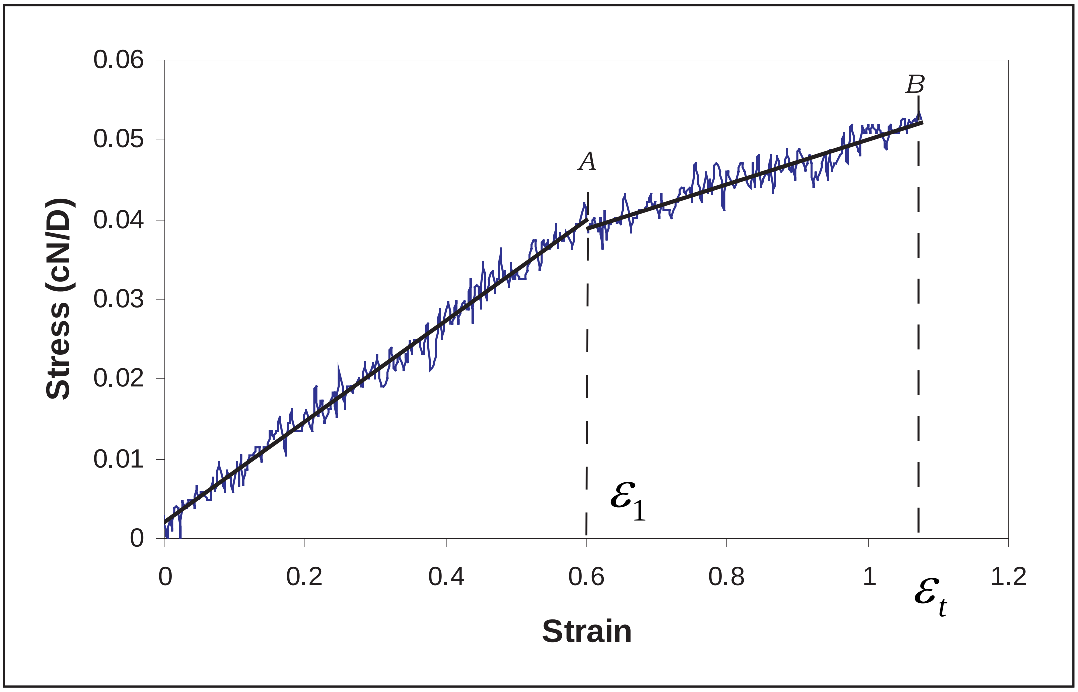

Figure 5.13 Stress versus strain curves of the PPy-coated PU yarn for strain energy densities analysis

$$\sigma = \begin{cases} E_1\varepsilon & 0<\varepsilon<\varepsilon_1 \\ (E_1 - E_2)\varepsilon_1 + E_2\varepsilon & \end{cases} \tag{5.3}$$

where *E* is the Young's modulus, *E₁* is the slope between OA and *E₂* is the slope between AB.

Elimination of stress between Equations (5.2) and (5.3) yields the density function in term of strain as:

$$U_d = \int_0^{\varepsilon_1} E_1\varepsilon d\varepsilon + \int_{\varepsilon_1}^{\varepsilon_2} \left[(E_1 - E_2)\varepsilon_1 + E_2\varepsilon\right] d\varepsilon \tag{5.4}$$

$$U_d = \frac{1}{2}E_1\,\varepsilon^2\Big|_0^{\varepsilon_1} + (E_1 - E_2)\varepsilon_1\,\varepsilon\Big|_{\varepsilon_1}^{\varepsilon_t} + \frac{1}{2}E_2\,\varepsilon^2\Big|_{\varepsilon_1}^{\varepsilon_t} \tag{5.5}$$

$$U_d = \frac{1}{2}E_1\varepsilon_1^{\ 2} + (E_1 - E_2)\varepsilon_1(\varepsilon_t - \varepsilon_1) + \frac{1}{2}E_2(\varepsilon_t^{\ 2} - \varepsilon_1^{\ 2}) \tag{5.6}$$

$$U_d = (E_2 - E_1)\varepsilon_1^{\ 2} + (E_1\varepsilon_1 - E_2\varepsilon_1)\varepsilon_t + \frac{1}{2}E_2\varepsilon_t^{\ 2} \tag{5.7}$$

where ε_t represents the total strain.

In the experiments, the PU yarn has been pre-extended at certain strain level which is called initial strain (ε_i). Then, the yarn will be further extended that is called relative strain (ε_r). Therefore, the strain energy density functions have been modified to handle initial deformation. The strain due to total deformation, referred to as total strain, is the sum of the relative strain and initial strain.

$$\varepsilon_t = \varepsilon_r + \varepsilon_i \tag{5.8}$$

In the definition of strain energy due to total deformation, the range of integration is taken from the existing initial strain (ε_i) with respect to the total strain (ε_t). Therefore, the strain energy density U_d^t of total deformation is obtained by substituting Equation (5.8) into (5.7) as follows:

$$U_d^t = (E_2 - E_1)\varepsilon_1^{\ 2} + (E_1\varepsilon_1 - E_2\varepsilon_1)(\varepsilon_i + \varepsilon_r) + \frac{1}{2}E_2(\varepsilon_i + \varepsilon_r)^2 \tag{5.9}$$

Since the total strain energy density is directly related to the initial strain, thus the PU yarn with larger pre-extension levels will store larger amount of strain energy inside the yarn leading to easier formation of cracks. From the above analysis and the in-situ SEM photographs, it is concluded that knitted structure with various pre-extension levels of PU yarn is one of the critical parameter that affects the strain sensitivity of the PPy-coated fabrics.

5.5 Fabric Structure and Deformation Mechanism of Weft Knitted Tactel/Lycra Plain Fabric

Figure 5.14 shows the stress-strain curves of PPy-coated fabric in the walewise and coursewise directions. It can be seen that the stress increases up to 0.14 MPa and 0.08 MPa at 50% of strain in the walewise and coursewise directions respectively. The different behaviour under tensile loading reflects different geometry and structural behaviour of the weft knitted fabric structure. PPy-coated fabric displays higher stiffness on the walewise direction than in the coursewise direction.

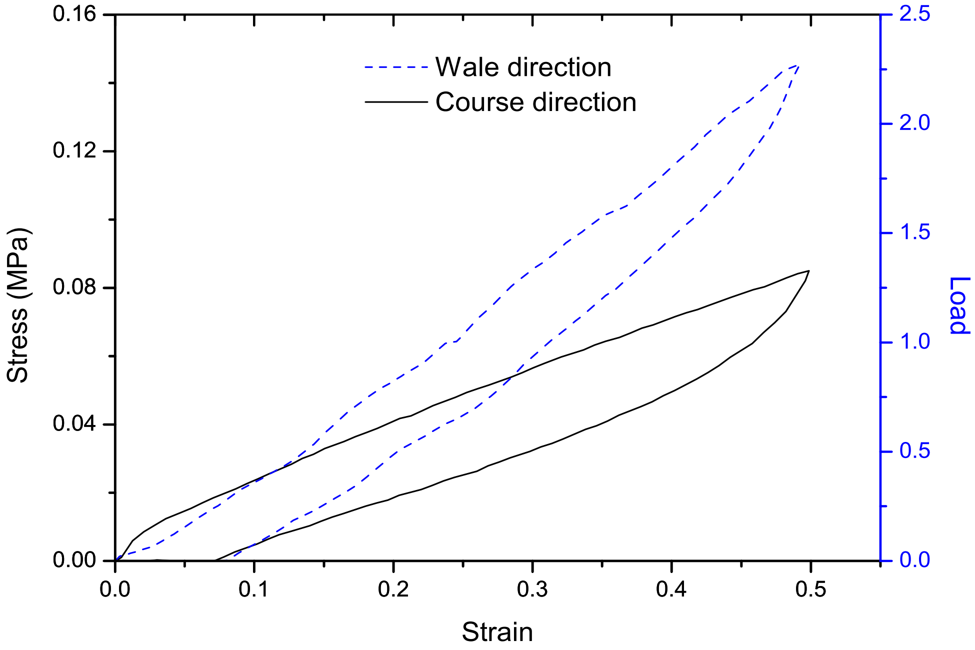

Figure 5.14 Tensile behaviours of PPy-coated fabrics along wale direction and course direction

Different strain sensitivities of the PPy-coated fabrics in the walewise and coursewise extensions are performed as shown in Figures 5.15 and 5.16. The strain sensitivities of the same PPy-coated fabric are 450 and 2.7 for the walewise and coursewise extension respectively.

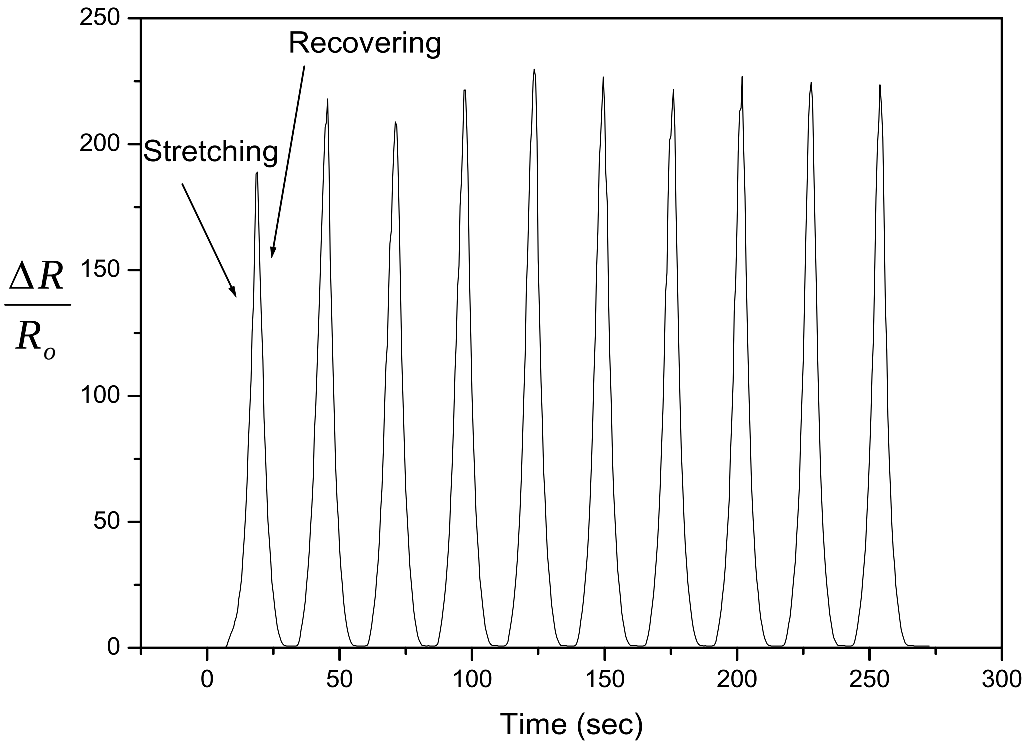

Figure 5.15 Relative resistance change as a function of time in a cyclic tensile test of the PPy-coated fabrics along the wale direction

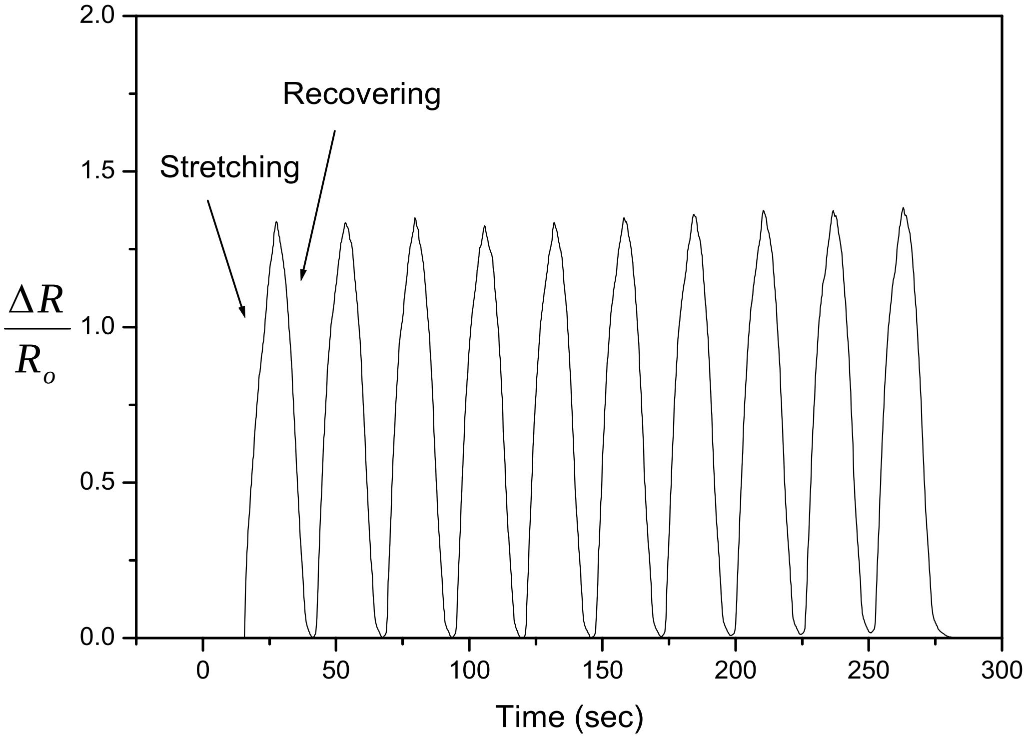

Figure 5.16 Relative resistance change as a function of time in a cyclic tensile test of the PPy-coated fabrics along the course direction

Figures 5.17 and 5.18 illustrate the fabrics at different strain levels in the wale and course directions respectively.

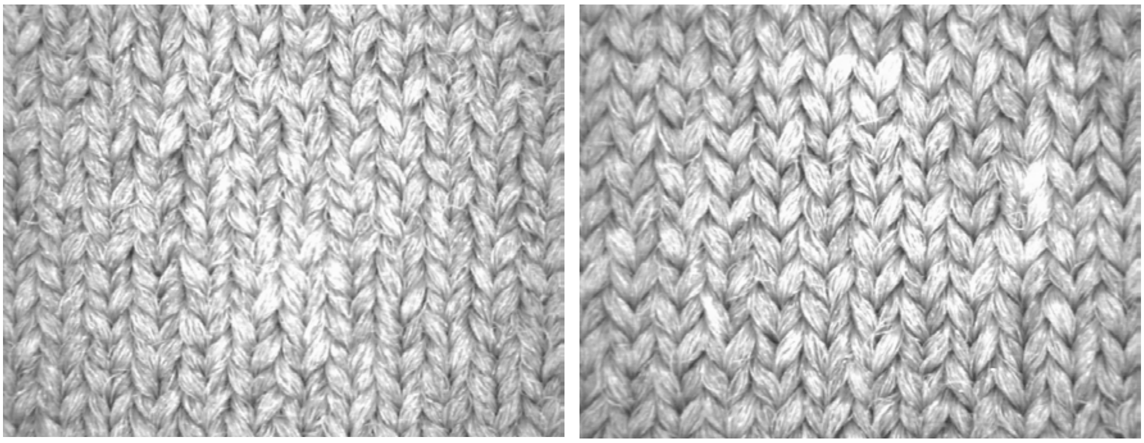

(a) $\varepsilon = 0$ (b) $\varepsilon = 0.20$

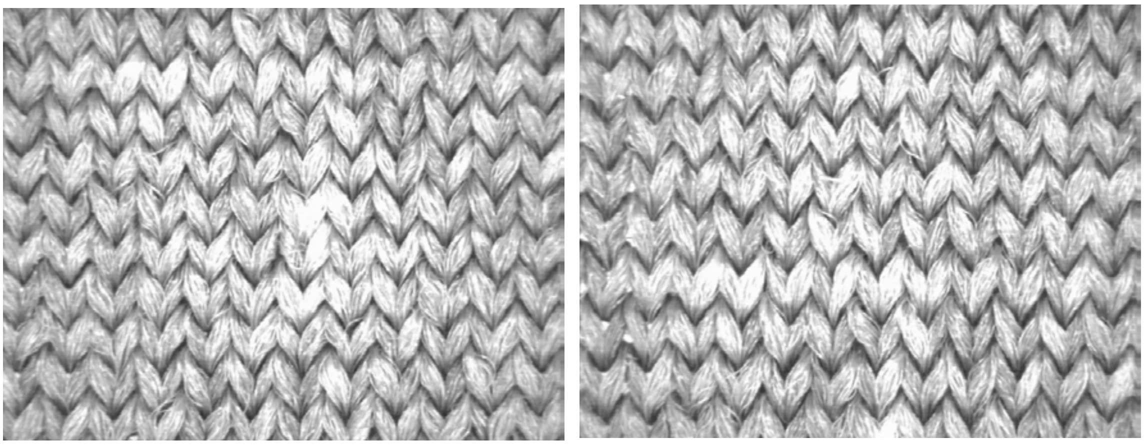

(c) $\varepsilon = 0.50$ (d) $\varepsilon = 0.70$

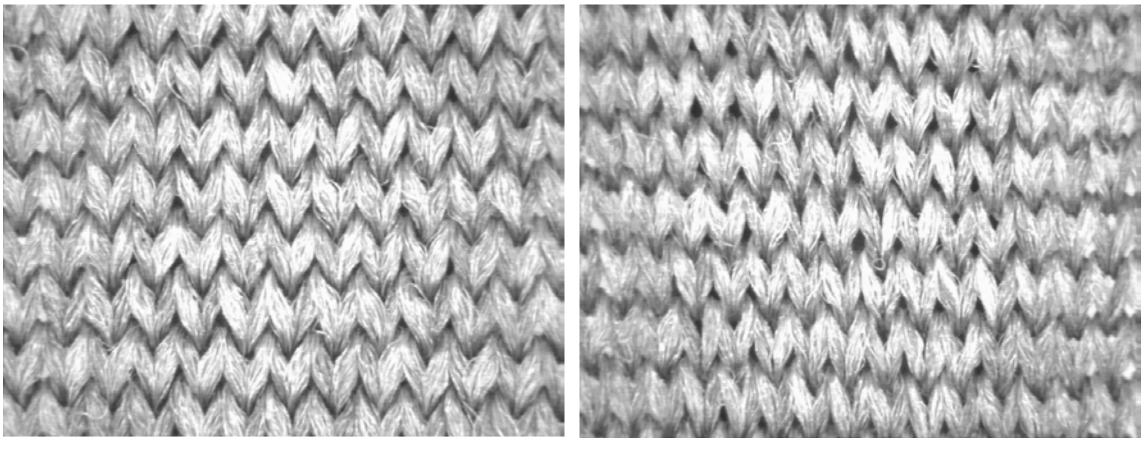

(e) $\varepsilon = 1.00$ (f) $\varepsilon = 1.50$

Figure 5.17 Photographs of the PPy-coated fabric at different strain levels in the wale direction

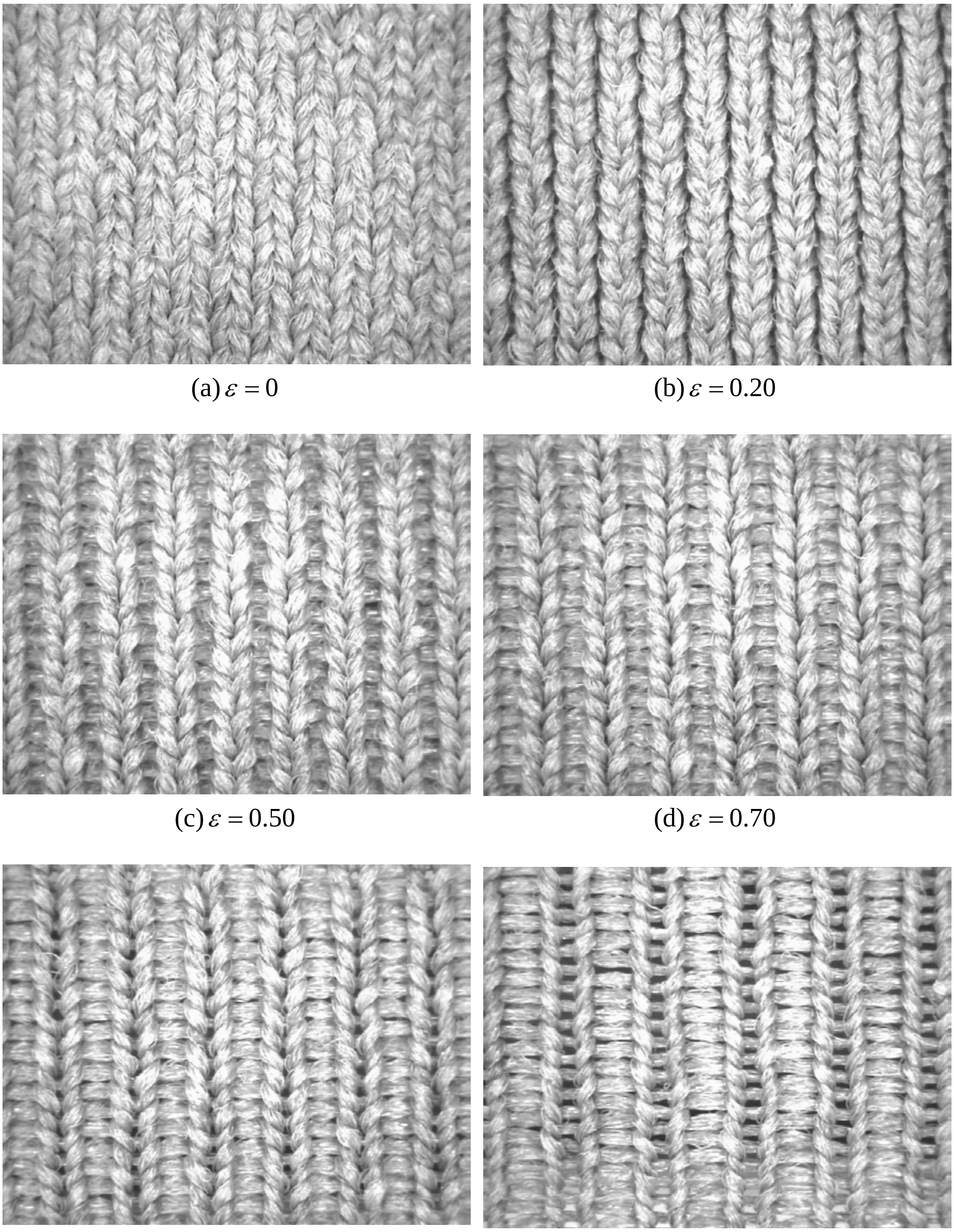

(a) $\varepsilon = 0$

(b) $\varepsilon = 0.20$

(c) $\varepsilon = 0.50$

(d) $\varepsilon = 0.70$

(e) $\varepsilon = 1.00$

(f) $\varepsilon = 1.50$

Figure 5.18 Photographs of the PPy-coated fabric at different strain levels in the course direction

From figures 5.17 and 5.18, two phenomenon can be observed that may ascribe to the strain sensitivity of PPy-coated fabric in different stretching direction. Firstly, the yarn contact in the loops is different in the wale and course directions. Secondly, the amount of yarns slippage is different in the wale and course directions.

The basic repeat unit of a plain weft knitted structure is shown in Figure 5.19. The point at which a yarn in a neighbouring loop crosses over another loop is called interlock (Farrington, 1995). When stretching the fabric, the fabric loop is deformed to share the load. Initially, the main cause of loop deformation is the slipping of yarns with respect to each other at the interlacing. During this deformation, energy is stored in the fabric as bending potential energy. Unless the yarns have poor bending elasticity, the fabric will probably recover from the deformation once the applied force is removed.

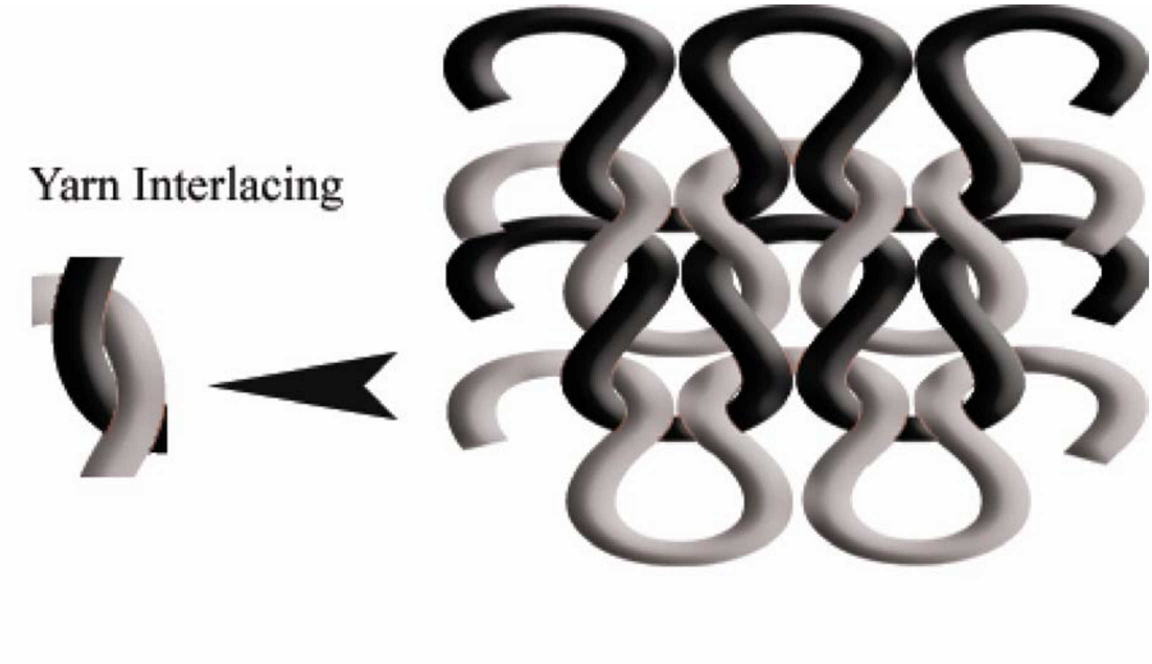

Figure 5.19 Graphical representation of the structure of a plain weft knitted fabric and indication of yarn interlacing

Since the fabric is tightly knitted, the knitted loops show very closed contact between the yarn interlacing. The yarn contact points getting lesser while stretching the fabric in the wale direction as shown in Figure 5.20. It is one of the reason that causing increment of electrical resistance in the initial phase when stretching the fabric in the wale direction.

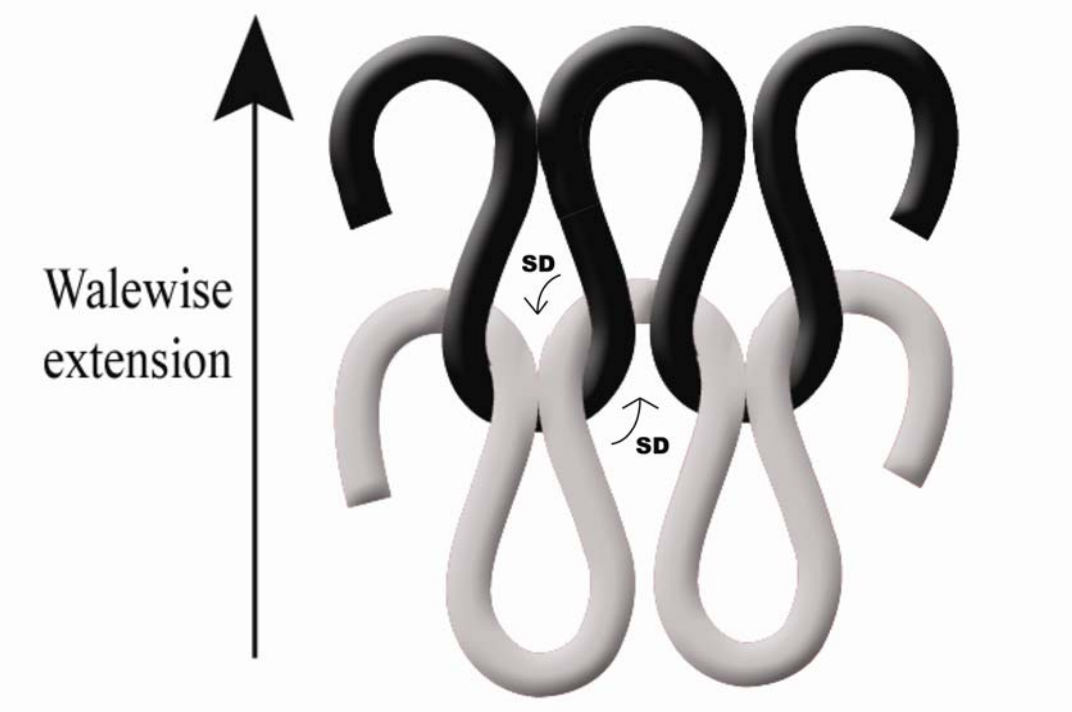

*SD = Yarn Slippage Direction

Figure 5.20 Graphical representation of fabric jamming in the course direction when walewise extension

Comparatively, the loops along the course are not that tightly contact as the loops along the wales when the fabric is in related state as shown in Figures 5.17 (a) and 5.19. Therefore, the yarn contact points are lesser than the wale direction. These contact points getting lesser while stretching the fabric in the course direction as shown in Figure 5.21. It is causing relatively lower increment of electrical resistance when stretching the fabric in the wale direction. The relative changing of electrical resistance versus fabric strain in the wale and course direction is exhibited in Figures 5.22 and 5.23. Figure 5.24 compares the resistance changes versus strain of the PPy-coated fabric stretched in different directions. It can be seen that the relative resistance changes more while the fabric is being stretched in the wale direction before 10% strain. Therefore, it is confirmed that the effect of yarn contact in the loops is one of the contributions on the strain sensitivity.

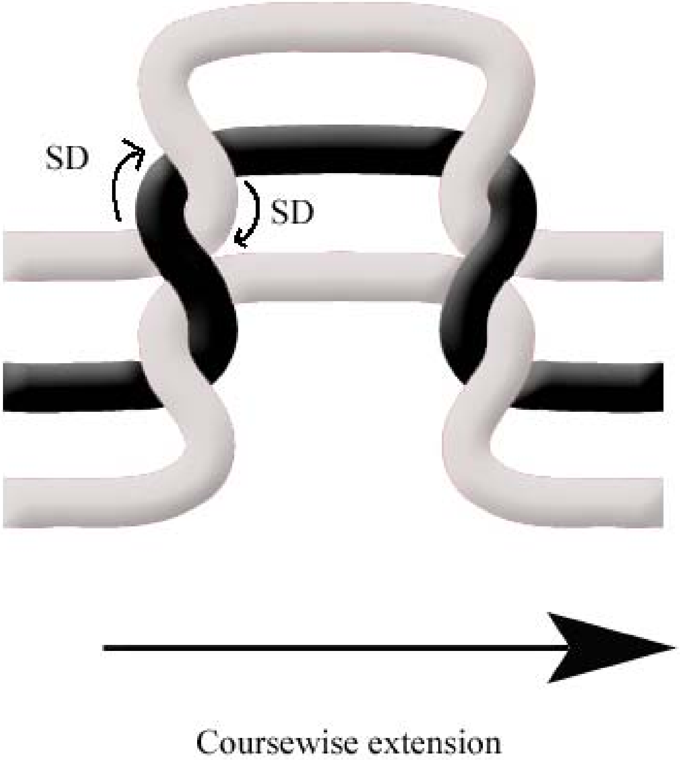

*SD = Yarn Slippage Direction

Figure 5.21 Graphical representation of fabric jamming in the wale direction when coursewise extension

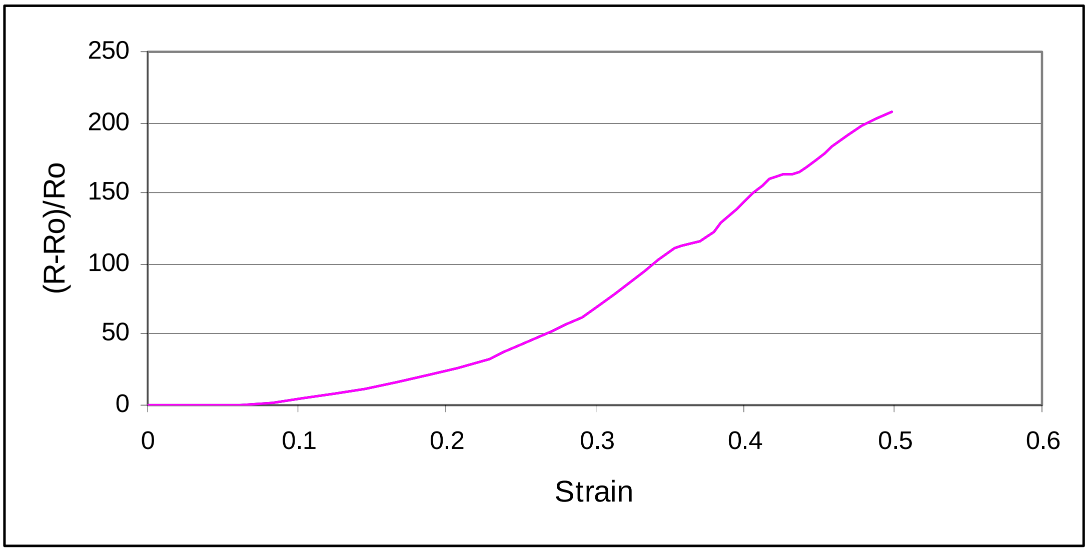

Figure 5.22 Relative resistance change versus strain in the fifth cycle tensile test of the PPy-coated fabrics along the wale direction

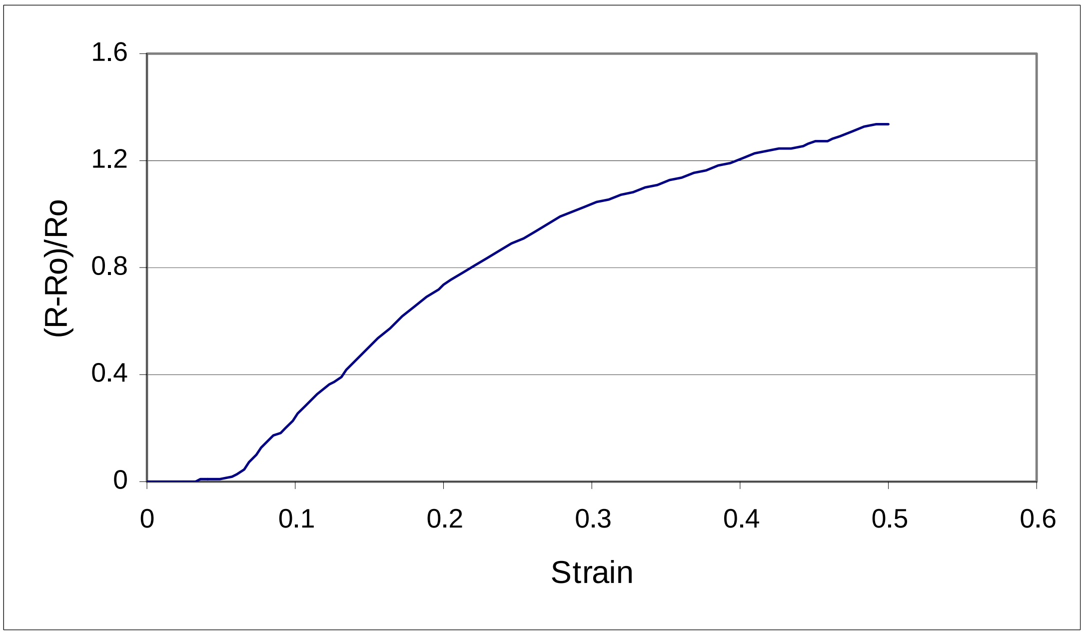

Figure 5.23 Relative resistance change versus strain in the fifth cycle tensile test of the PPy-coated fabrics along the course direction

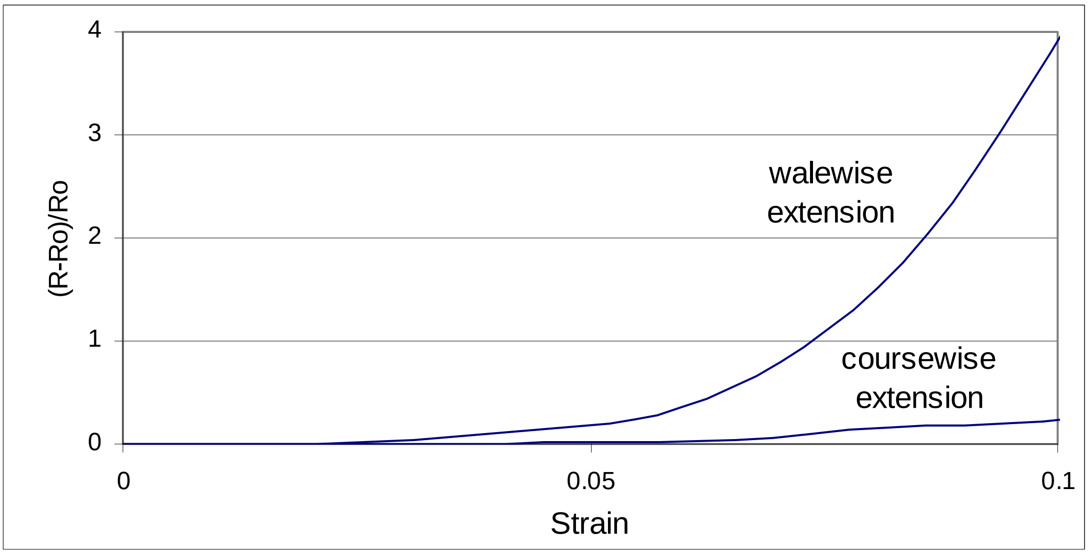

Figure 5.24 Relative resistance change versus strain in the fifth cycle tensile test of the PPy-coated fabrics along the wale and course directions

In addition to the yarn contact effects on the strain sensitivity, the yarn slippage during fabric stretching may also attribute to the fabric strain sensitivity. From Figures 5.17 to 5.21, it can be seen that more yarn slip in the V-segment of the loop during extension in wale direction while more yarn slip in the loop arc during extension in course direction. As there is thickness associated with a yarn and a fixed amount of yarn in each loop, there is a limit to the extension and contraction of a fabric due to yarn slipping. Figures 5.20 and 5.21 show the graphical representation of the jamming geometry of a plain knitted fabric. It demonstrates the examples of stretching the fabrics by yarn slipping in the walewise and coursewise directions. When a knitted fabric is stretched in the wale direction, the wale spacing will be reduced and the yarn will slip more in the stem of the loop until the yarns in the neighbouring wales start touching each other. This phenomenon is called “fabric jamming” (Farrington, 1995). At this point, no more yarn slipping can occur and so any additional extension of the fabric will be the result of yarn being stretched (Figure 5.20). A similar effect but to a lesser degree exists when a knitted fabric is loaded in the course direction as shown in Figure 5.21. The course spacing is reduced and the direction of slippage puts more yarn in the loop arc, until the yarns in the neighbouring courses touch each other and then the yarns are stretched. Since the deformational characteristics of the wale and course directions are not the same, thus an anisotropic material will be produced. In general, coursewise extensibility is generally greater than walewise extensibility because of the ease of yarn straightening in the arc of the loop. As for the same amount of fabric extension in the walewise and coursewise directions for large deformation, the yarns are stretched earlier with larger loads for walewise extension. This structural behaviour can explain why higher stress is required for performing the same level of strain in the walewise direction tensile loading.

For the same amount of fabric strain, i.e. 50%, the PU yarn inside fabric is subjected to higher stretching in the walewise extension than in the coursewise extension. Therefore, the film cracking on the PU yarn is easily happened when the fabric stretching in the wale direction, and resulting obvious electrical resistance changes.

There were many researchers studied the geometrical properties of plain knitted fabrics (Farrington, 1995). Pierce (1947) developed a geometric model which was based on the assumption that the fabric was jammed in the course and wale directions giving the tightest possible structure. Popper (1966) developed a similar model showing that the fabric undergoes several deformations of considerable magnitude when fabric stretching. The deformations depend on yarn properties, slippage, straightening of the curved yarns and the ratio of the imposed stresses. In present study, it is aimed to quantify the difference between the maximum jamming conditions during fabric deformation in wale and course directions.

Figure 5.25 shows a unit cell in a plain knitted fabric which is composed of two interlacing yarn quarter loops with below assumptions:

i. The load is enough to straighten the yarns completely.
ii. The yarns are straight except at the crossing points.
iii. The fabric will deform uniformly.
iv. The projected yarn lengths on the plane of the fabric are equal to the actual yarn length.

Below are the parameters which define the knitted structure:

L = loop length

c = course spacing

w = wale spacing

r = yarn radius

θ = yarn inclination

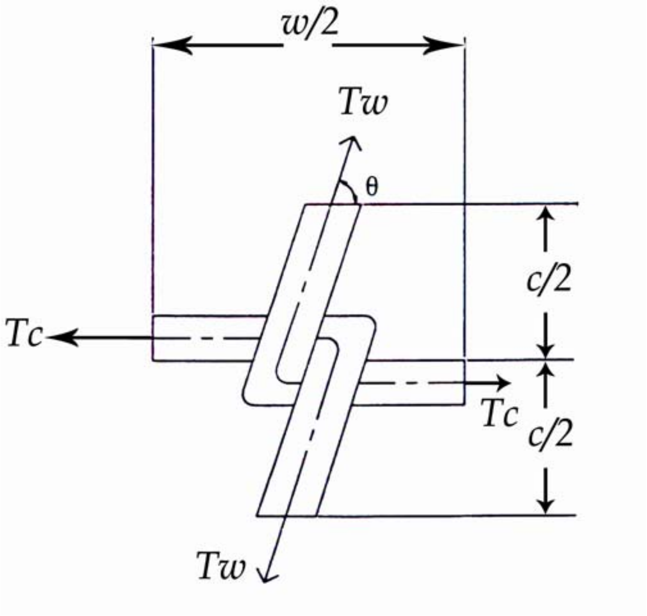

Figure 5.25 The basic element in the knitted structure

By performing a geometric analysis, an expression for the half loop length can be determined in terms of course and wale spacing (Farrington, 1995).

$$\frac{L}{2} = \frac{w}{2} + \frac{c}{\sin\theta} + \pi r \tag{5.10}$$

When jamming occurred in the course direction, the course spacing, *c*, is at a minimum (c_{min}) and the wale spacing, w, is at a maximum (w_{max}) as shown in Figure 5.26. Therefore, through a geometric analysis it can be proven that the minimum course spacing must be equal to four yarn radii.

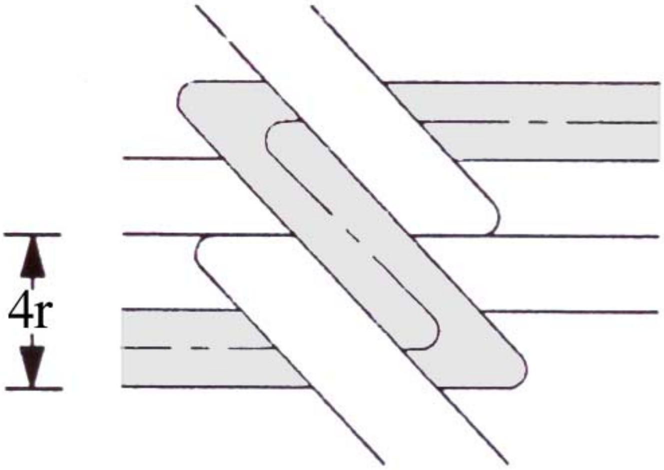

Figure 5.26 Fabric under maximum extension in course direction

$$c_{\min} = 4r \tag{5.11}$$

By substituting the minimum course spacing into Equation (5.10), an expression for the maximum wale spacing in terms of the yarn radius can be derived:

$$\frac{w}{2} = \frac{L}{2} - \frac{c}{\sin\theta} - \pi r \tag{5.12}$$

When jamming in the course direction,

$$\cos\theta = \frac{1}{2} \qquad \theta=60^{\circ}$$

By substituting θ=60° into Equation (5.12), the maximum wale spacing is expressed by the following equation:

$$\frac{w_{\max}}{2}=\frac{L}{2}-\frac{2\times 4r}{\sqrt{3}}-\pi r \qquad (5.13)$$

$$w_{\max}=2\left(\frac{L}{2}-4.6r-\pi r\right) \qquad (5.14)$$

When jamming occurred in the wale direction, the course spacing is at a maximum (c_{max}) while the wale spacing is at a minimum (w_{min}) as shown in Figure 5.27.

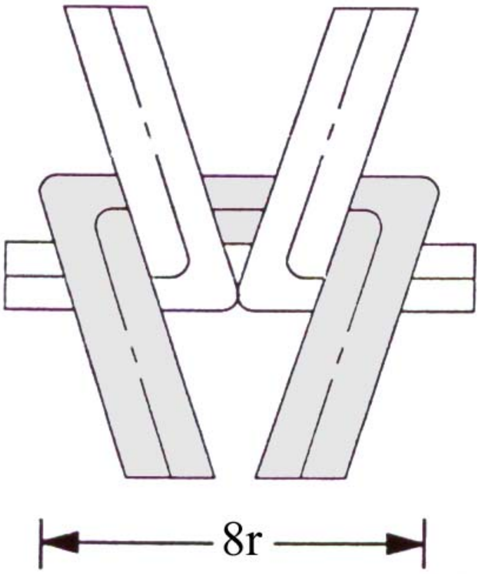

Figure 5.27 Fabric under maximum in wale direction

$$w_{\min}=8r \qquad (5.15)$$

By substituting the minimum wale spacing into Equation (5.10), an expression for the maximum course spacing in terms of the yarn radius can be derived:

$$\frac{c}{\sin\theta}=\frac{L}{2}-\frac{w}{2}-\pi r \tag{5.16}$$

When jamming in the wale direction, it is assuming the yarn inclination is almost $\theta=\frac{\pi}{2}$ which the vertical section of the yarn segments are perpendicular to the wales. Thus, the maximum course spacing can be expressed as the following equation by substituting $\theta=\frac{\pi}{2}$ into Equation (5.16).

$$\frac{c_{\max}}{\sin\frac{\pi}{2}}=\frac{L}{2}-\frac{8r}{2}-\pi r \tag{5.17}$$

$$c_{\max}=\frac{L}{2}-4r-\pi r \tag{5.18}$$

By quantifying the ratio between maximum wale spacing and maximum course spacing at the jamming situation during fabric strain in the course direction and wale direction respectively, the ratio is derived as follows:

$$\frac{w_{\max}}{c_{\max}}=\frac{2\left(\frac{L}{2}-\pi r-4.6r\right)}{\left(\frac{L}{2}-\pi r-4r\right)} \tag{5.19}$$

$$\frac{w_{\max}}{c_{\max}}\approx 2 \tag{5.20}$$

It is found that when the plain knitted fabric stretched in the wale and course direction, the amount of yarn slippage to the loop arc during coursewise extension is at least double higher than the yarn slipping to the v-segment of the loop during the walewise extension. It can further explain the yarns are stretched earlier with larger loads for walewise extension. Therefore, it can be concluded that yarn slippage in knitted structure is one of but not the main of the parameter contributes to the strain sensitivity of the PPy-coated fabric. After studied the effect of substrate fibers, pre-extension level of PU yarn and the fabric structure in terms of yarn contact and yarn slippage in the loops on the strain sensing capacity of PPy-coated fabric, the excellent strain sensing behaviour of the LT PPy-coated fabrics are mainly attributed to the high performance of the PPy-coated PU yarn, the crack-opening and crack-closing mechanism which happen on the fibre surface.

5.6 Concluding Remarks

In this chapter, the electro-mechanical behaviour of the LT PPy-coated fibres and mechanism of the PPy-coated flexible strain sensor have been investigated. Micro-scale in-situ observation technique has been utilised for mechanisms investigation. Excellent strain sensing behaviour of the LT PPy-coated electrically conducting fabrics are mainly attributed to the high performance of the PPy-coated PU yarn, the crack-opening and crack-closing mechanism which happen on the fibre surface, as well as the excellent properties of knitted fabric structure.

CHAPTER 6

DESIGN AND DEVELOPMENT OF PROTOTYPE BY USING FABRIC SENSORS

6.1 Introduction

In the twenty-first century, textile products are entering a new generation apart from traditional textiles. Garment is not only used for aesthetic or traditional protection, but can also be transformed into an interactive, intelligent infrastructure to facilitate pervasive information processing. In Chapters 3 and 4, it has been found that various fabrication methods, stabilisation treatments and polymerisation temperature can produce the polypyrrole (PPy)-coated fabric sensors with different sensing capacity. Chapter 5 explores that the PPy-coated polyurethane (PU) fibres can be used as flexible fibre strain sensor with specific sensing capacity. PPy-coated conductive fibres and fabrics with various performances can be used for a large range of product developments.

In this chapter, a new concept of incorporating an array of electro-textiles (e-textile) sensors into a instrumental dancing garment (IDG) has been realised to combine music and dance together when performing art. The unique system is aimed at providing flexibility of movements and comfort for the dancers. The prototype development comprises four key areas of research, namely (i) sensor development,

(ii) connector design, (iii) circuit design and (iv) computing programme design, which will be discussed in detail in this chapter.

6.2 Design Concept

The first prototype of dancing garments was used for band instrumental sound dancing, the design of garment with modern and rock feeling, plus comfortable for dancing. In addition, the function of dancing garment is to control the instrumental sound during dancing.

The developed e-textile sensors were used for the prototype development of IDG. The e-textile sensors were installed at particular joint positions of human as soft switches to trigger function modes. The integration of the e-sensors with the music-instrumental dancing garment allows the device to transform the dancing posture into electrical signals so as to control the musical sound. Figure 6.1 shows the design and collection of the IDG. Each dancing garment has been pre-defined to produce a particular instrumental music in a dancing band including guitar, drum, piano and bass guitar etc. As a result, no other physical musical instruments are needed for this band since the e-textile IDG worn by the players can control digital sounds from various music instruments. The schematic diagram of the first prototype for specific drum sound player is shown in Figure 6.2. It can be seen that there is no significant difference in appearance between the IDG and traditional dancing dress because this specific IDG has no bulky connectors or circuit boards that affect the natural, violent and enthusiastic dancing. Textile e-sensor and textile connector has been used for developing this IDG in order to facilitate light weight and tight fitting properties.

Figure 6.1 Collection of the instrumental dancing garments

Figure 6.2 Schematic diagram of drum sound IDG

6.3 Design Layout of Instrumental Dancing Garment

The design of IDG should include many particular technology integration such as washability, flexibility, size requirement of the fabric sensors, shock resistance of the textile connectors, and the interconnection between the fabric sensor and textile connectors. The design layout contains flexible fabric strain sensor, textile connectors, circuit board and computing programme with wireless system as shown in Figure 6.3. The prototype is demonstrated in Figure 6.4.

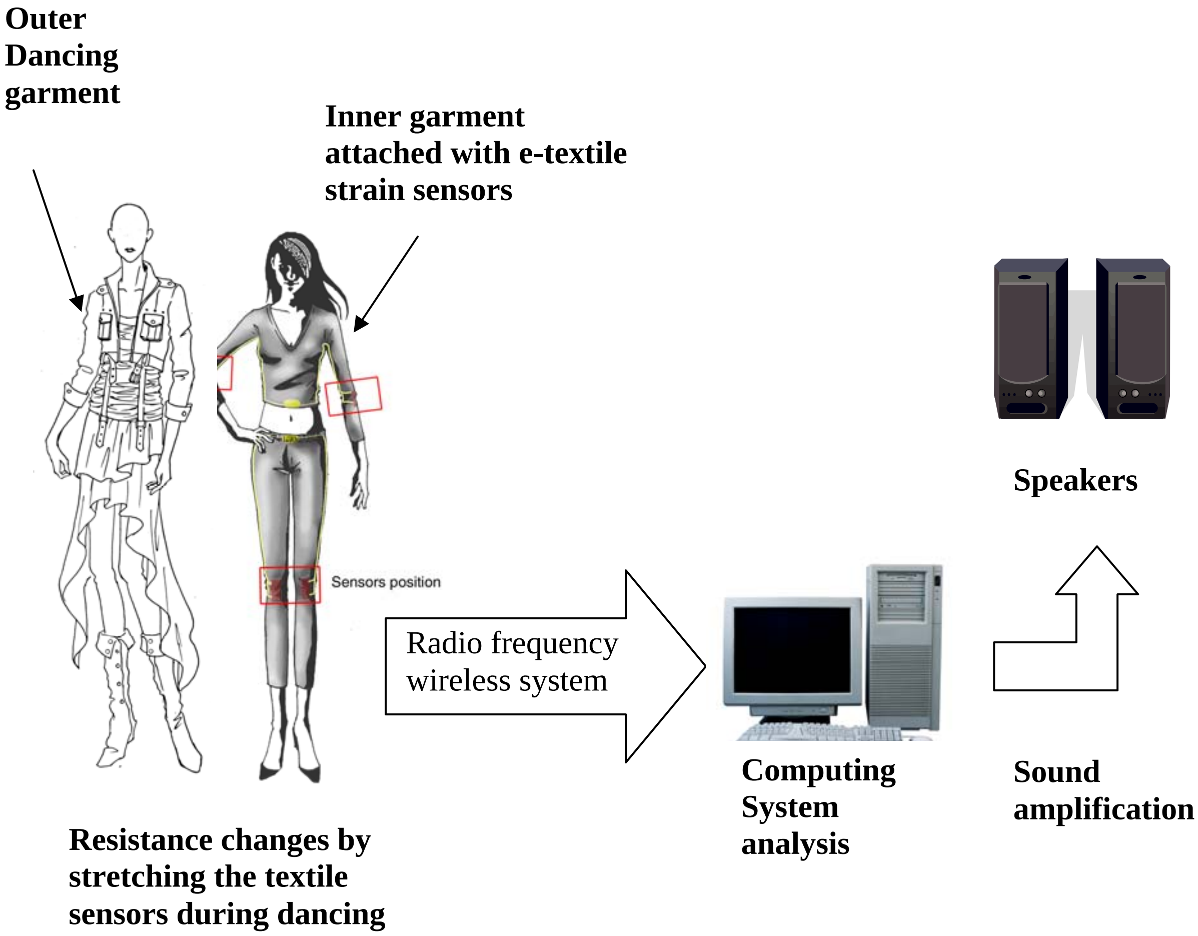

Figure 6.3 Design layout of IDG

Figure 6.4 Demonstration of IDG with drum sound

6.3.1 Fabric sensors

For making the first prototype of IDG, fabric strain sensors with appropriate electrical conductivity, strain sensitivity as well as environmental stability are necessary. The PPy-coated fabrics fabricated by padding followed with chemical vapour deposition (Pad-CVD) under extremely low temperature with sodium dodecylbenzenesulphonate (DBS) application and vacuum heat treatment (VHT) were produced and applied to this IDG development. The fabric sensors have initial resistance of 8.76kΩ/in^2, up to 450 strain sensitivity and only 5% changes in electrical resistance after 1 year of storage as discussed in Chapter 4. The fabric strain sensors were used to function as soft switches. The electrical resistance changes when stretching the fabric sensor; and the switches will be triggered once the resistance reaches the pre-set value. Hence, the strain sensitivity of fabric sensor is very important because a higher strain sensitivity can provide clear switch modes with lower noise signals.

Figure 6.5 shows the schematic diagram of the basic block of the IDG’s inner garment, while Figure 6.6 demonstrates the position of fabric switches installed at the joint positions of the garment. During body movement, strain variation can be transformed to the pre-set music sound. The pre-determined music such as drum sound is recorded on a voice chip and transmitted via a speaker and amplifier. During dancing performance, the e-textile sensors originally interconnected with garment parts by intrinsic conductive wires will be extended up to 45%. The resistance change of e-textile sensors will transform the signal to the switch “ON” of the circuit and produce musical sound.

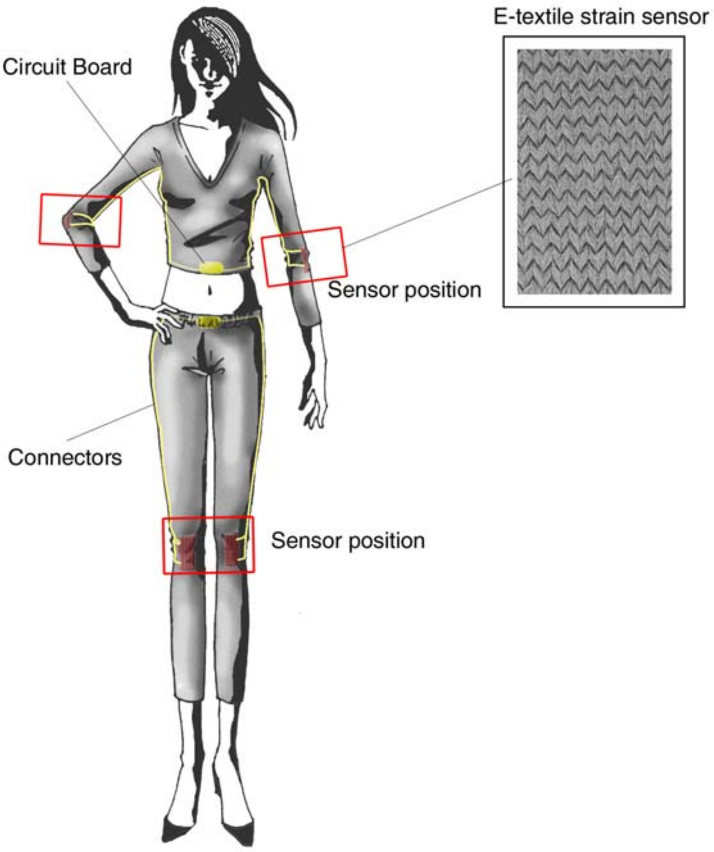

Figure 6.5 Schematic diagram of the IDG's inner garment

Figure 6.6 Positions of e-sensor on wearer's elbow

As discussed in Chapter 2, one of the major reasons for PPy films degradation is the attack of oxygen and/or water. The PPy-coated fabrics developed by the new fabrication method and treated with stabilisation treatments manifest very good environmental stability on the electrical resistance. However, it may still encounter contact problems between sensors and human skin during the IDG development. To tackle this problem, specific sandwich design of the placement of sensors was developed as demonstrated in Figure 6.7. This is a three-layers design used for placing the fabric sensor inside two protective fabrics which are made of the same material as the inner garment of IDG. The inner garment is made of Nylon/Lycra knitted fabric which has excellent stretch and recovery property suitable for making tight fitting garments. The first layer of the sandwich next to skin is used for avoiding the sweat attacking the fabric strain sensor. The second layer is the sensor and the third layer is the cover layer to protect the sensor from the interferences of external environment such as rain, abrasion or snagging during dancing. All three layers are packed in the form of circular tube tightly fit to the wearer in order to ensure that the fabric strain sensor can be stretched according to the movement of wearer as shown in Figure 6.8.

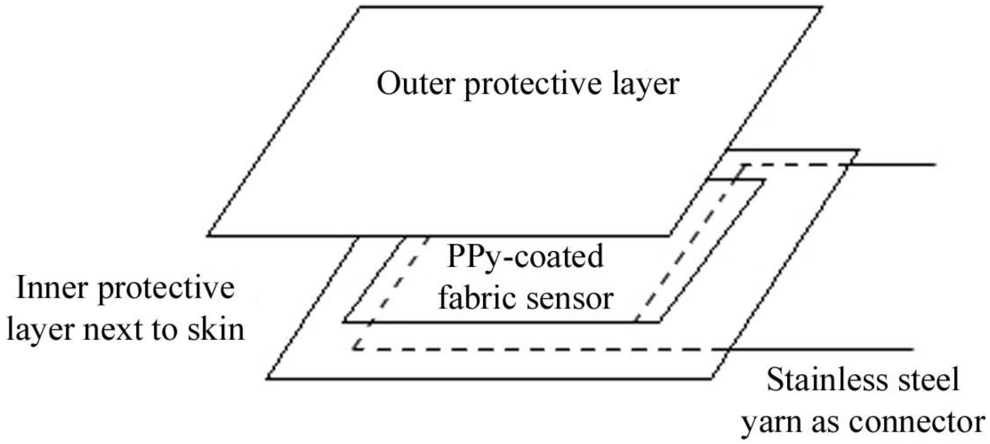

Figure 6.7 Sandwich design of fabric sensor placements

Figure 6.8 Circular tube sandwich design of fabric sensor placements

6.3.2 Textile connectors

As shown in Figures 6.5 and 6.6, the fabric sensors are attached to the tightly fit inner garment by simple sewing. Stainless steel yarns supplied by BEKINOX are used as contactors to form a network linking the sensors with the data processing unit as shown in Figure 6.9. By means of this arrangement, the sensor contact and data transmission cable made by stainless steel fibres will not affect the comfort of wearers. The electric resistivity of the stainless steel yarn is in the range of $10^{-6}\Omega$-m. A strip of woven fabric is attached to the stainless steel yarn aiming to protect the yarn from stretching or other deformation during the wearing process. Hence, the resistance of the connectors will not change when stretching or relaxing the e-textile sensors. The resistance of the fabric sensor varies from approximately $9k\Omega/in^2$ to

2MΩ/in^2 when the fabric is stretched from 0% to 50% strain. At the same time, the resistance of the connector remains constant at around 20Ω as shown in Figure 6.10. The length of connector measured from the sensor at the joint position to the circuit board is about 70cm. The connector stripes together with the stainless steel yarn are covered with flexible thermoplastic polyurethane (TPU) adhesive tape in order to avoid shocking between the connectors and different sensors. The TPU adhesive tape is so soft and thin that it will not affect the handle, softness and comfort of the garment.

Figure 6.9 Stainless steel yarns sewn on the woven fabrics as connectors

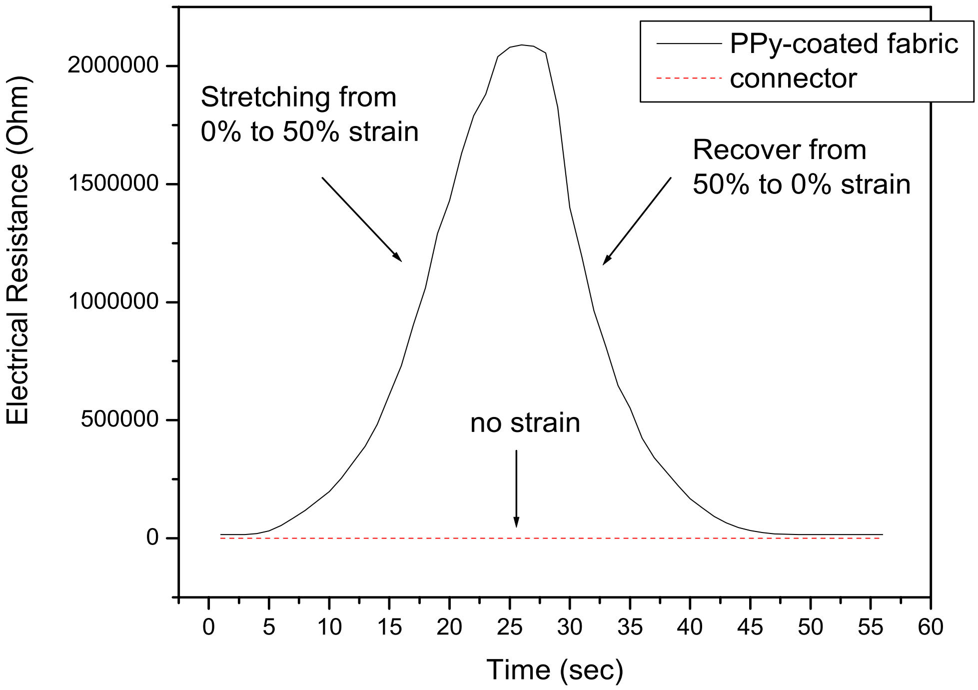

Figure 6.10 Electrical resistance changes versus strain of the PPy-coated fabric and stainless steel yarn

The wireless data transmission system design is shown in Figure 6.3. The flow of data transmission is summarised as follows: (i) the fabric sensors are stretched by the movement of the wearer, (ii) the changes of resistance corresponding to strain are transmitted to the circuit board by the connector containing stainless steel yarns, (iii) different levels of radio frequency are transmitted from the dress to the computing platform by means of a radio frequency wireless system, (iv) a software programme is designed and installed for recognising the level of radio frequency and transforming them into pre-determined instrumental music sounds, and (v) instrumental music sounds are then generated from the speakers connected with amplifiers.

6.3.3 Circuit design

The schematic circuit design is shown in Figure 6.11. The function of this circuitry is to digitise analogue signals by transforming the resistance changes of the fabric sensors into digital signals. It also modulates digital signals into different levels of frequency for recognising the correlation between signals and fabric sensors. In this circuitry, the fabric sensors are regarded as the input device while the radio frequency is the output information. There are five key elements in this circuit design; namely (i) fabric sensor, (ii) programmable shunt regulator, (iii) variable resistor (VR), (iv) photocoupler and (v) transmitter. The fabric sensor installed at the dancing garment is used for sensing the movements caused by stretching the fabric sensor.

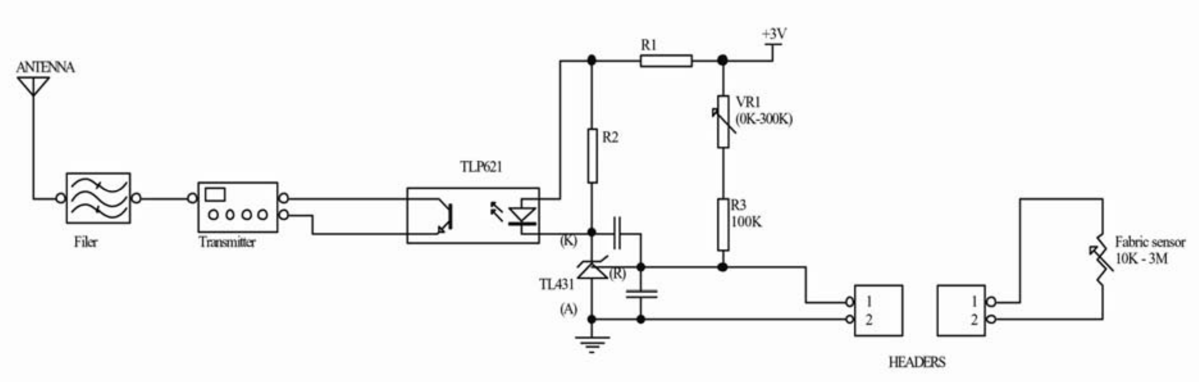

Keys:

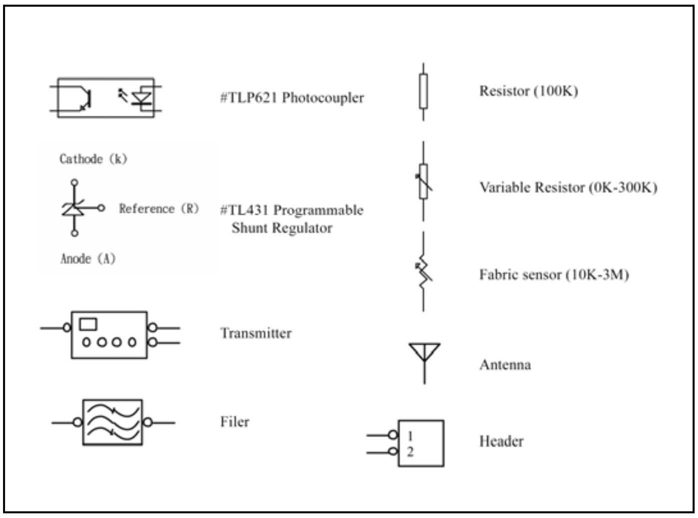

Figure 6.11 Schematic diagram of circuit design

The full circuit design of the dancing garment is shown in Figure 6.12. There are totally 4 fabric sensors installed at 4 specific joint positions, 2 at the tightly fit inner garment's top and 2 at the garment's bottom. Connectors are sewn from the fabric sensors to the garment's waist position where a small waist bag with the circuit board inside is worn by the dancer as shown in Figure 6.5. There are two headers, one header groups the connectors from the top while the other header groups the connectors from the bottom and then connects them to the circuit board. Headers are used for making the circuit board that can be attachable to the dress. Hence, the dancing garment is easy to handle and washable when detached from the circuit board.

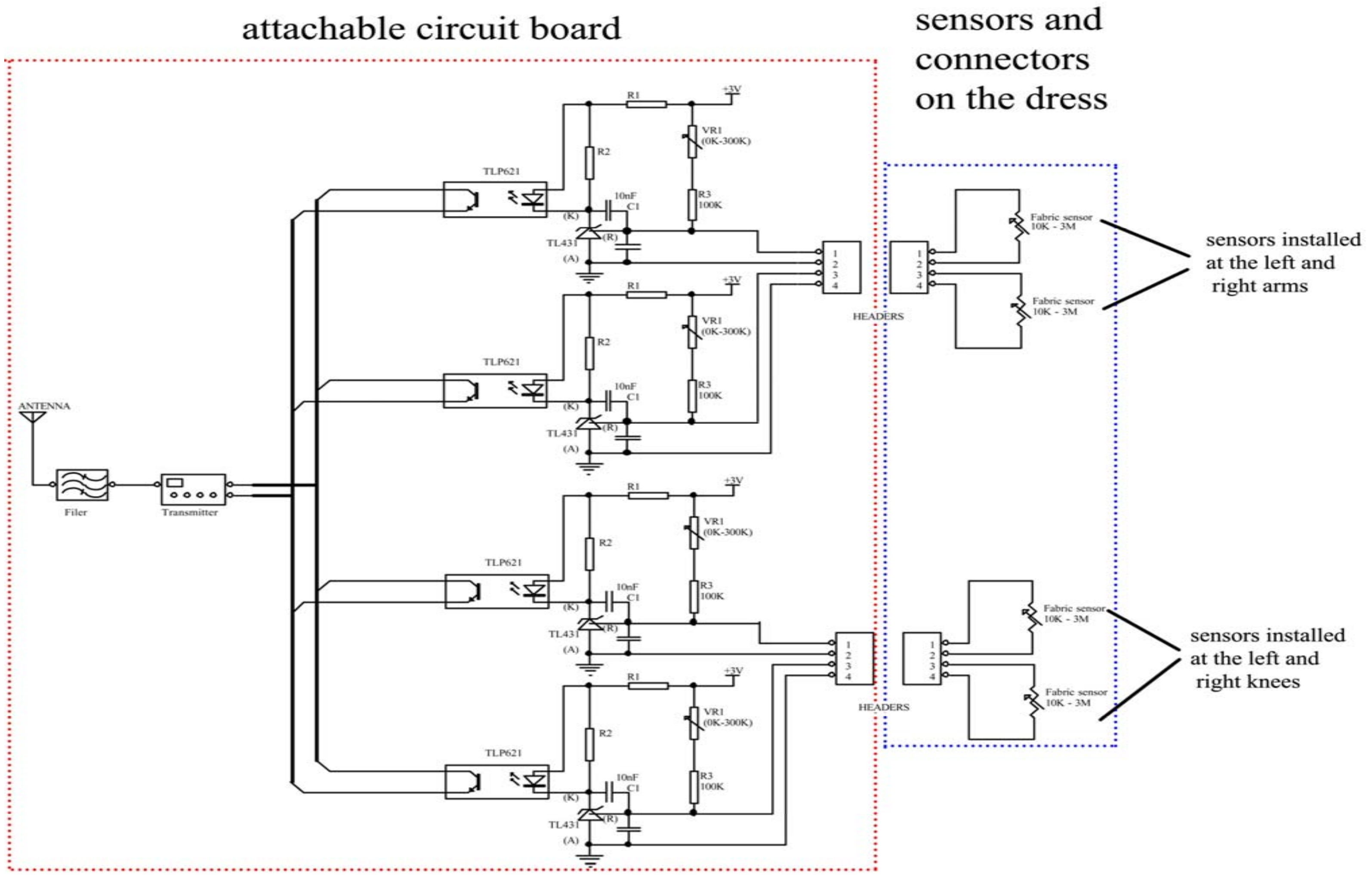

Figure 6.12 Diagram of circuit design

Programmable shunt regulator is a three-terminal adjustable regulator which is used for comparing the output voltage at Reference pin (R) (resistor bridge with the variable resistor and a resistor, VR1+R3) with the voltage reference (V_{REF}). The V_{REF} is set to be 2.5 volts. If the output voltage at Reference pin (R) is higher than V_{REF}, the output of the voltage loop at Cathode pin (K) will decrease. A useful component of this circuit design is the variable resistor which is tunable for adjusting the value of output voltage of Reference pin (R), thereby controlling the sensitivity of the digital signals. Higher sensitivity of the digital signals means lesser fabric strain can produce sound in this application. The value of variable resistor should be adjusted to a higher resistance value. Another advantage of using variable resistor is to provide flexibility for the re-installation of fabric sensors. Therefore, this circuit design is suitable for applying different fabric sensors to dancing garments with different strain sensitivities, i.e. from 10kΩ to 3MΩ. Moreover, the photocoupler is a photo-transistor optically coupled to an infrared emitting diode. This element is used as the isolation device for noise protection in this product design. When the photocoupler current increases to 10mA, it will close the circuit and the switch “ON” signal is then transmitted to the transmitter. The transmitter is used for modulating the digital signals to different levels of radio frequency which are pre-set with respect to the fabric sensors installed at different joint positions. The information is finally transmitted to the computing platform by the frequency modulation of radio frequency wireless system for musical sound processing.

An example of the working principle of the circuit design is illustrated in Figure 6.13. When the fabric sensor is stretched up to 35% strain by the posture movement of the dancer; musical sound will be generated meaning that the resistance of the fabric sensor reaches the level of around 700kΩ. The variable resistor should then be adjusted to 40kΩ according to the following calculation:

$$V_{REF} = 3V \frac{700k}{700k + (VR1 + R3)} > 2.5V \tag{6.1}$$

Where V_{REF} is voltage reference of programmable shunt regulator,

VR1 is the electrical resistance value of the variable resistor,

R3 is the electrical resistance value of the resistor in the same bridge of variable resistor, and

Supply voltage is 3 volt.

When the voltage at R pin of the regulator is higher than V_{REF} caused by stretching the fabric sensor up to 35% strain, K will decrease while the photocoupler current will increase and resulting in the closing of the circuit. Switch “ON” signal is then transmitted to the transmitter where the digital signal is transformed into specific radio frequency which is subsequently sent to the computing platform by means of radio frequency wireless system in frequency modulation. The computing platform contains the receiver for collecting the information, and a programme is designed to identify the radio frequencies for musical sound processing. A specific sound is finally generated from the speaker.

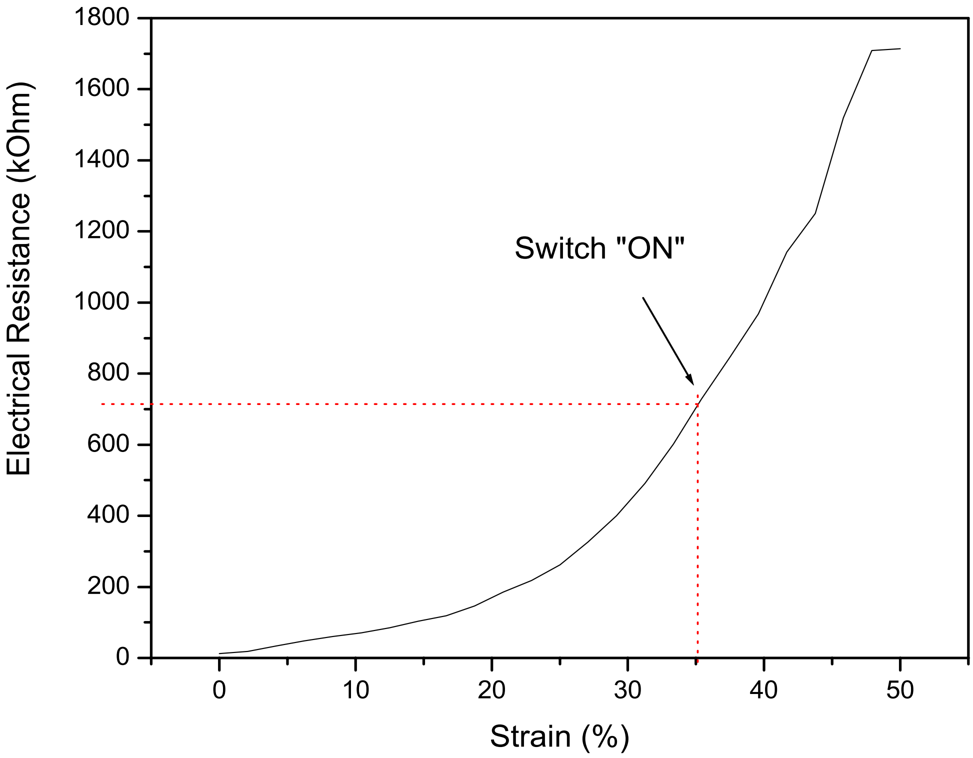

Figure 6.13 Electrical resistance changes versus strain of the PPy-coated fabric sensor for circuit design

6.3.4 Computing programme design

The design of programme is aimed at analysing the signals generated from the movement of wearers and transforming them to different drum sounds immediately. The computing programme design is separated into 3 steps as follows:

Step 1: Select the specific music files which are representing different drum sounds for this prototype development, and establish the connection between the music files, fabric sensors on the IDG and specific function key. For example, the fabric sensor is placed on dancer’s left elbow connected to function key 1 which is then connected to drum sound 1.

Step 2: Analyse the signals generated from the dancer and recognise them with respect to the specified function keys.

Step 3: Load the music file according to the function key of the dancer who produce and plays it immediately.

The above steps are simply illustrated in Figure 6.14 with the Flash programme being used for designing the computing programme. Flash codes and commands are programmed as shown in Appendix 1.

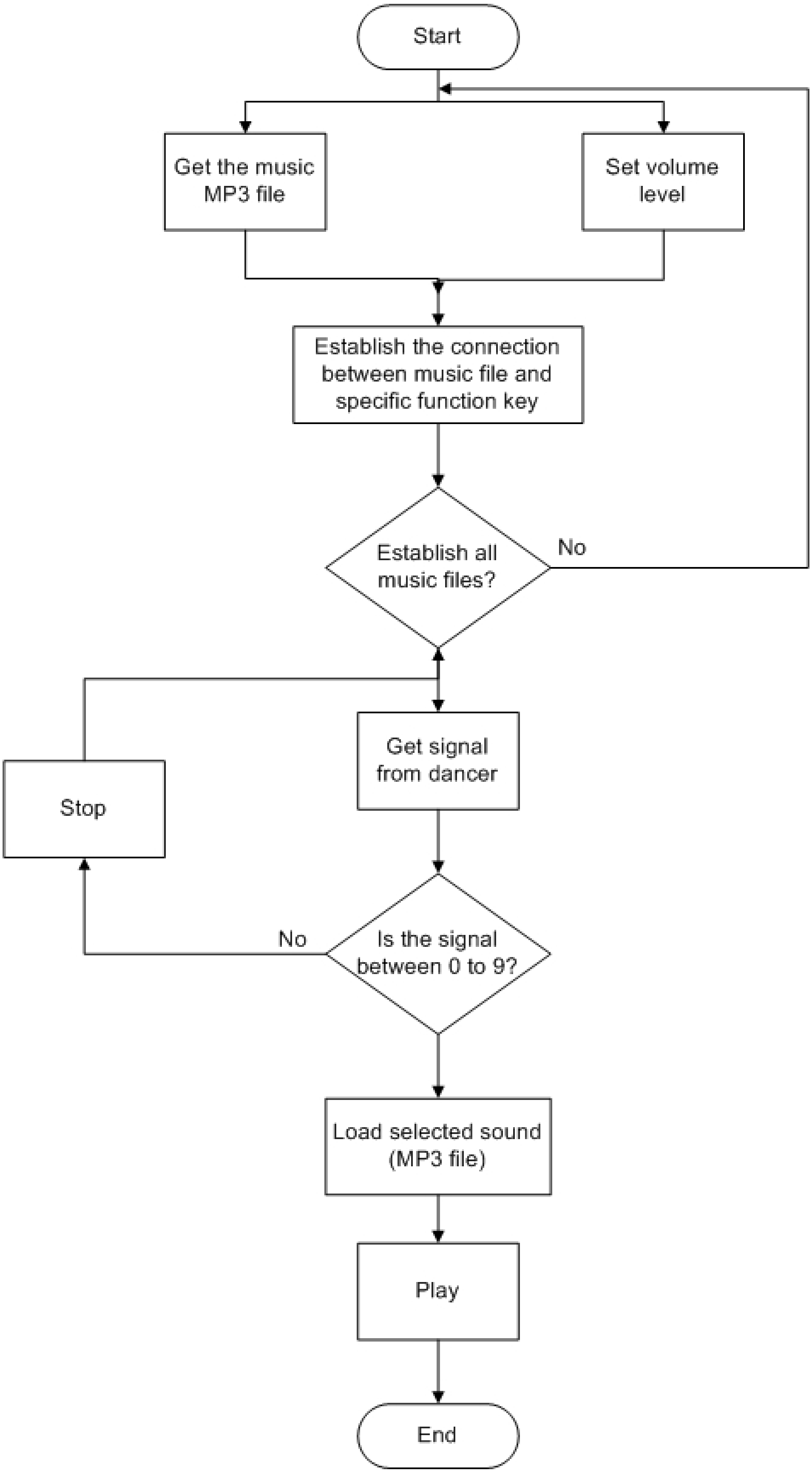

Figure 6.14 Flow chart of computing programme

6.4 Other Potential Applications of the PPy-Coated Textiles

There are innumerable applications of the PPy-coated textiles as discussed in Chapter 2. As for the PPy-coated fabrics sensor fabricated by the new methods and treated with stabilisation treatments, extremely high strain sensitivity, good conductivity as well as good environmental stability of e-sensors can be acquired. There is wide range of applications of the flexible e-textile sensors with above properties other than the IDG. Li (2005) explored the usage of this PPy-coated fabric e-sensor for a sensing glove development which could operate the toy car by remote control.

The PPy-coated fabric sensors can also be used for remote monitoring of some vital signals generated from patients for health care. It is aimed to perform health status monitoring such as measurement of physiological parameters including ECG, heart rate, or respiratory rate. Based on the use of flexible, smart fabric sensors which are conformable to the human body, this will help improve the autonomy and life quality of patients. Since the wearable bio-medical sensor can be stretched and relaxed during humans' breathing and heart beating, thus the change in electrical resistance signals can be transmitted and transformed to the computer platform.

Another potential application of the PPy-coated fabric sensors with high strain sensitivity is the rehabilitation field. The fabric sensors can be placed at the joint positions of elbow or knee etc. It can monitor the patients' training exercises for the restoration of fracture problems by transmitting the report to their doctors or physiotherapists. Hence, patients can practice the training at their home or anywhere if they feel comfortable.

Apart from the game applications such as sensing glove and IDG development, it is realised that wearable bio-medical sensor systems represent a potentially large research and development area. The impact expectation on health-care and quality of life is high as they can enhance capabilities for supporting personalised disease prevention and rehabilitation at home. It offers continuous monitoring by avoiding unnecessary hospitalisation which is beneficial to both patients and doctors.

6.5 Concluding Remarks

An instrumental dancing garment has been developed by installing the PPy-coated stretchable fabric sensors at particular joint positions. The newly developed sensors possess good conductivity (less than $10k\Omega/in^2$), very high strain sensitivity (up to 450 at 50% strain) and excellent long term stability (around 5% conductivity loss for 1 year) which are very suitable for advanced product developments.

An innovative application of the system composing of an instrumental dancing garment has been demonstrated. It comprises four key areas of research, namely (i) sensor development, (ii) connector design, (iii) circuit design and (iv) computing programme design. The IDG is a collection of garments that transform body movement to music associated with dancing rhythm. By combining the traditional fashion design with material science, electronic engineering and computing system design, the dancers wearing a collection of electro-sensing garments are able to compose a rhythmic song with different types of musical instrument sounds. Other applications of the PPy-coated fabric strain sensor in the fields of games as well as wearable bio-medical devices and systems are proposed and suggested.

CHAPTER 7

CONCLUSIONS AND FUTURE WORK

7.1 Summary of Major Findings and Conclusions

Based on the extensive literature review of the environmental stability and sensing capacity of the electrically conductive polymer coated textiles, a new class of PPy-coated textiles has been further developed and studied experimentally and theoretically in this thesis. The multi-scale study of sensing properties of PPy-coated textiles has achieved all the objectives of this thesis. In the study, the major findings obtained from the experiments and the conclusions are summarised in the following.

(1) Fabrication of the PPy-coated textiles and the study of their corresponding pure PPy powders and PPy-coated fibres have been conducted. After optimising the processing parameters, the screen printing followed by chemical vapour deposition (Print-CVD) and padding followed by chemical vapour deposition (Pad-CVD) have been further developed for producing the PPy-coated fabrics. It is found that both fabrication methods will not affect the mechanical property of the textile substrates, therefore, the advantages of using textiles as substrates such as flexibility, comfortability and light weight can be retained.

(2) The two developed fabrication methods and the conventional solution polymerisation fabrication method have been investigated and compared. In terms

of the sensing performance of the PPy-coated fabrics, the samples prepared by CVD method exhibits higher strain sensitivity up to 20 at 50% strain. Furthermore, they demonstrate excellent linearity of the sensing curves within ten cycles when compared with other fabrication processes reported by the other researchers.

CVD method is successfully applied for producing thinner and more uniform PPy layer coated fabric sensor with good sensing properties. As characterised by the scanning electron microscopy, there is no obvious difference of the fibres diameters between the Pad-CVD samples or Print-CVD samples and the diameter of uncoated fibre is around 13μm. However, the fibre diameters of the samples fabricated by the conventional solution polymerisation are in the range of 15μm to 20μm.

(3) The sensing electrical resistance, strain sensitivity and environmental stability of the PPy-coated fabrics with different stabilisation treatments such as vacuum drying (VD), vacuum heat treatment (VHT) and sodium dodecylbenzenesulphonate (DBS) dopant application have been studied. The experimental results reveal that the VHT thermal annealing method under vacuum can significantly enhance the strain sensitivity without affecting the initial resistance and the repeatability of the sensing function. Furthermore, the samples fabricated with DBS and subjected to VHT can further enhance the strain sensitivity up to 184 at 50% strain, and also significantly improve the environmental stability of electrical conductivity. The proposed stabilisation treatments are very suitable for the PPy-coated stretchable sensors containing spandex or elastane materials.

Characterisations of the PPy-coated fabrics and pure PPy powders with different stabilisation treatments have been conducted by using SEM, thermalgravimetric analysis (TGA), x-ray diffraction (XRD) and contact angle measurement. It is found that the stabilisation treatments can improve the thermal stability, PPy-chain ordering, surface smoothness and fabric hydrophobicity, resulting in enhancing the environmental stability as well as strain sensitivity.

After comparing the performance of the three proposed stabilisation treatments, it is obvious that fabrication process with the addition of DBS dopant and subsequent vacuum drying followed by VHT is the most promising method for stabilising the PPy-coated fabric. It is also found that very thin, smooth and dense PPy coating layer can be formed on the fibre surface by means of the optimum stabilisation treatment.

(4) A comparison study of polymerisation temperatures for fabricating the PPy-coated fabric sensor has been carried out. Electrically conductive fabrics prepared by CVD process at low temperature (LT) exhibit excellent strain sensitivity factor of over 400 at the strain of 50% with very large workable range of more than 50% which is the highest strain sensing capacity in the world. Furthermore, LT CVD can produce the fabric sensor with higher electrical conductivity as well as better environmental stability. It is found that the particle size of PPy coating formed by LT CVD is much smaller than that obtained at room temperature (RT) CVD. This produces a more oriented and structured nano-film on the fabrics. The results of different characterisation methods including TGA, XRD, SEM and scanning probe microscopy (SPM) etc. confirm that LT CVD can deposit a thinner, continuous and

more ordered structure of PPy film on the fabric surface, which is beneficial to the sensing performance. US Patent regarding the invention of extremely low polymerisation temperature for fabricating the PPy-coated fabrics with the application number of 11/222,179 has been applied.

(5) The sensing performance of the PPy-coated fabrics may be governed by (i) the structure of the coating layer, (ii) interface between the coating and textile substrate, (iii) thickness and (iv) the surface morphology of PPy coating. Dynamic force microscopy (DFM) mode has been utilised to provide more detailed topography information about the structures formed on the PPy layer coated on the polyurethane (PU, Lycra) fibres in micro-scale and nano-scale. It is found that the PPy film fabricated by LT CVD is composed of well-connected PPy granules, covering the whole fibre surface with finer, denser, more uniform grains and uniformly distributed layers than those of the PPy coating fabricated by RT CVD. Other surface analyses of SPM called “grain size analysis” and “surface smoothness analysis” have been utilised to provide additional information beyond the standard morphology measurements. Since smaller grain size of PPy with narrower distribution are produced at low temperature, thus more smooth and uniform coating layer can be formed.

(6) Surface potential detection by SPM has been used in this project for determining the coating thickness of PPy-coated fibres. This characterisation method has proved that the PPy coating thickness of 200nm on the textile fibres prepared by LT CVD is thinner than that of 350nm of RT CVD. It is found that lower polymerisation temperature can slow down the PPy growth rate on the textile substrate leading to the

formation of thinner, smoother, denser, more uniform and better orientation of PPy coating.

(7) The mechanism governing the electro-mechanical behaviour of the PPy-coated flexible strain sensor has been analysed. The comparison of sensing performance between PA6 and PU yarn has been conducted. It is found that the excellent strain sensing behaviour of the PPy-coated fabrics is mainly attributed to the high performance of the PPy-coated PU yarn. By utilising the in-situ SEM observation of the PPy-coated PU yarn for characterisation, the crack-opening and crack-closing mechanism during fibre strain can be observed on the fibre surface. The sensing mechanisms between the samples prepared at RT and LT have been compared. It is found that the surface damage of the LT PPy-coated PU yarn occurs only at longer strain due to the better quality of PPy film formed on the fibre. Therefore, the strain sensitivity of the LT PPy-coated PU yarn is higher than RT sample.

(8) The effect of knitted fabric structure on strain sensing behaviour has been conducted by studying the pre-extension levels of PU yarn. The in-situ SEM observation demonstrates that higher pre-extension level will cause the formation of a lot of deeper and wider cracks on the PPy film at the same strain level resulting in higher electrical resistance changes versus strain. Therefore, it is obvious that the excellent properties of knitted fabric structure are beneficial to the strain sensing behaviour of the PPy-coated fabrics.

(9) An Instrumental Dancing Garment (IDG) has been developed by installing the PPy-coated stretchable fabric sensors at particular joint positions of human. Four

key areas of research, namely (i) sensor development, (ii) connector design, (iii) circuit design and (iv) computing programme design have been involved. The IDG is a collection of garments that transform body movement to music associated with dancing rhythm. By combining traditional fashion design with material science, electronic engineering and computing system design, IDG development has manifested the functions and advantages of the PPy-coated flexible strain sensors.

On the whole, the further developed fabrication methods, polymerisation condition and stabilisation treatments have been successfully designed to alter the surface morphology, structure and quality of the PPy coating on textile substrates in order to improve the sensing performance. It has demonstrated that all the proposed methods and treatments can provide better sensing performance of the PPy-coated fabric strain sensors including electrical resistance, strain sensitivity, environmental stability with respect to temperature and relative humidity as well as long term stability. The successful outcome of this research study does provide an impetus for the future development of electrically conductive textiles in the application area of wearable electronics.

7.2 Recommendations for Future Work

Based on the study of the PPy-coated textiles presented in this thesis, the following future research works are suggested.

(1) The relative electrical resistance versus unidirectional tensile strain of the developed PPy-coated fabric has been measured. It is anticipated that the investigation and development of a fabric sensor for multi-directional strain sensing

will be extremely valuable in widening up the potential application of the PPy-coated fabric strain sensors. Hitherto, there is no measurement technique available for evaluating the multi-directional strains of conductive fabrics. Hence, further development and application of some new techniques for measuring the relative resistance change versus multi-directional strains distribution are extremely useful.

(2) The experimental results prove that extremely LT polymerisation can form thinner, smoother, denser PPy coating with higher orientation on textile substrates. However, the growth mechanism of PPy chains formed step by step on textile substrate is still not clear. Hence, more future studies are required to investigate the PPy growth mode and the interaction between the PPy and substrate polymers.

(3) In addition to the study of thermal annealing and large sized dopant application for enhancing the environmental stability of PPy-coated fabrics, the aftertreatments of LT plasma treatment with fluorocarbon groups or silicon coating on the PPy-coated textiles are highly recommended in order to create a thin and fine hydrophobic layer onto the PPy-coated textiles. It is also recommended to systematically investigate the effect of the aftertreatments on the sensing performance of the PPy-coated textile sensors including electrical conductivity, strain sensitivity and environmental stability.

(4) It is valuable to theoretically study the decoupling of the multi-parameter responses of fabric sensors with respect to strain, temperature and humidity. A mathematical model correlating all the mentioned parameters can be further

developed in order to provide more understanding of the actual interaction between all parameters of the fabric sensors in the real environment.

(5) The existing prototype of IDG is developed to demonstrate the flexible conductive textile sensor incorporate into garment as a soft switch function. More innovative products can be further developed for heart beat monitoring, body kinematics, posture and gesture monitoring by incorporating the newly developed flexible textile strain sensors into garments.

REFERENCES

Beuth, J. L. (1992) Cracking of thin bonded films in residual tension. *International Journal of Solids Structures*, 29 **(13)**: 1657-1675.

Bhat, N. V., Seshadri, D. T., Nate, M. M. & Gore, A. V. (2004) Conductive textiles for smart fabrics. *BTRA SCAN*, 34 **(1)**: 9-15.

Billingham, N. C., Calvert, P. D., Foot, P. J. S. & Mohammad, F. (1987) Stability and degradation of some electrically conducting polymers. *Polymer Degradation and Stability*, 19 **(4)**: 323-341.

Bloor, D., Hercliff, R. D., Galiotis, C. G. & Young, R. J. (1985) Electronic properties of polymers and related compounds. *Springer Series in Solid State Sciences*, 63: 179.

Brady, S., Diamond, D. & Lau, K.-T. (2005) Inherently conducting polymer modified polyurethane smart foam for pressure sensing. *Sensors and Actuators A: Physical*, 119: 398-404.

Brady, S., Lau, K. T., Megill, W., Wallace, G. G. & Diamond, D. (2005) The development and characterisation of conducting polymeric-based sensing devices. *Synthetic Metals*, 154: 25-28.

Carpi, F. & De Rossi, D. (2005) Electroactive polymer-based devices for e-textiles in biomedicine. *IEEE Transactions on Information Technology in Biomedicine*, 9 **(3)**: 295-318.

Cassignol, C., Olivier, P. & Ricard, A. (1998) Influence of the dopant on the polypyrrole moisture content: Effects on conductivity and thermal stability. *Journal of Applied Polymer Science*, 70: 1567-1577.

Catrysse, M., Puers, R., Hertleer, C., Langenhove, L. V., Egmond, H. v. & Matthys, D. (2004) Towards the integration of textile sensors in a wireless monitoring suit. *Sensors and Actuators A: Physical*, 114: 302-311.

Cheah, K., Forsyth, M. & Truong, V. T. (1998) Ordering and stability in conducting polypyrrole. *Synthetic Metals*, 94: 215-219.

Cheah, K., Forsyth, M., Truong, V. T. & Olsson-Jacques, C. (1997) Mechanisms governing the enhanced thermal stability of acid and based treated polypyrrole. *Synthetic Metals*, 84: 829-830.

Chen, F., Zhang, J., Wang, F. & Shi, G. (2003) Raman spectroscopic studies on the structural changes of electrosynthesized polypyrrole films during heating and cooling processes. *Journal of Applied Polymer Science,* 89: 3390-3395.

Chen, X. B., Devaux, J., Issi, J. P. & Billaud, D. (1994) The stability of polypyrrole electrical conductivity. *European Polymer Journal,* 30 **(7)**: 809-811.

Chen, Z., Cotterell, B. & Wang, W. (2002) The fracture of brittle thin films on compliant substrates in flexible displays. *Engineering Fracture Mechanics,* 69: 597-603.

Cheng, K. B., Ramakrishna, S. & Lee, C. E. (2000a) Development of conductive knitted-fabric-reinforced thermoplastic composites for electromagnetic shielding applications. *Journal of Thermoplastic Composite Materials,* 13 **(5)**: 378-399.

Cheng, K. B., Ramakrishna, S. & Lee, K. C. (2000b) Electromagnetic shielding effectiveness of copper/glass fiber knitted fabric reinforced polypropylene composites. *Composites: Part A,* 31: 1039-1045.

Cheng, K. B., Ueng, T. H. & Dixon, G. (2001) Electrostatic discharge properties of stainless steel/poyester woven fabrics. *Textile Research Journal,* 71 **(8)**: 732-738.

Cheung, K. M. & Stevens, D. B. C. (1988) Characterization of polypyrrole electropolymerized on different electrodes. *Polymer,* 29 **(9)**: 1709-1717.

Child, A. D. & Kuhn, H. H. (1994) Degradation of conductivity in polypyrrole coated textiles. *Polymer Preprints (American Chemical Society, Division of Polymer Chemistry),* 35 **(1)**: 249-250.

Child, A. D. & Kuhn, H. H. (1997) Enhancement of the thermal stability of chemically synthesized polypyrole. *Synthetic Metals,* 84: 141-142.

Child, A. D. (1998a) *Method of Enhancing the Stability of Conductive Polymers,* US Patent 5,716,896

Child, A. D. (1998b) *Method of Enhancing The Stability of Conductive Polymers,* US Patent 5,833,884

Cho, J. W. & Choi, J. S. (2000) Relationship between electrical resistance and strain of carbon fibers upon loading. *Journal of Applied Polymer Science,* 77: 2082-2087.

Cho, J. W., Choi, J. S. & Yoon, Y. S. (2002) Electromechanical behavior of hybrid carbon/glass fiber composites with tension and bending. *Journal of Applied Polymer Science,* 83: 2447-2453.

Cook, J. G. (1984) Polyurethane Fibres. *Handbook of Textile Fibres -- II - Man-made Fibres.* Merrow.610-638

Coosemans, J., Hermans, B. & Puers, R. (2006) Integrating wireless ECG monitoring in textiles. *Sensors and Actuators A: Physical*, 130-131: 48-53.

Cottet, D., Grzyb, J., Kirstein, T. & Troster, G. (2003) Electrical characterization of textile transmission lines, *IEEE Transactions on Advanced Packaging*, 26:182-190

Crowley, K. & Cassidy, J. (2003) In situ resonance Raman spectroelectrochemistry of polypyrrole doped with dodecylbenzenesulfonate. *Journal of Electroanalytical Chemistry,* 547: 75-82.

De Paoli, M. A., Panero, S., Passerini, P. & Scrosati, B. (1990) Study of the electrochromism of polypyrrole/dodecylsulfate in aqueous solutions. *Electrochimica Acta,* 35 **(7)** : 1145-1148.

De Rossi, D., Carpi, F., Lorussi, F., Mazzoldi, A., Scilingo, E. P. & Tognetti, A. (2002) Electroactive fabrics for distributed, conformable and interactive systems, *Proceedings of IEEE Sensors, IEEE International Conference on Sensors,* 1st, Orlando, FL, United States, June 12-14:1608-1613

De Rossi, D., Della Santa, A. & Mazzoldi, A. (1997) Dressware: Wearable piezo- and thermoresisitive fabrics for ergonomics and rehabilitation, *Proceedings - 19th International Conference - IEEE/EMBS,* Chicago, IL. USA, Oct. 30 - Nov. 2:1880-1883

De Rossi, D., Della Santa, A. & Mazzoldi, A. (1999) Dressware: Wearable hardware. *Material Science and Engineering,* 7 **(31)**.

De Rossi, D., Loriga, G., Lorussi, F., Paradiso, R., Taccini, N., Tesconi, M. & Tognetti, A. (2005) Wearable systems for personalised health care. *Textile Asia,* 12: 37-42.

De Rossi, D., Lorussi, F., Mazzoldi, A., Rocchia, W. & Scilingo, E. P. (2001) A Strain amplified electroactive polymer actuator for haptic interfaces, *Proceedings of SPIE*:43-53

Digital Instruments Inc. (1997) Scanning *Probe Microscopy Manuals*, CA, Santa Barbara.

Dillingham, T. R., Cornelison, D. M. & Bullock, E. (1994) Investigation of vapour-deposited polyaniline thin films. *Journal of Vacuum Science & Technology A*, 12 **(4)**: 2436-2440.

Ennis, B. C. & Truong, V. T. (1993) Thermal and electrical stability of polypyrrole at elevated temperatures. *Synthetic Metals,* 59: 387-399.

Farringdon, J., Moore, A. J., Tilbury, N., Church, J. & Biemond, P. D. (1999) Wearable sensor badge & sensor jacket for context awareness, *The Third International Symposium on Wearable Computers*:107-113

Farrington, C. E. (1995) PhD thesis, *Mathematical modeling of plain weft knitted structures,* North Carolina State University

Gao, J. & Tian, Z. (1995) Electrochemical and in-situ Raman spectroscopic studies of dodecylbenzenesulfonate doped polypyrrole. *Journal of Xiamen University (Natural Science),* 34 **(2)**: 226-233.

Gaynor, J. F. & Desu, S. B. (1994) Room temperature copolymerization to improve the thermal and dielectric properties of polyxylylene thin films by chemical vapor deposition. *Journal of Materials Research,* 9 **(12)**: 3125-3130.

Gaynor, J. F., Senkevich, J. J. & Desu, S. B. (1996) A new method for fabricating high performance polymeric thin films by chemical vapor polymerization. *Journal of Materials Research,* 11 **(7)**: 1872.

Gregory, R. V., Kimbrell, W. C. & Kuhn, H. H. (1989) Conductive textiles. *Synthetic Metals,* 28 **(1-2)**: 823-835.

Gregory, R. V., Kimbrell, W. C. & Kuhn, H. H. (1991) Electrically conductive non-metallic textile coatings. *Journal of Coated Fabrics,* 20: 167-175.

Guernion, N., Ewen, R. J., Pihlainen, K., Ratcliffe, N. M. & Teare, G. C. (2002) The fabrication and characterisation of a high sensitive polypyrrole sensor and its electrical responses to amines of differing basicity at high humidities. *Synthetic Metals,* 126: 301-310.

Gustafsson, G., Inganas, O., Nilsson, J. O. & Liedberg, B. (1988) Thermal undoping in poly(3-alkylthiophenes). *Synthetic Metals,* 26 **(3)**: 297-309.

Gustafsson, G., Lundstrom, I., Liedberg, B., Wu, C. R. & Wennerstrom, O. I. (1989) The interaction between ammonia and poly(pyrrole). *Synthetic Metals,* 31 **(2)**: 163-179.

Harlin, A., Nousiainen, P., Puolakka, A., Pelto, J. & Sarlin, J. (2005) Development of polyester and polyamide conductive fibre. *Journal of Materials Science,* 40: 5365-5371.

Heisey, C. L., Wightman, J. P., Pittman, E. H. & Kuhn, H. H. (1993) Surface and adhesion properties of polypyrrole-coated textiles. *Textile Research Journal,* 63 **(5)**: 247-256.

Hertleer, C., Grabowska, M., Langenhove, L. V., Catrysse, M., Hermans, B., Puers, R., Kalmar, A., Egmond, H. v. & Matthys, D. (2004) The use of electroconductive textile material for the development of a smart suit, *World Textile Conference - 4th AUTEX Conference*, Roubaix, June 22-24:O-1W4

Hu, E., Kaynak, A. & Li, Y. (2005) Development of a cooling fabric from conducting polymer coated fibres: Proof of concept. *Synthetic Metals,* 150: 139-143.

Inganas, R. E. & Salaneck, I. L. R. (1985) XPS and electrical characterization of BF4-doped polypyrrole exposed to oxygen and water. *Synthetic Metals,* 10 **(5)**: 303-318.

Jiang, X., Tessier, D., Dao, L. H. & Zhang, Z. (2002) Biostability of electrically conductive polyester fabrics: An in vitro study. *Journal of Biomedical Materials Research,* 62 **(4)**: 507-513.

Kang, E. T., Neoh, K. G. & Ong, Y. K. (1991) Thermal stability and degradation of some chemically synthesized polypyrrole complexes. *Thermochimica Acta,* 181: 57-70.

Kaynak, A. & Beltran, R. (2003) Effect of synthesis parameters on the electrical conductivity of polypyrrole-coated poly(ethylene terephthalate) fabrics. *Polymer International,* 52: 1021-1026.

Kaynak, A. & Hakansson, E. (2005) Generating heat from conducting polypyrrole-coated PET fabrics. *Advances in Polymer Technology,* 24 **(3)**: 194-207.

Khalkhali, R. A. & Keivani, M. B. (2005) Thermogravimetry analysis of electrochemically synthesized polypyrrole conducting polymer films. *Asian Journal of Chemistry,* 17 **(3)**: 1483-1489.

Kim, B., Koncar, V., Devaux, E., Dufour, C. & Viallier, P. (2004) Electrical and morphological properties of PP and PET conductive polymer fibers. *Synthetic Metals,* 146: 167-174.

Kim, D. Y., Lee, J. Y., Moon, D. K. & Kim, C. Y. (1995) Stability of Reduced Polypyrrole. *Synthetic Metals,* 69: 471-474.

Kim, H. K., Byun, S. W., Jeong, S. H., Hong, Y. K., Joo, J. S., Song, K., Park, Y. H. & Lee, J. Y. (2002) Environmental stability of EMI shielding PET fabric/polypyrrole composite. *Molecular Crystals Liquid Crystal,* 377: 369-371.

Kim, H. K., Kim, M. S., Chun, S. Y., Park, Y. H., Jeon, B. S., Lee, J. Y., Hong, Y. K., Joo, J. & Kim, S. H. (2003) Characteristics of electrically conducting polymer-coated textiles. *Molecular Crystals Liquid Crystal,* 405: 161-169.

Kim, M. S., Kim, H. K., Byun, S. W., Jeong, S. H., Hong, Y. K., Joo, J. S., Song, K. T., Kim, J. K., Lee, C. J. & Lee, J. Y. (2002) PET fabric/polypyrrole composite with high electrical conductivity for EMI shielding. *Synthetic Metals,* 126: 233-239.

Kim, S. H., Jang, S. H., Byun, S. W., Lee, J. Y., Joo, J. S., Jeong, S. H. & Park, M.-J. (2003) Electrical properties and EMI shielding characteristics of polypyrrole-nylon 6 composite fabrics. *Journal of Applied Polymer Science,* 87: 1969-1974.

Kim, S. H., Oh, K. W. & Bahk, J. H. (2004) Electrochemically synthesized polypyrrole and Cu-plated nylon/spandex for electrotherapeutic pad electrode. *Journal of Applied Polymer Science*, 91: 4064-4071.

Kirstein, T. (2004) Medical applications of electronic clothing. *Medical Device Technology,* Sept: 22-24.

Kuhn, H. H. & Child, A. D. (1998) Electrically conducting textiles. *Handbook of Conducting Polymer*.993-1013

Kuhn, H. H. & Kimbrell, W. C. US Patent 4803096

Kuhn, H. H. (1993) Characterization and Application of Polypyrrole-coated Textiles. In Aldissi, M. (Ed.) *Intrinsically Conducting Polymers: An Emerging Technology*. Netherlands, Kluwer Academic Publishers.25-34

Kuhn, H. H. (1997) Adsorption at the liquid/ solid interface: conductive textiles based on polypyrrole, *Book of Papers, International Conference and Exhibition - AATCC,* Atlanta:114-122

Kuhn, H. H., Child, A. D. & Kimbrell, W. C. (1995) Toward real applications of conductive polymers. *Synthetic Metals,* 71: 2139-2142.

Kuhn, H. H., Kimbrell, W. C., Fowler, J. E. & Barry, C. N. (1993) Properties and applications of conductive textiles. *Synthetic Metals*, 55-57: 3707-3712.

Kurosawa, S. (2004) PhD thesis, *Supercritical processing of electrically conducting polymers,* Chemical Engineering, Georgio Institute of Technology

Lascelles, S. F., McCarthy, G. P., Butterworth, M. D. & Armes, S. P. (1998) Effect of synthesis parameters on the particle size, composition and colloid stability of polypyrrole-silica nanocomposite particles. *Colloid Polymer Science,* 276: 893-902.

Lee, J. Y., Park, D. W. & Lim, J. O. (2003) Polypyrrole-coated woven fabric as flexible surface-heating element. *Macromolecular Research,* 11 **(6)**: 481-487.

Lee, K. K.-Y. (2001) PhD thesis, *Growth and characterization of vapor-deposited conjugated polymer thin films,* Chemical Engineering, University of Pennsylvania

Li, R. W. M. (2005) BA thesis, *A Study of the Fabrication of the Polypyrrole-Coated E-Textile Strain Sensors and Product Development,* Institute of Textiles and Clothing, The Hong Kong Polytechnic University

Li, Y., Cheng, X. Y., Leung, M. Y., Tsang, J., Tao, X. M. & Yuen, M. C. W. (2005) A flexible strain sensor from polypyrrole-coated fabrics. *Synthetic Metals,* 155 **(1)**: 89-94.

Liu, Y.-C. & Chung, K.-C. (2003) Characteristics of conductivity - improved polypyrrole films via different procedures. *Synthetic Metals,* 139 **(2)**: 277-281.

Liu, Y.-C. & Hwang, B.-J. (2001) Mechanism of conductivity decay of polypyrrole exposed to water and enhancement of conductivity stability of copper(I) - modified polypyrrole. *Journal of Electroanalytical Chemistry,* 501: 100-106.

Marculescu, D., Marculescu, R., Zamora, N. H., Stanley-Marbell, P., Khosla, P. K., Park, S., Jayaraman, S., Jung, S., Lauterbach, C., Weber, W., Kirstein, T., Cottet, D., Grzyb, J., Troster, G., Jones, M., Martin, T. & Nakad, Z. (2003) Electronic textiles: A platform for pervasive computing, *Proceedings of the IEEE*, 91:1995-2018

Mazzoldi, A., De Rossi, D., Lorussi, F., Scilingo, E. P. & Paradiso, R. (2002) Smart textiles for wearable motion capture systems. *AUTEX Research Journal*, 2 **(4)**: 199-203.

Meoli, D. & May-Plumlee, T. (2002) Interactive electronic textile development: A review of technologies. *Journal of Textile and Apparel, Technology and Management,* 2 **(2)**: 1-12.

Morgan, N. (2000) Spin doctoring to porduce electrically conductive fibres. *Technical Textiles International,* 3: 24-26.

Moss, B. (1992) PhD thesis, *Thermal and Environmental Ageing Studies of Polypyrrole*, School of Chemical Engineering and Industrial Chemistry, University of New South Wales

Munstedt, H. (1986) Properties of polypyrroles treated with base and acid. *Polymer,* 27 **(6)**: 899-904.

Munstedt, H. (1988) Ageing of electrically conducting organic materials. *Polymer,* 29 **(2)**: 296-302.

MyHeart, http://www.extra.research.philips.com/euprojects/myheart

Neoh, K. G., Young, T. T., Kang, E. T. & Tan, K. L. (1997) Structural and mechanical degradation of polypyrrole films due to aqueous media and heat treatment and the subsequent redoping characteristics. *Journal of Applied Polymer Science,* 64 **(3)**: 519-526.

Nowak, C. K. J. (1995) PhD thesis, *Specific Interactions Between Electrically Conductive Polypyrrole and Nylon 6,6*, Textiles, Fibers and Polymer Science, Clemson University

Oh, K. W., Park, H. J. & Kim, S. H. (2003) Stretchable conductive fabric for electrotherapy. *Journal of Applied Polymer Science,* 88: 1225-1229.

Oh, K. W., Park, H. J. & Kim, S. H. (2004) Electrical property and stability of electrochemically synthesized polypyrrole films. *Journal of Applied Polymer Science*, 91: 2659-2666.

Omastova, M., Kosina, S., Pionteck, J., Janke, A. & Pavlinec, J. (1996) Electrical properties and stability of polypyrrole containing conducting polymer composites. *Synthetic Metals,* 81: 49-57.

Omastova, M., Pavlinec, J., Pionteck, J. & Simon, F. (1997) Synthesis, electrical properties and stability of polypyrrole-containing conducting polymer composites. *Polymer International,* 43: 109-116.

Ouyang, J. & Li, Y. (1995) Enhancement of the electrical conductivity of polypyrrole films on applying higher voltage. *Synthetic Metals*, 75: 1-3.

Otero, T. F., Tejada, R. & Elola, A. S. (1987) Formation and modification of polypyrrole films on platinum electrodes by cyclic voltammetry and anodic polarization. *Polymer,* 28 **(4)**: 651-658.

Pacelli, M., Loriga, G., Taccini, N. & Paradiso, R. (2006) Sensing fabrics for monitoring physiological and biomechanical variables: E-textile solutions, *Proceeding of the 3rd IEEE-EMBS International Summer School and Symposium on Medical Devices and Biosensors,* MIT, Boston, USA, Sept 4-6, 2006

Patnaik, S. N. & Hopkins, D. A. (2003) *Strength of Materials - A New Unified Theory for the 21th Century,* Elsevier Butterworth Heinemann.

Pei, Q. & Qian, R. (1991) Protonation and deprotonation of polypyrrole chain in aqueous solutions. *Synthetic Metals,* 45: 35-48.

Pierce, F. T. (1947) Geometrical principles applicable to the design of functional fabrics. *Textile Research Journal,* **(3)**: 123.

Plank, R. V., DiNardo, N. J. & Vohs, J. M. (1997) Chemical and electronic properties of vapor-deposited polyaniline films on metal substrate. *Synthetic Metals,* 89 **(1)**: 1-9.

Popper, P. (1966) The theoretical behavior of a knitted fabric subjected to biaxial stresses. *Textile Research Journal,* **(2)**: 148.

Porter, T. L., Caple, K. & Caple, G. (1994) Structure of chemically prepared free-standing and vacuum evaporated polyaniline thin films. *Journal of Vacuum Science & Technology A,* 12 **(4)**: 2441-2445.

Post, E. R., Orth, M., Russo, P. R. & Gershenfeld, N. (2000) E-broidery: Design and fabrication of textile-based computing. *IBM Systems Journal,* 39 **(3&4)**: 840-860.

Post, M. O. E. R. (1997) Smart fabric, or wearable clothing. *Proceeding of First International Syposium on Wearable Computers*.

Rapi, S., Bocchi, V. & Gardini, G. P. (1988) Conducting polypyrrole by chemical synthesis in water. *Synthetic Metals*, 24: 217-221.

Rodie, J. B. (2004) Textile sensitivity. *Textile World,* June: 82.

Rodriguez, J., Grande, H. J. & Otero, T. F. (1997) Polypyrroles: from basic research to technological applications. In Nalwa, H. S. (Ed.) *Handbook of Organic Conductive Molecules and Polymers: Vol. 2. Conductive Polymers: Synthesis and Electrical Properties.* John Wiley & Sons Ltd.415-469

Rupprecht, L. (1999) *Conductive Polymers and Plastics in Industrial Applications,* US, Plastics Design Library.

Salmon, M., Diaz, A. F., Logan, A. J., Krounbi, M. & Bargon, J. (1982) Chemical modification of conducting polypyrrole films. *Molecular Crystals Liquid Crystal,* 83 **(1-4)**: 1297-1308.

Samuelson, L. A. & Druy, M. A. (1986) Kinetics of the degradation of electrical conductivity in polypyrrole. *Marcomolecules,* 19: 824-828.

Scilingo, E. P., Lorussi, F., Mazzoldi, A. & De Rossi, D. (2003) Strain-sensing fabrics for wearable kinaesthetic-like systems. *IEEE Sensors Journal,* 3 **(4)**: 460-467.

Scrosati, B. (1993) *Application of Electroactive Polymers.* 1st Edition ed., Chapman & Hall, London.229

Seiko-SPI4000-series (2002) *SPM Handbook Manual*.

Selampinar, F., Toppare, L., Akbulut, U., Yalcin, T. & Suzer, S. (1995) A conducting composite of polypyrrole II. As a gas sensor. *Synthetic Metals,* 68 **(2)**: 109-116.

Shirota, Y. (1997) Electrically conducting polymers and their applications as functional materials. In Takemoto, K., Ottenbrite, R. M. & Kamachi, M. (Eds.) *Functional Monomers and Polymers.* Second Edition ed. New York, Basel, Hong Kong, Marcel Dekker, Inc.

Silk, T., Hong, Q., Tamm, J. & Compton, R. G. (1998a) AFM studies of polypyrrole film surface morphology I. The influence of film thickness and dopant nature. *Synthetic Metals,* 93: 59-64.

Silk, T., Hong, Q., Tamm, J. & Compton, R. G. (1998b) AFM studies of polypyrrole film surface morphology II. Roughness characterization by the fractal dimension analysis. *Synthetic Metals,* 93: 65-71.

Singh, R., Narula, A. K., Tandon, R. P., Rao, S. U. M., Panwar, V. S., Mansingh, A. & Chandra, S. (1996) Growth kinetics of polypyrrole, poly(N-methyl pyrrole) and their copolymer, poly(N-methyl pyrrole-pyrrole): effect of annealing on conductivity and surface structure. *Synthetic Metals,* 79: 1-6.

Smartex, http://www.smartex.it

Smith, W. C. (1988) Metallized fabrics -- Techniques and applications. *Journal of Coated Fabrics,* 17 **(4)**: 242-253.

Spinks, G. M., Wallace, G. G., Liu, L. & Zhou, D. (2002) Conducting polymers and carbon nanotubes as electromechanical actuators and strain sensors, *Materials Research Society Symposium Proceeding -- Electroactive Polymers and Rapid Prototyping*, 698:17-28

Spinks, G. M., Wallace, G. G., Liu, L. & Zhou, D. Z. (2003) Conducting polymers electromechanical actuators and strain sensors. *Macromolecules Symp.*, 192: 161-169.

Sree, U., Yamamoto, Y., Deore, B., Shiigi, H. & Nagaoka, T. (2002) Characterisation of polypyrrole nano-films for membrane-based sensors. *Synthetic Metals,* 131: 161-165.

Street, G. B. (1986) *Handbook of Conducting Polymers,* New York, Marcel Dekker, Inc.

Suarez, M. F. & Compton, R. G. (1999) In situ atomic force microscopy study of polypyrrole synthesis and the volume changes induced by oxidation and reduction of the polymer. *Journal of Electroanalytical Chemistry,* 462: 211-221.

Tan, S. N. & Ge, H. (1996) Investigation into vapour-phase formation of polypyrrole. *Polymer,* 37 **(6)**: 965-968.

Tao, X. (2001) *Smart Fibers, Fabrics and Clothing,* England, The Textile Institute.

Tao, X. (2005) *Wearable Electronics and Photonics*, The Textile Institute, Woodhead Publishing Limited.

Tao, X. M. (2001) *Smart Fibers, Fabrics and Clothing,* England, The Textile Institute.

Tao, X. M., Leung, M. Y., Yuen, C. W. M., Kwok, W. Y. & Ho, H. L. (2005) *Patterned Electrical Textile Sensors and Device,* US Patent 11-029,674

Thieblemont, J. C., Brun, A., Marty, J., Planche, M. F. & Calo, P. (1995) Thermal analysis of polypyrrole oxidation in air. *Polymer,* 36 **(8)**: 1605-1610.

Thieblemont, J. C., Gabelle, J. L. & Planche, M. F. (1994) Polypyrrole overoxidation during its chemical synthesis. *Synthetic Metals,* 66: 243-247.

Thieblemont, J. C., Planche, M. F., Petrescu, C. & Bouvier, J. M. (1993) Stability of chemically synthesized polypyrrole films. *Synthetic Metals,* 59: 81-96.

Thieblemont, J. C., Planche, M. F., Petrescu, C., Bouvier, J. M. & Bidan, G. (1994) Kinetics of degradation of the electrical conductivity of polypyrrole under thermal aging. *Polymer Degradation and Stability,* 43: 293-298.

Truong, V. T., Ennis, B. C. & Forsyth, M. (1995) Enhanced thermal properties and morphology of ion-exchanged polypyrrole films. *Polymer,* 36 **(10)**: 1933-1940.

Truong, V. T., Ennis, B. C., Turner, T. G. & Jenden, C. M. (1992) Thermal stability of polypyrroles. *Polymer International,* 27: 187-195.

Turcu, R., Neamtu, C. & Brie, M. (1993) Effects of thermal annealing on the electrical conductivity of polypyrrole films. *Synthetic Metals,* 53: 325-332.

Wallace, G. G., Spinks, M. G., Kane-Maguire, L. A. P. & Teasdale, P. R. (2003) *Conductive Electroactive Polymers, 2nd Edition,* New York, CRC Press.

Wang, X. & Chung, D. D. L. (1996) Continuous carbon fibre epoxy-matrix composite as a sensor of its own strain. *Smart Materials and Structures,* 5 **(6)**: 796-800.

Wang, Y. & Rubner, M. F. (1990) Stability studies of the electrical conductivity of various poly(3-alkylthiophenes). *Synthetic Metals,* 39 **(2)**: 153.

Wang, Y. & Rubner, M. F. (1991) Stability studies of electrically conducting polyheterocycles. *Synthetic Metals,* 41-43: 1103-1108.

Xue, P. & Tao, X. M. (2004) Multi-scale investigation on electromechanical behaviour of polypyrrole-coated fibres, *World Textile Conference - 4th AUTEX Conference,* Roubaix, June 22-24

Xue, P. & Tao, X. M. (2005) Morphological and electromechanical studies of fibers coated with electrically conductive polymer. *Journal of Applied Polymer Science,* 98: 1844-1854.

Xue, P., Tao, X. M., Kwok, K. W. Y. & Leung, M. Y. (2004) Electromechanical behaviour of fibers coated with an electrically conductive polymer. *Textile Research Journal,* 74 **(10)**: 929-936.

Xue, P., Tao, X., Leung, M. Y. & Zhang, H. (2005) Electromechanical properties of conductive fibres, yarns and fabrics. In Tao, X. (Ed.) *Wearable Electronics and Photonics.* The Textile Institute.81-104

Yoon, C. O., Sung, H. K., Kim, J. H., Barsoukov, E., Kim, J. H. & Lee, H. (1999) The effect of low-temperature conditions on the electrochemical polymerization of polypyrrole films with high density, high electrical conductivity and high stability. *Synthetic Metals,* 99: 201-212.

You, L., Yang, G.-R., Lang, C.-I., Moore, J. A., Wu, P., McDonald, J. F. & Lu, T.-M. (1993) Vapor deposition of parylene-F by pyrolysis of dibromotetrafluoro-p-xylene. *Journal of Vacuum Science & Technology A,* 11 **(6)**: 3047-3052.

Zhang, H., Tao, X. M., Wang, S. & Yu, T. (2005) Electro-mechanical properties of knitted fabric made from conductive multi-filament yarn under unidirectional extension. *Textile Research Journal*, 75 **(8)**: 598-606.

Zhang, Z., Roy, R., Tessier, F. J. D. & Dao, L. H. (2001) In vitro biocompatibility study of electrically conductive polypyrrole-coated polyester fabrics. *Journal of Biomed Materials*, 57: 63-71.

Computing program design for the Instrumental Dancing Garment by Flash:

```
//Init and Start BG Music
bgSound = new Sound();
bgSound.loadSound("sound.mp3"); //Get the music file
bgSound.setVolume(90);  //Set Volume Level
bgSound.start(0, 0);  //Start Play Sound

//Repeat the BG Music
bgSound.onSoundComplete = function() {
 bgSound.start(.1, 0);
};

var myListener:Object = new Object();
var cKey:Number=0;

//fun the function when enter the any key
myListener.onKeyDown = function () {
var k:Number=chr(Key.getAscii());  //get the key which the user entered
 //check is the key is between 0 to 9
 if ((k>0 & k<=9) && (cKey != k)){
   cKey=tt2=k;
   //Start play the selected sound
   mysound = new Sound();
   mysound.loadSound("sound"+cKey+".mp3");  //load the mp3 file
   mysound.setVolume(90);  //set Volume Level
   mysound.start(-21, 999);  //Start Play

 }
}

//
myListener.onKeyUp = function () {
 cKey=0;
 mysound.stop();  //Stop the selected sound
}

Key.addListener(myListener);
```